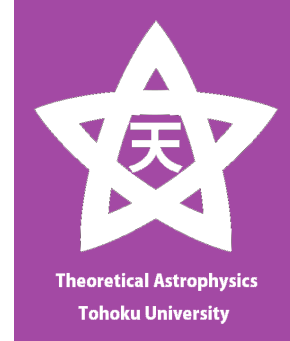


ガンマ線バースト・ 高速電波バースト 研究の現状、 宇宙論との関係



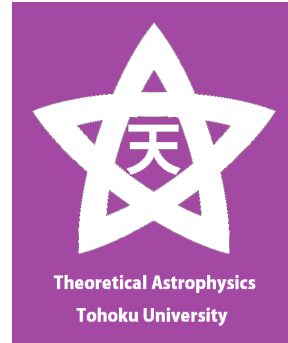
Kunihito Ioka (KEK)



HIGH ENERGY ACCELERATOR RESEARCH ORGANIZATION



ガンマ線バースト・ 高速電波バースト 研究の現状、 宇宙論との関係

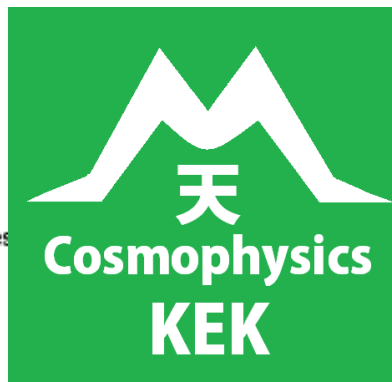


Theoretical Astrophysics
Tohoku University

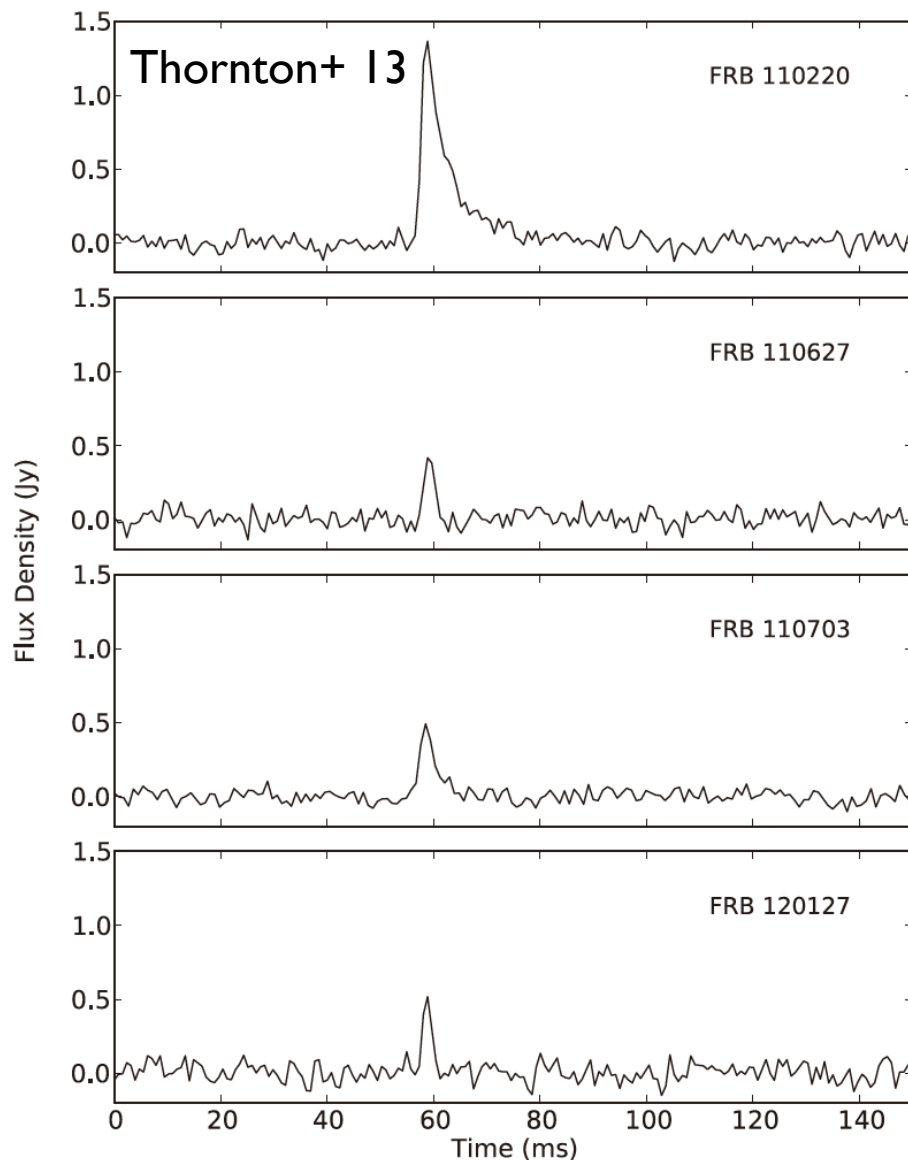
Kunihito Ioka (KEK)



HIGH ENERGY ACCELERATOR RESEARCH ORGANIZATION



Fast Radio Bursts



F=0.6-8.0 Jy ms !!!
Most luminous
radio transients
if cosmological

~10年前

GRB Cosmology

Massive star origin \Rightarrow High redshift GRBs

Like QSO

Like Supernova

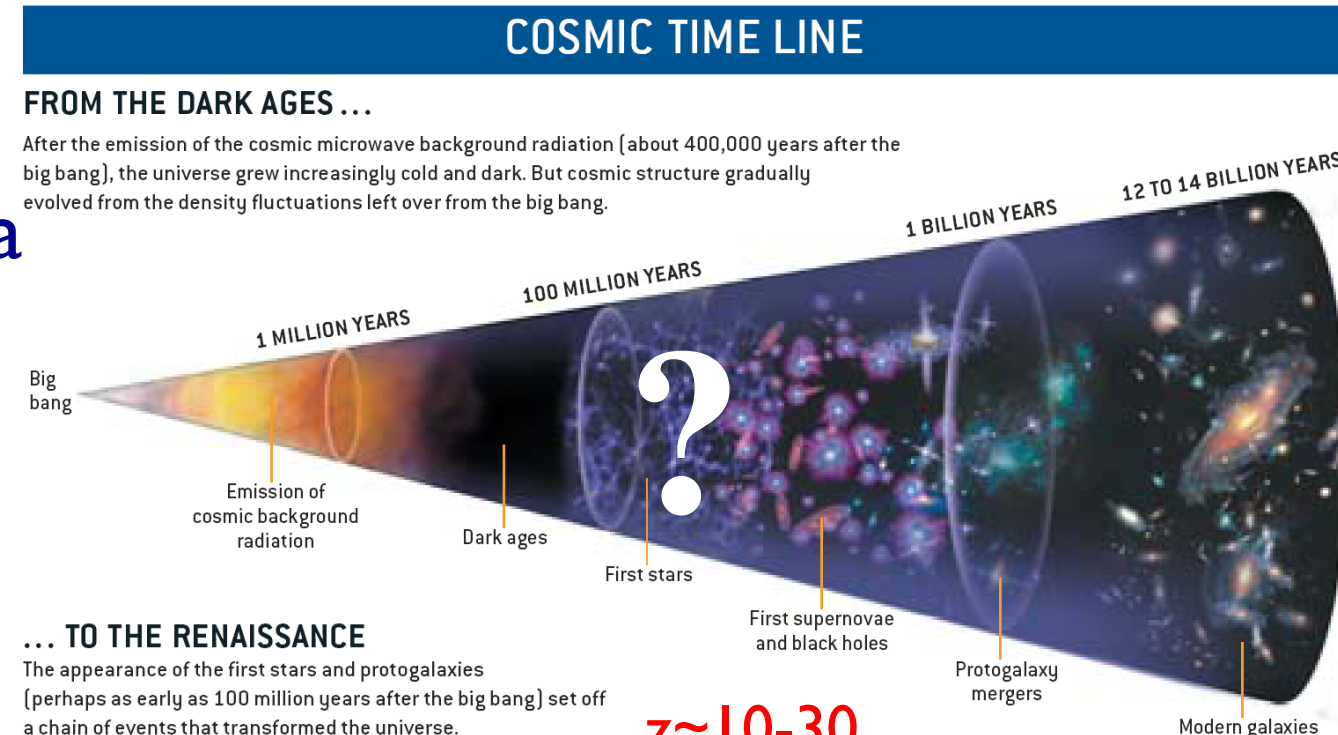
Star formation

Reionization

Metal, Dust

Dark energy

...

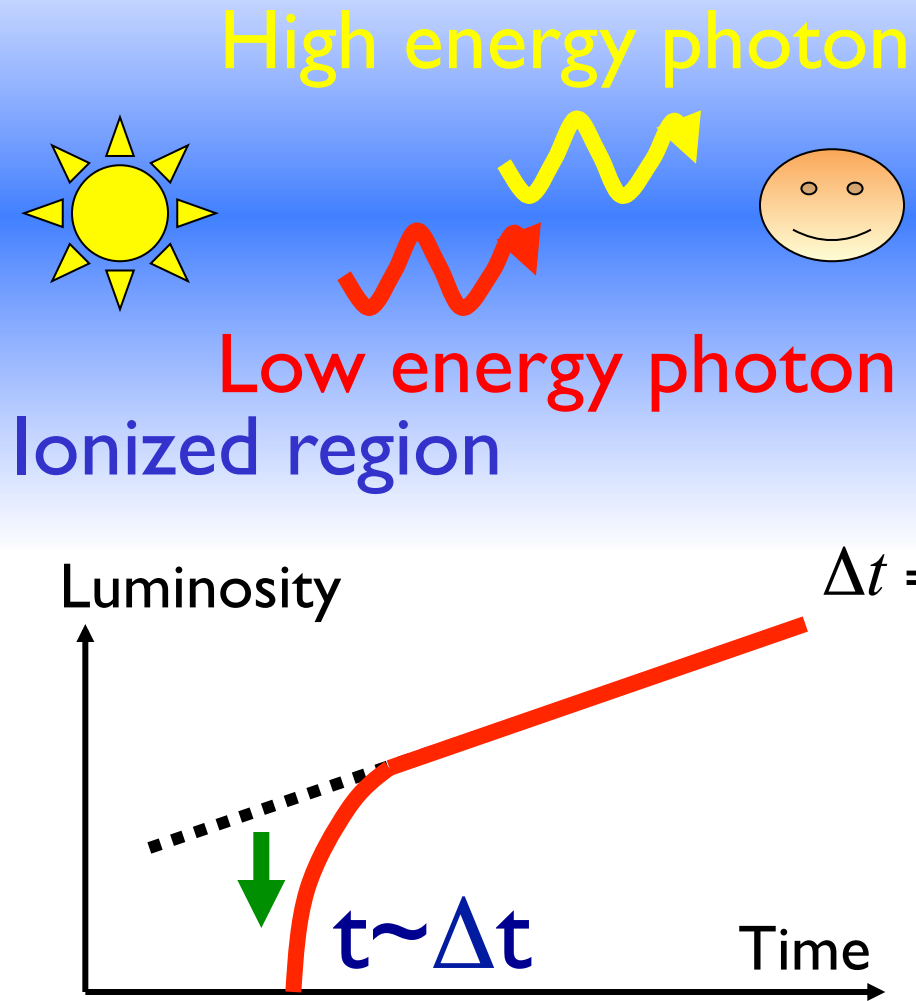


Larson & Bromm 02

GRBs are useful
for probing high-z

GRB ←
QSO, galaxy ←

Radio Dispersion



In a plasma, a light signal is delayed

$$\omega^2 = k^2 c^2 + \omega_p^2$$

$$\omega_p = \sqrt{\frac{4\pi n e^2}{m}} = 5.63 \times 10^4 n^{1/2} \text{ s}^{-1}$$

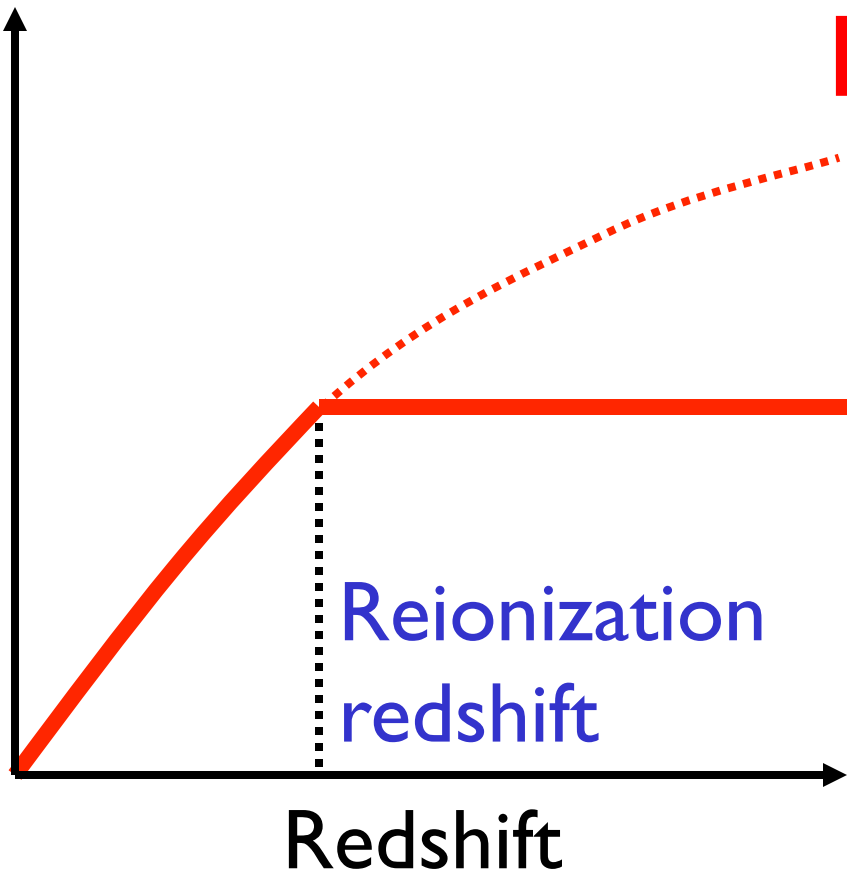
$$\Delta t = 4.15 \text{ s} \left(\frac{\nu}{1 \text{ GHz}} \right)^{-2} \left(\frac{\text{DM}}{10^3 \text{ pc cm}^{-3}} \right)$$

Distortion in light curve
 ⇒ DM
 ⇒ Reionization History

Dispersion Measure

is the column density of free electrons along light path

Dispersion Measure



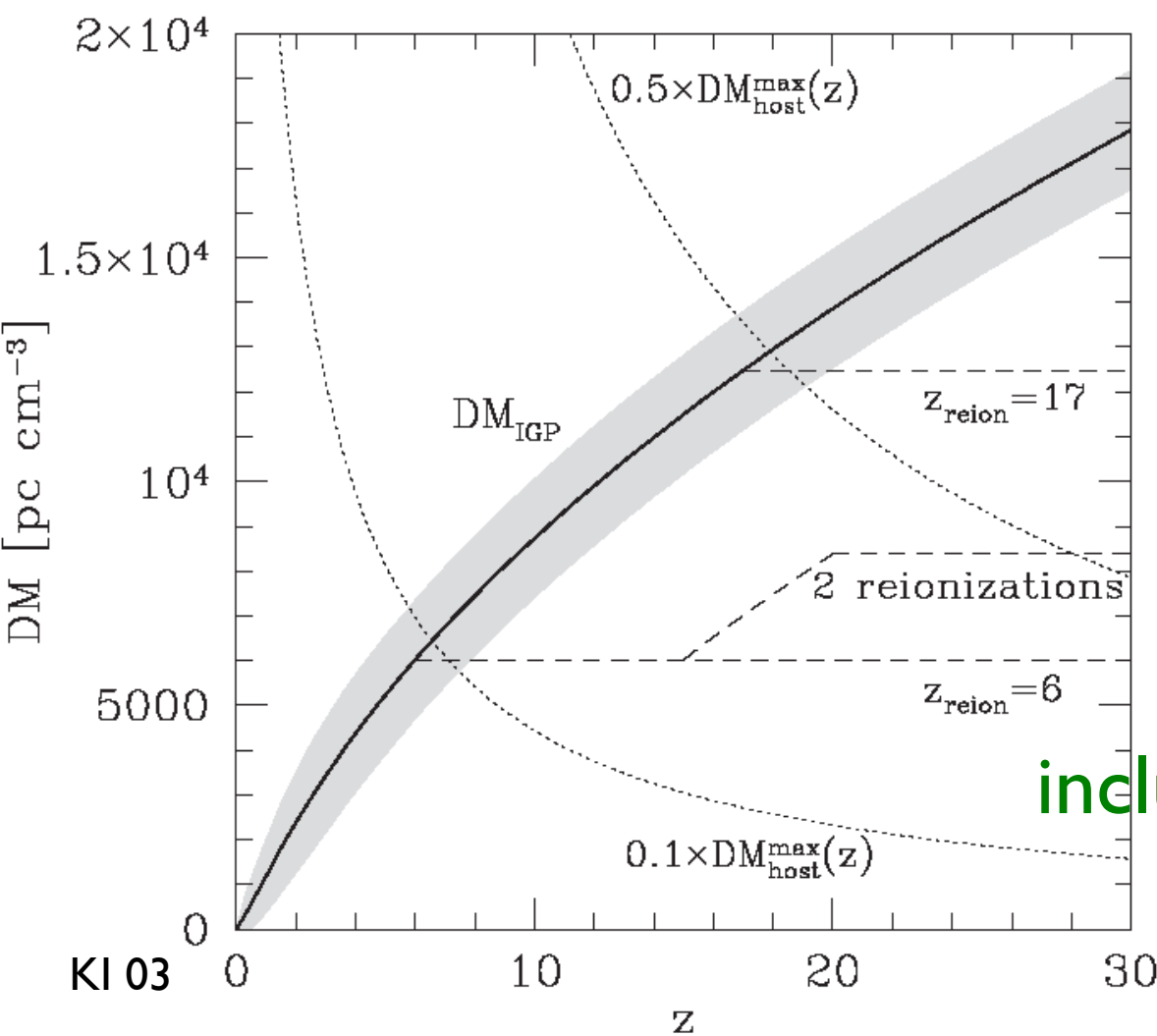
Dispersion Measure



Reionization
History

Recombined electrons
provide no DM

Intergalactic DM



$$\Delta t = \int_0^z dz \frac{dt}{dz} \frac{1}{2} \frac{(1+z)\nu_p^2}{[(1+z)\nu]^2}$$

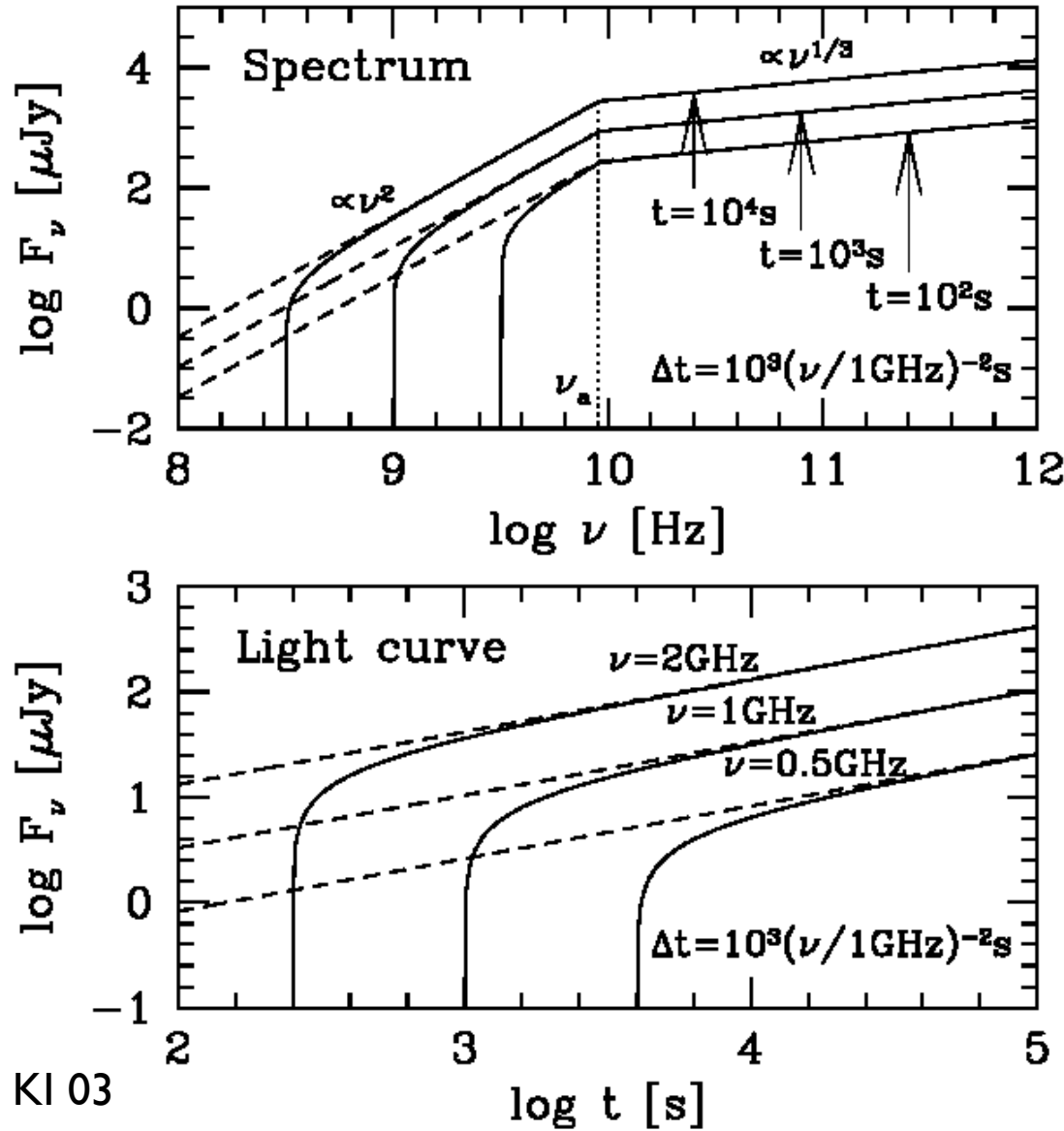
$$= \frac{e^2}{2\pi m_e c} \frac{1}{\nu^2} \times$$

$$\frac{cn_0}{H_0} \int_0^z \frac{(1+z)dz}{[\Omega_m(1+z)^3 + \Omega_\Lambda]^{1/2}}$$

DM_{IGP}

$DM_{Galaxy} \sim 30-10^3\ pc\ cm^{-3}$

DM from Afterglow

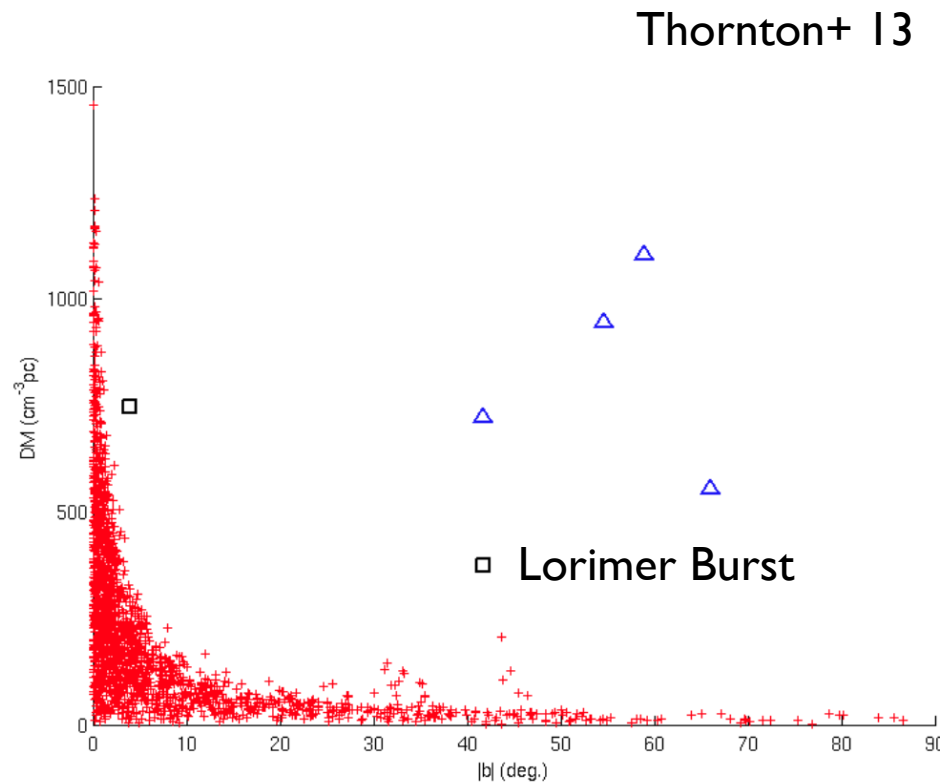
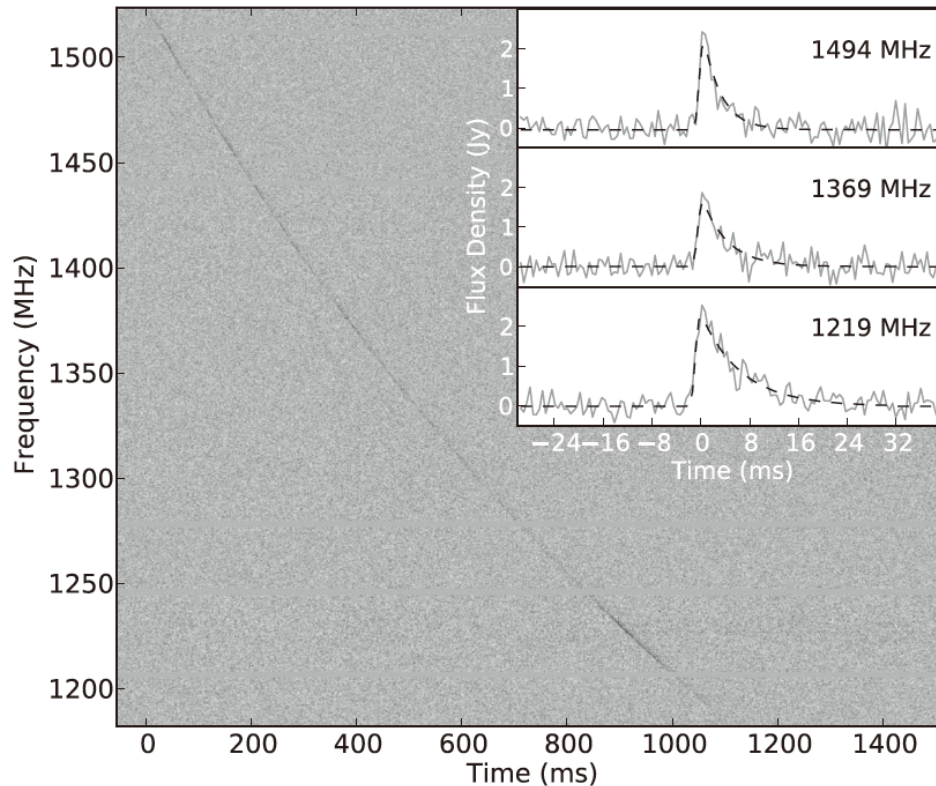


Distortion
at $t \sim \Delta t$
 \Rightarrow DM

$$\Delta t \propto \nu^{-2}$$

Unfortunately
radio afterglows
are not so bright

Dispersion Measure



$$\delta t \propto DM \cdot v^{-2}$$

Galactic latitude

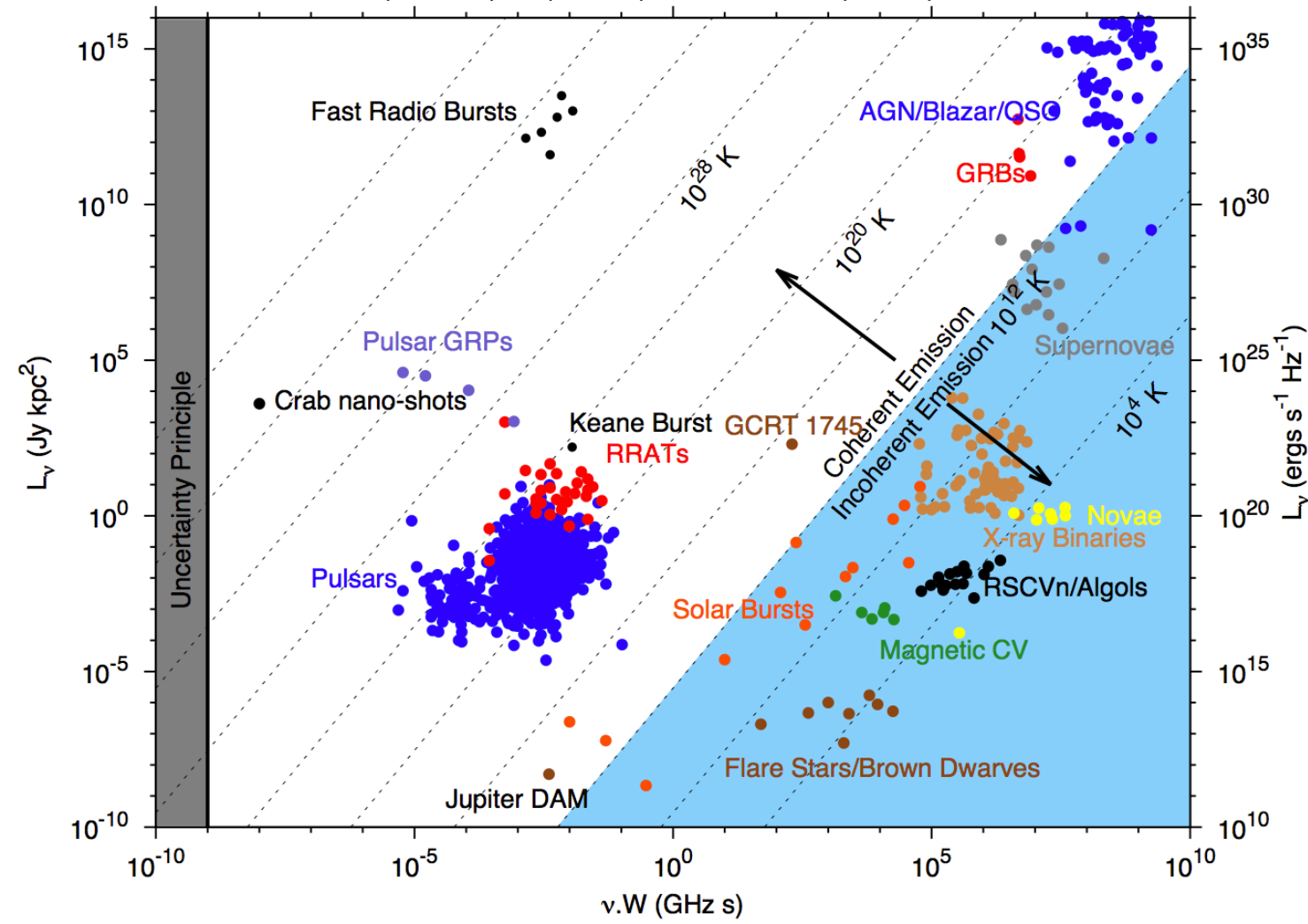
$DM=500-1000 \text{ cm}^{-3} \text{ pc}$

Brightness Temperature

$$T_B \simeq 10^{36} \text{ K} \left(\frac{S_{\text{peak}}}{\text{Jy}} \right) \left(\frac{\text{GHz}}{\nu} \right)^2 \left(\frac{\text{ms}}{\Delta t} \right)^2 \left(\frac{d}{\text{Gpc}} \right)^2 \frac{(1+z)^4}{\gamma^2}$$

d: comoving distance

- $P \sim |E|^2$
- $\sim |E_1 + \dots + E_N|^2$
- $\sim N|E_1|^2$
- (incoherent)
- $\sim N^2|E_1|^2$
- (coherent)



Summary of FRB Obs.

- $\text{DM}=500\text{-}1000 \text{ cm}^{-3} \text{ pc}$ ($z=0.5\text{-}1$, $d_L \sim 2\text{-}6 \text{ Gpc}$)
- $S_\nu \sim Jy \Rightarrow E_{\text{iso}} \sim 10^{39\text{-}41} \text{ erg}$ ($\sim 10x$ if $\Delta\nu \sim \nu$)
- $\delta t = 5.6 \text{ ms}, < 4.3, 1.4, 1.1 \text{ ms}$
 $\Rightarrow c\delta t(1+z)^{-1} < 1500(1+z)^{-1} \text{ km}$
- Rate $\sim (1 \pm 0.5) \times 10^4 / \text{sky/day} \sim 10^{-3} / \text{yr/galaxy}$
 $\Leftrightarrow \text{Supernova rate } 10^{-2} / \text{yr/galaxy}$
- High brightness temperature $> 10^{35} \text{ K}$
- No repeats & No counterparts so far

Expected Rate

Hassall+ 13
Lorimer+ 13
Trott+ 13

High Scattering

Low frequency component SKA I could find an extragalactic burst every hour

Spectral Index

- 0.0
- 1.0
- 2.0
- 3.0
- 4.0

I event/hour

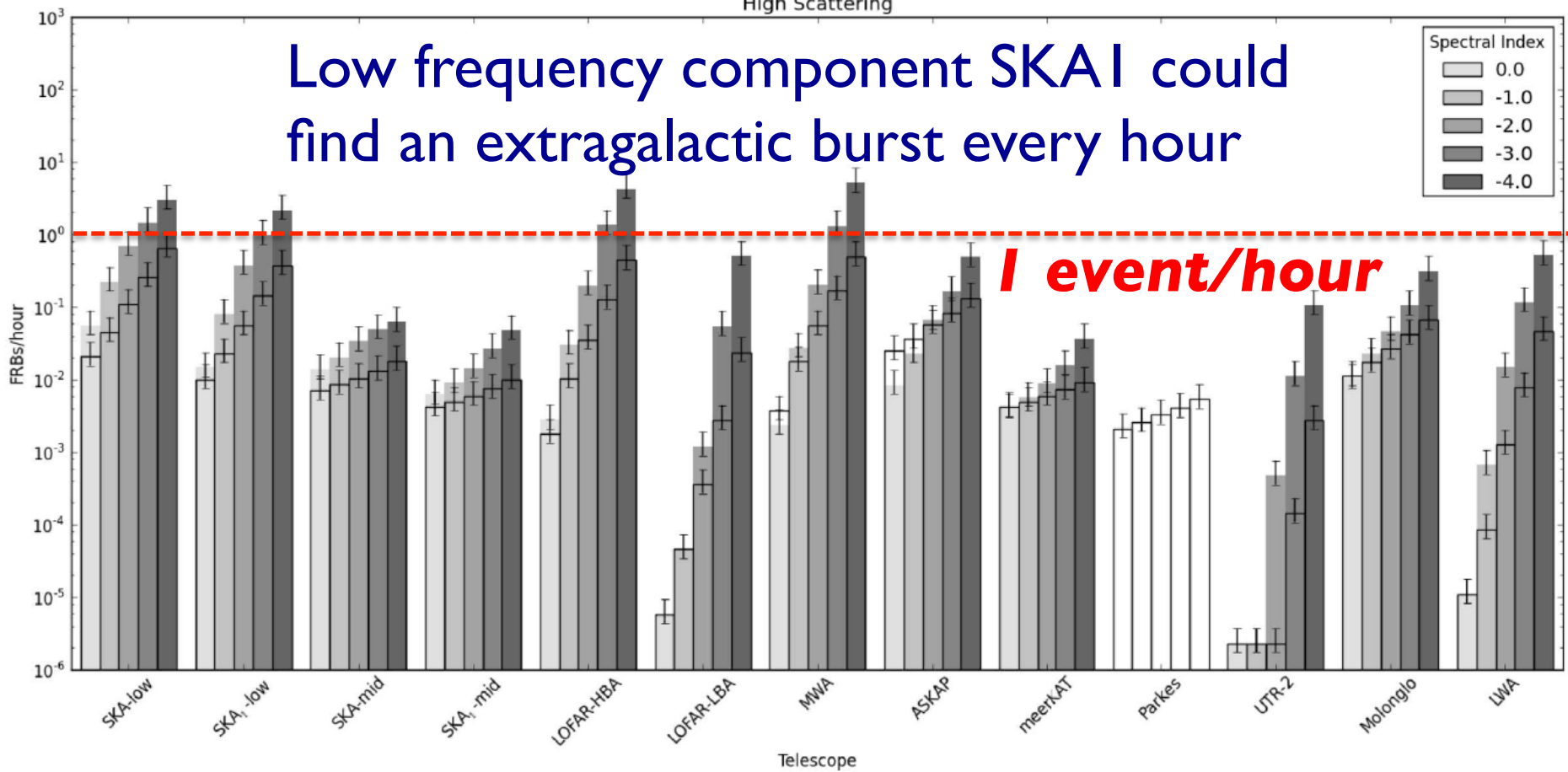


Figure 2. Expected number of FRBs per hour for various observatories in the high-scattering simulations. The solid bars show the number of FRBs detectable in imaging surveys, assuming different spectral indices of: 0.0 (white), -1.0, -2.0, -3.0 and -4.0 (darkest grey). The number of FRBs detectable in beamformed surveys are indicated by the corresponding transparent bars. The DM range used was $0 - 6000 \text{ pc cm}^{-3}$.

Contents for FRB

- ***Possible origins***
- Real cosmic signal?
- Galactic?
- FRB cosmology

Possible Origins

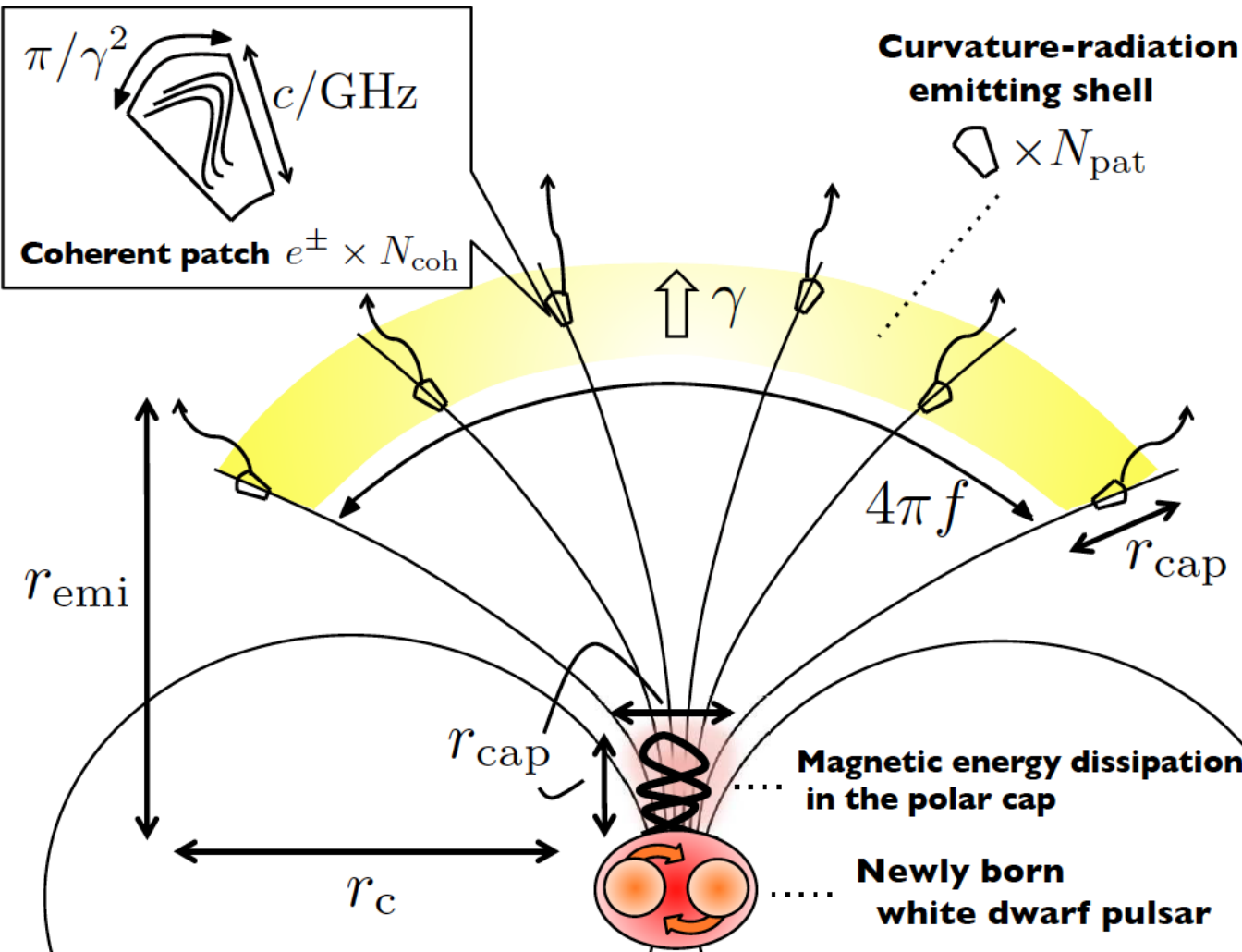
- **Perytons** Burke-Spolaor+ 11; Kulkarni+ 14
- **Galactic**
 - Nearby flaring star Loeb+ 13
 - RRAT (Rotating Radio Transient; intermittent pulsar)
- **Extragalactic**
 - Magnetar giant flare Popov & Postnov 07; Thornton+ 13; Lyubarsky 14; Penn & Conner 15
 - NS-NS merger Hansen & Lyutikov 01; Totani 13
 - WD-WD merger Kashiyama+ 13
 - Collapse of hypermassive NS Falcke & Rezzolla 13; Zhang 13
 - Supernova into a nearby star Colgate+ 71,75; Egorov & Postnov 09
 - Supergiant pulse Cordes & Wasserman 15
 - Pulsar-orbiting bodies Mottez & Zarka 14

Possible Exotics

- **Evaporation of BH** Rees 77; Blandford 77; Kavic+ 08; Keane+ 12
- **PBH to white hole** Barrau+ 14
- **Superconducting cosmic strings** Cai+ 12; Yu+ 14
- **Axion stars** Iwazaki+ 14; Tkachev+ 14
- ...

Binary White Dwarf Mergers?

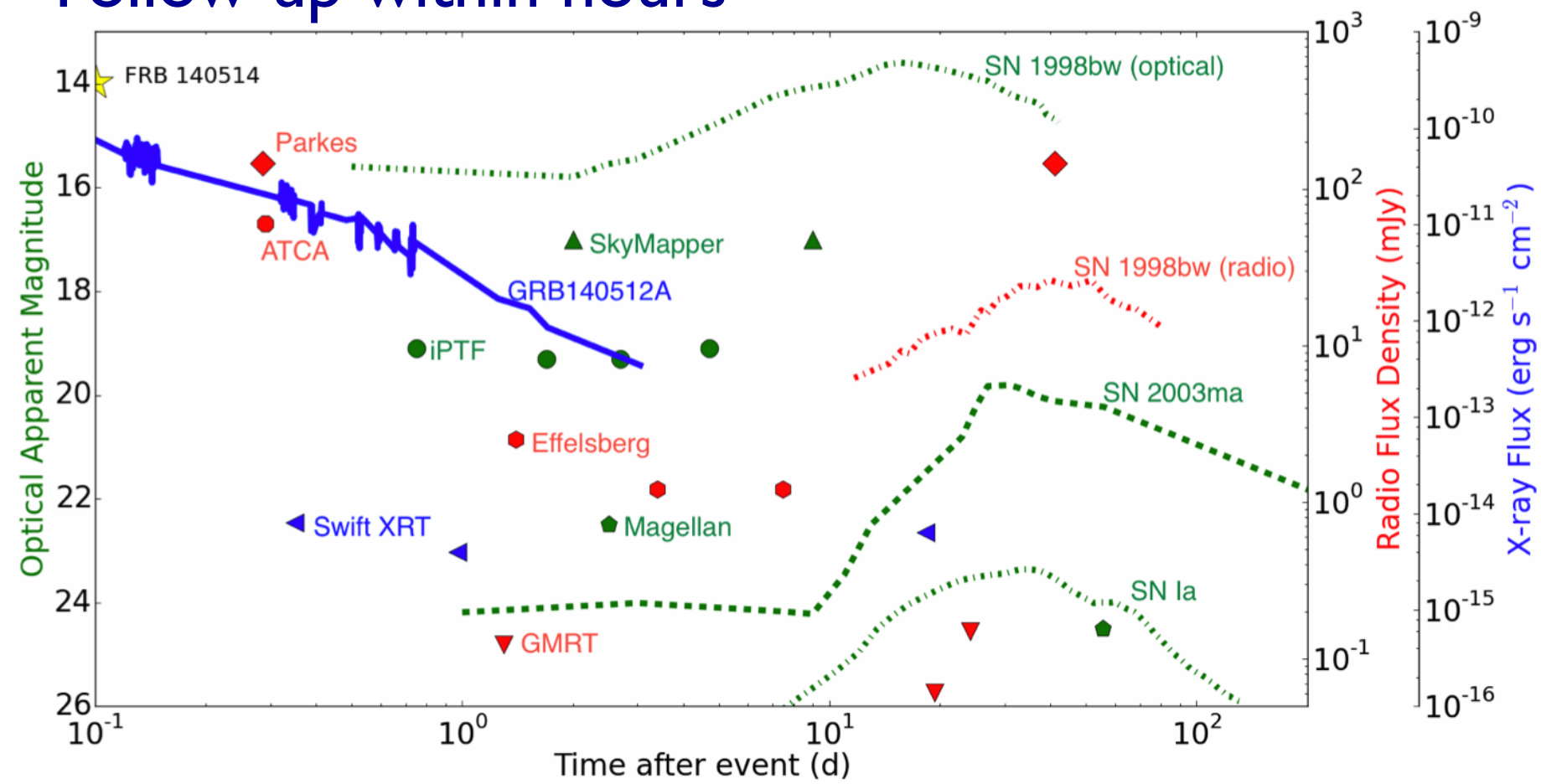
Kashiyama, KI & Meszaros 13



- **Energetics**
 $E_B \sim 10^{40} \text{ erg}$
- **Timescale**
 $r_{\text{cap}}/c \sim \text{ms}$
- **Event rate**
 $\sim \text{SN Ia}$
- **SN Ia as a counterpart?**

No Counterpart So Far

Follow-up within hours

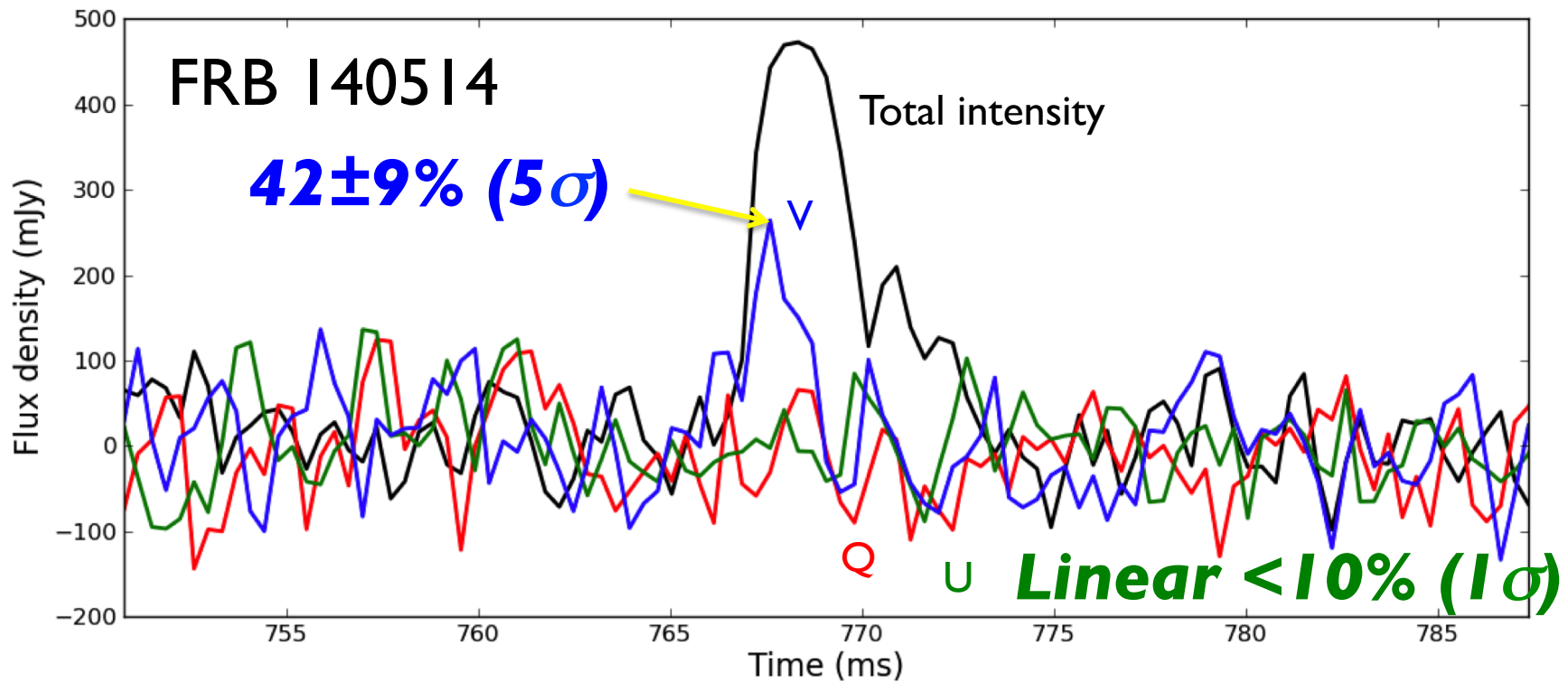


Rule out supernovae and long GRBs

Petroff+ 14

Circular Polarization

$21 \pm 7\% (3\sigma)$ circular polarization!!!



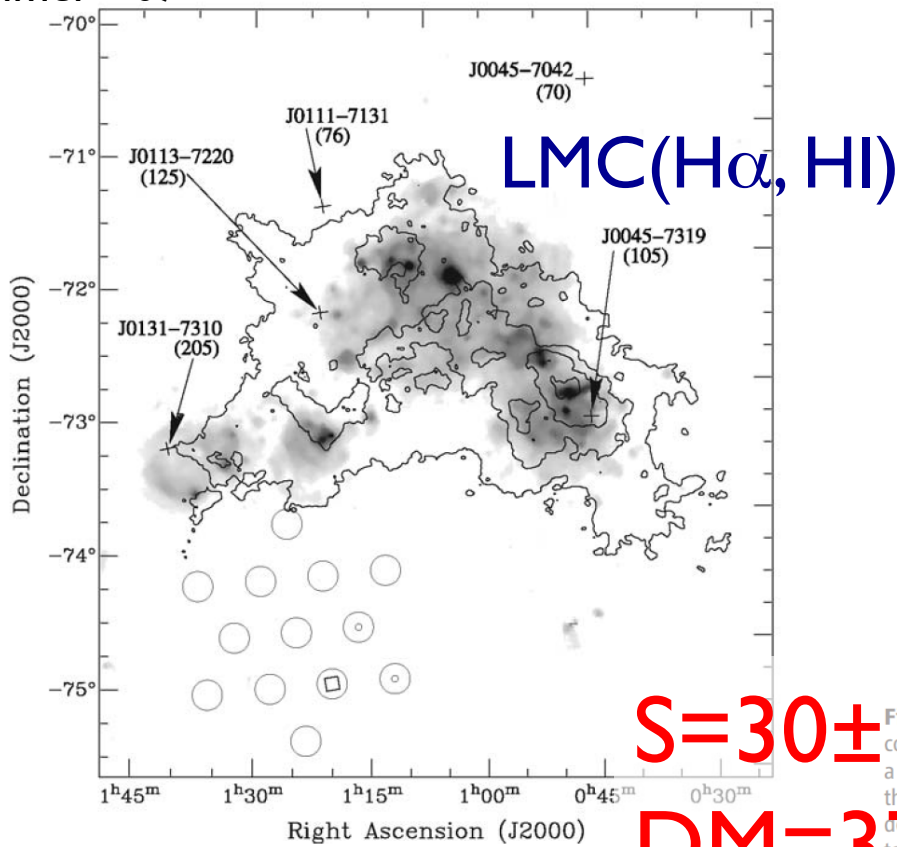
Intrinsic? (Cyclotron maser in flare stars 90-100%, AGN ~0.3%, Pulsar pulses)
Faraday conversion from linear to circular? (not likely)
Scintillation-induced CP?

Contents for FRB

- Possible origins
- ***Real cosmic signal?***
- Galactic?
- FRB cosmology

Lorimer Burst 010724

Lorimer+ 07



Right Ascension (J2000)

Declination (J2000)

Fig. 1. Multiwavelength image of the field surrounding the burst. The gray scale and contours respectively show H α and H I emission associated with the SMC (32, 33). Crosses mark the positions of the five known radio pulsars in the SMC and are annotated with their names and DMs in parentheses in units of cm $^{-3}$ pc. The open circles show the positions of each of the 13 beams in the survey pointing, with diameter equal to the half-power width. The strongest detection saturated the single-bit digitizers in the data acquisition system, indicating that its S/N >> 23. Its location is marked with a square at right ascension 01 $^{\text{h}}$ 18 $^{\text{m}}$ 06 $^{\text{s}}$ and declination -75 $^{\circ}$ 12' 19'' (J2000 coordinates). The other two detections (with S/Ns of 14 and 21) are marked with smaller circles. The saturation makes the true position difficult to localize accurately. The positional uncertainty is nominally $\pm 7'$ on the basis of the half-power width of the multibeam system. However, the true position is probably slightly (a few arcmin) northwest of this position, given the nondetection of the burst in the other beams.

$S = 30 \pm 10 \text{ Jy}$, $\delta t < 5 \text{ ms}$
 $DM = 375 \text{ cm}^{-3} \text{ pc} \Rightarrow z \sim 0.1 - 0.3$
 $W \propto f^{-4.8 \pm 0.4}$, $S \propto f^{-4}$
 $b = -41.8 \text{ deg}$

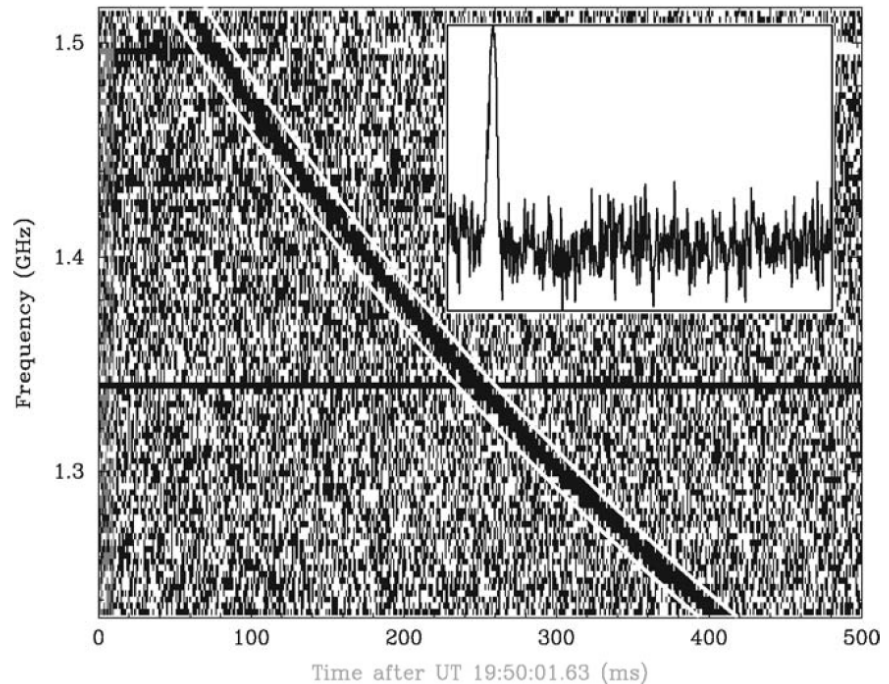
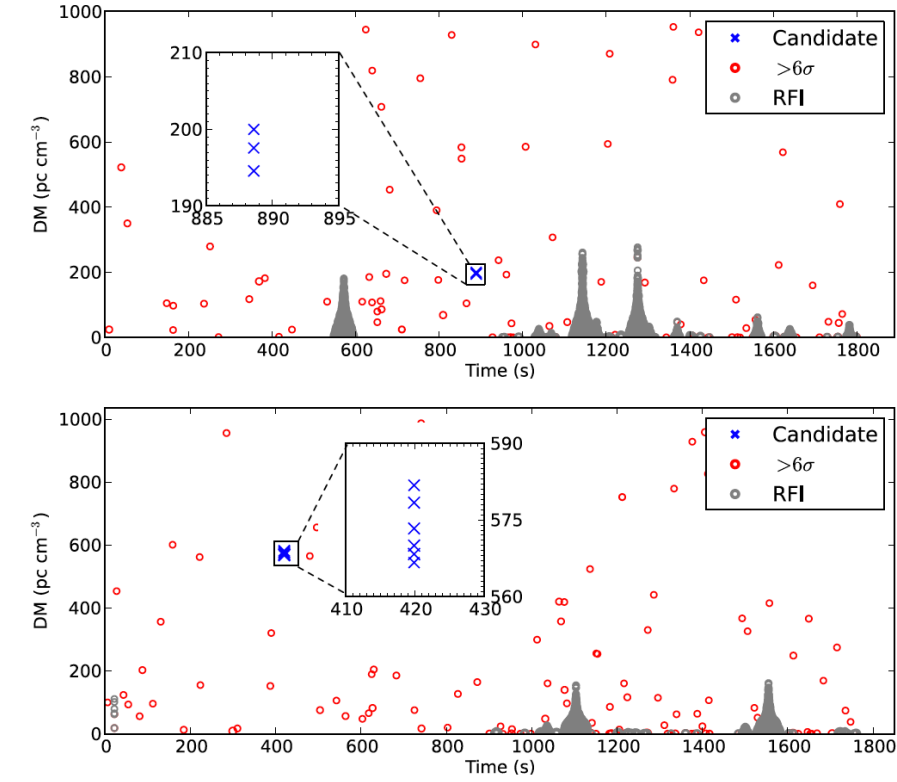
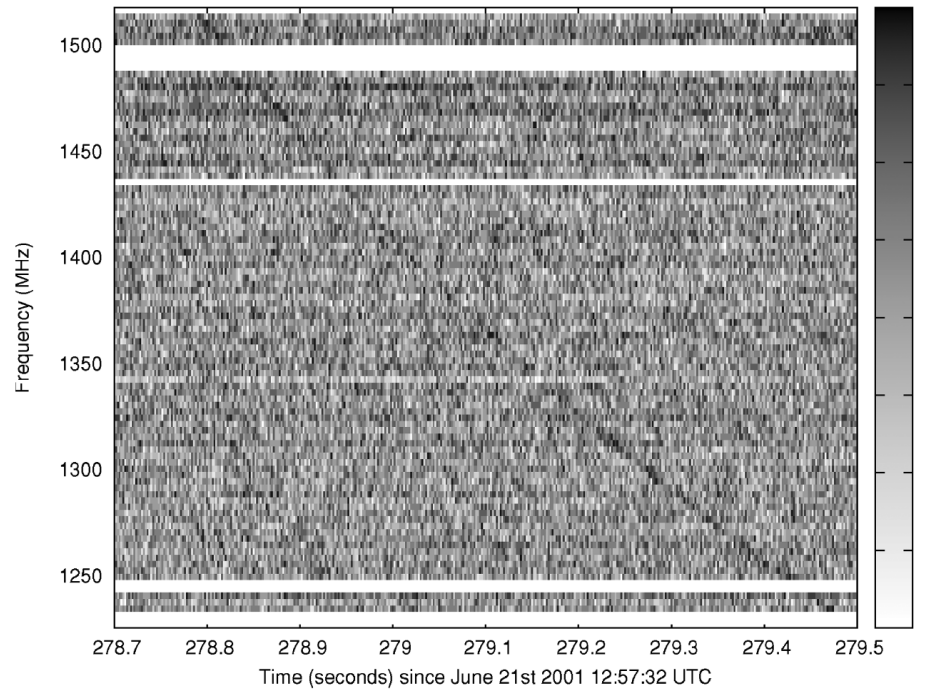


Fig. 2. Frequency evolution and integrated pulse shape of the radio burst. The survey data, corrected for 2 August 2011, are shown here as a two-dimensional “waterfall plot” of intensity as a function of radio frequency versus time. The dispersion is clearly seen as a quadratic sweep across the frequency band, with broadening toward lower frequencies. From a measurement of the pulse delay across the receiver band, we used standard pulsar timing techniques and determined the DM to be $375 \pm 1 \text{ cm}^{-3} \text{ pc}$. The two white lines separated by 5 ms that bound the pulse show the expected behavior for the cold-plasma dispersion law assuming a DM of $375 \text{ cm}^{-3} \text{ pc}$. The horizontal line at $\sim 1.34 \text{ GHz}$ is an artifact in the data caused by a malfunctioning frequency control; this plot is for one of the offset beams in which the digitizers were not saturated. By splitting the data into four frequency subbands, we have measured both the half-power pulse width and flux density spectrum over the observing bandwidth. Accounting for pulse broadening due to known instrumental effects, we determine a frequency scaling relationship for the observed width $W = 4.6 \text{ ms} (f/1.4 \text{ GHz})^{-4.8 \pm 0.4}$, where f is the observing frequency. A power-law fit to the mean flux densities obtained in each subband yields a spectral index of -4 ± 1 . The time axis on the inner figure also spans the range 0 to 500 ms.

Similar Events?



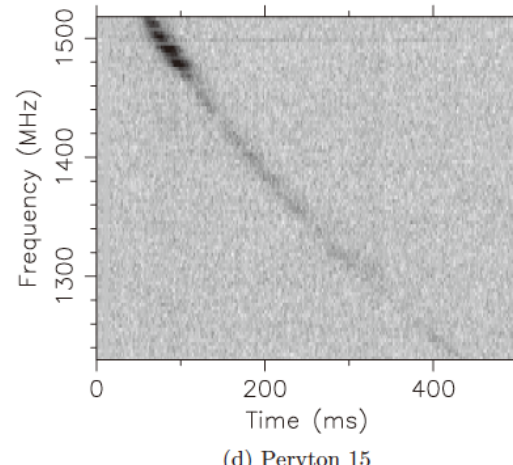
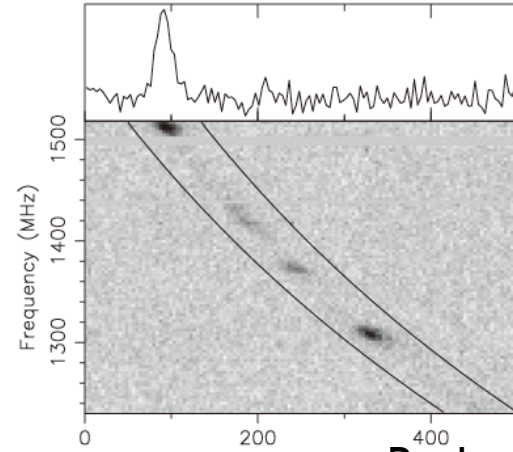
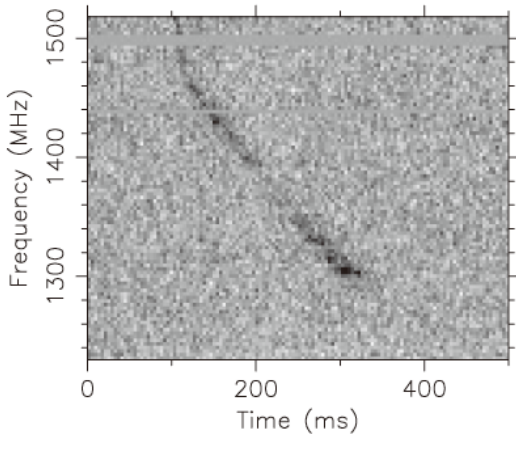
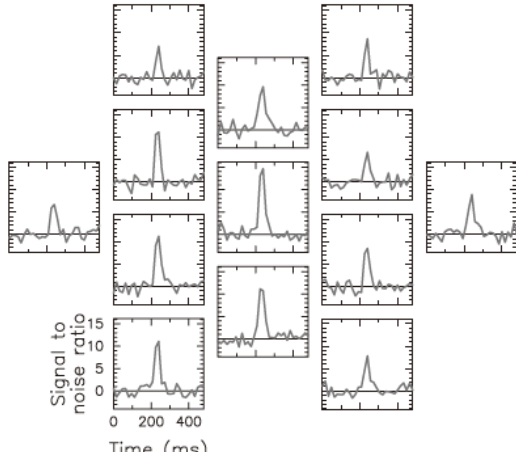
J1852-08 (Keane FRB 01062I)

DM=746 cm $^{-3}$ pc
400mJy, 7.8ms

Keane+ 12
Bannister+ 12
Rubio-Herrera+ 13

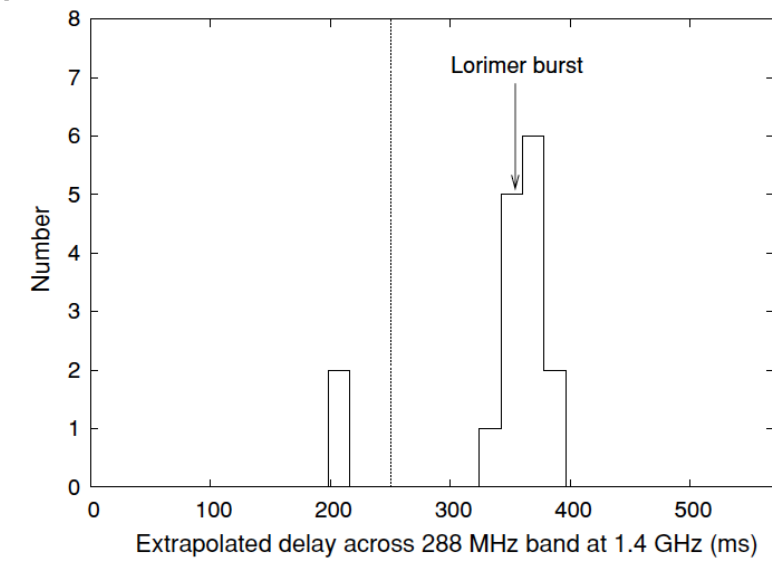
GRB100704A
GRB101011A

Terrestrial?



16 “Perytons” in all
13 telescope receivers

Burke-Spolaor+ 11; Kocz+ 12; Saint-Hilaire+ 12



Lightening, Aircraft, Electronics, ...?

Dispersion Measure

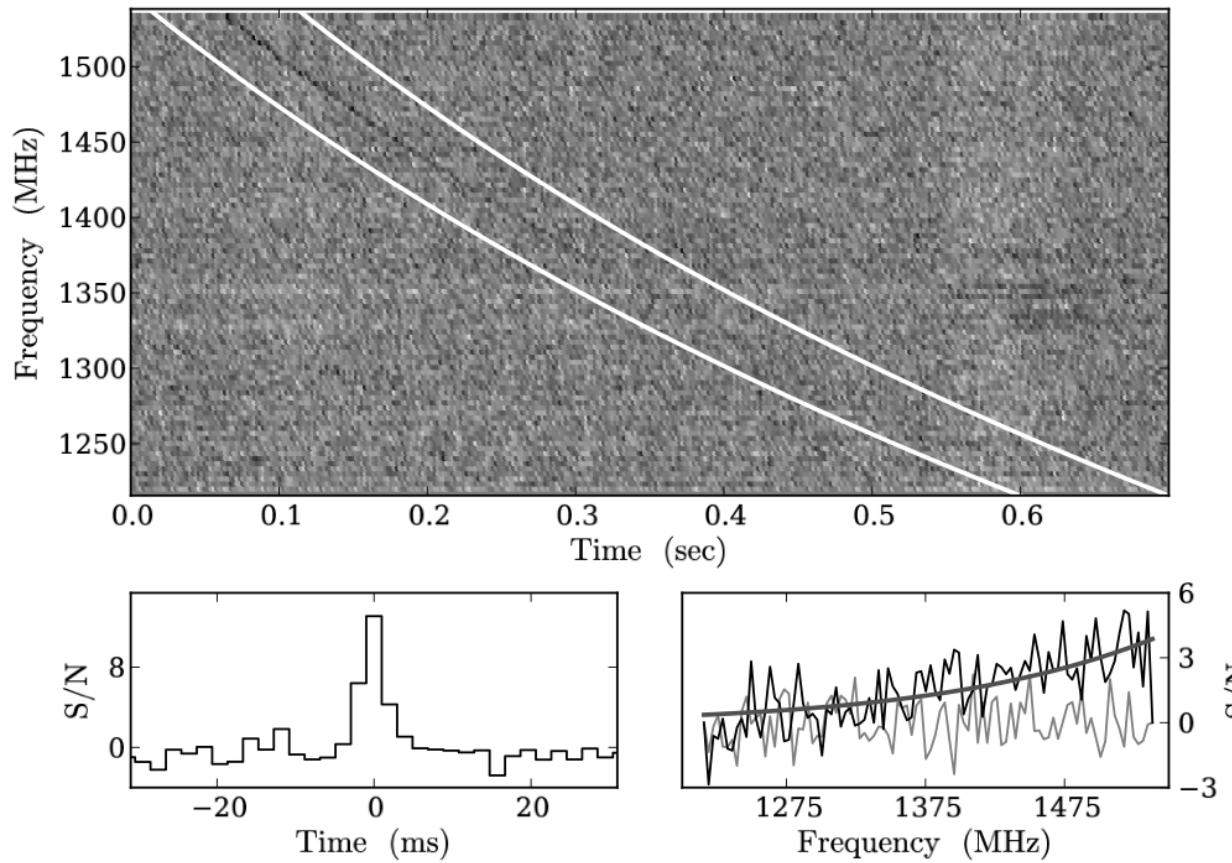


Not Terrestrial?

- Perytons have symmetric $W > 20$ msec which is larger than 4 FRBs by > 3
- FRB 110220 has an exponential tail
- Perytons have $DM \sim 375$ cm $^{-3}$ pc
 $< DM \sim 500-1000$ cm $^{-3}$ pc for 4 FRBs
- 4 FRBs are only detected in a single beam
- Perytons prefer daytime, and recur

Arecibo FRB (not Parkes)

A different telescope also detected FRB



FRB 121102
 Galactic anti-center
 $b = -0.2 \pm 0.2^\circ$
 $DM = 557.4 \pm 3 \text{ pc/cm}^3$
 delay $\beta = -2.01 \pm 0.03$
 Width $3 \pm 0.5 \text{ ms}$
 No scattering signal
 Spectral $\alpha \sim 10$
 (sidelobe effect?)
Rate is consistent

Still in Chaos

- No FRB at intermediate Galactic latitude ($-15^\circ < b < 15^\circ$) by Parkes HTRU Petroff+ 14
 - Non-uniform sky distribution (99%CL)
 - Disfavor a Galactic origin Burke-Spoliar & Bannister 14
- FRB 011025 in Parkes archives ($5^\circ < |b| < 30^\circ$)
 - Rate $\sim 2 \times 10^3 / \text{sky/day} \sim (1/5) \times (\text{Thornton+ 13})$
- FRB 131104 toward Carina dwarf Sph Ravi+ 14
- Keane FRB 010621 is Galactic? Bannister & Madsen 14
- VLA & LOFAR detect no FRB Law+ 14; Coenen+ 14

FRB 011025

- Parkes archival data ($5^\circ < |b| < 30^\circ$)
- Rate $\sim 2 \times 10^3 / \text{sky/day} \sim 5 \times$ (Thornton+ 13)

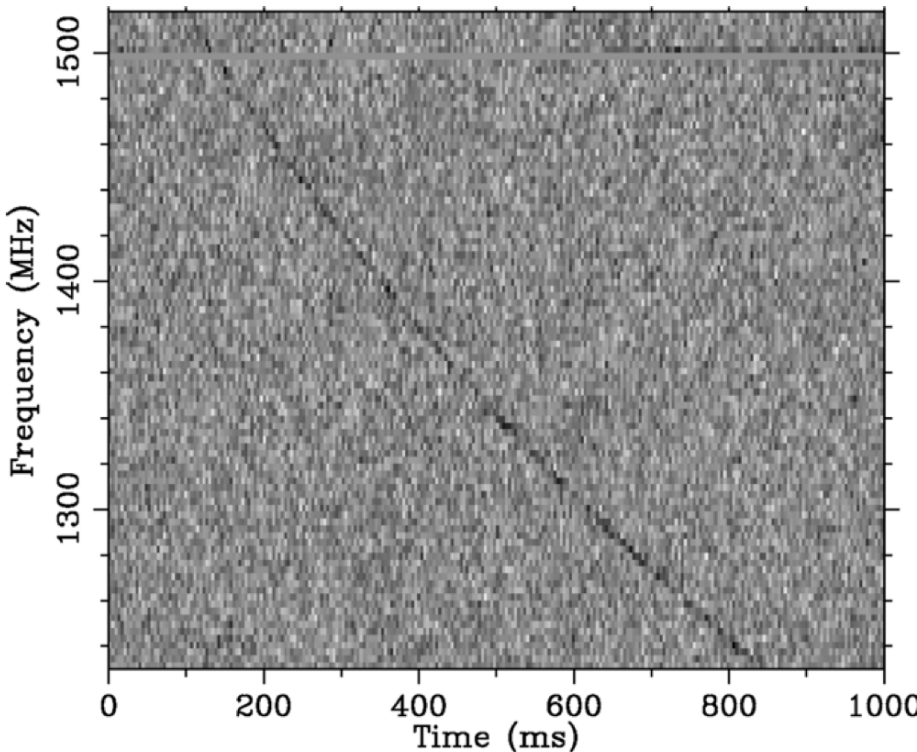
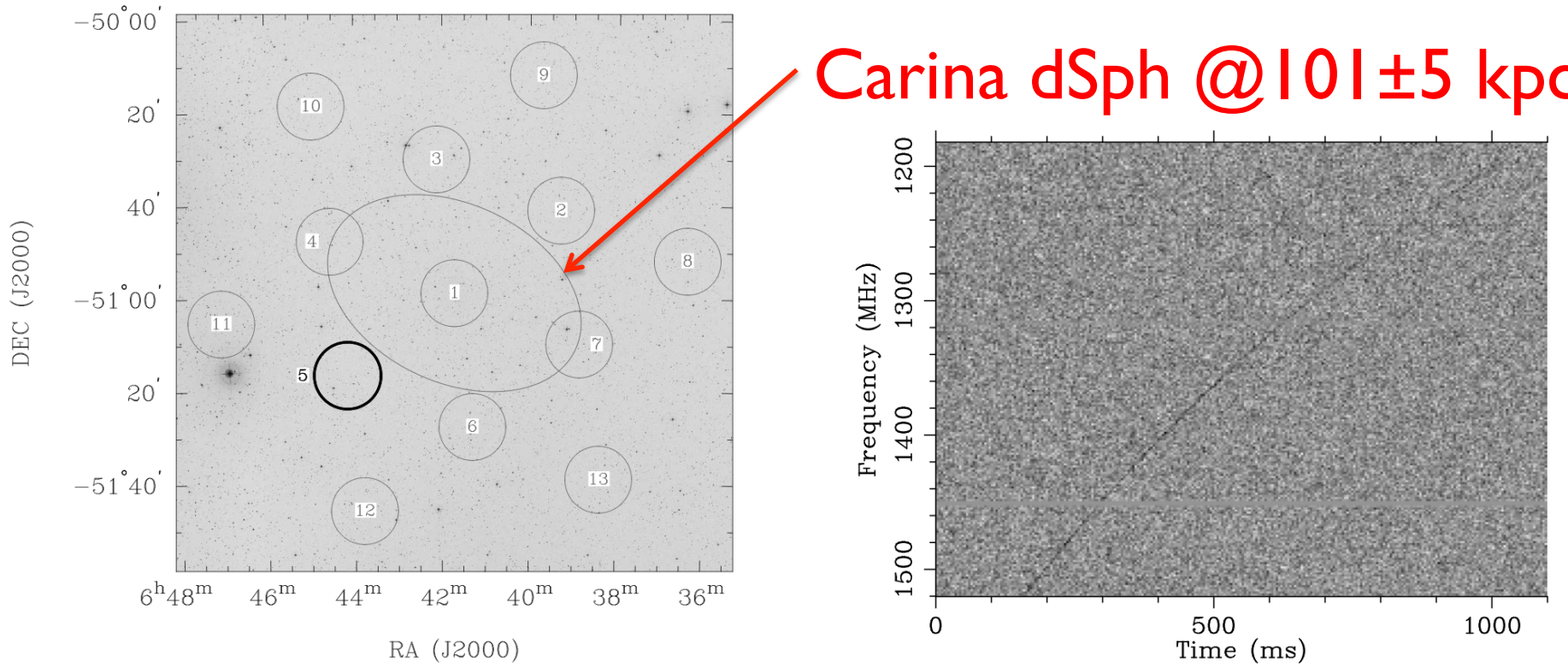


Table 1
Properties of FRB011025

| | |
|---|-------------------------------------|
| Pointing R.A., decl. (J2000) | 19:06:53.0, $-40:37:14.4$ |
| Pointing gl, gb | 356.641, -20.021 |
| $t_{1516.5}$ (UTC Y-M-D, h:m:s) | 2001 Jan 25, 00:29:13.23 ± 0.02 |
| Delay index ($dt \propto f^a$) | -2.00 ± 0.01 |
| DM | $790 \pm 3 \text{ pc cm}^{-3}$ |
| DM _E | 680 pc cm^{-3} |
| w_{50} | $9.4 \pm 0.2 \text{ ms}$ |
| Scattering index ($w_{50} \propto f^\mu$) | -4.2 ± 1.2 |
| Peak, min | 300 mJy |
| Fluence | $<2.82 \times 10^{-3} \text{ Jy s}$ |

Note. Parameter $t_{1516.5}$ refers to the arrival time of the burst at 1516.5 MHz.

FRB 131104



Parkes

Table 1
Details of time-frequency fits (all uncertainties are the 95% confidence intervals).

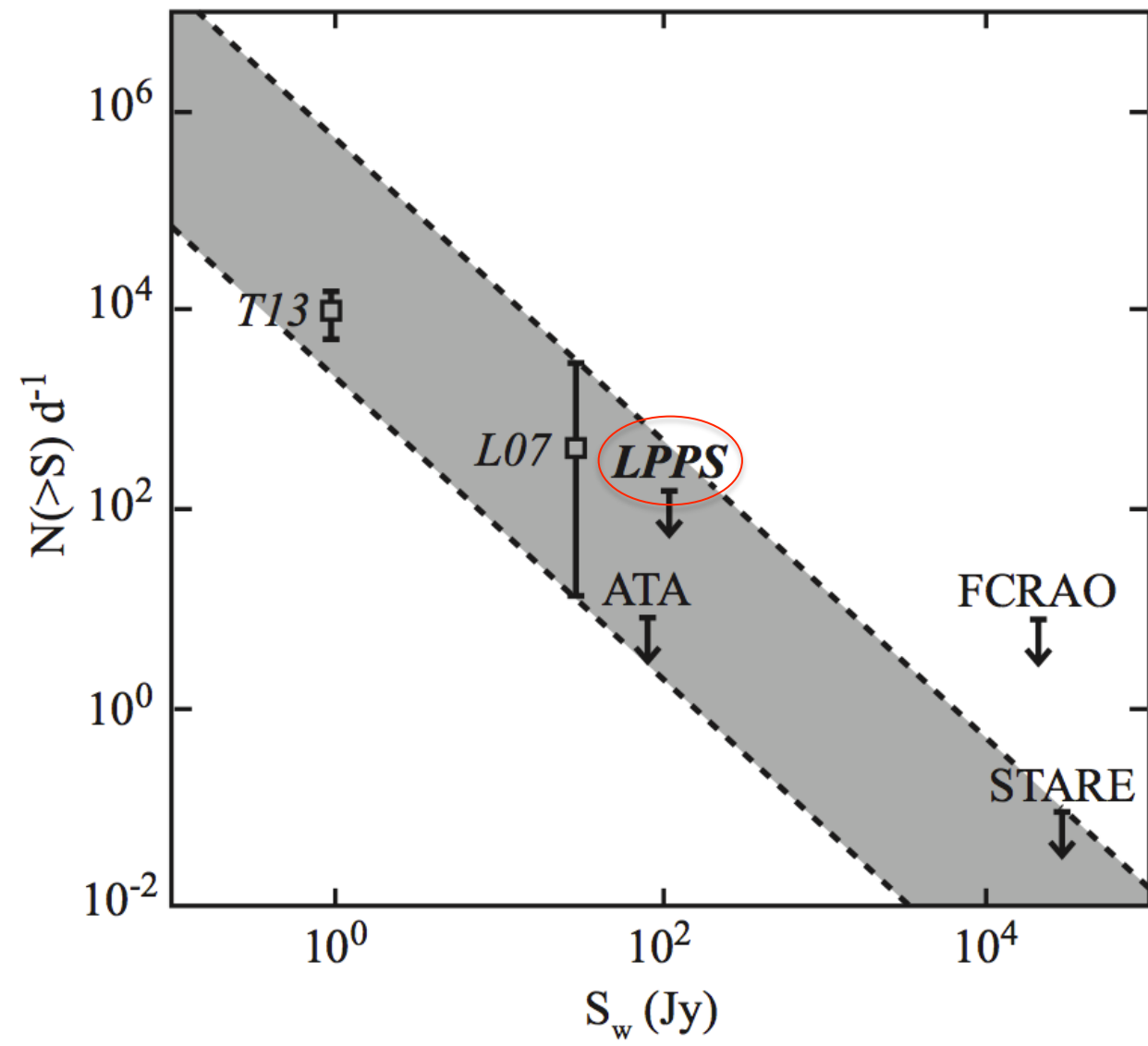
Ravi+ 14

| Model | c_{1232} (Jy ms) | c_{1332} (Jy ms) | c_{1432} (Jy ms) | c_{1532} (Jy ms) | DM ($\text{cm}^{-3} \text{ pc}$) | τ_s (ms) | α | t_0 (s) | ΔBIC |
|-------|------------------------|------------------------|------------------------|---------------------|------------------------------------|---------------------|---------------------|---|--------------------|
| 0 | $0.65^{+0.07}_{-0.07}$ | $0.78^{+0.04}_{-0.08}$ | $1.16^{+0.09}_{-0.09}$ | $1.7^{+0.1}_{-0.3}$ | $779.1^{+0.1}_{-0.2}$ | — | — | $1.03435^{+7 \times 10^{-5}}_{-8 \times 10^{-5}}$ | 0 |
| 1 | $0.78^{+0.07}_{-0.07}$ | $0.78^{+0.08}_{-0.04}$ | $0.99^{+0.04}_{-0.09}$ | $1.4^{+0.1}_{-0.1}$ | $779.0^{+0.2}_{-0.2}$ | $1.1^{+0.1}_{-0.1}$ | — | $1.0338^{+1 \times 10^{-4}}_{-1 \times 10^{-4}}$ | -299 |
| 2 | $0.9^{+0.1}_{-0.1}$ | $0.8^{+0.2}_{-0.2}$ | $0.95^{+0.04}_{-0.09}$ | $1.2^{+0.1}_{-0.1}$ | $778.5^{+0.2}_{-0.3}$ | $2.0^{+0.8}_{-0.5}$ | $4.4^{+1.6}_{-1.8}$ | $1.0340^{+1 \times 10^{-4}}_{-1 \times 10^{-4}}$ | -306 |

2nd FRB with exponential tail (after FRB110220)

$W_{\text{intrinsic}} < 0.64 \text{ ms}$

LOFAR



$\sim 142 \text{ MHz}$
 $R < 150 / \text{day/sky}$
for $S > 107 \text{ Jy}$

VLA Interferometer

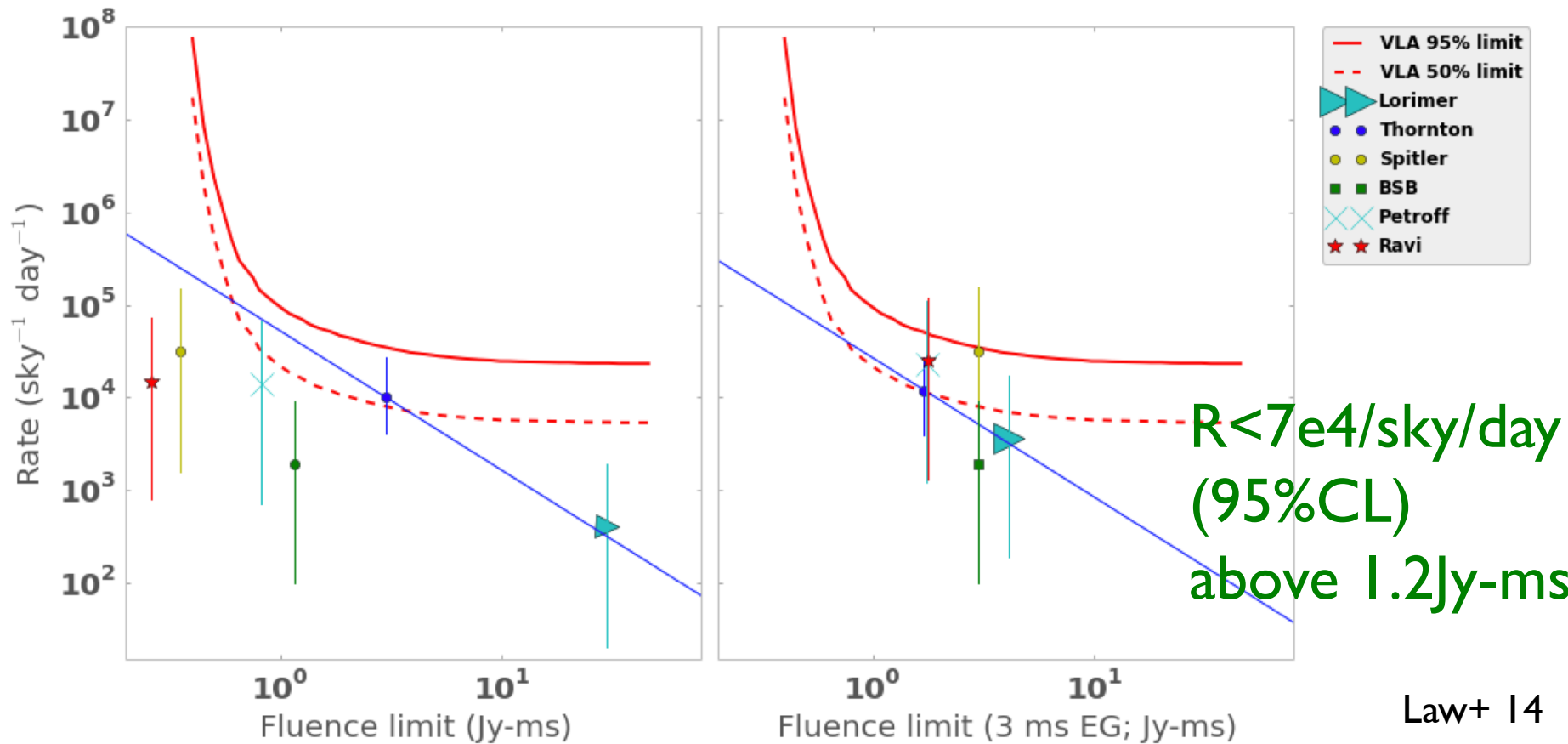
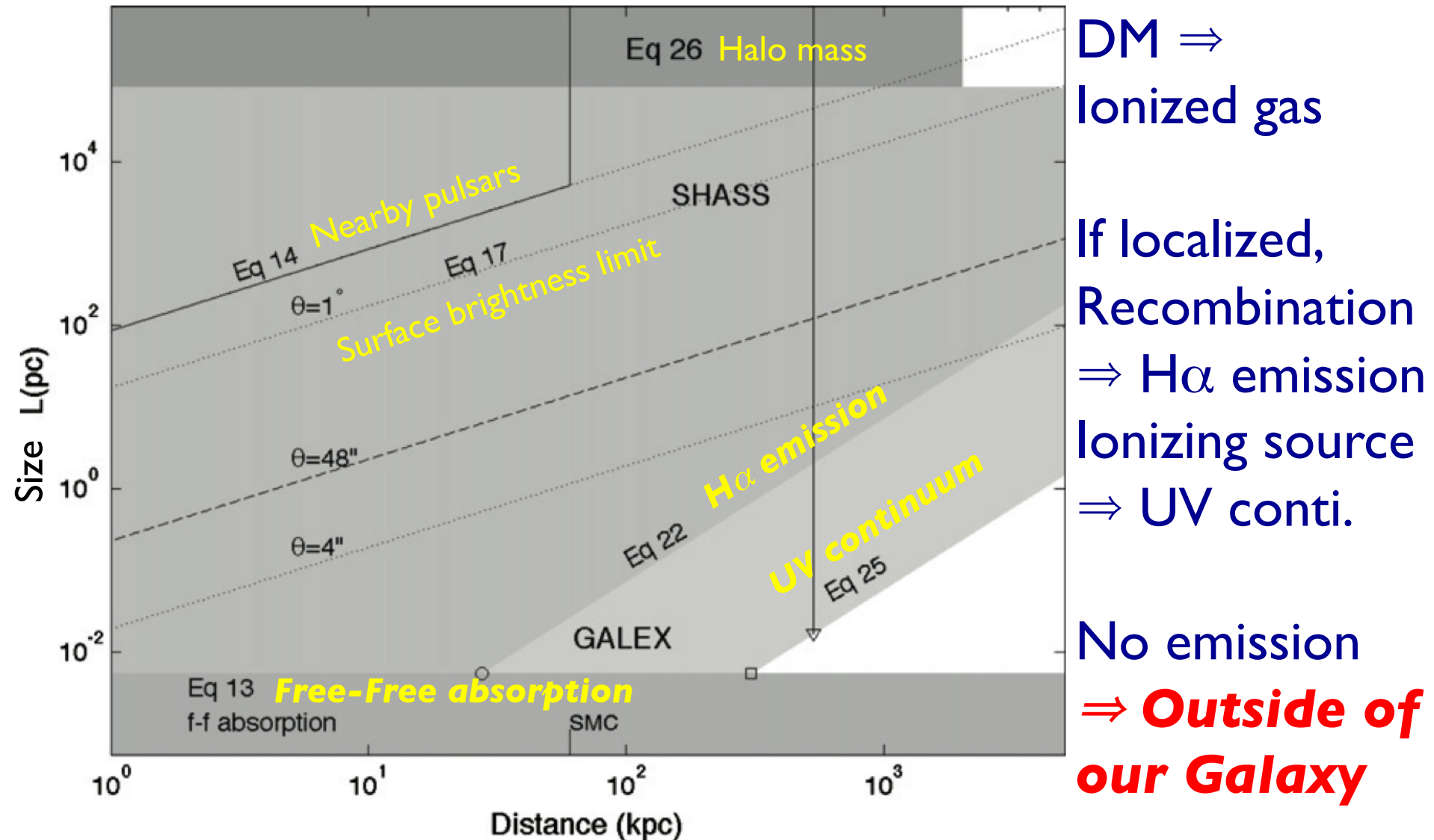


FIG. 9.— *Left:* FRB rates and VLA rate limit as a function of limiting fluence as quoted in (or inferred from) publications (Lorimer et al. 2007; Thornton et al. 2013; Spitler et al. 2014; Burke-Spolaor & Bannister 2014; Ravi et al. 2014; Petroff et al. 2014a). The blue line shows an extrapolation of the rate of Thornton et al. (2013), assuming a Euclidean distribution ($-3/2$ powerlaw slope in this space) from a fluence limit of 3 Jy-ms. The VLA 50% and 95% upper limits are shown with a dashed and solid line, respectively. The VLA rate limit is not complete at very high fluences (far right) as described in §6.4. The fluence limit of Lorimer et al. (2007) is a lower limit recently calculated in a reanalysis (Keane & Petroff 2014). *Right:* Same as the left panel, but for recalculated flux limits. All flux limits assume a 3 ms pulse width and that FRBs originate outside the Galaxy with DM of 779 pc cm^{-3} .

Contents for FRB

- Possible origins
- Real cosmic signal?
- ***Galactic?***
- FRB cosmology

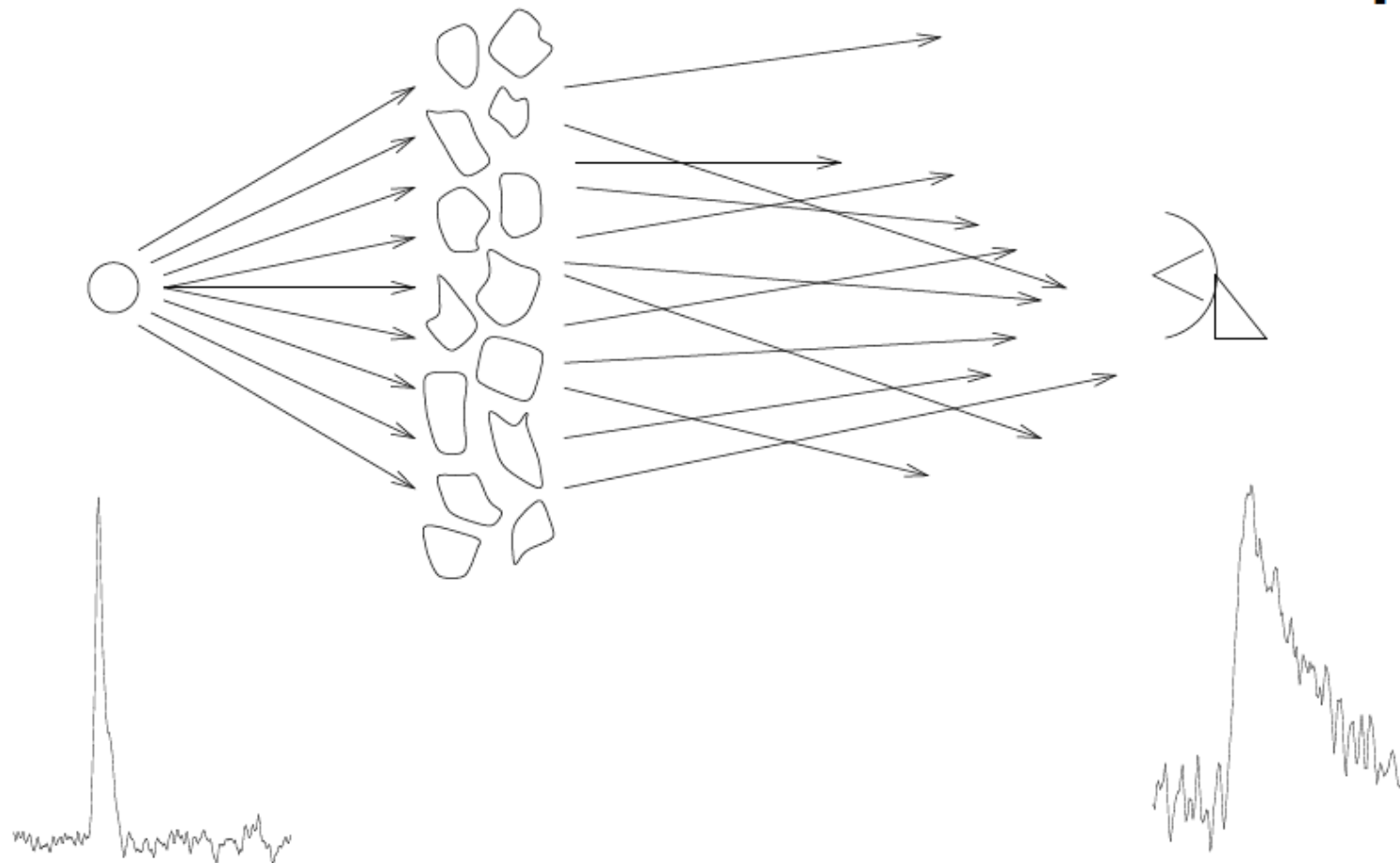
Distance to DM Nebula



Pulse Scattering

Pulsar

Telescope

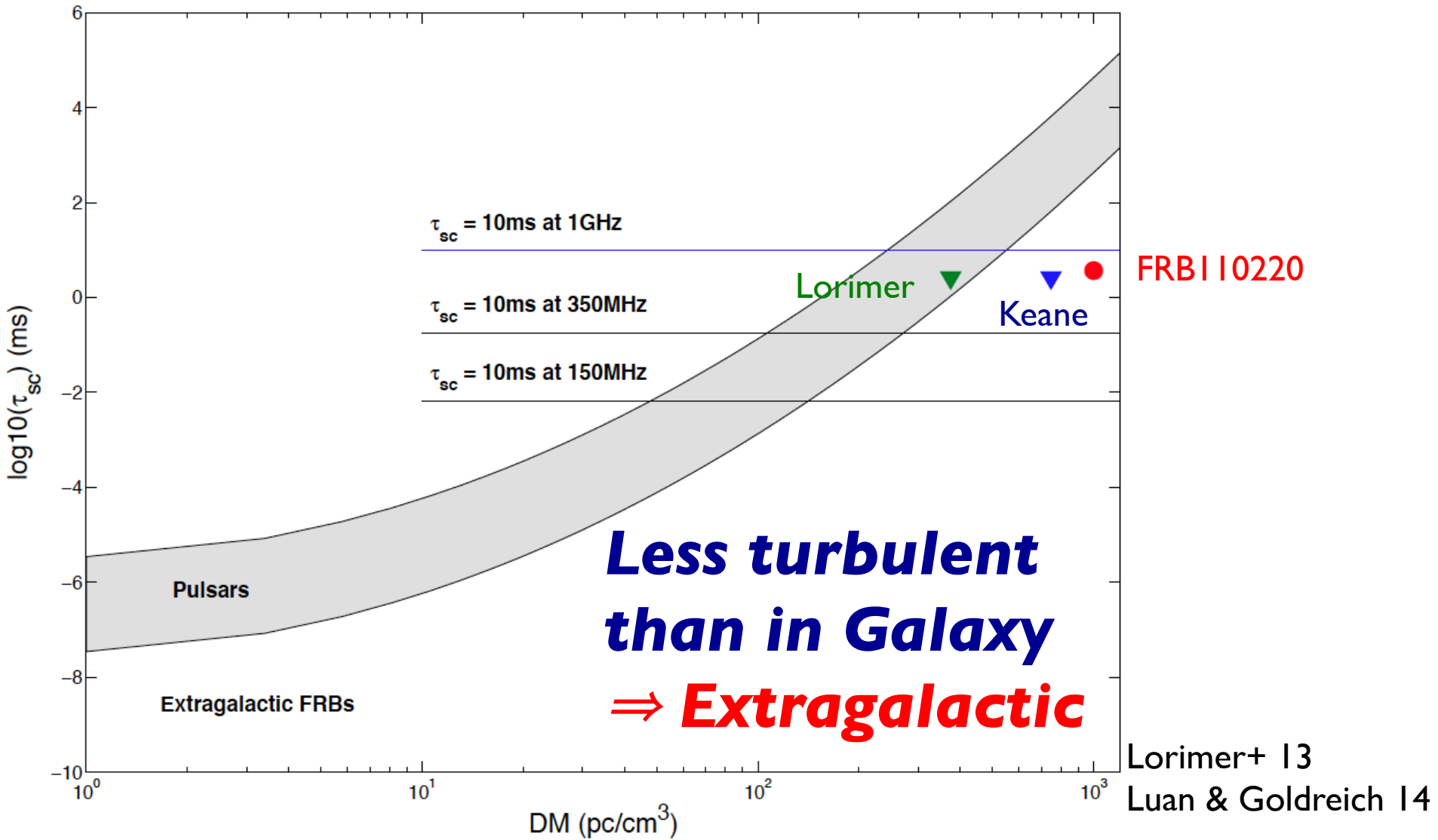


Emitted Pulse

Lorimer 08

Detected Pulse

Less Scattering



Host galaxy

- Most likely, scattering occurs in host galaxies
- Also in the turbulent region
- Center of host galaxy? $DM > 700 \text{ cm}^{-3} \text{ pc}$
 - $W \propto D_{\text{bs}} D_{\text{os}} / (D_{\text{bs}} + D_{\text{os}})^2$ Kulkarni+ 14; Luan & Goldreich 14
 - $D_{\text{bs}} \ll D_{\text{os}}$ \Rightarrow the pulse width is small as observed
- Elliptical host: low DM
- Spiral host: $DM > 700 \text{ cm}^{-3} \text{ pc}$ if $i > 87\text{deg}$ (5%)
- Intervening galaxies: $P < 5\%$

Contents for FRB

- Possible origins
- Real cosmic signal?
- Galactic?
- *FRB cosmology*

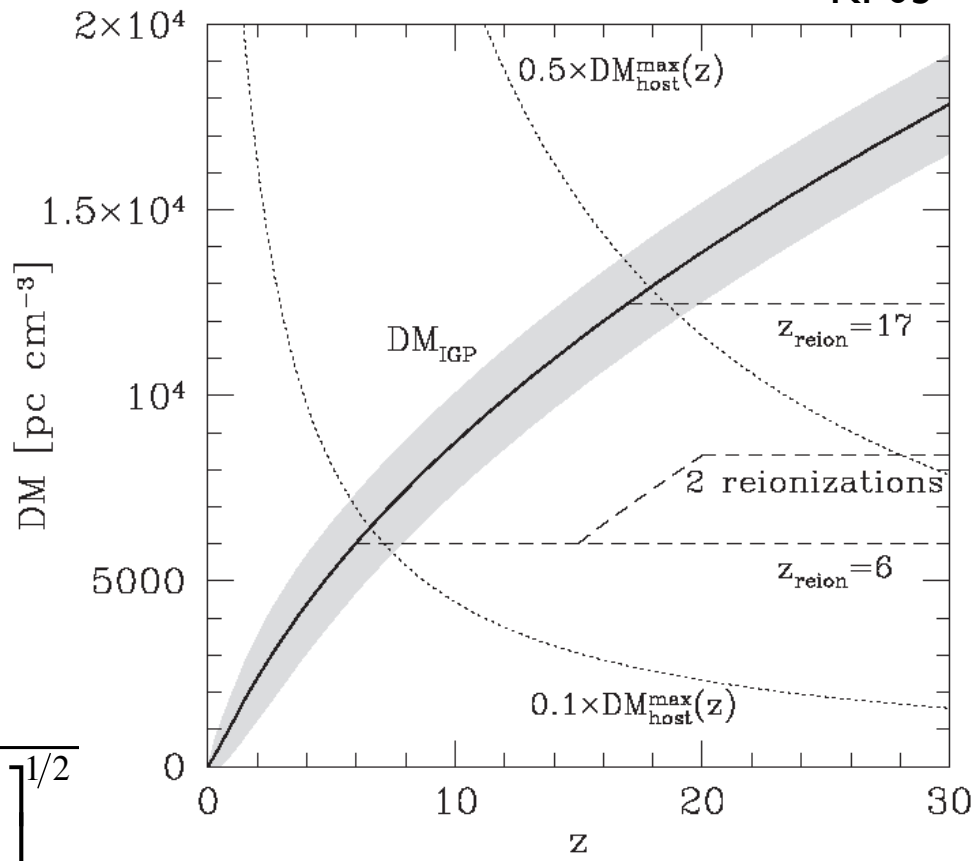
FRB Cosmology

KI 03

- Reionization
- Missing baryon
- Dark energy, cosmological parameters

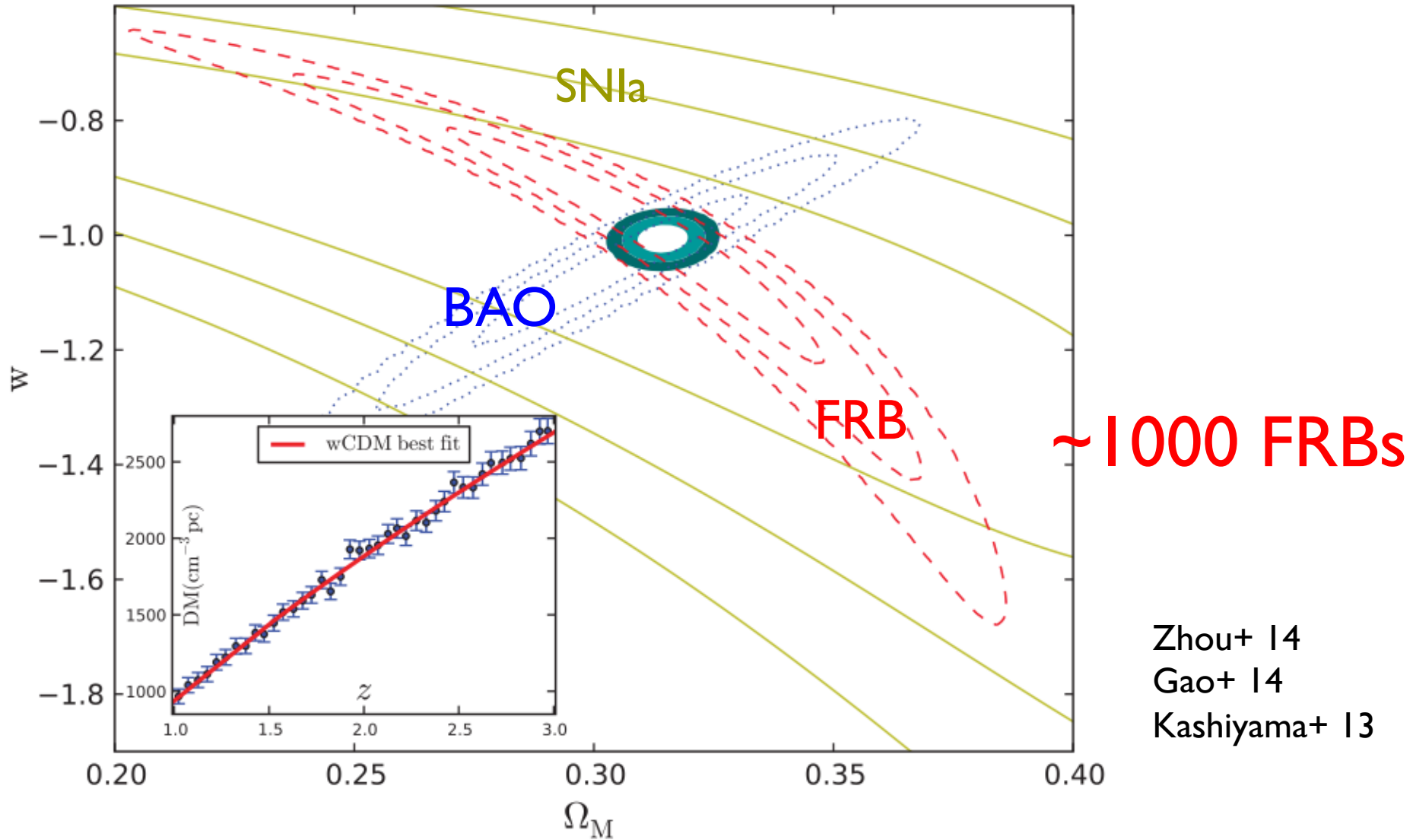
$$\text{DM}_{\text{IGP}} = \frac{3cH_0\Omega_b}{8\pi G m_p} \int_0^z \frac{(1+z)dz}{\left[\Omega_m(1+z)^3 + \Omega_\Lambda\right]^{1/2}}$$

$$d_L = \frac{c(1+z)}{H_0} \int_0^z \frac{dz}{\left[\Omega_m(1+z)^3 + \Omega_\Lambda\right]^{1/2}}$$

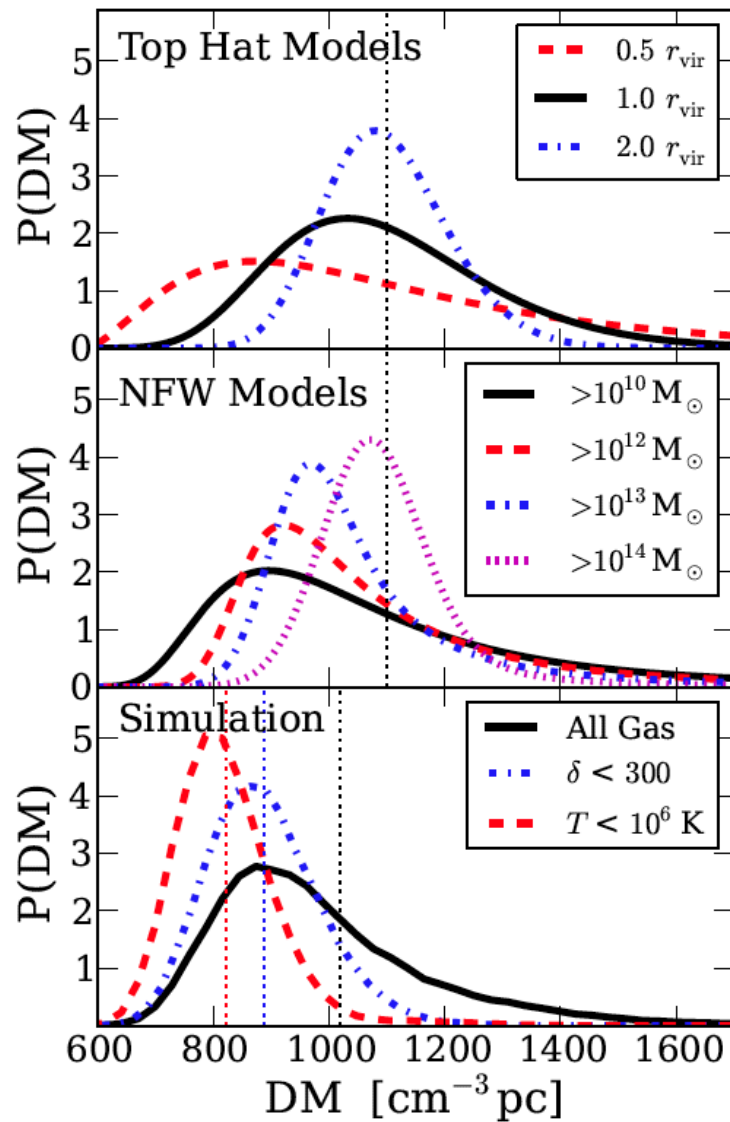


**Fast radio bursts
as cosmological tools
New frontier?**

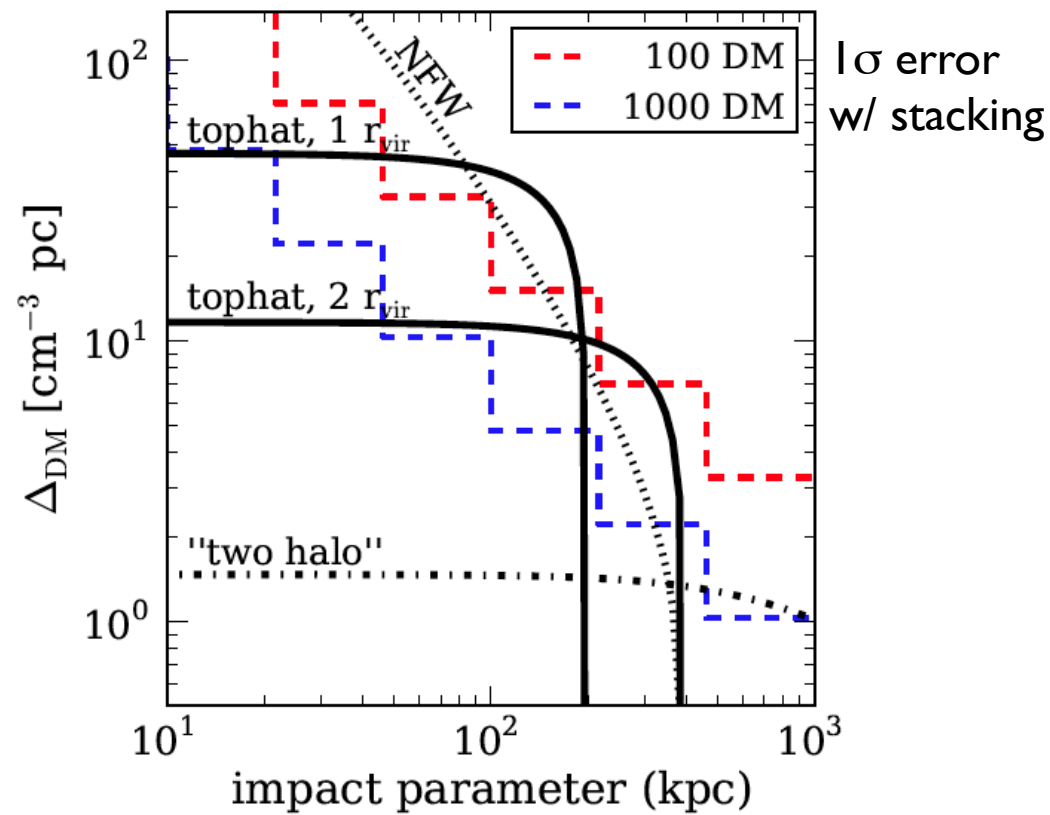
Dark Energy



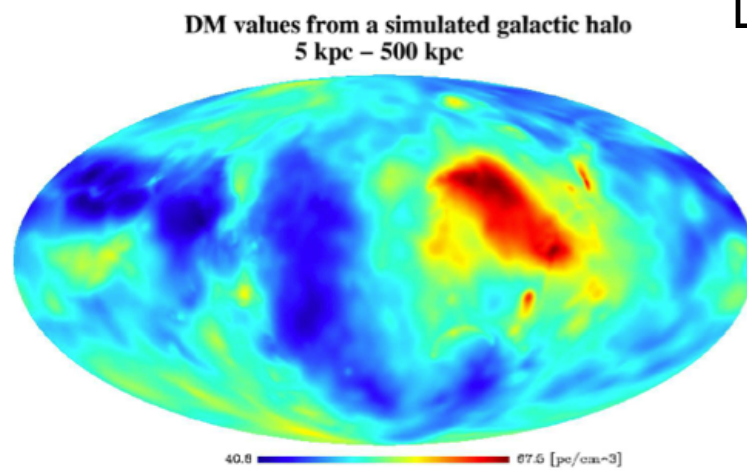
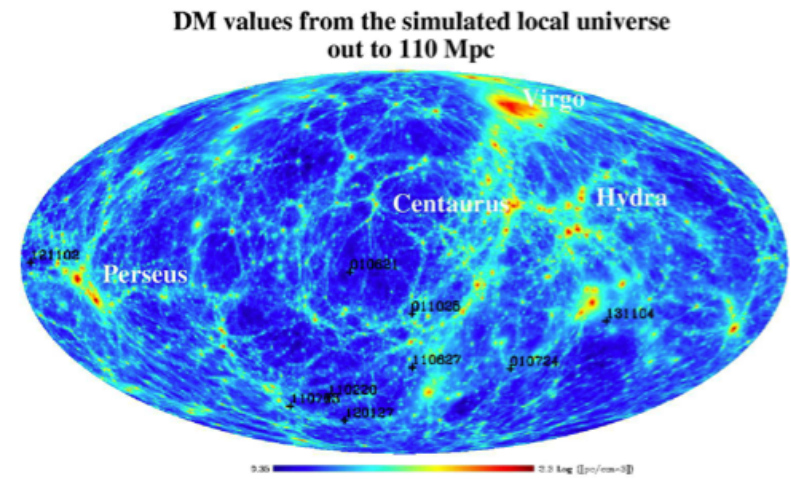
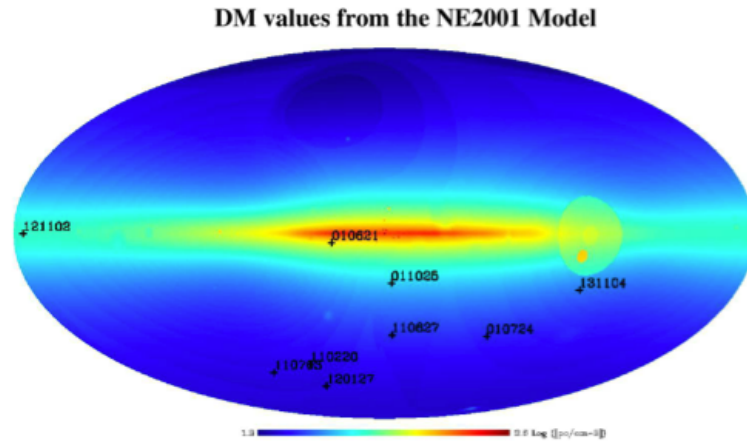
Locating Missing Baryon



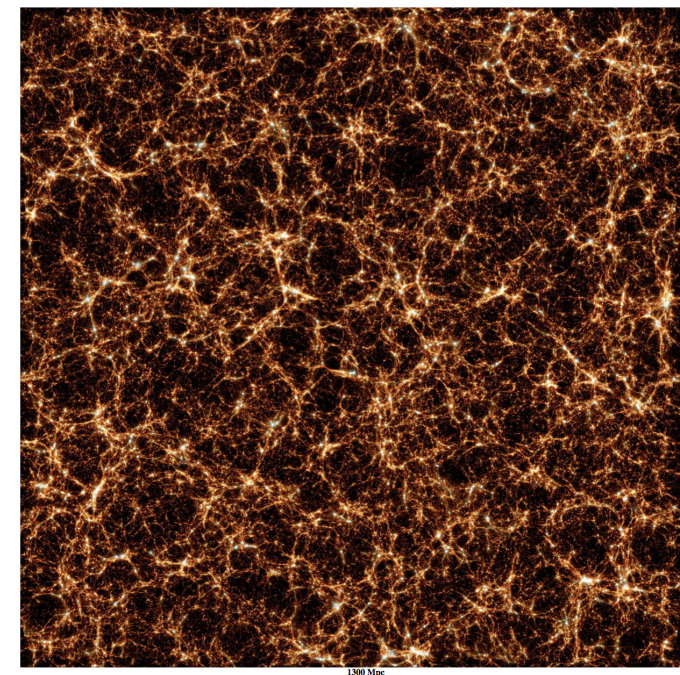
Half of baryon is missing
DM is sensitive its distribution



Cosmological Simulation

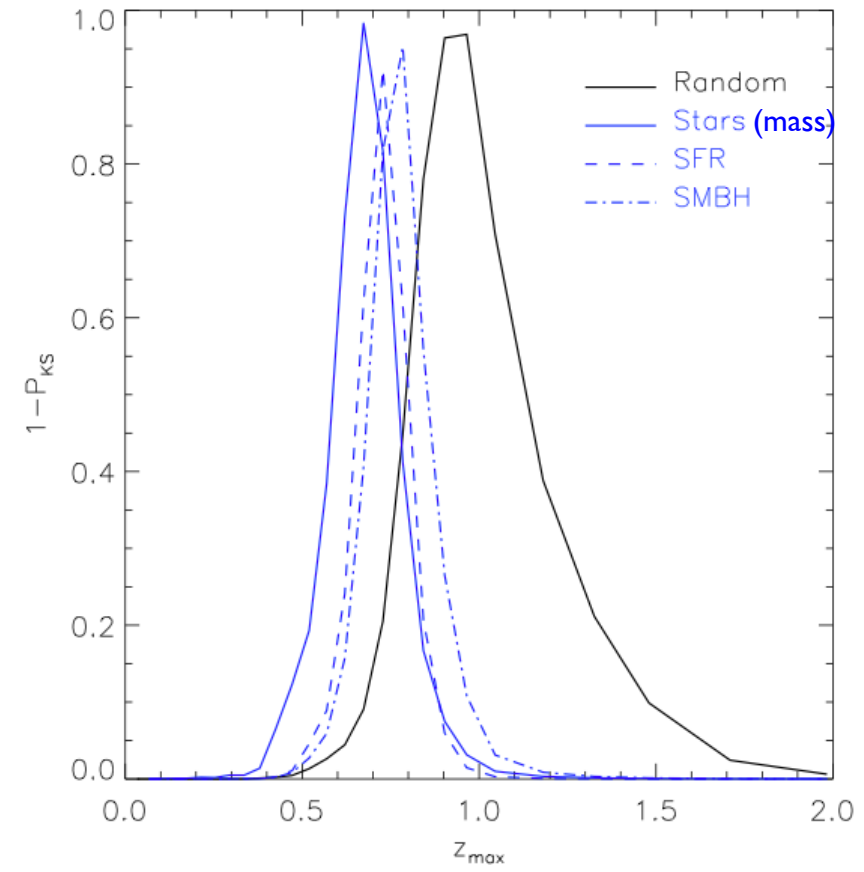
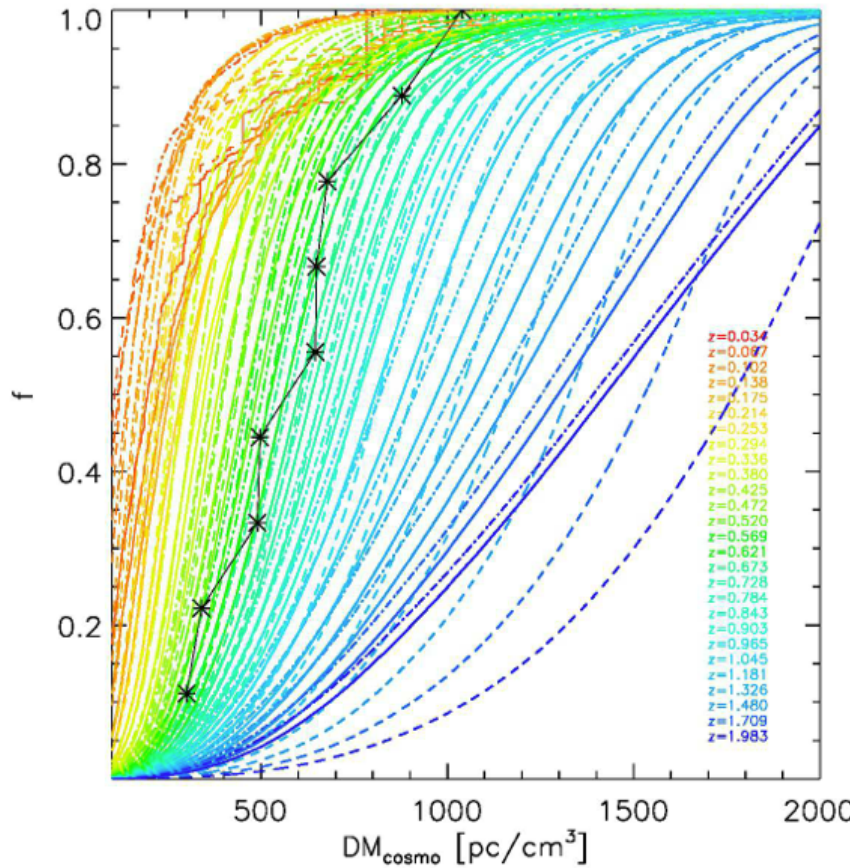


Dolag+14



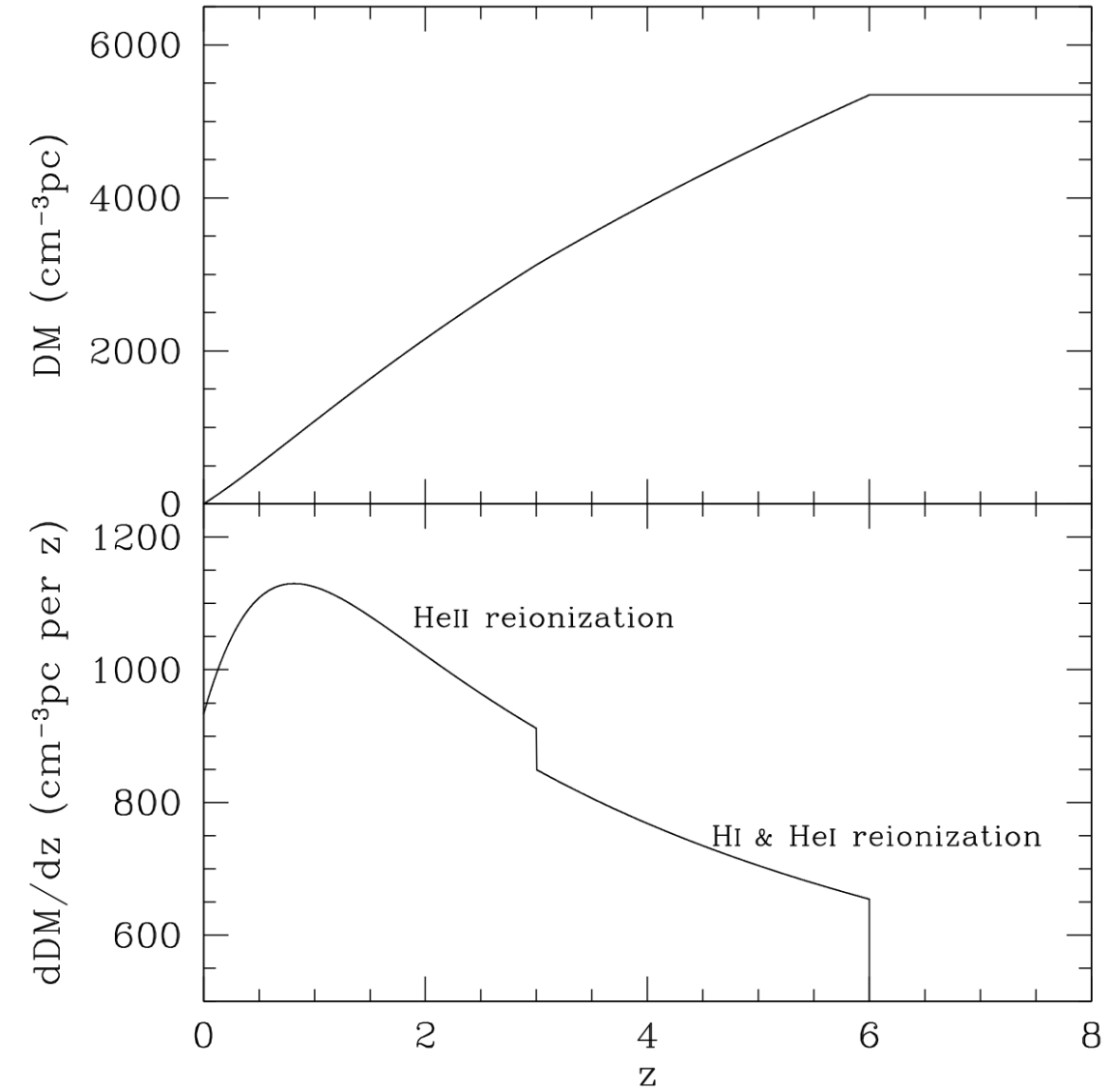
$\text{DM}_{\text{halo}} \sim 30 \text{ pc/cc} \sim \text{DM}_{\text{Gal}}$
Distribution of DM_{cosmo}

DM Distribution



Distribution is consistent with extragalactic origin
Depend on FRB location

He Reionization



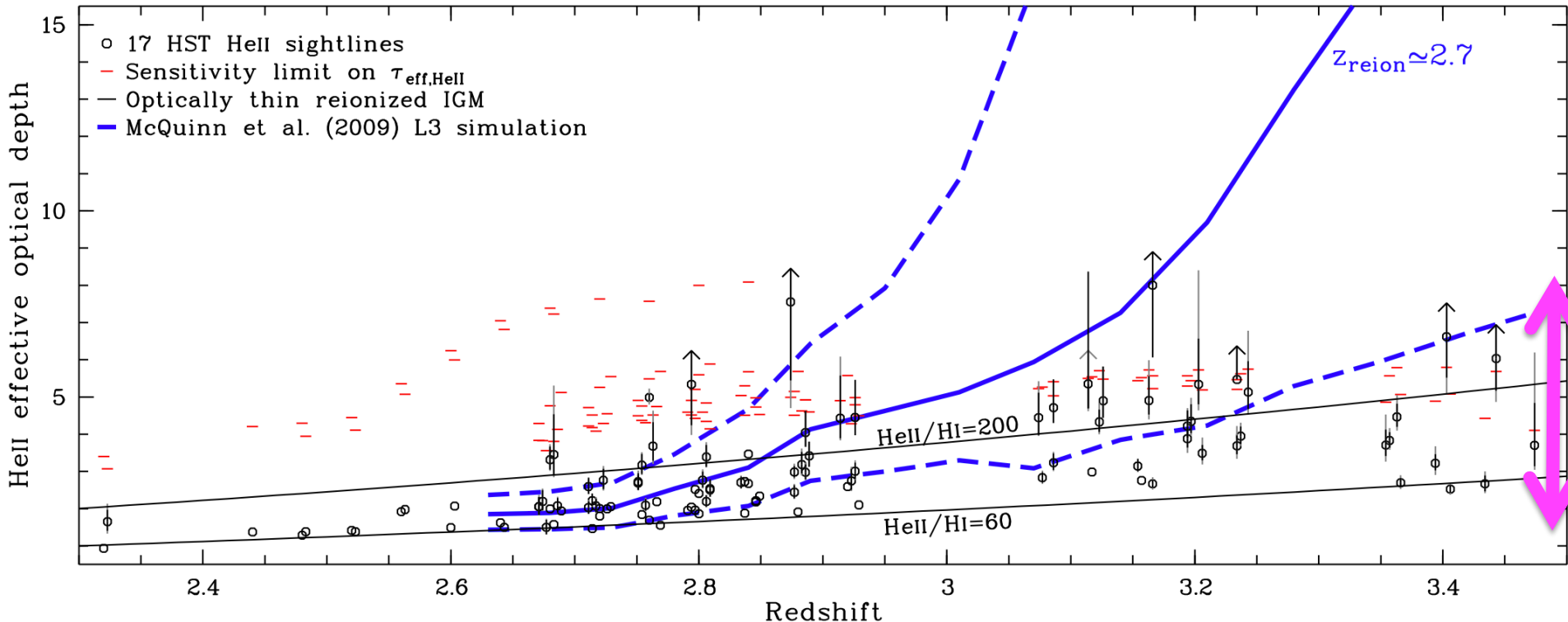
H I: 13.6 eV
He I: 24.6 eV
He II: 54.4 eV
He II reionized @ $z < 3$

Probing AGN (X-ray)

Zheng+ 14
Deng & Zhang 14
Zhou+ 14

Extended He Reionization

He II reionization is still unclear



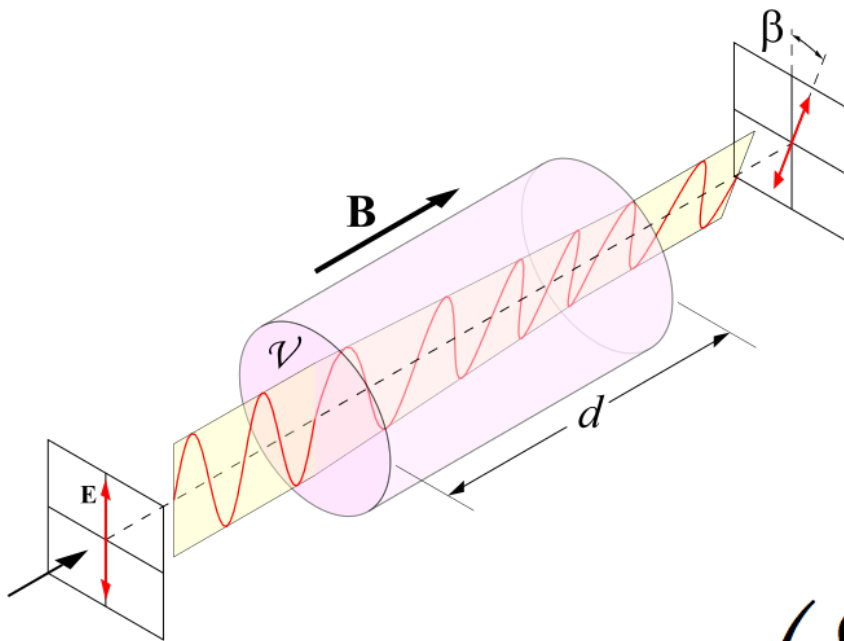
17 quasars, HST

A strong sightline-to-sightline variance

Average $x_{\text{HeII}} \sim 0.003$ @ $z \sim 0.34 \Rightarrow$ ionized at early times?

Worseck+ 14

Magnetic Field

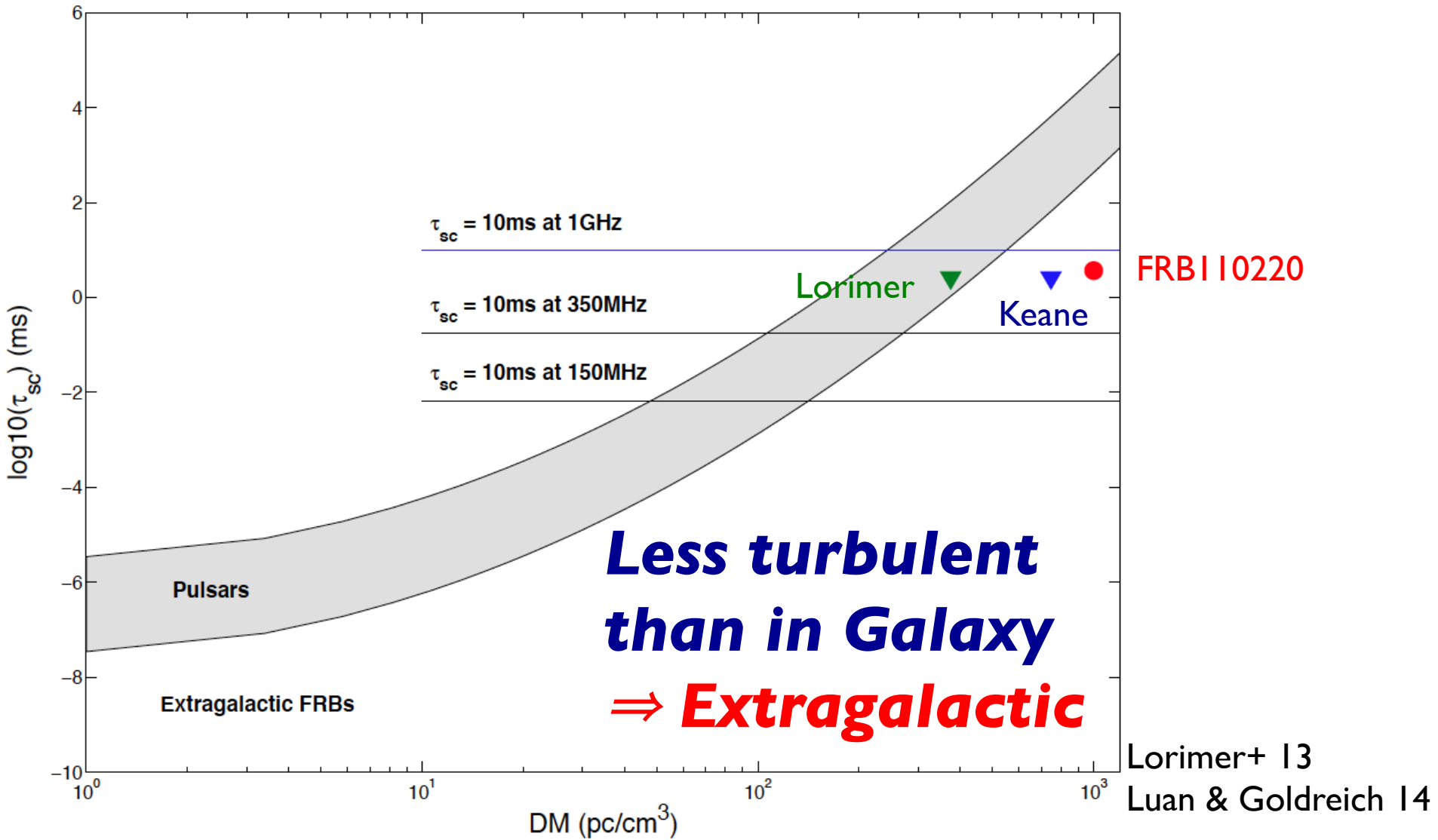


Faraday rotation \Rightarrow
Still unknown IGM B

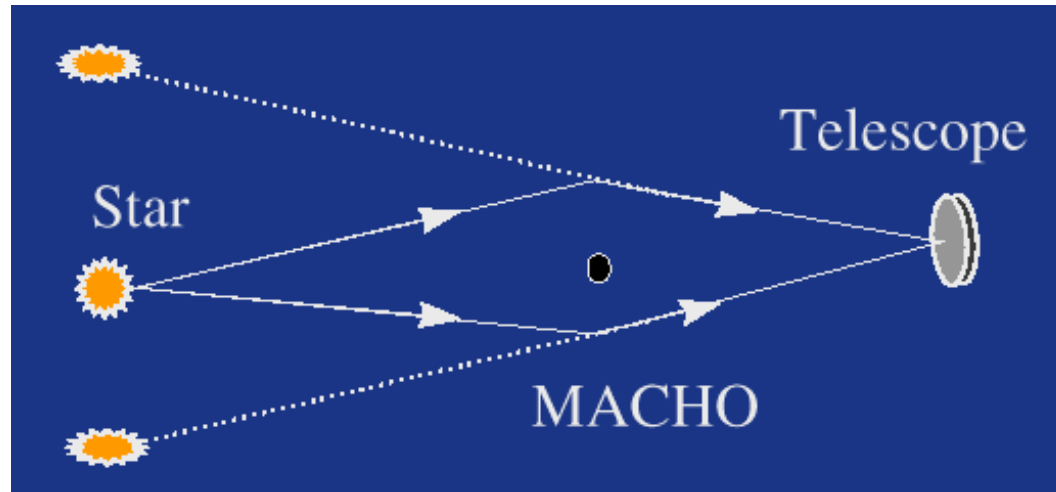
$$\text{RM} = 8.61 \text{ rad m}^{-2} \left(\frac{\Omega_b h^2}{0.022} \right) \left(\frac{h}{0.7} \right)^{-1} \left(\frac{B_0}{10 \text{ nG}} \right)$$

$$\times \int_0^z \frac{f_e(z) b_{\parallel}(z) dz}{\sqrt{\Omega_m(1+z)^3 + \Omega_{\Lambda}}} . \quad b_{\parallel}(z) \equiv B_{\parallel}(z)/B_0$$

Turbulence



Femto-Lensing



$$\Delta t_l = 41(1 + z_l)(M/1 M_\odot) \mu\text{s.}$$

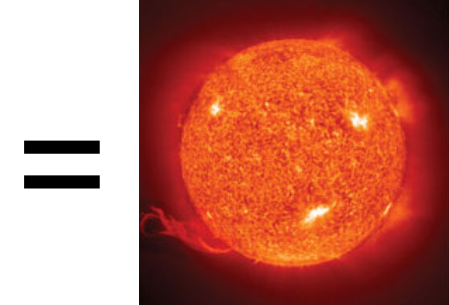
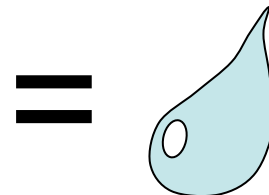
$$A(\omega) = \frac{u^2 + 2}{u\sqrt{u^2 + 4}} + \frac{2}{u\sqrt{u^2 + 4}} \cos(\omega\Delta t_l),$$

Interference fringe in spectrum

$$\nu = \omega/(2\pi)$$

Gamma-Ray Burst

$E=mc^2$ (by Einstein)



Atomic bomb $\sim 1\text{ kg}$

GRB
 $\sim 10^{52}\text{ erg}$

Sun
 $\sim 10^{33}\text{ g}$

In \sim sec, GRB release energy Sun emit over lifetime

GRB is the most luminous object

GRB in a Nutshell

Relativistic Jet

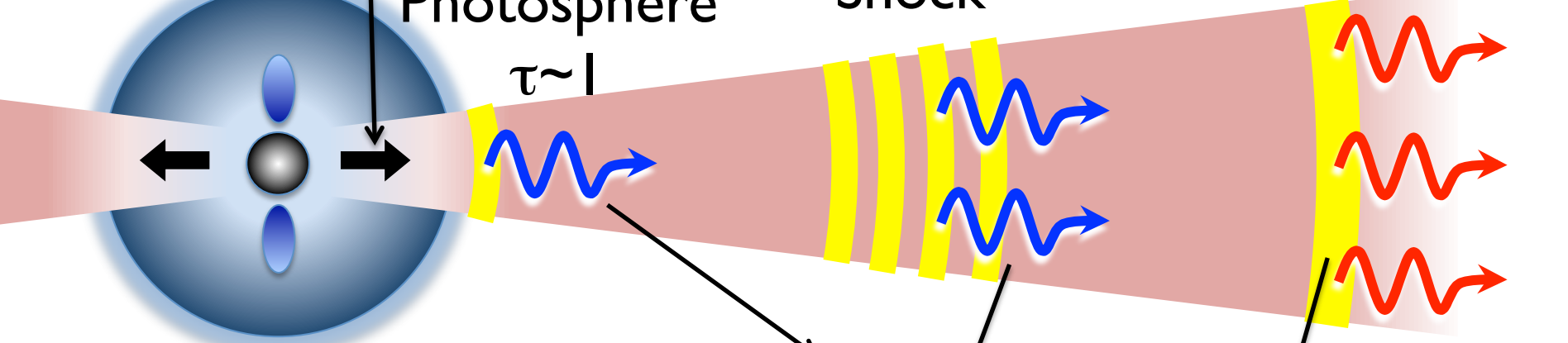
$\Gamma > 100$

Photosphere

$\tau \sim 1$

Internal Shock

External Shock
ISM

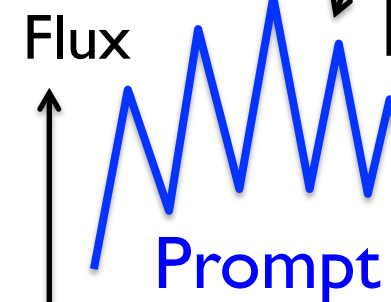


$\sim 2\text{-}3/\text{day}$ @ Cosmological

Long: Massive Stellar
Collapse to BH/NS

Short: NS-NS/BH merger?
Magnetar? WD/NS AIC?

Flux



$E_{\text{kin}}/B \Rightarrow E_\gamma$

Prompt

$\sim 2\text{-}100\text{s}$
 $\sim 0.01\text{-}2\text{s}$

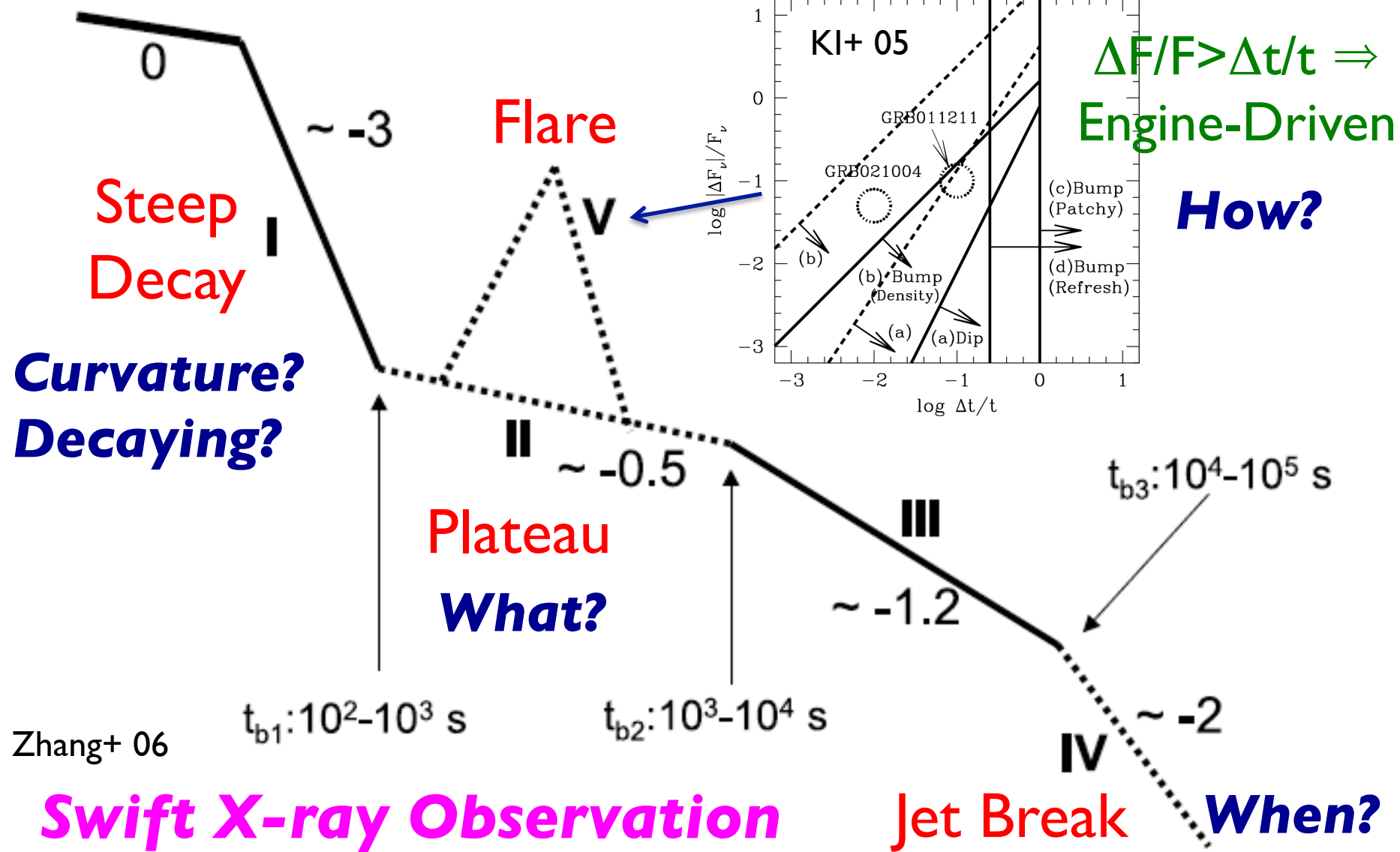
Afterglow

Time

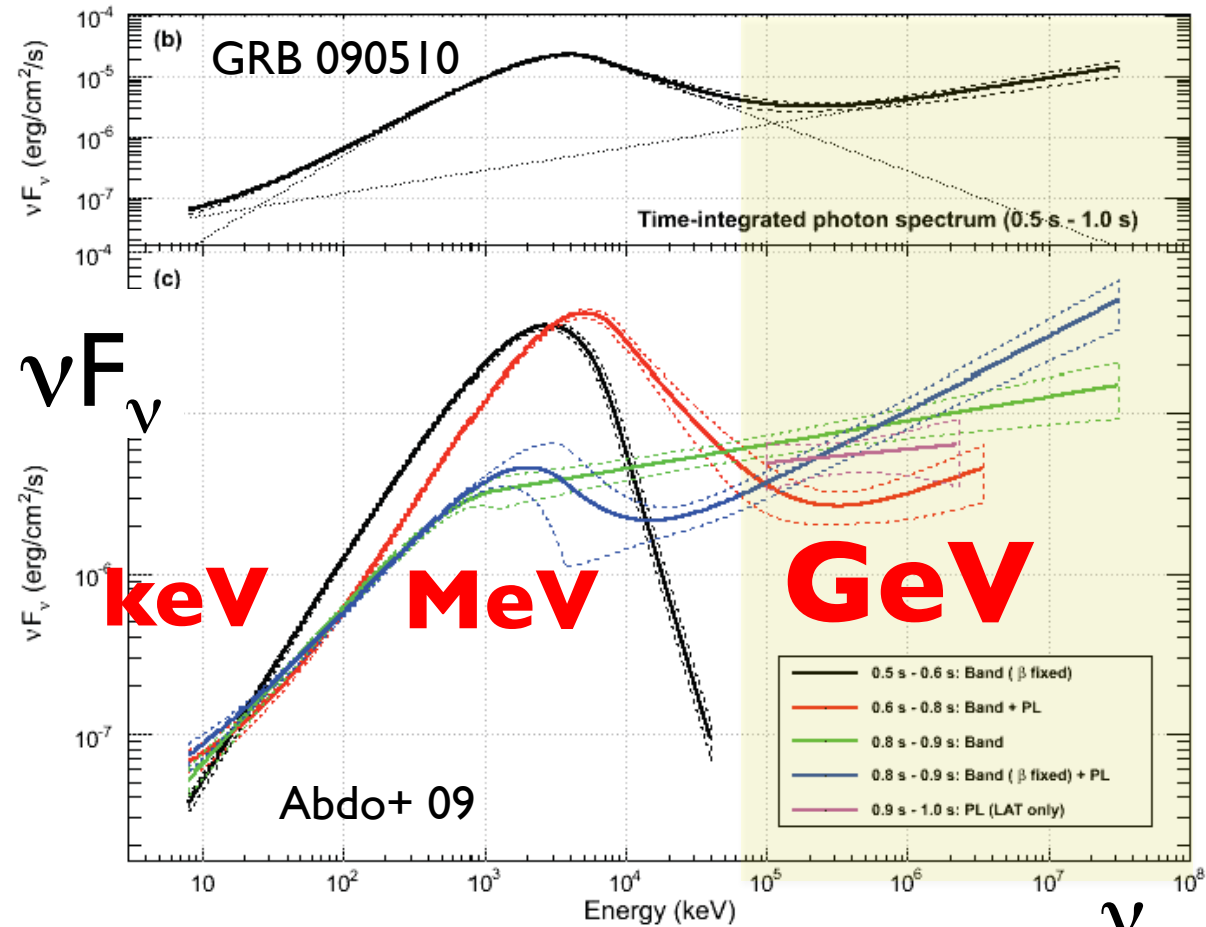
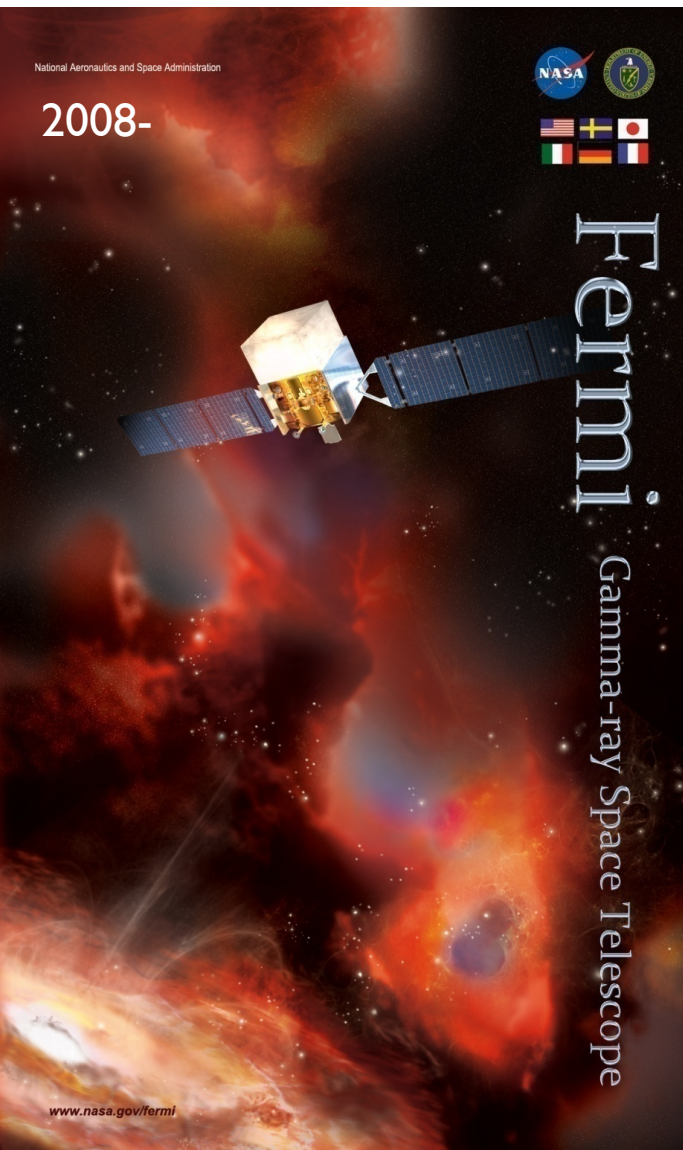
Unresolved Problems

- ***Early X-ray afterglow (First 3hr)***
 - Steep decay, Flare, Plateau, Optical flash
- ***Prompt GRB emission mechanism***
 - Photosphere or Poynting (γ jet or B jet)
 - Band spectrum (E_{peak} relation, Spectral index)
 - GeV γ -ray
- ***Central engine***
 - Black hole or Magnetar (High-B neutron star)
 - Blandford-Znajek or $\nu\nu$ annihilation

Early Afterglow Puzzles



>GeV γ -ray from GRBs

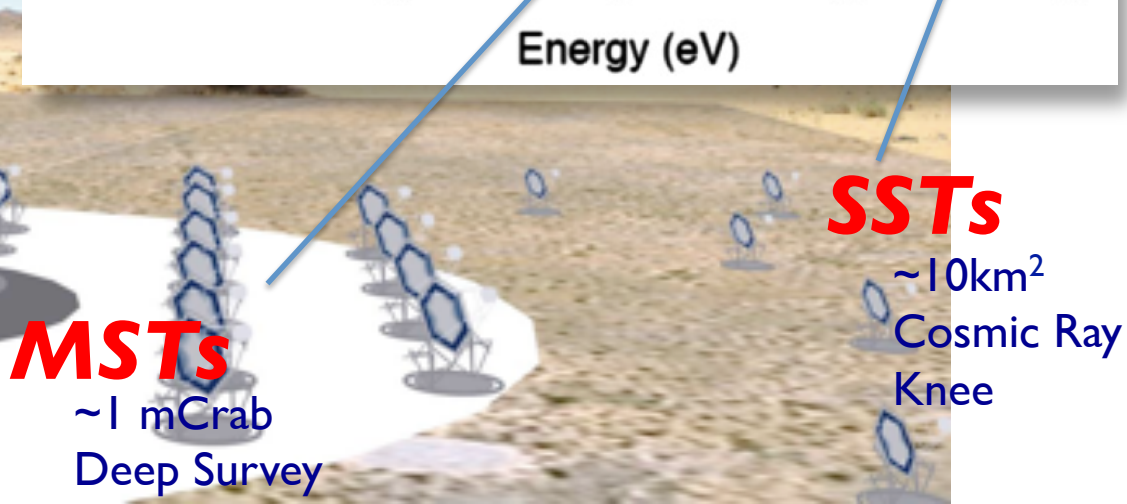
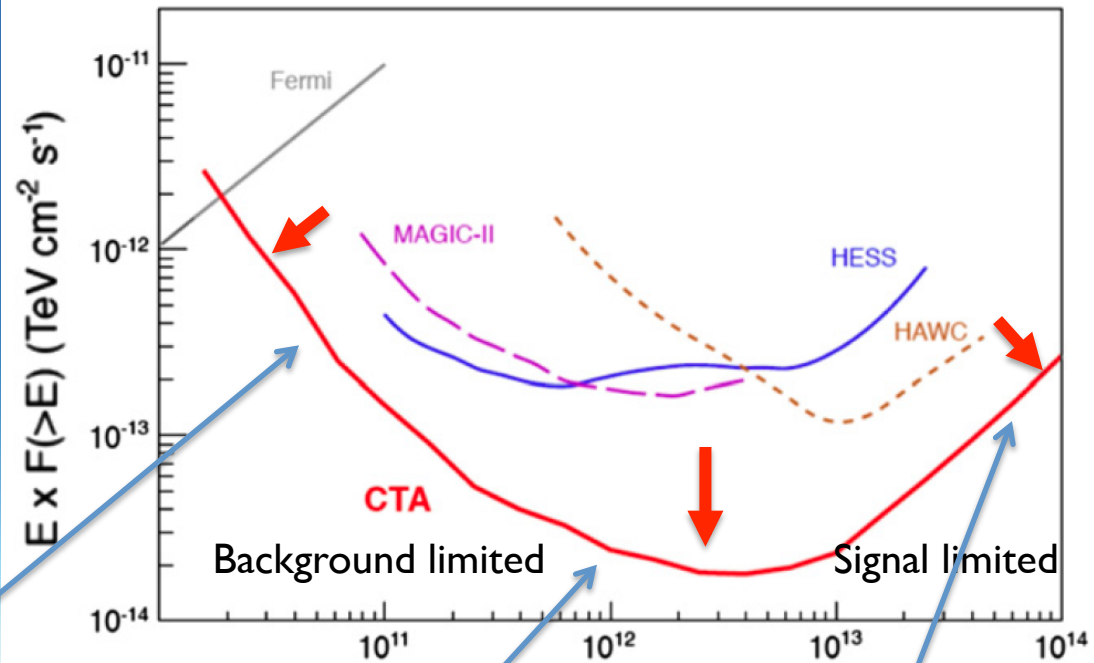


- $\Gamma > 1000$ to avoid $\gamma\gamma \rightarrow e^+e^-$
- $> 10^{17} \text{ eV } p + \gamma \rightarrow \pi \rightarrow \gamma, e?$

CTA



- ~20GeV-100TeV
- ×10 Sensitivity
- $\Delta\theta \sim 1-2$ min
- FOV $\sim 5-10$ deg
- ~20 s slew (LST)
- ~2015-
- ~150€



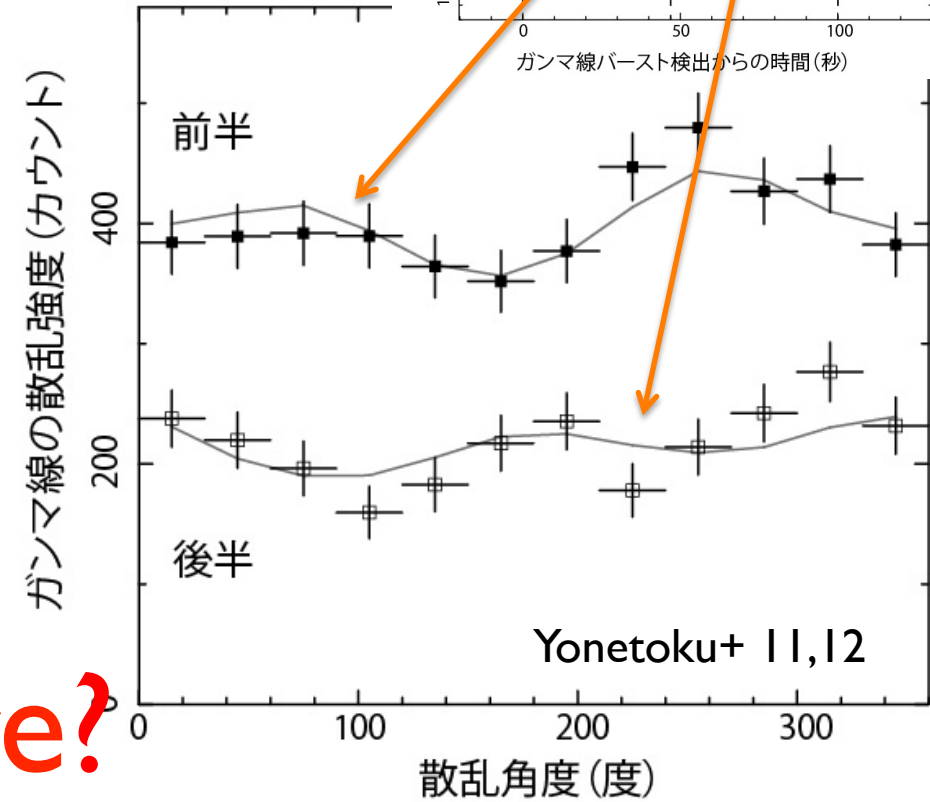
Detectability: Kakuwa+ 12; Inoue+ 13

GRB Polarization

*Tsubame soon
Ask Toma-kun*



GRBI00826A
 $27 \pm 11\% (2.9^\circ)$
Rotation (3.5°)



Patchy B? γ -shere?

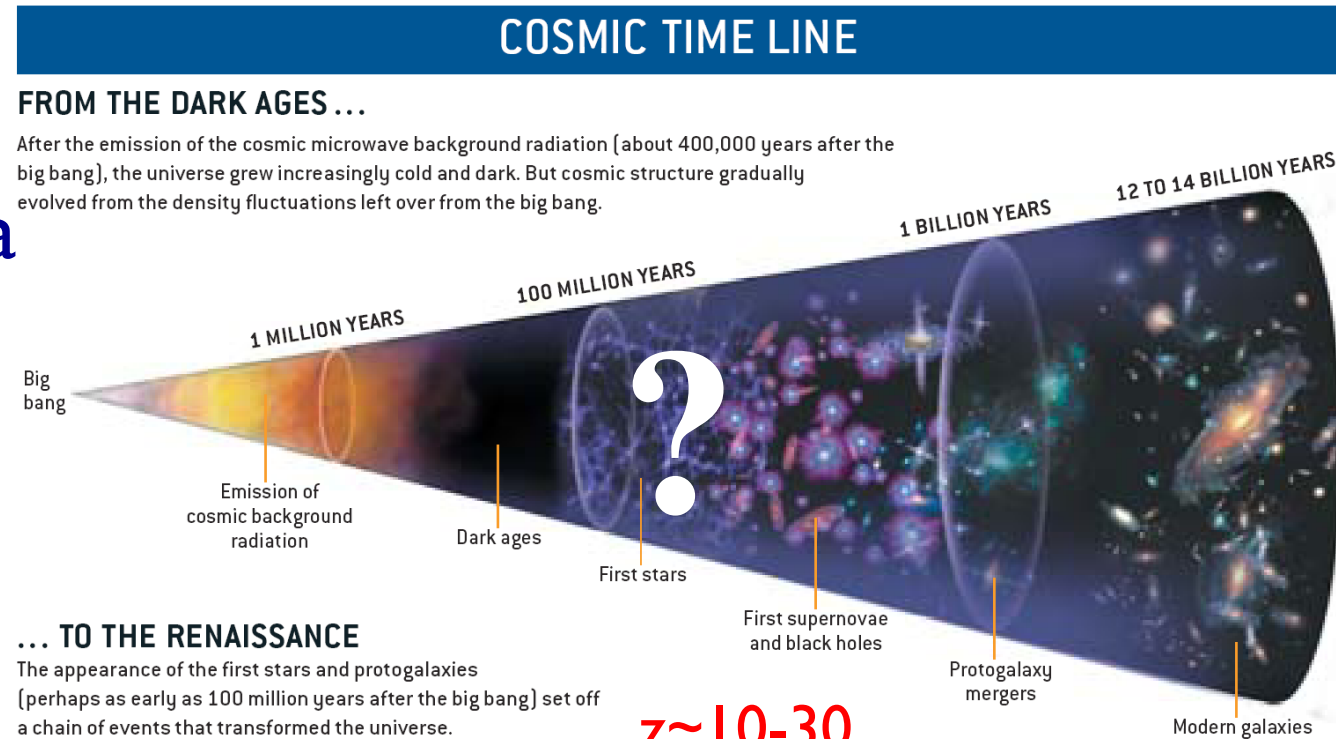
Contents for GRB

- ***GRB Cosmology***
- Pop III GRB
- Ultralong GRB
- Short GRB
- Other topics

GRB Cosmology

Massive star origin \Rightarrow High redshift GRBs

- Like QSO
- Like Supernova
- Star formation
- Reionization
- Metal, Dust
- Dark energy
- ...



Larson & Bromm 02

GRBs are useful
for probing high-z

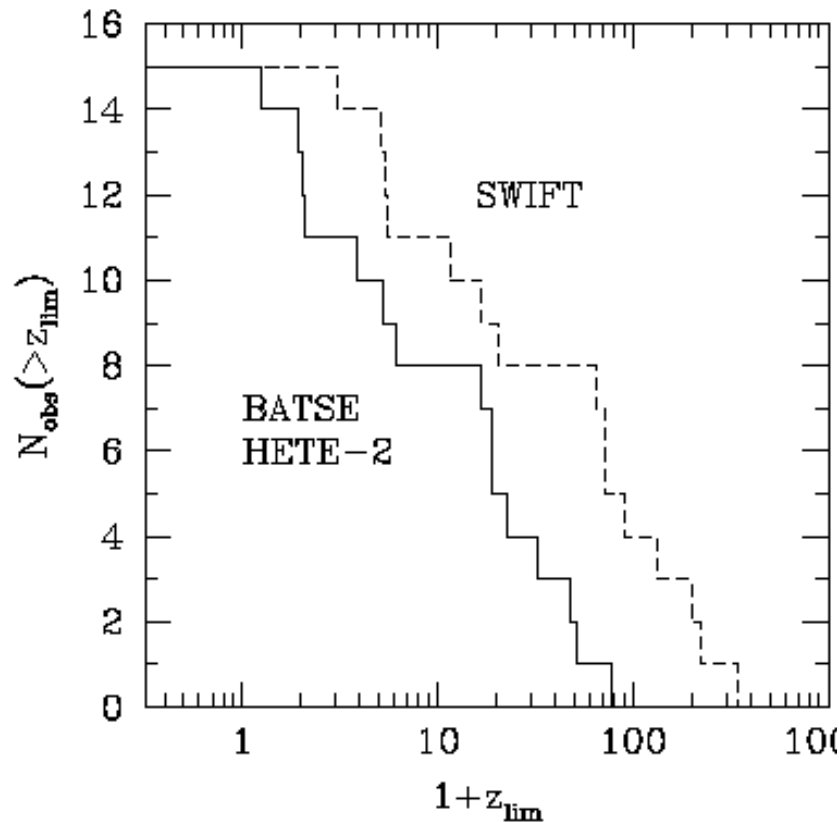
GRB \longleftrightarrow
QSO, galaxy

$z \sim 10-30$

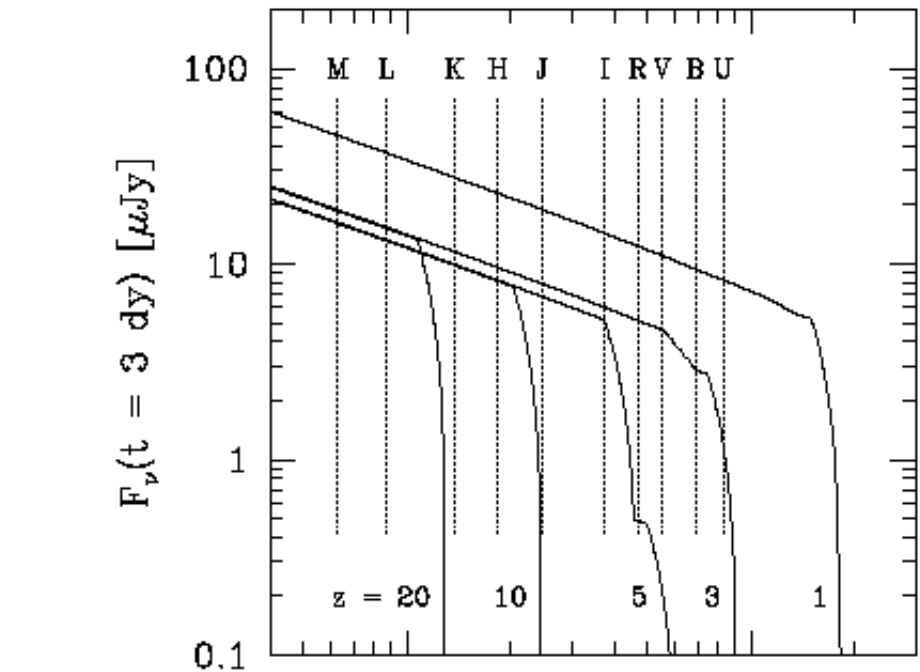
$z \sim 8$

Anticipated from ~2000

Lamb & Reichart 01, Ciardi & Loeb 00

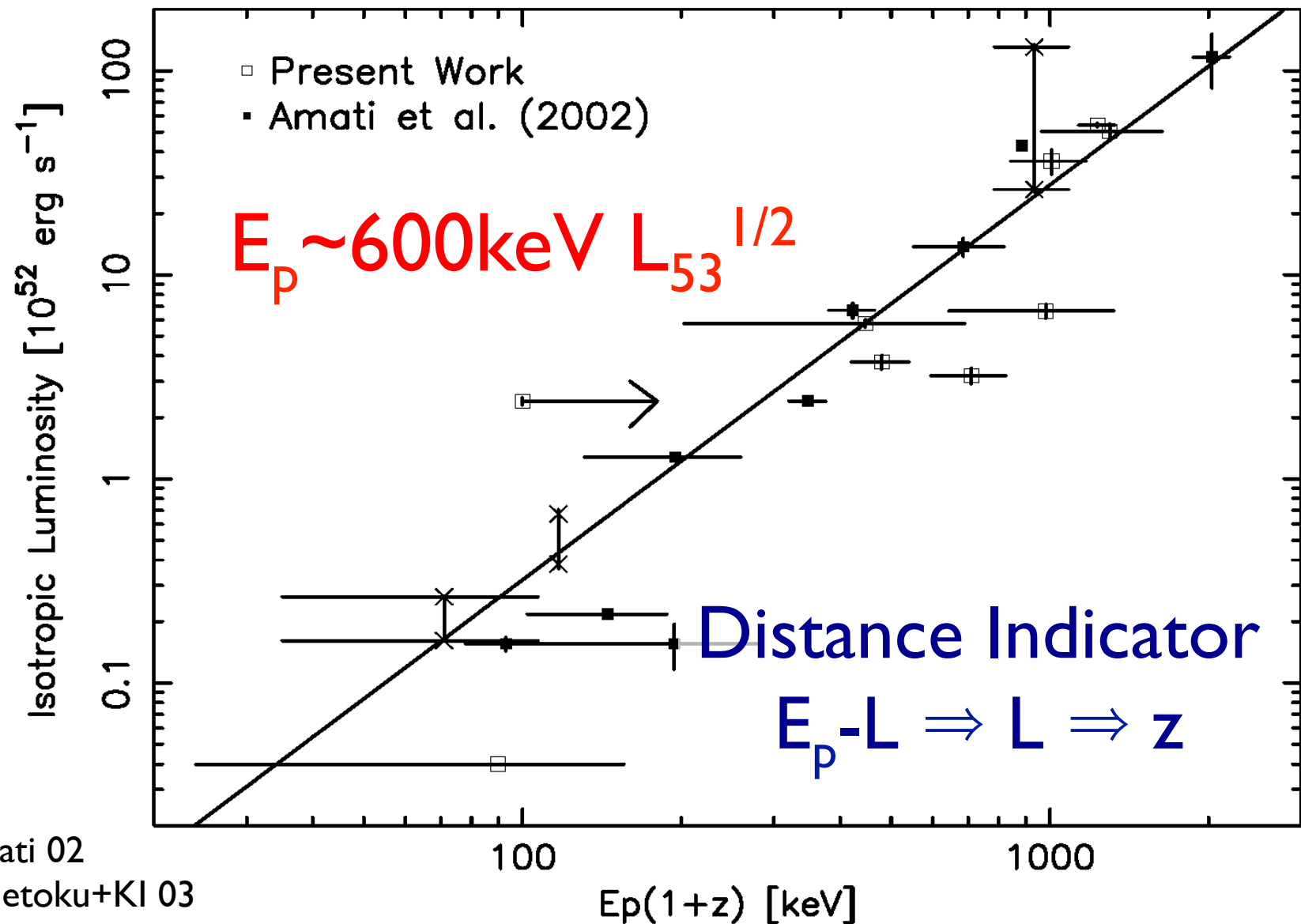


GRB is detectable
up to $z \sim 100$

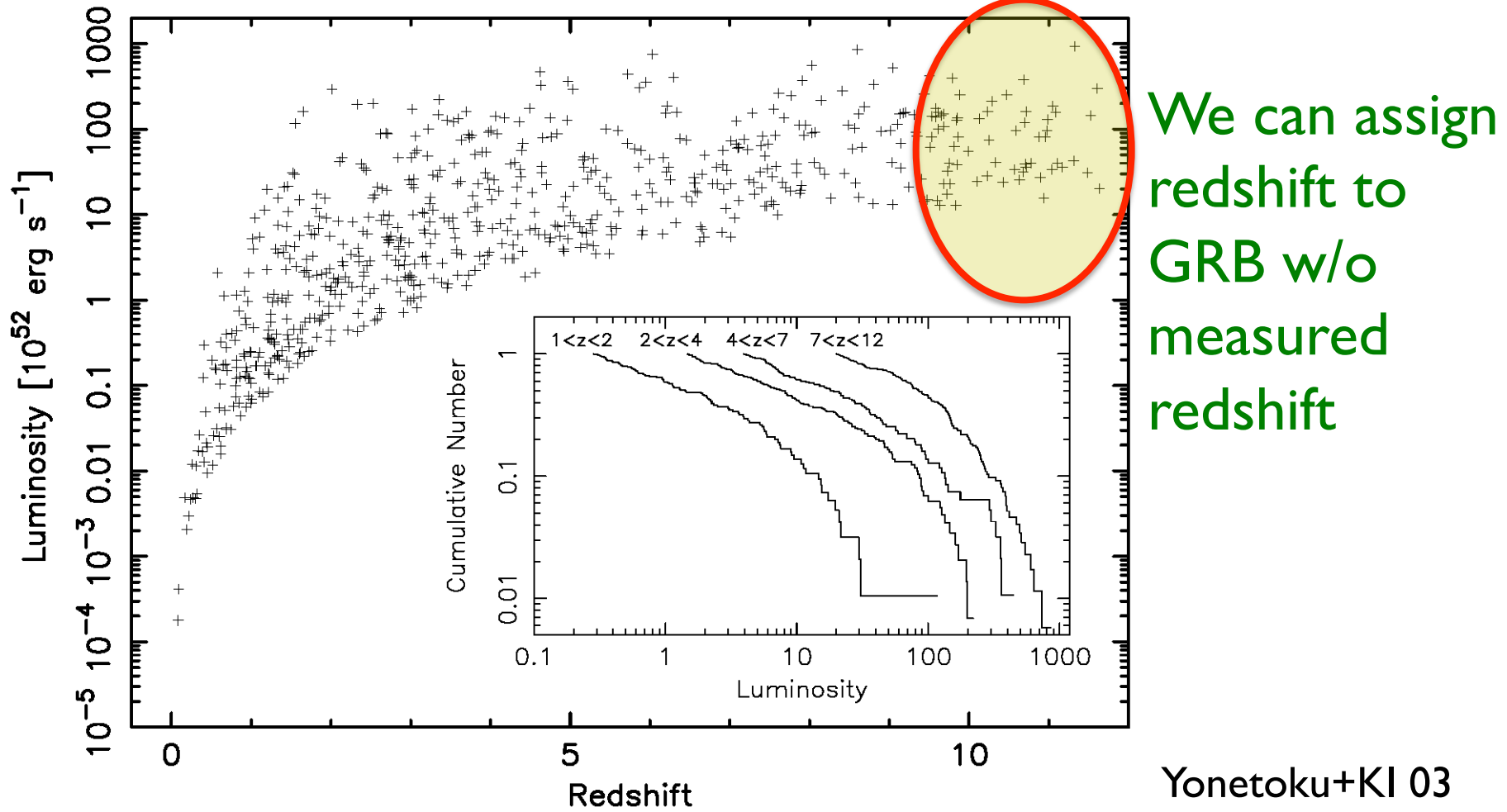


t dilation + K-corr. \Rightarrow
AG is detectable @high-z
Ly α trough \Rightarrow redshift

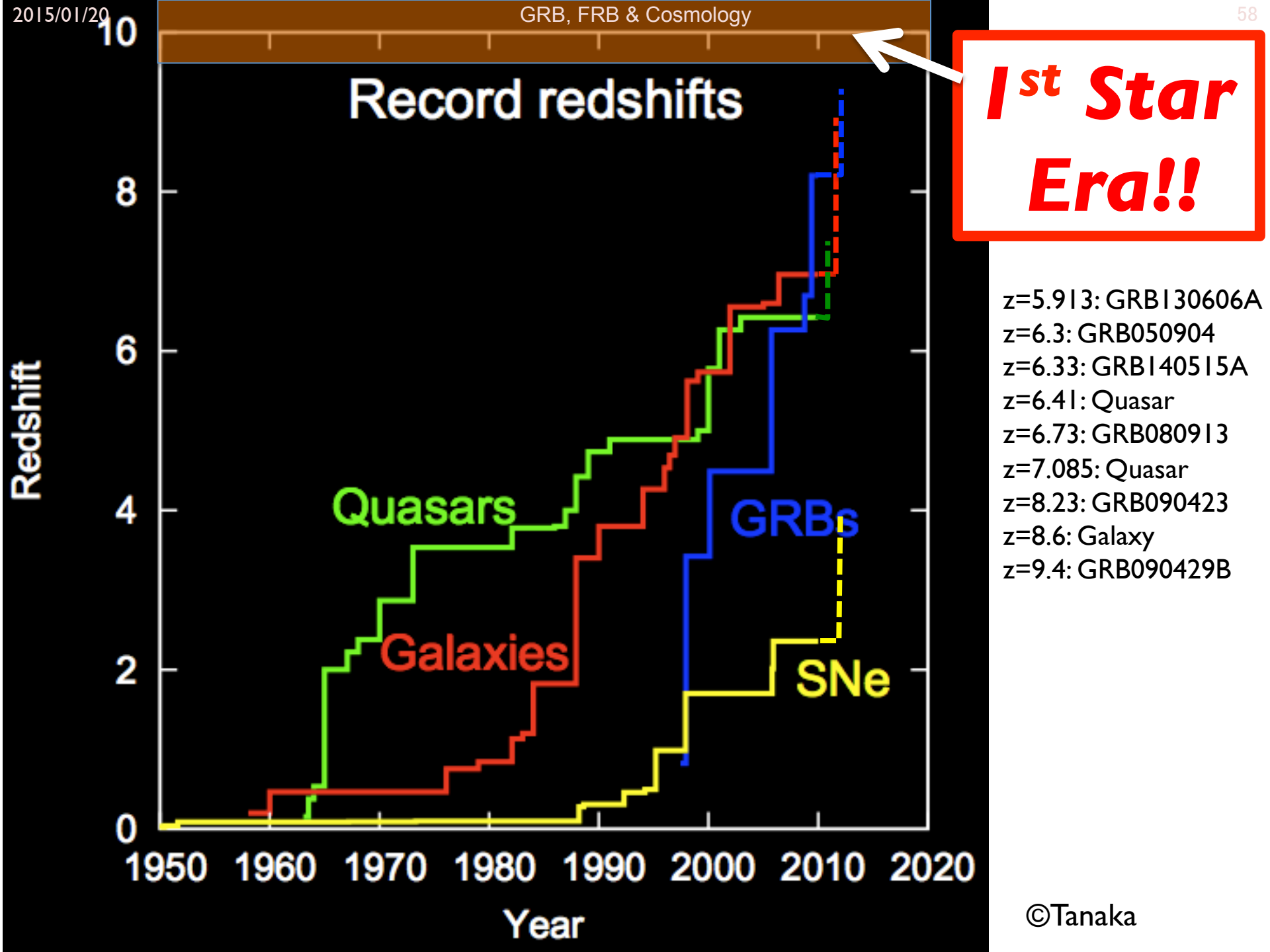
Amati/Yonetoku Relation



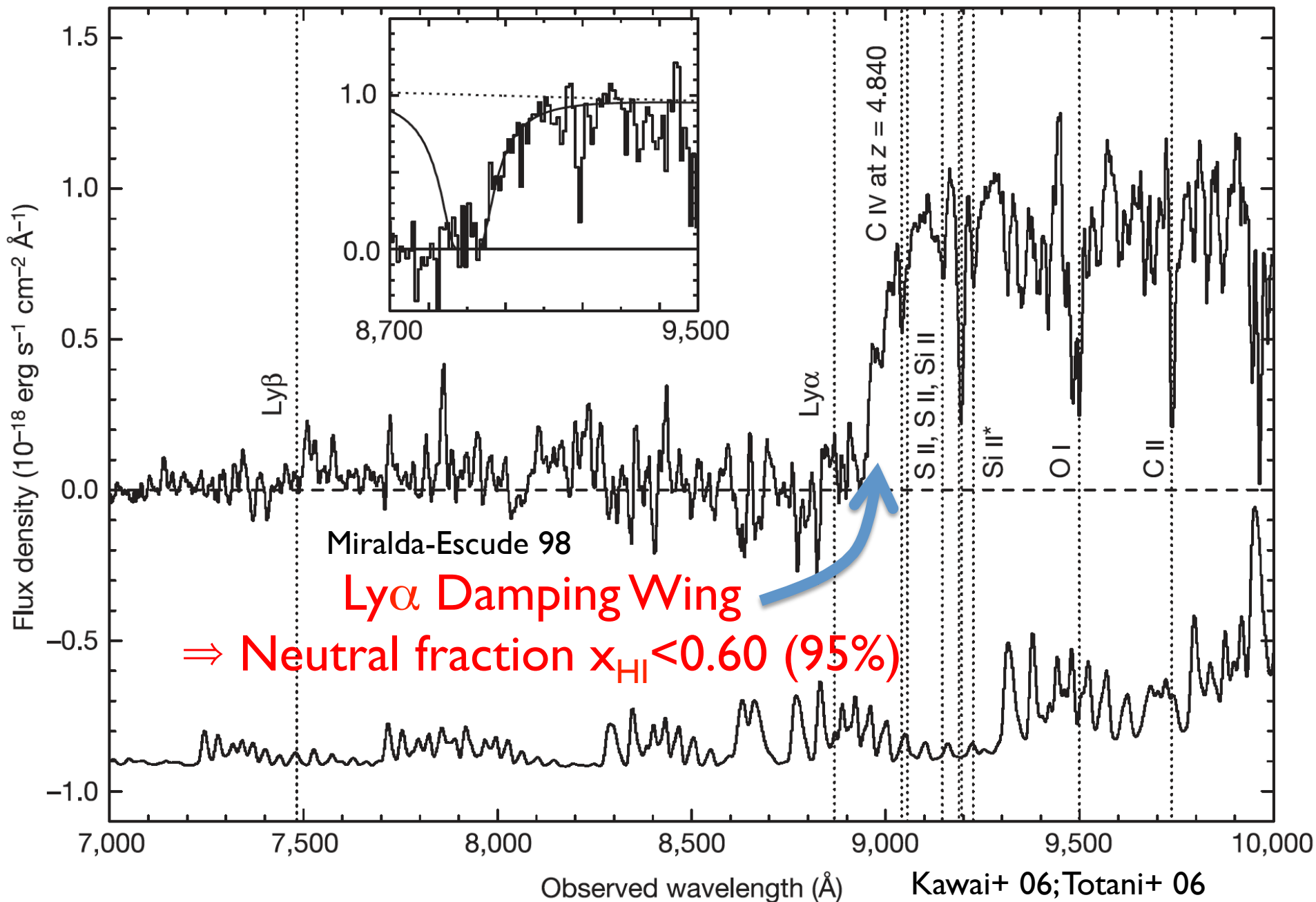
E_p -L imply $z > 10$ GRB



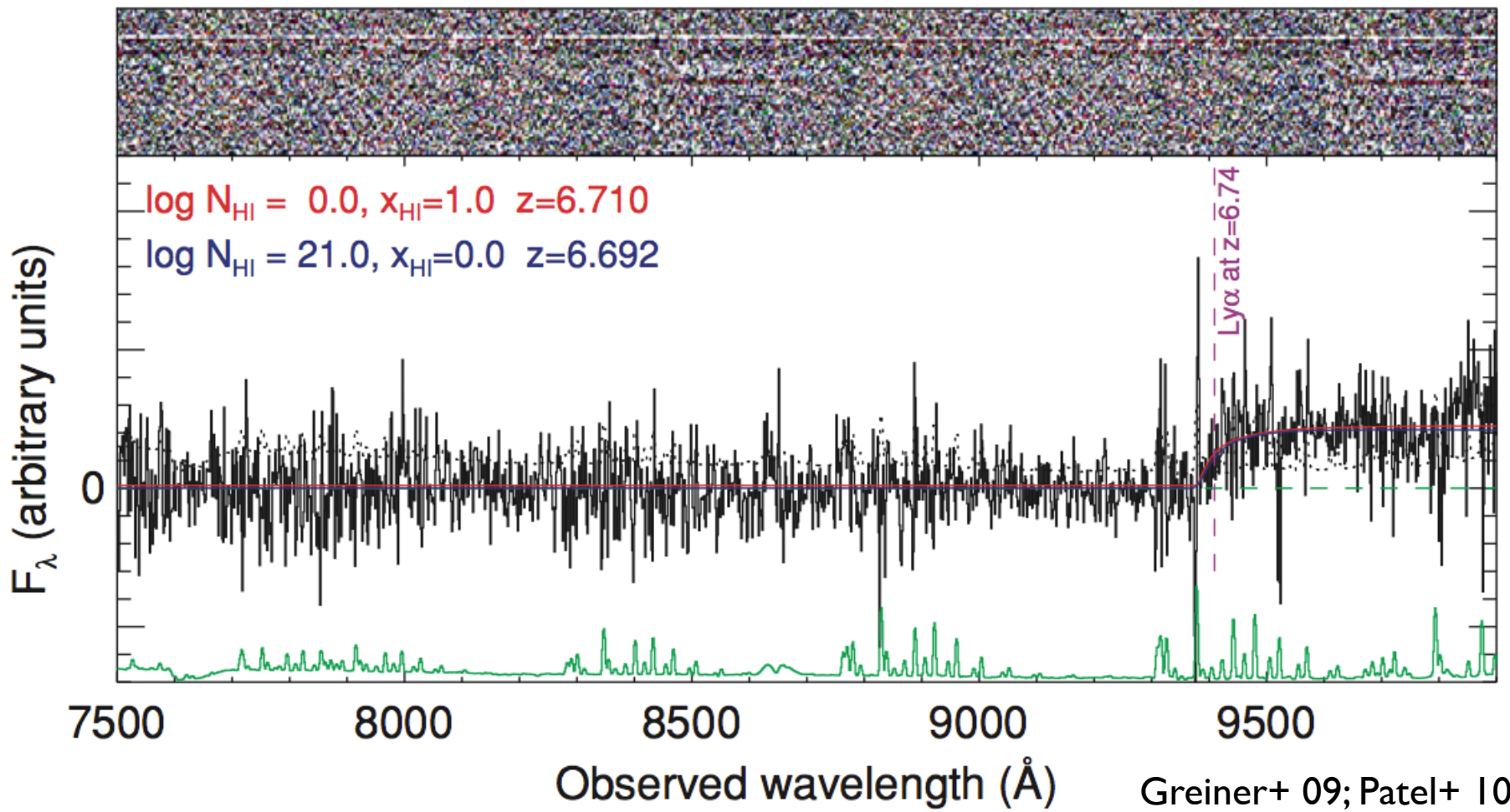
$z > 10$ GRBs have been already detected!?



$z=6.295$, GRB050904 at $t=3.4$ d, Subaru FOCAS 4.0 hrs

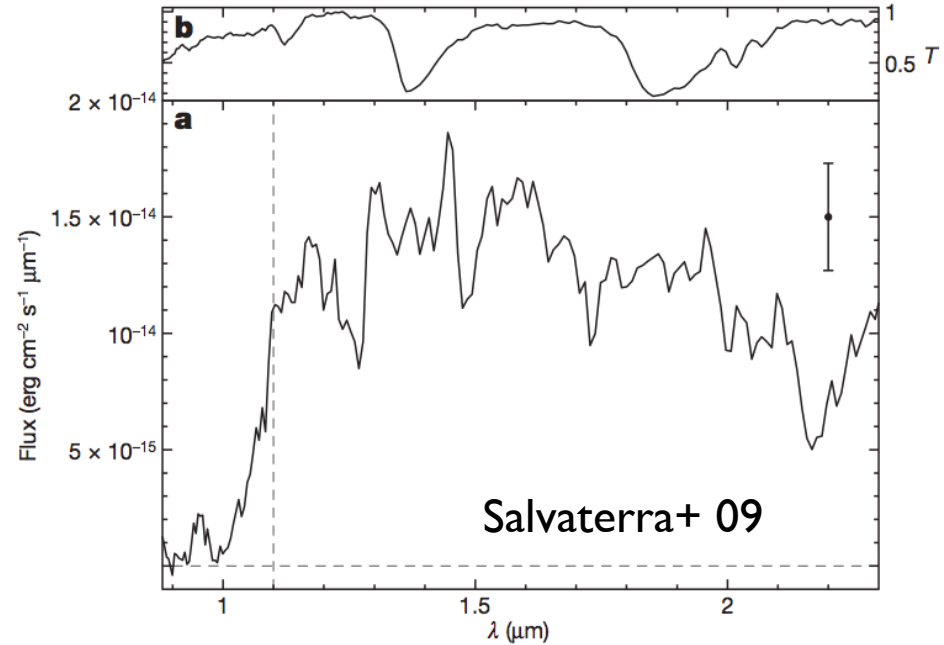
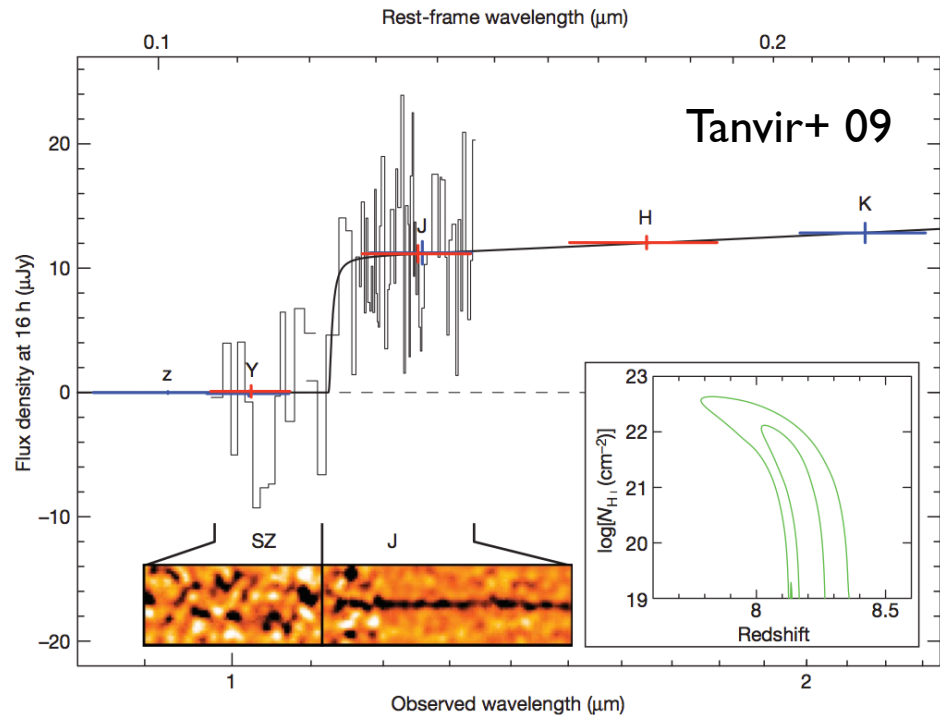


GRB 080913 @ $z \sim 6.7$

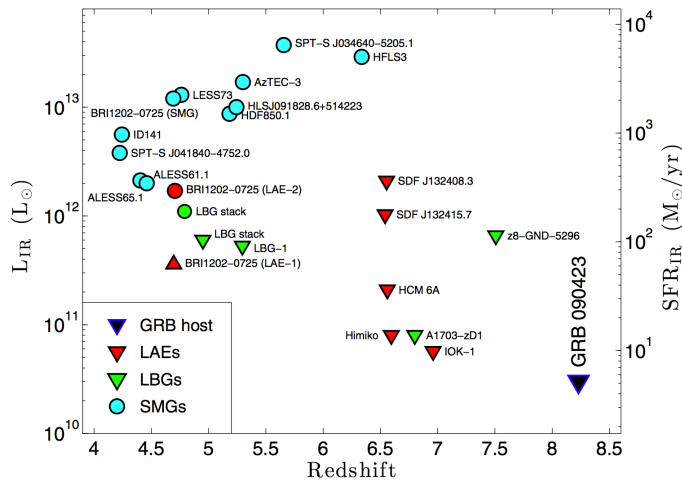


Damping wing does not discriminate DLA or IGM

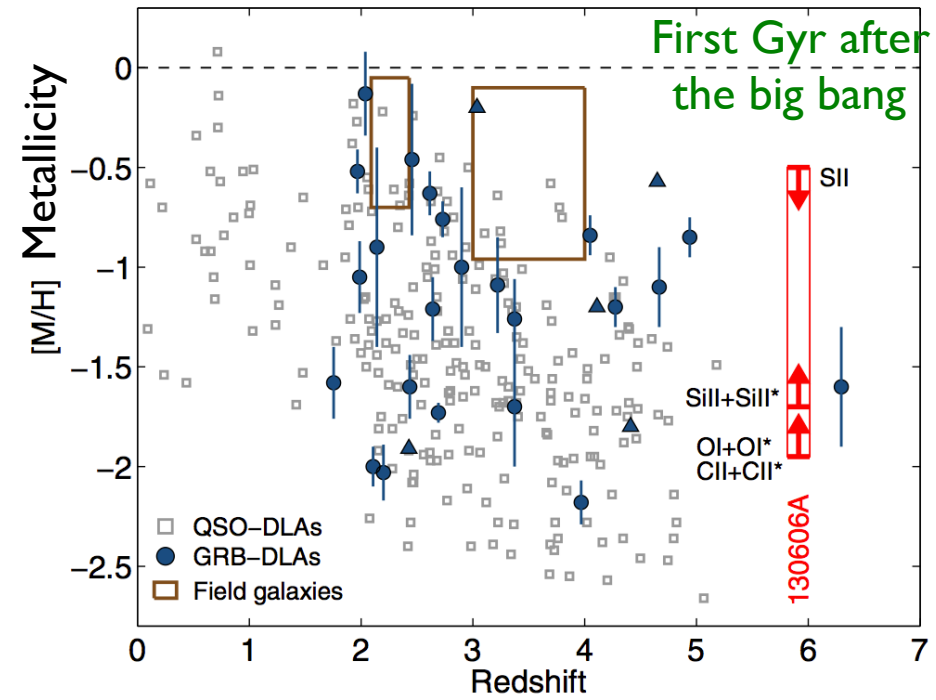
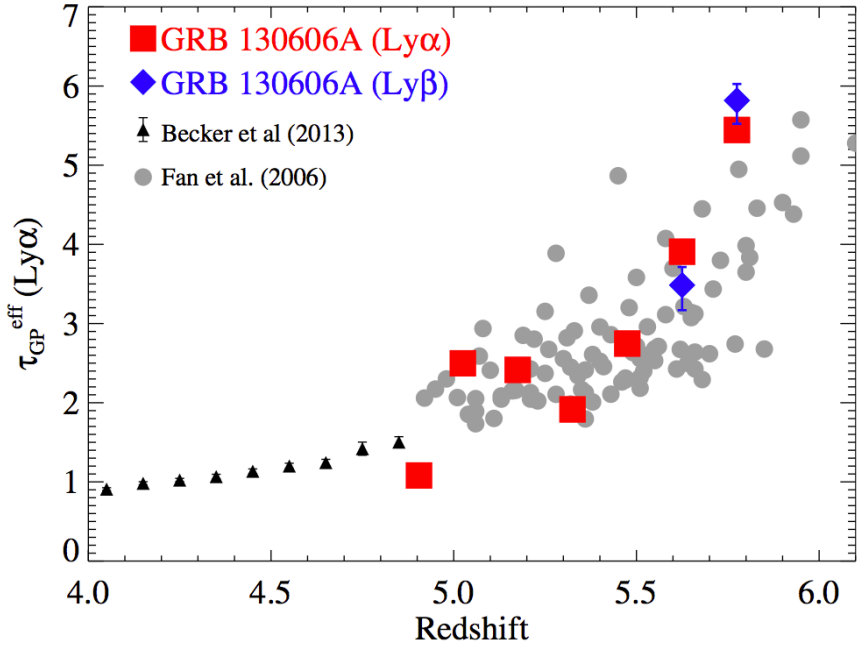
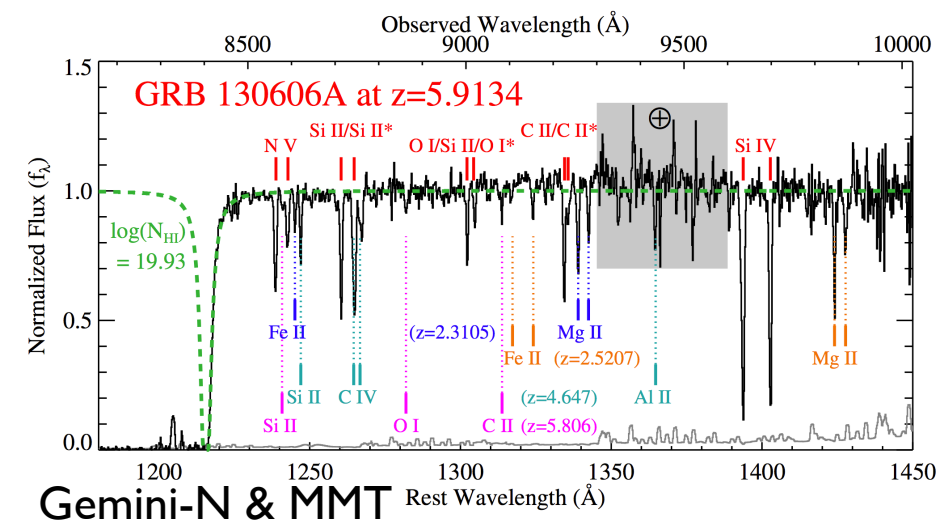
GRB 090423 @ $z \sim 8.2$



Only upper bound on N_{HI}
(Unclear damping wing)



GRB 130606A @z~5.9



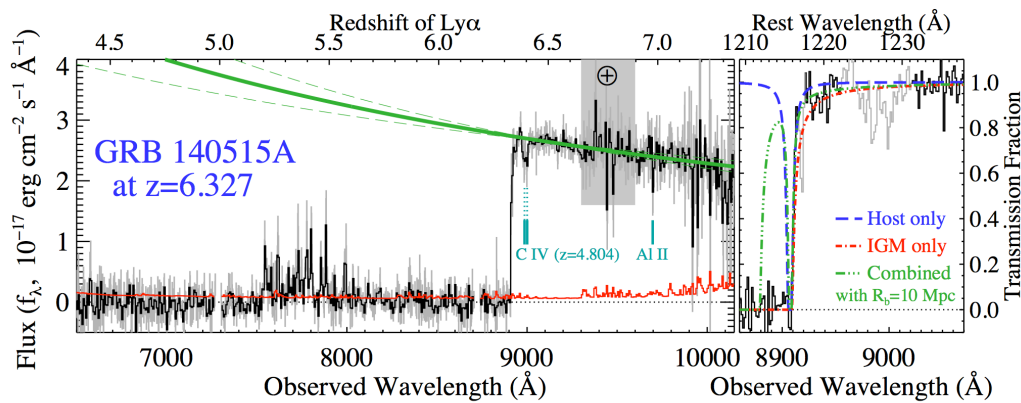
$x_{\text{HI}} < 0.11 \text{ (2}\sigma\text{)}$ Chornock+ 13

$\sim 0.1 - 0.5$ Totani+ 14 (Subaru)

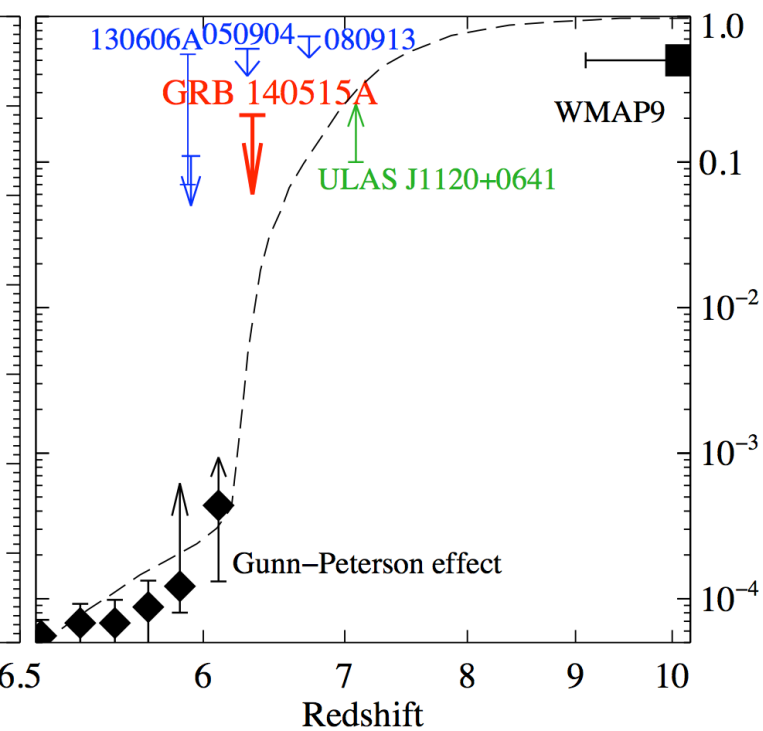
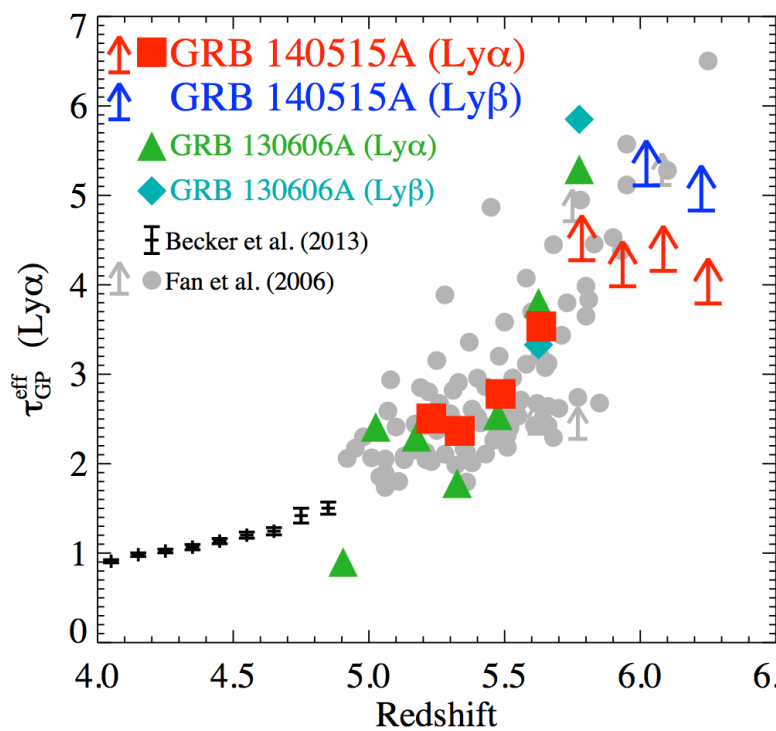
$< 0.03 \text{ (3s)}$ Hartoog+ 14

(VLT/X-shooter), Castro-Tirado+ 14 (GTC)

GRB 140515A @ $z \sim 6.3$

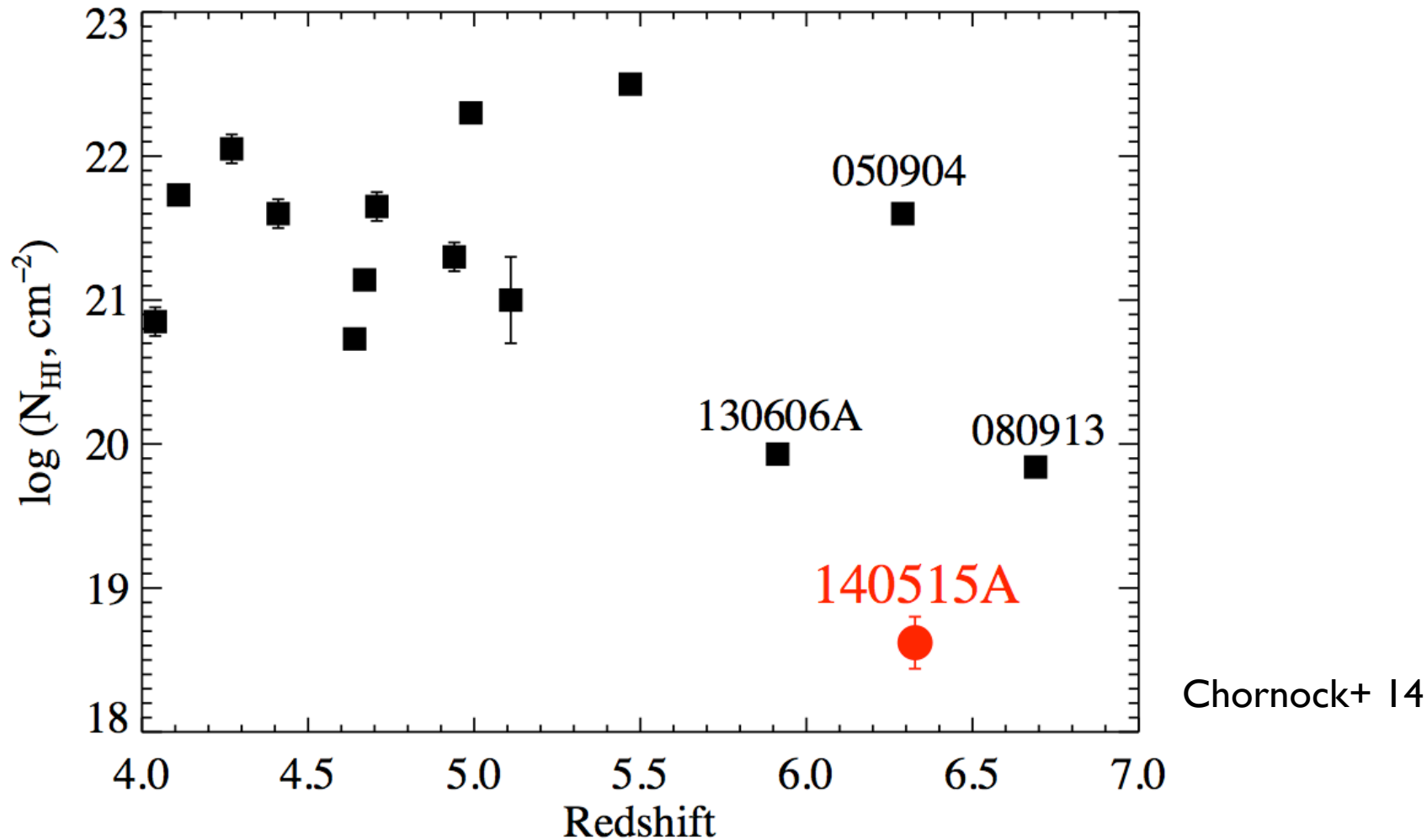


Gemini-North
 High- z was serendipitous
DLA+IGM: $x_{\text{HI}} \sim 0.12 \pm 0.05$
No metal line: $[\text{Z}/\text{H}] < -0.8$



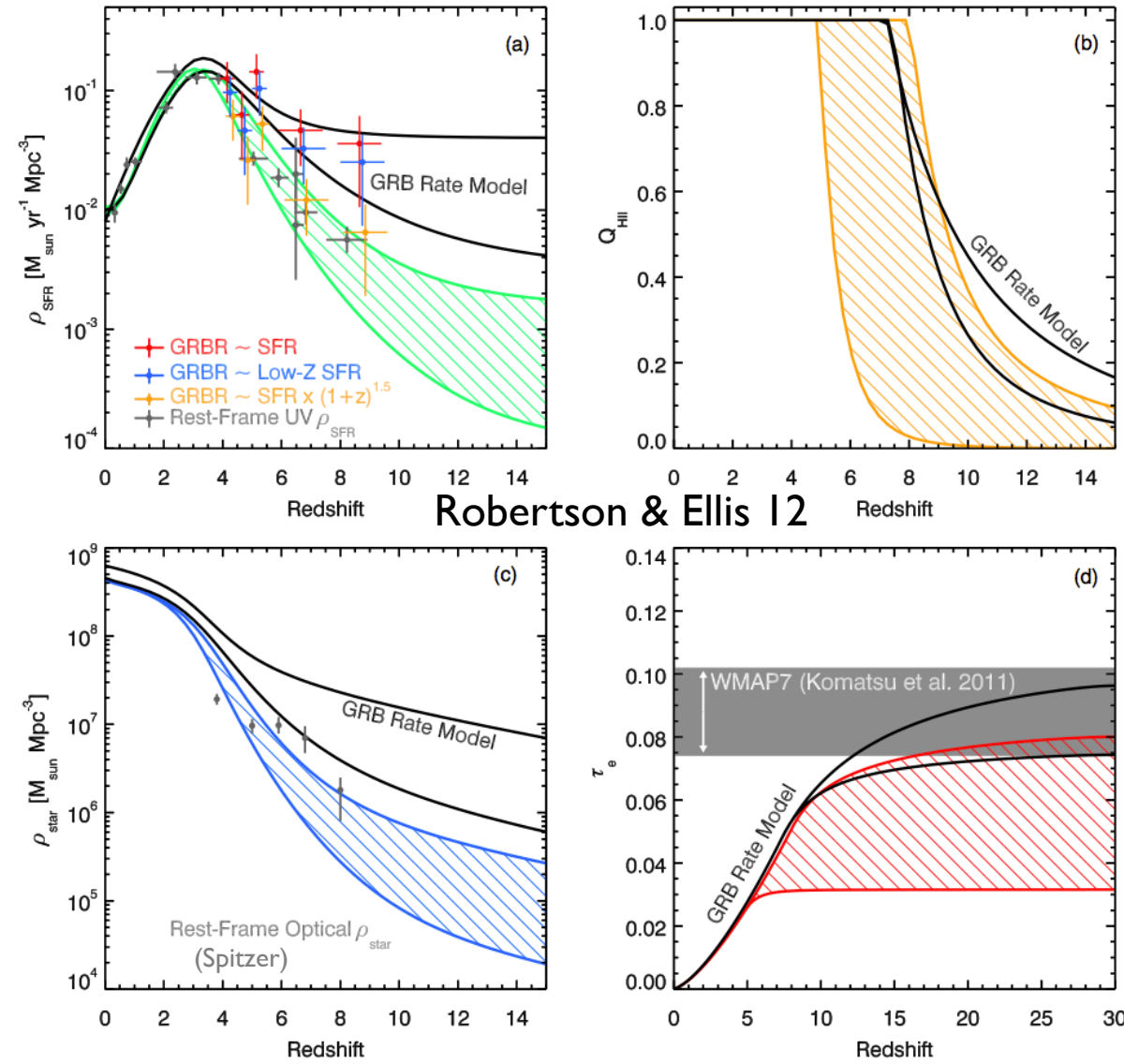
DLA only:
 $N_{\text{HI}} \sim 18.62 \pm 0.08$
IGM only:
 $x_{\text{HI}} \sim 0.056 \pm 0.011$

Host Absorption



Escape fraction of ionizing photons increases at $z>6$?

GRB & Reionization



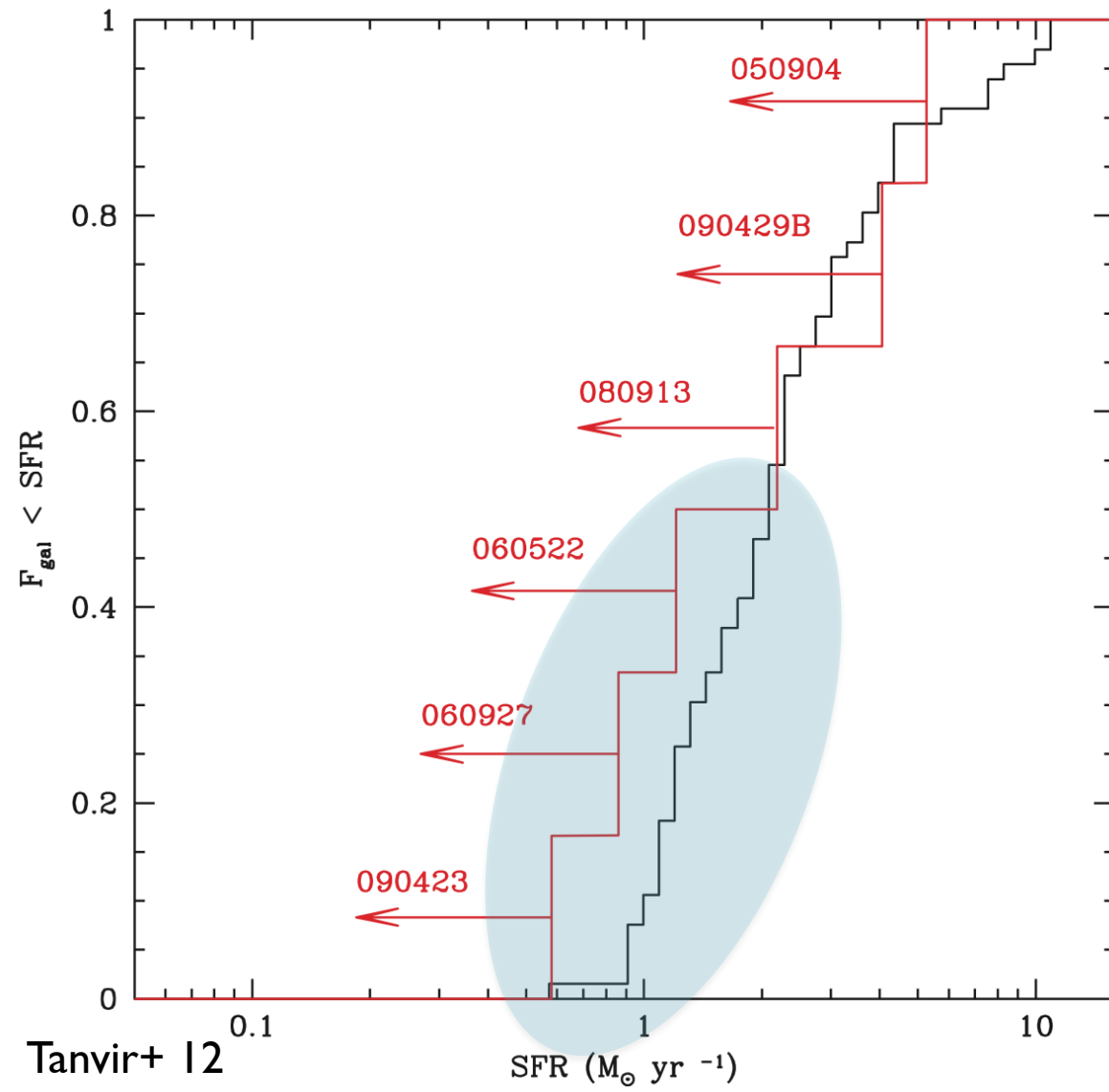
$\text{GRB} \propto \text{SFR} (1+z)^{1.5}$
to match GRB & UV

$\text{GRB} \propto \text{SFR} (1+z)^{0.5}$
 \Rightarrow Reionization implied
by CMB polarization

But, overproduce
stellar mass density?

$Z \sim 0.2 Z_\odot$
Clumpiness = 3 (up), 2.5 (low)
 $f_{\text{esc}} = 0.06$ (up), 0.2 (low)

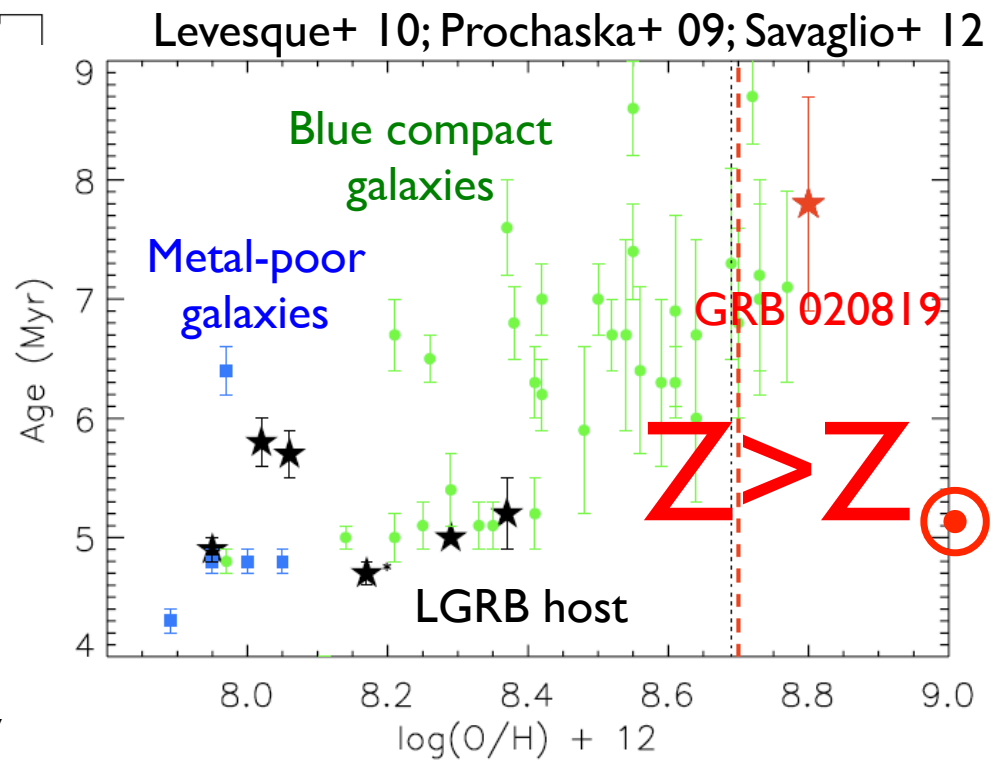
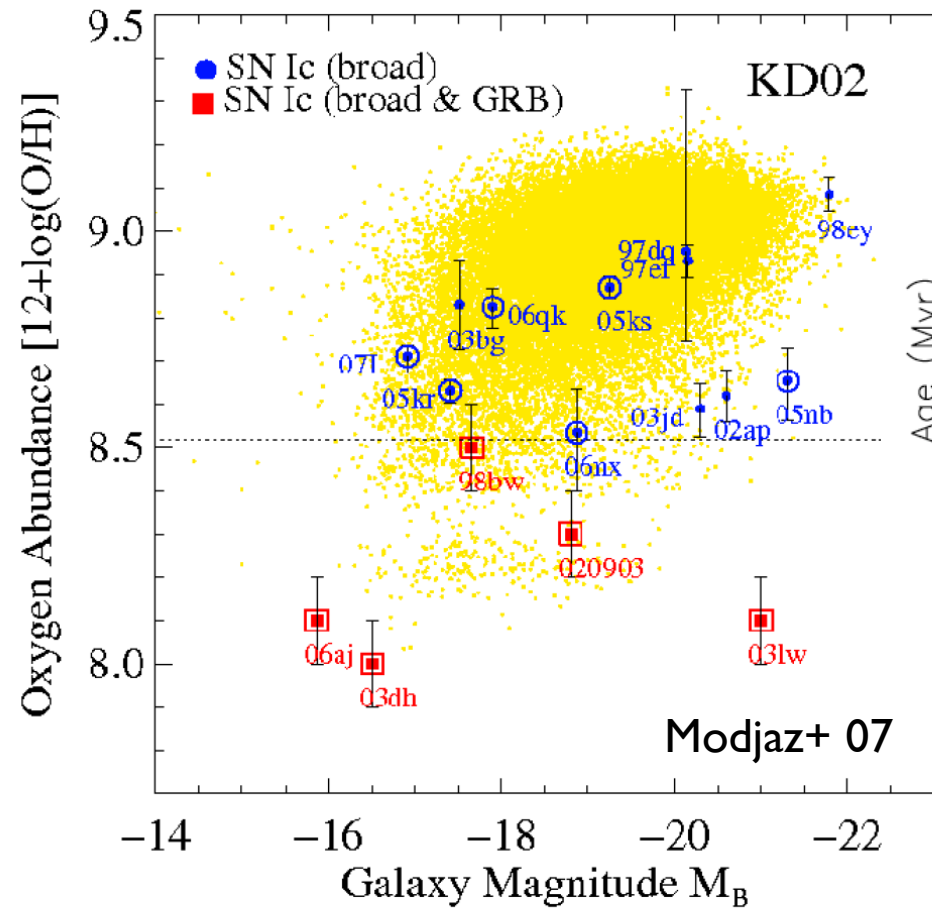
GRB & Star Formation



GRB @ $z>5$ v.s.
Hubble UDF gal. @ $z\sim 7$

If $\text{GRB} \propto \text{SFR}$ (Totani+97)
⇒ **Much star formation (UV photons) arises in faint galaxies?**

Low Metal for GRB?



Fundamental plane

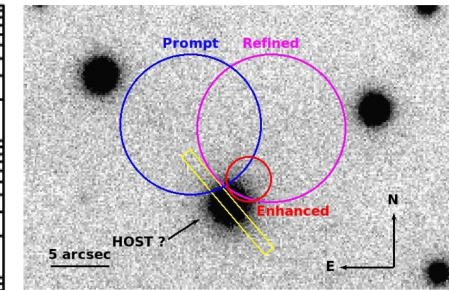
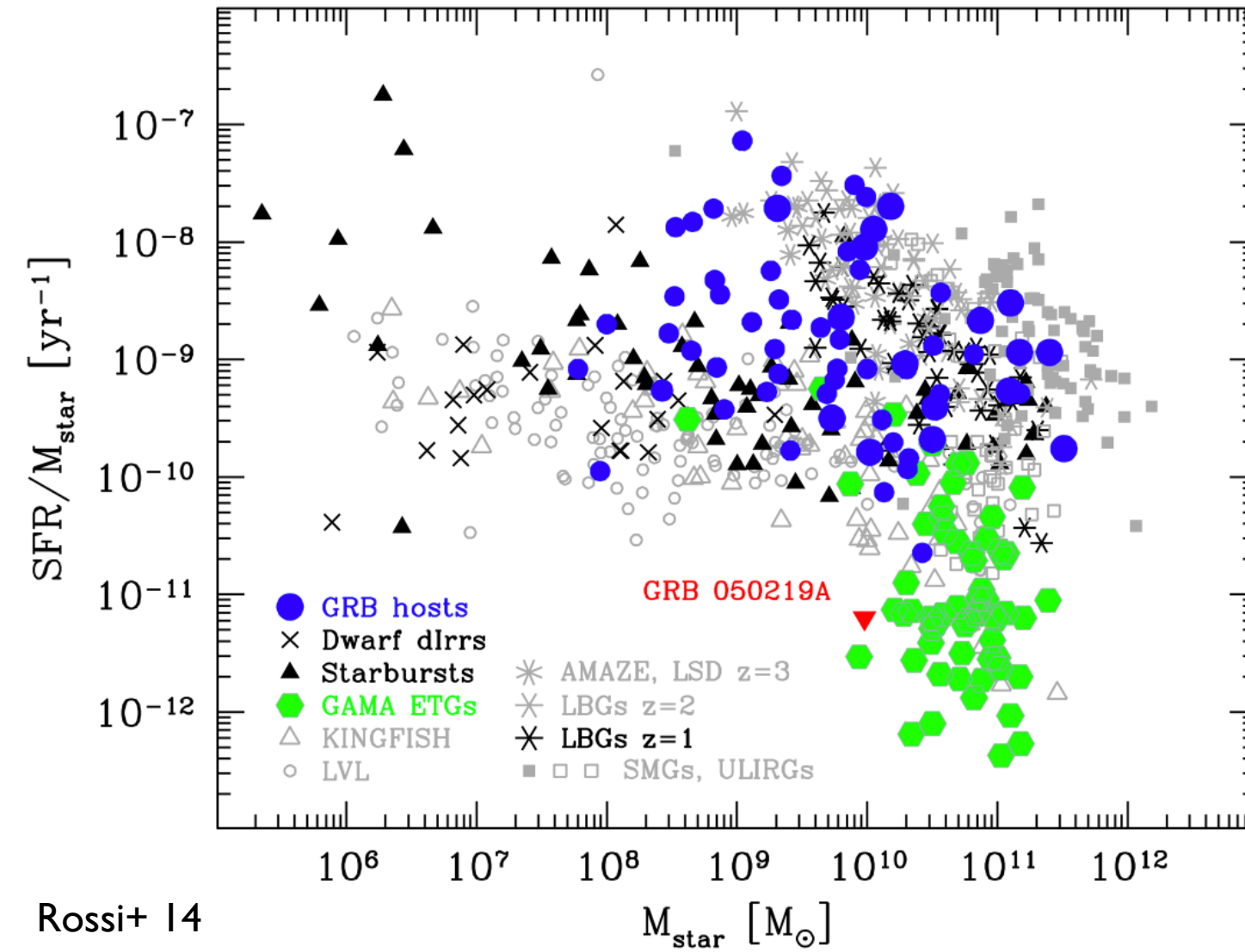
SFR-Metal-Mass
Host is typical?

Mannucci 11

Metal \Rightarrow Wind \Rightarrow

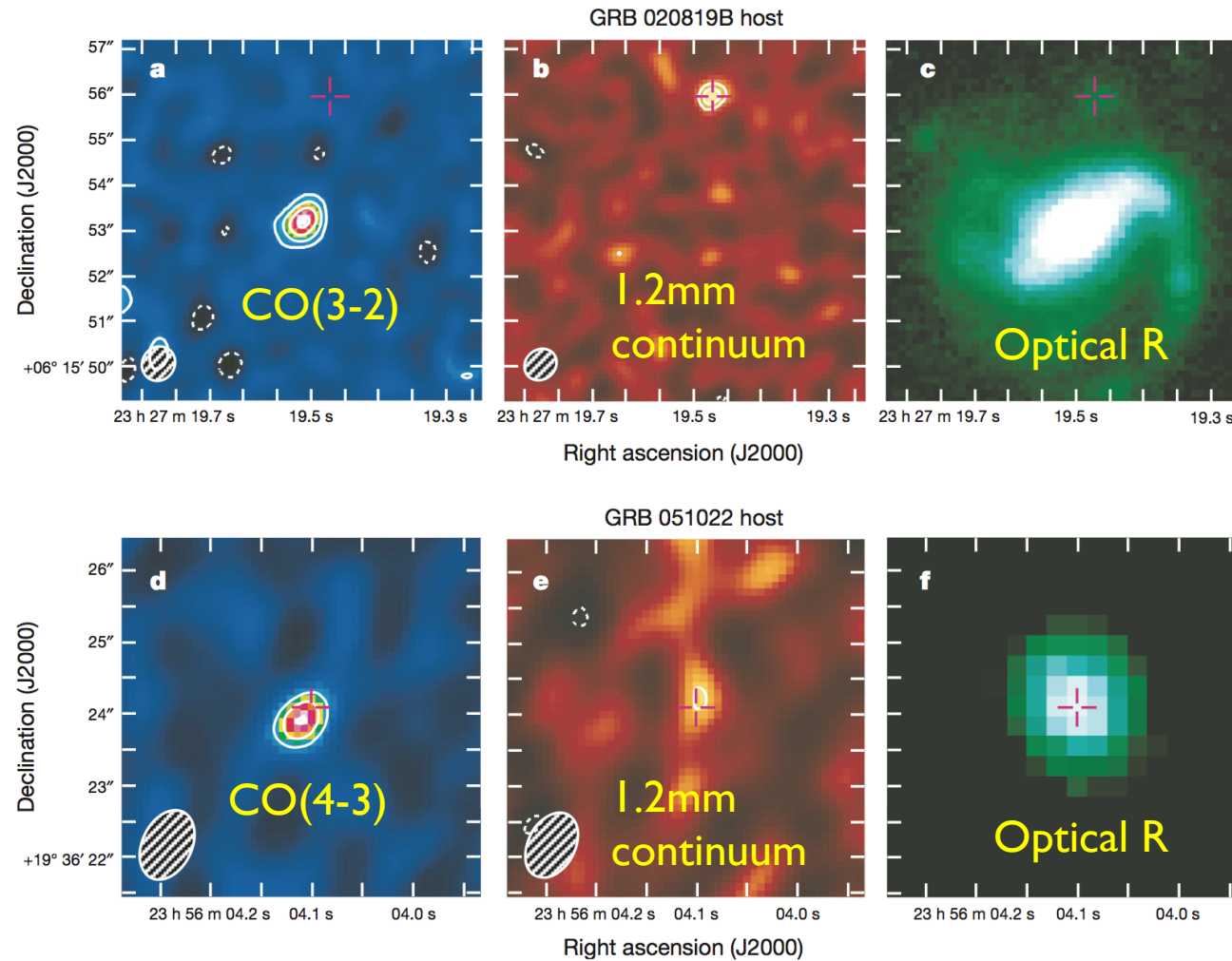
Ang. Mom. Loss \Rightarrow No GRB?

LGRB in Early-Type Gal.



$z=0.211$
3Gy-old ETG
Not *forming

Small Gas-to-Dust Ratio



CO line by ALMA
⇒ Molecular gas
mm continuum
⇒ Dust

$M_{\text{gas}}/M_{\text{dust}} < 9-14$
(GRB 020819)
< Star-forming gal.

Gas into stars?

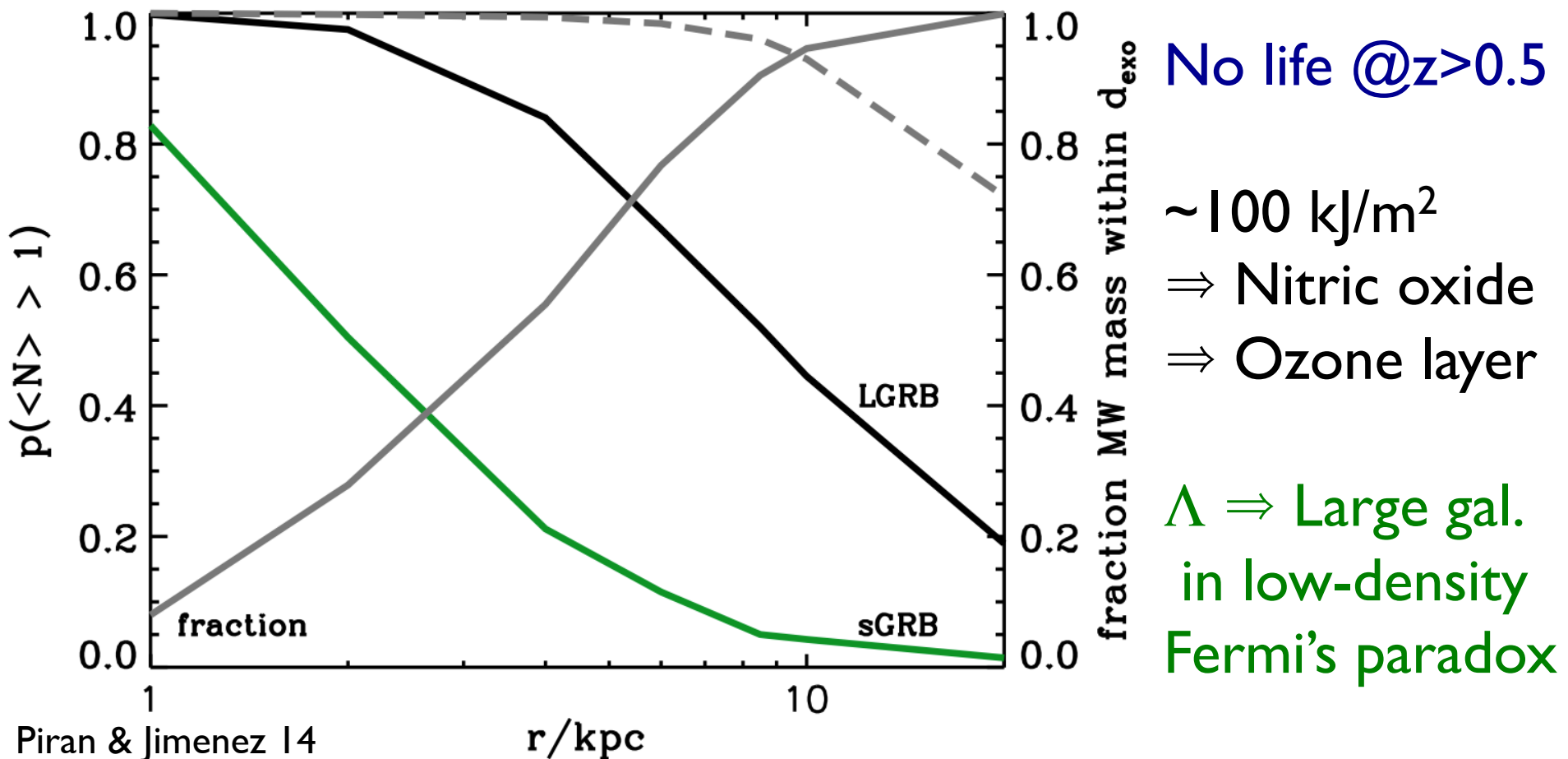
Dust extinction
⇒ Dark afterglow

Hatsukade+ 14
Stanway+ 14 for GRB 080517

Life Extinction

Lethal GRBs are abundant in the inner Galaxy

Low-density region in the outskirts of large galaxies is safe



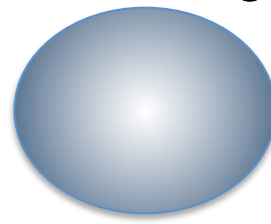
Contents for GRB

- GRB Cosmology
- ***Pop III GRB***
- Ultralong GRB
- Short GRB
- Other topics

Very Massive Pop III Star?

**Present Day
Massive Star**

$\sim 20M_{\odot}$



Abel+ 02; Bromm+ 02;
Omukai+ 03; Yoshida+ 08

**Pop III
(Zero Metal)**
 $\sim 1000M_{\odot}$
(!?)

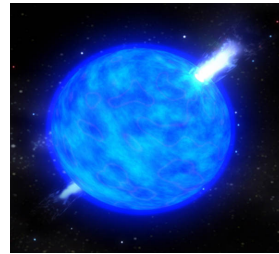
Mini halo (first object): $\sim 1000M_{\odot}$

If all the mass is accreted to a proto-star,

First stars are very MASSIVE?

Pop III GRB?

Present Day GRB

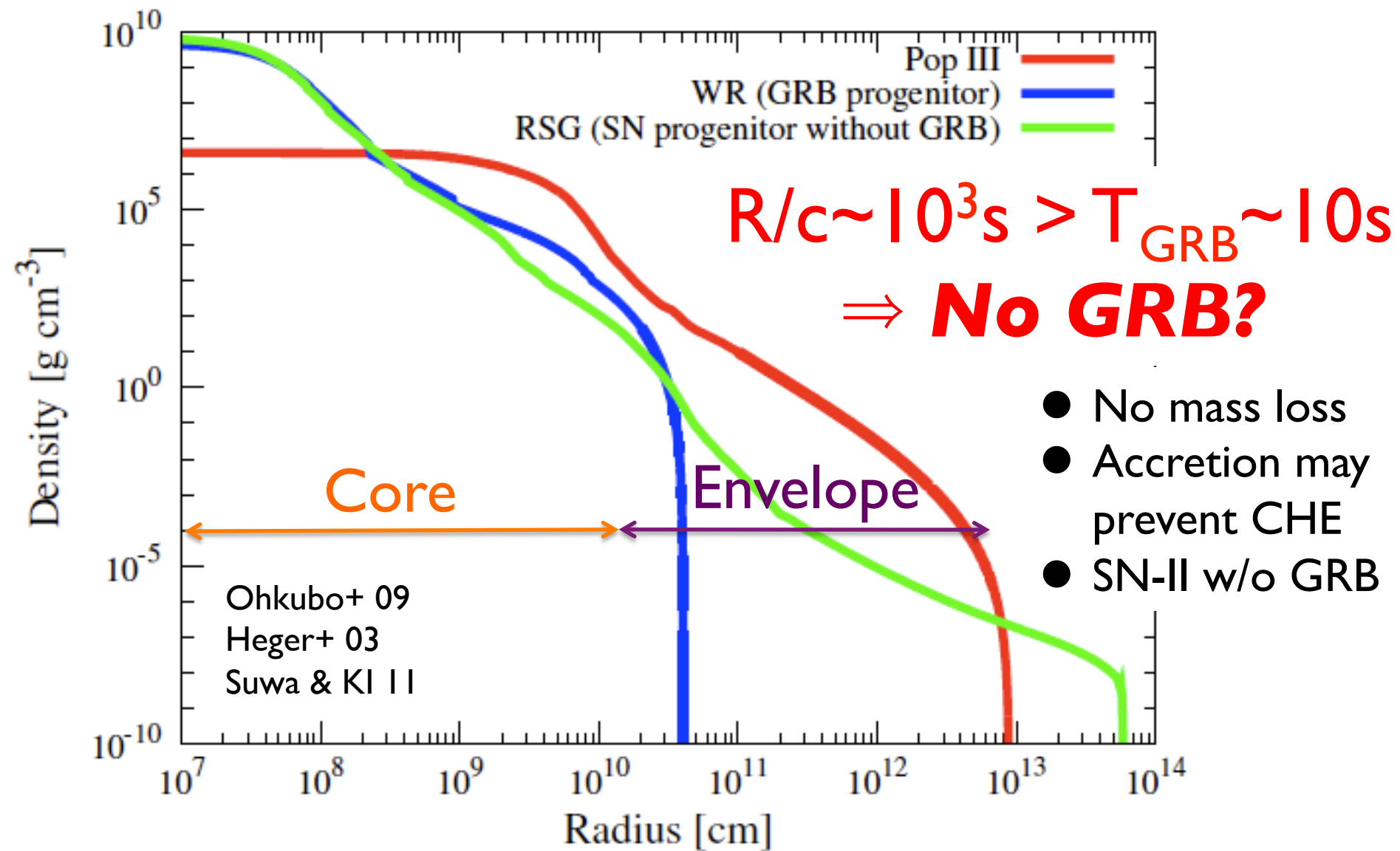


Komissarov & Barkov 10
Meszaros & Rees 10
Suwa & KI 11
Nagakura, Suwa & KI 12



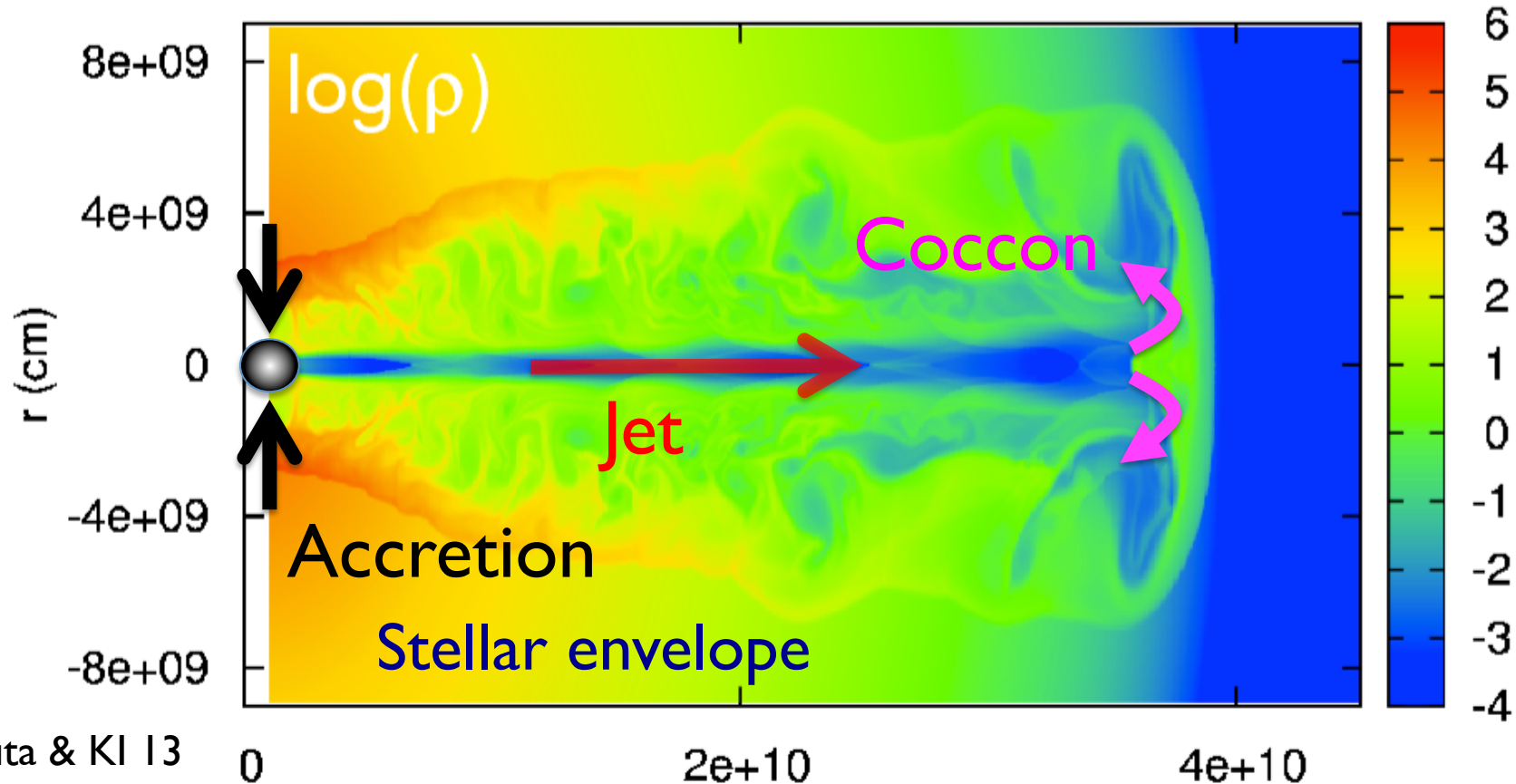
Gigantic ($\times 100$) GRB @ $z \sim 10-30???$

Massive Envelope



Duration ~ 10 sec?

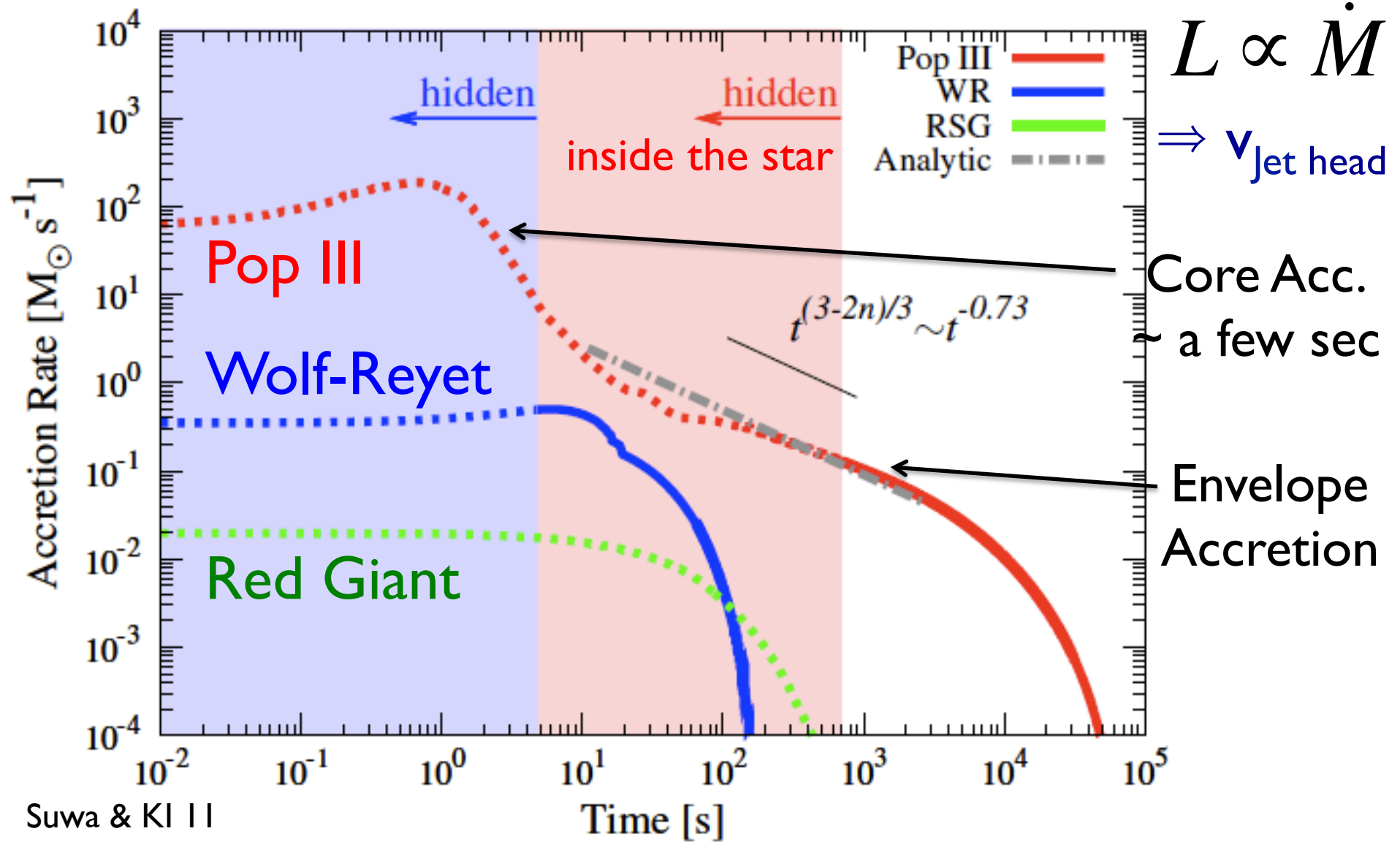
Loophole: $T_{Pop\ III\ GRB} \sim 10$ sec?

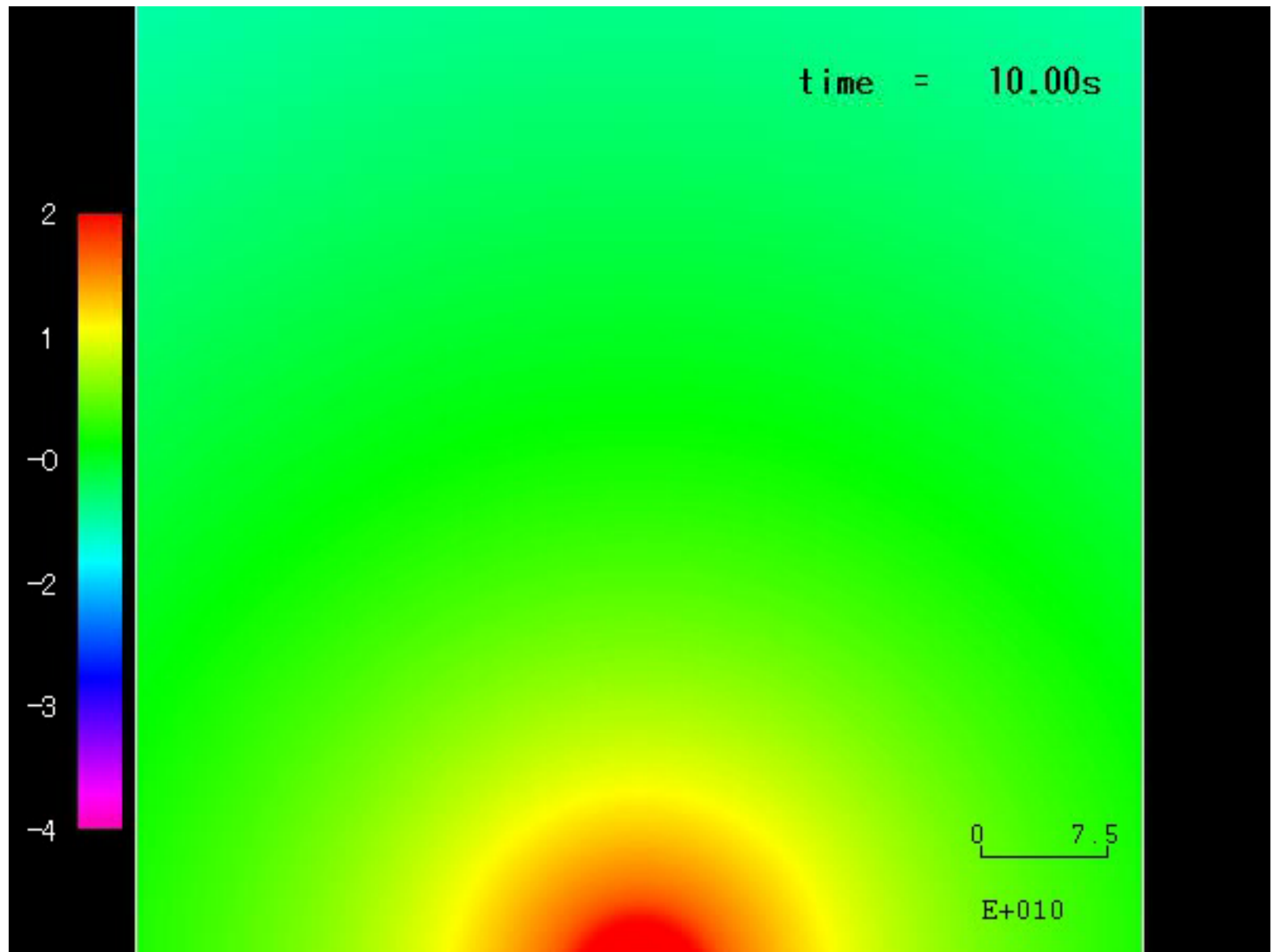


Mizuta & Ki 13

Big envelope is \circlearrowleft for jet injection but \times for penetration

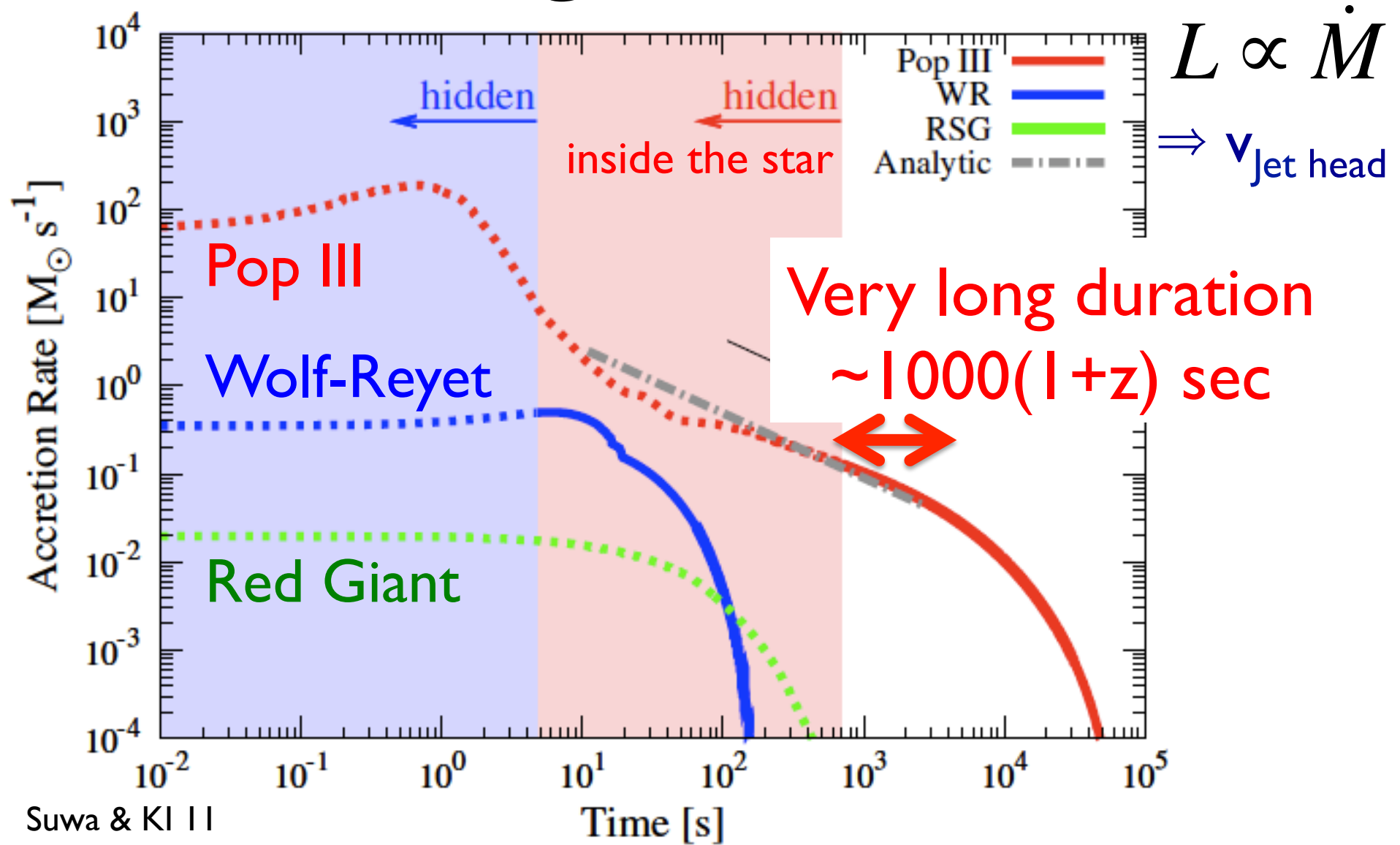
Envelope Accretion



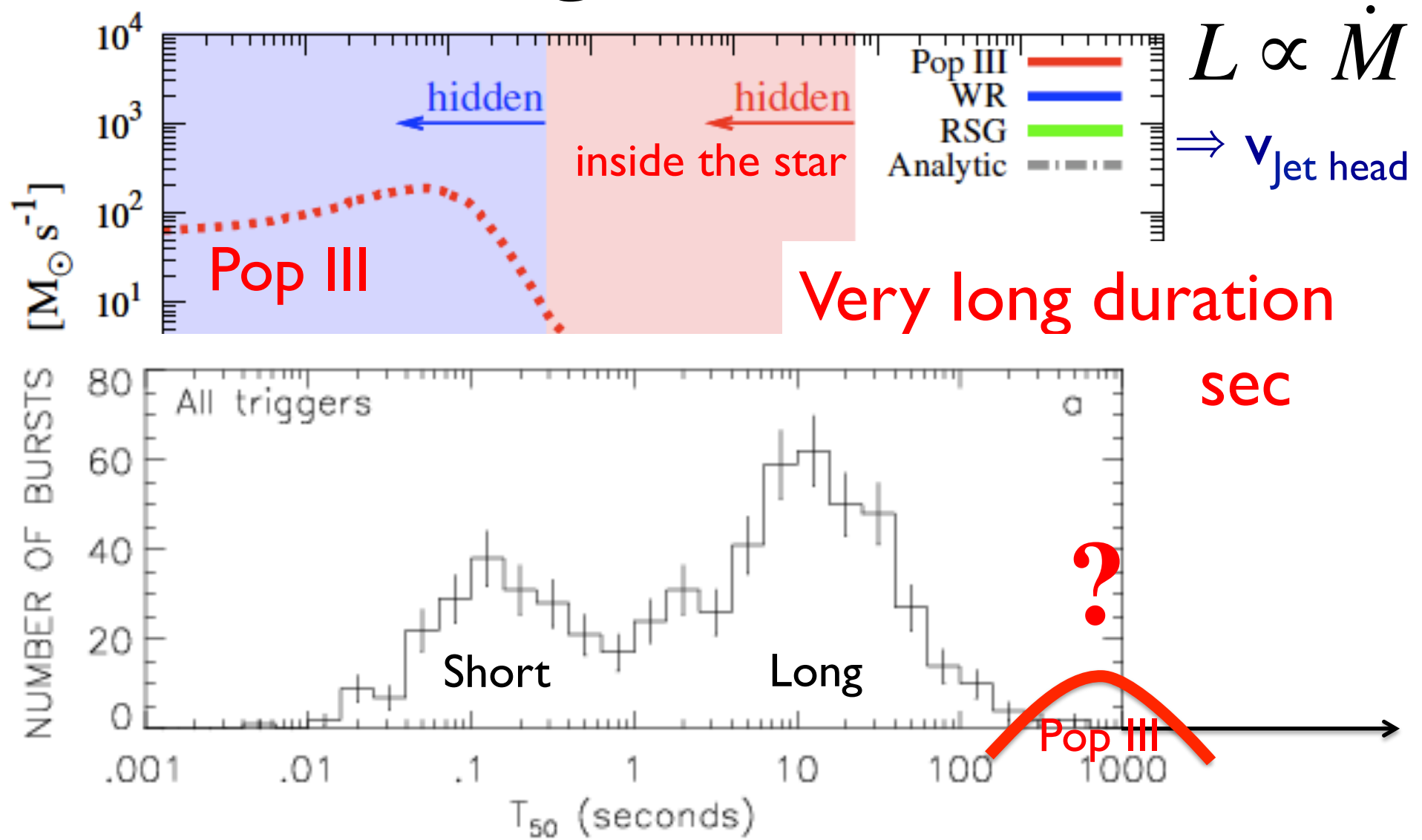


Nagakura+ 12 2D, rela-hydro, Mass accretion from inner boundary \Rightarrow Jet

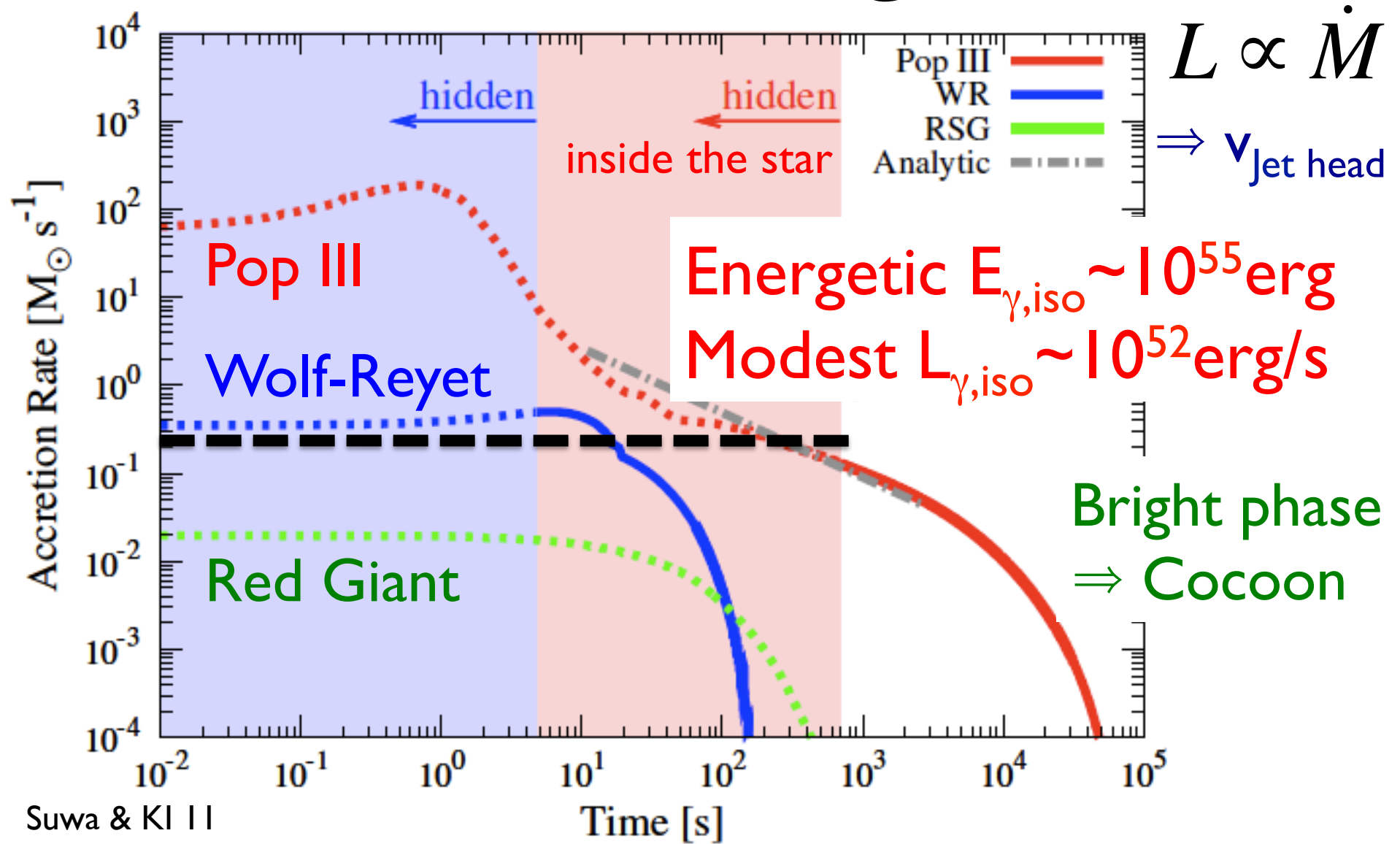
Long Duration



Long Duration



Not so Bright

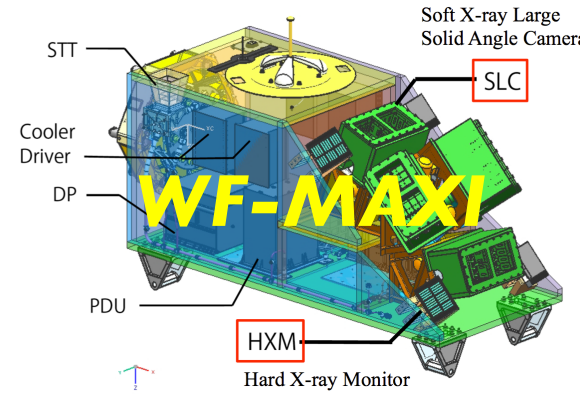
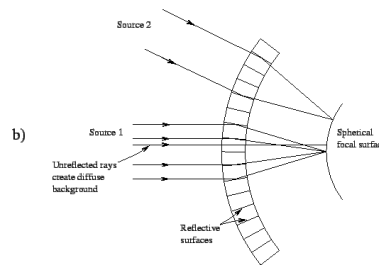


Detectability

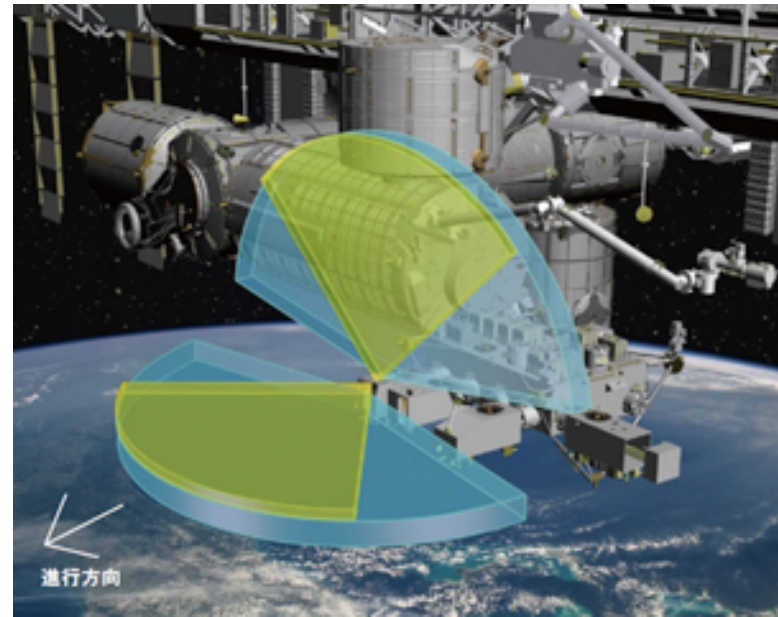
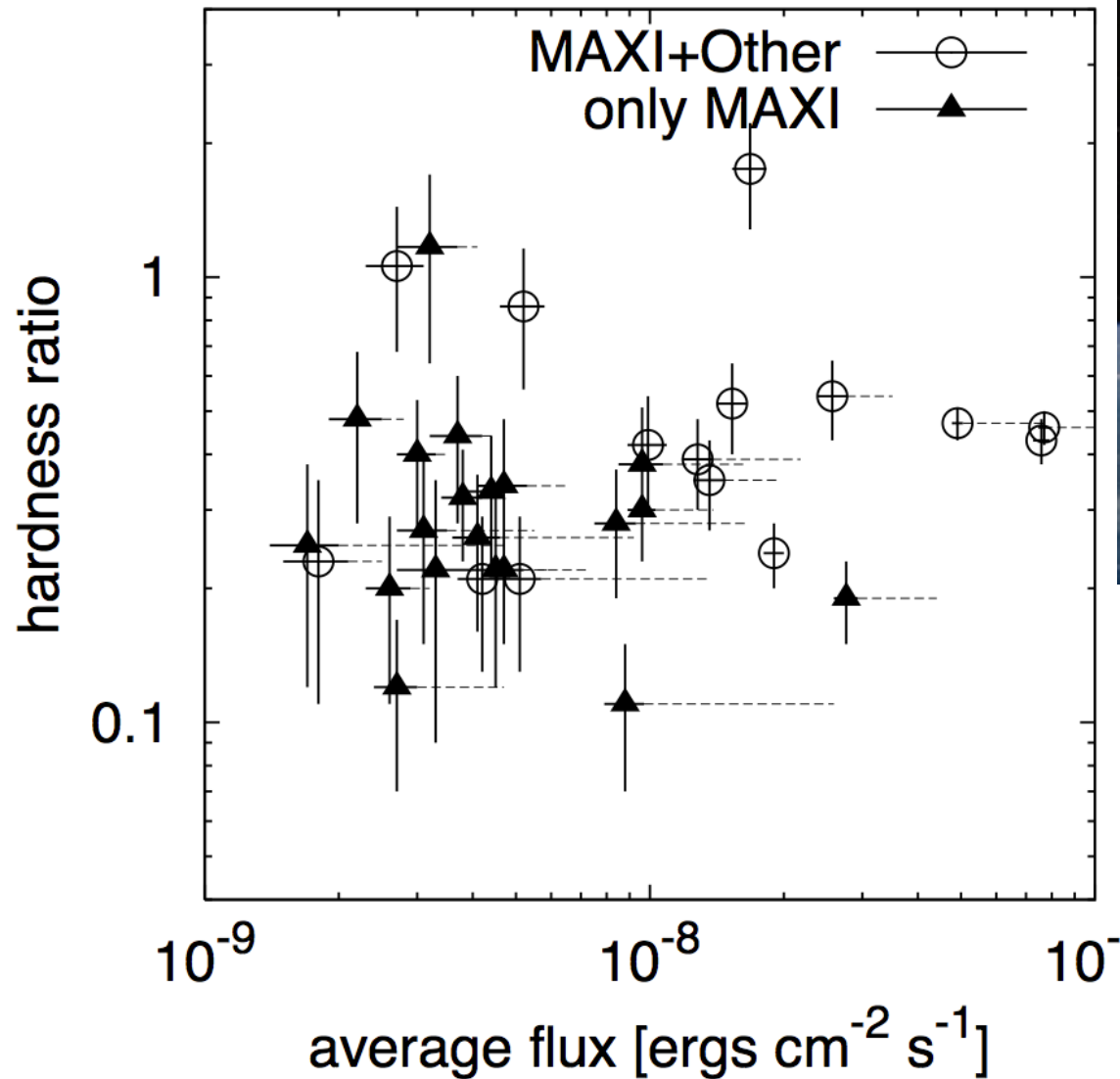
- Pop III GRB at $z \sim 20$

$$F = \frac{\varepsilon_\gamma L_{\text{iso}}}{4\pi r_L^2} \sim 10^{-9} \text{ erg cm}^{-2} \text{ s}^{-1}$$

- Swift BAT sensitivity $\sim 10^{-8} \text{ erg cm}^{-2} \text{ s}^{-1}$
- *Future soft X-ray surveys*

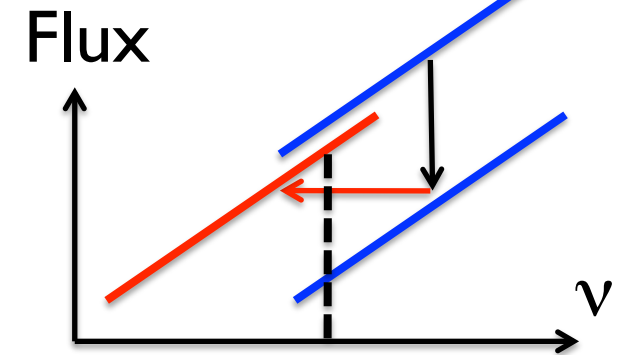
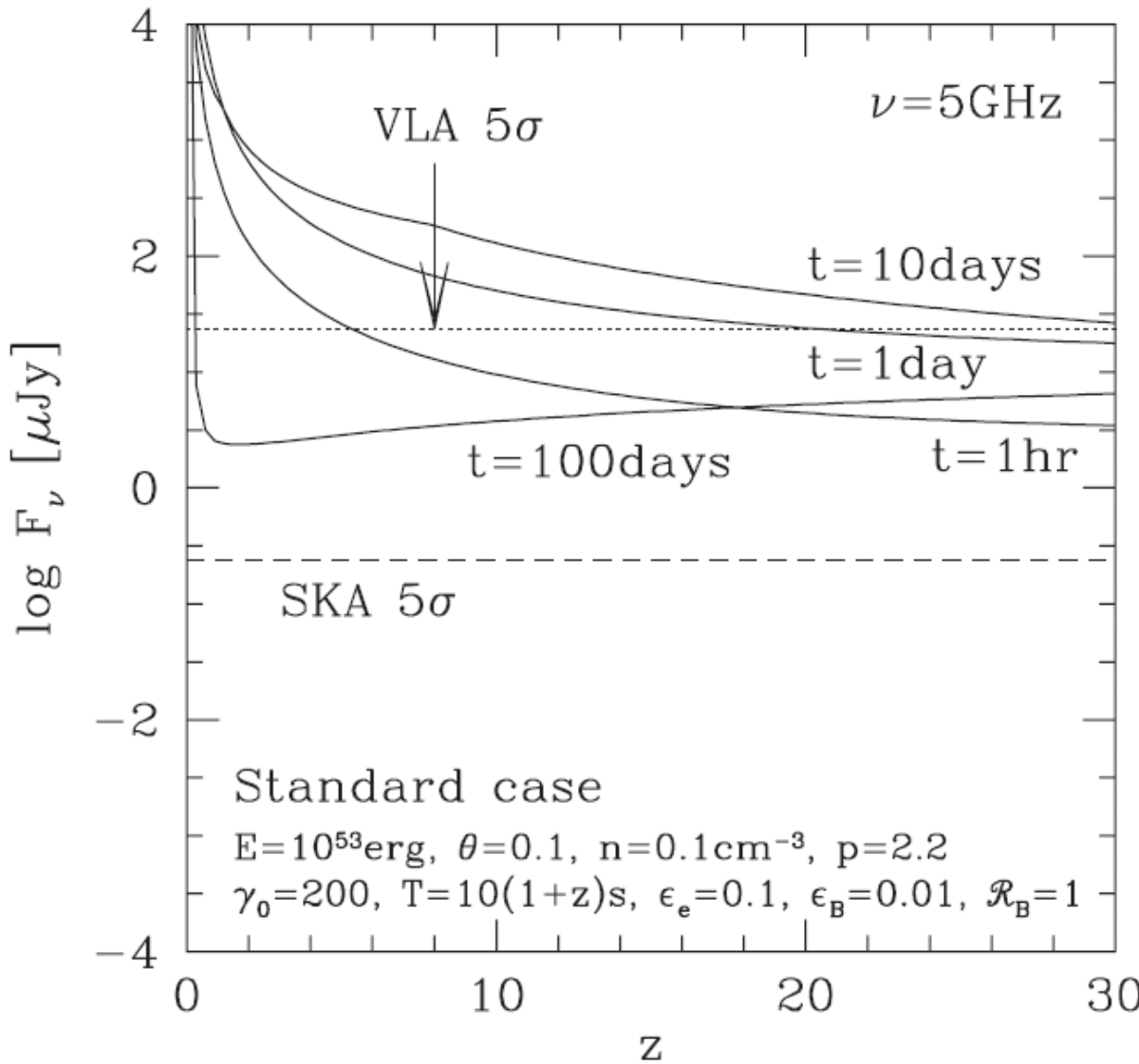


MAXI GRB



MAXI detects soft GRB,
such as **X-Ray Flashes**
(2-30 keV) (Aug 09-13)

Radio Afterglow

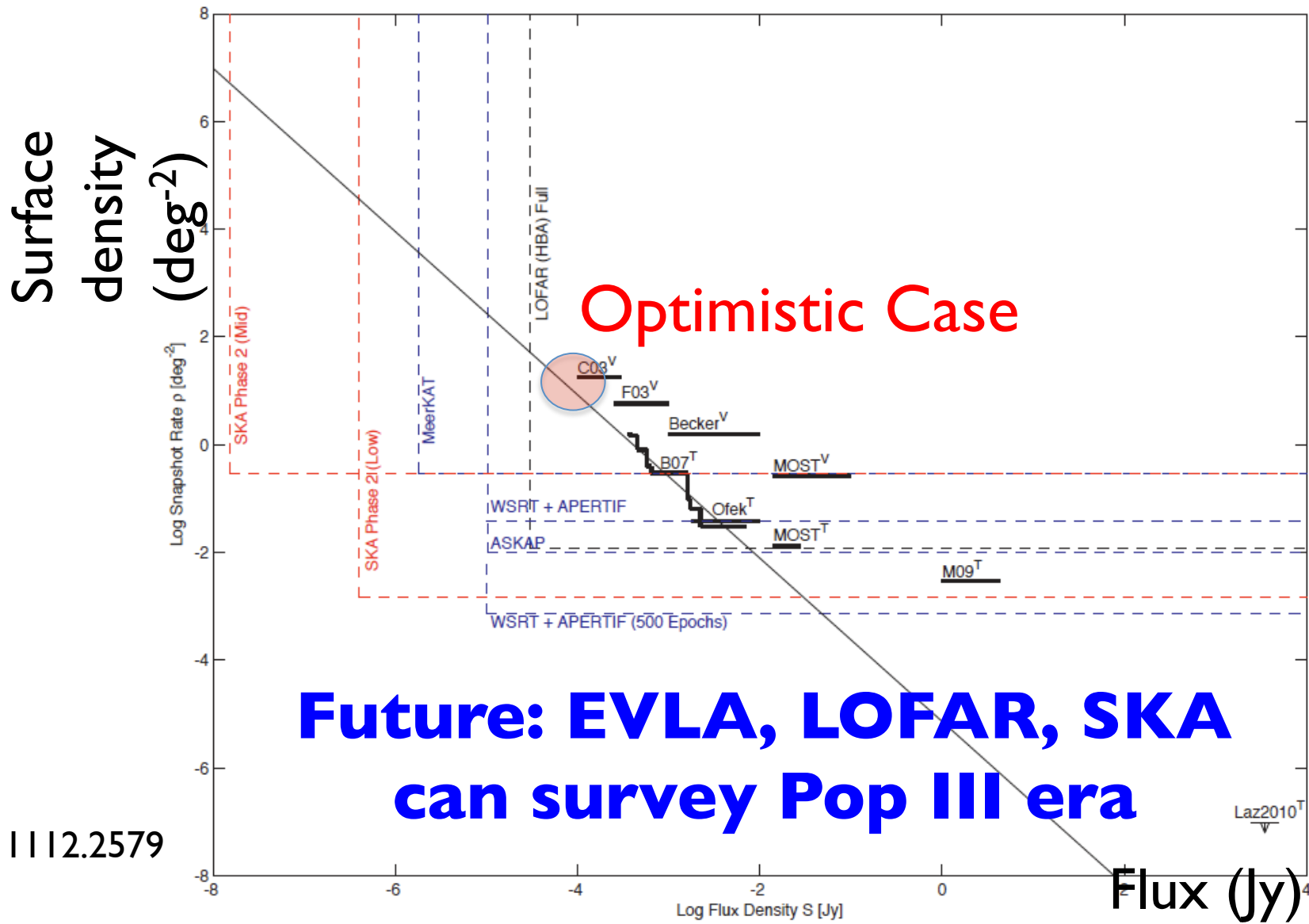


K-correction \Rightarrow
Not dim @high-z

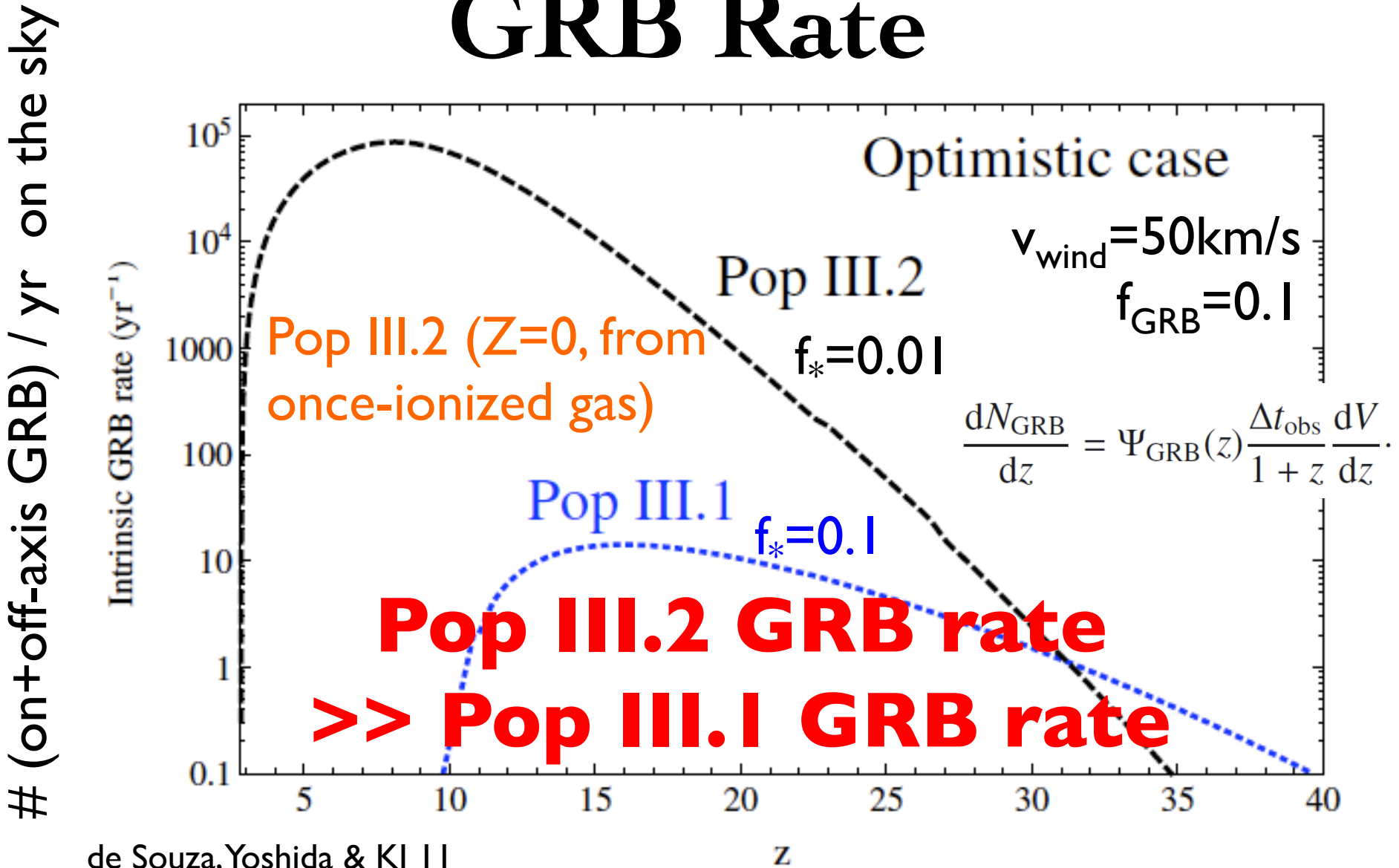
Spherical after
jet break

KI & Meszaros 05
Inoue+ 07, Toma+ 10

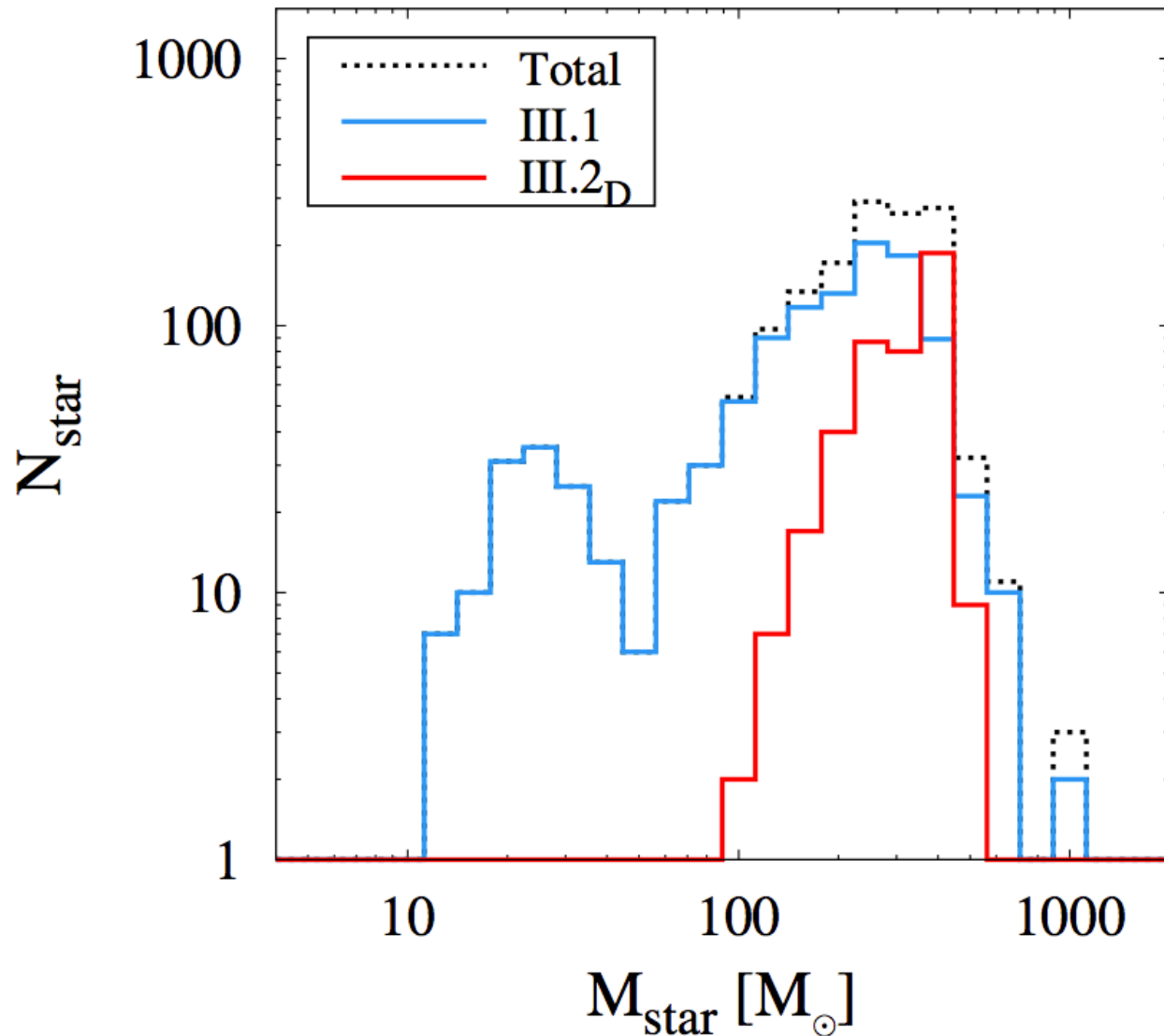
Future Radio Transient



Pop III.1 & III.2 GRB Rate



Pop III.2_D



#(Pop III.2)
< #(Pop III.2_D)

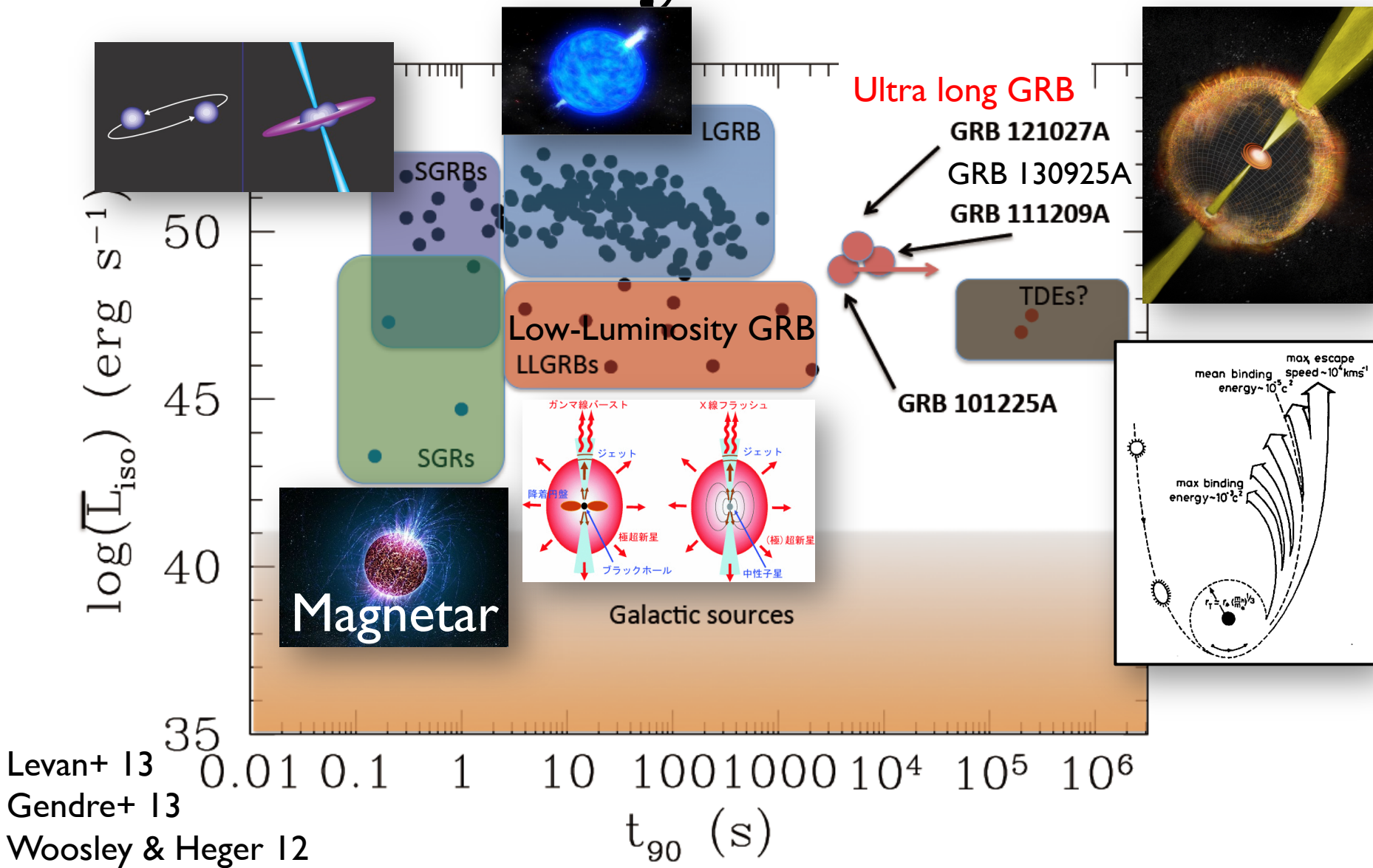
GRB III.2_D is
more energetic
than GRB III.2
(easy to detect)

Hirano+ 14

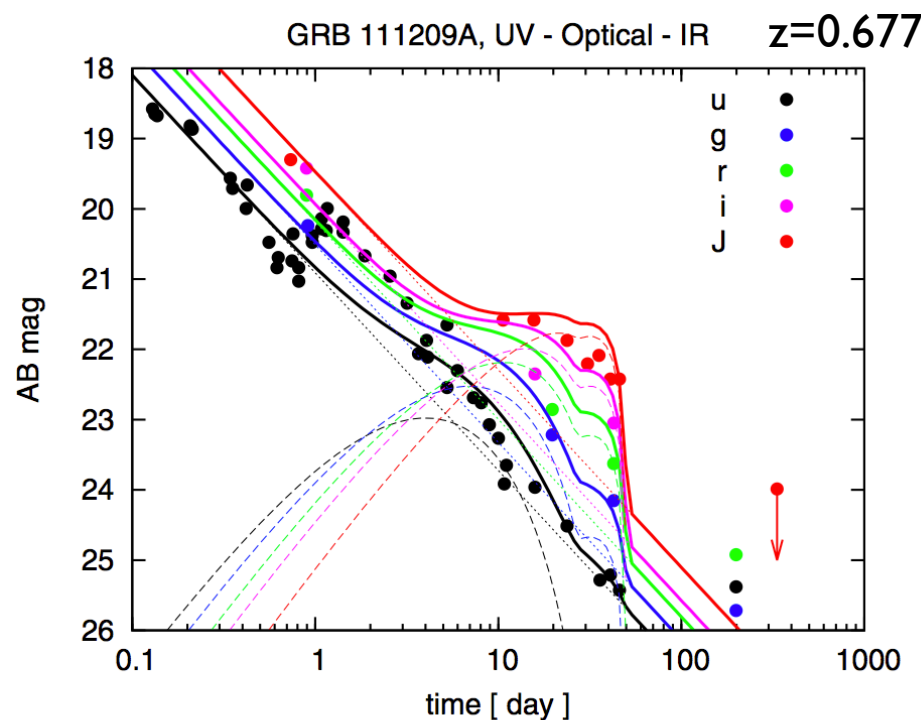
Contents for GRB

- GRB Cosmology
- Pop III GRB
- ***Ultralong GRB***
- Short GRB
- Other topics

Diversity of GRB

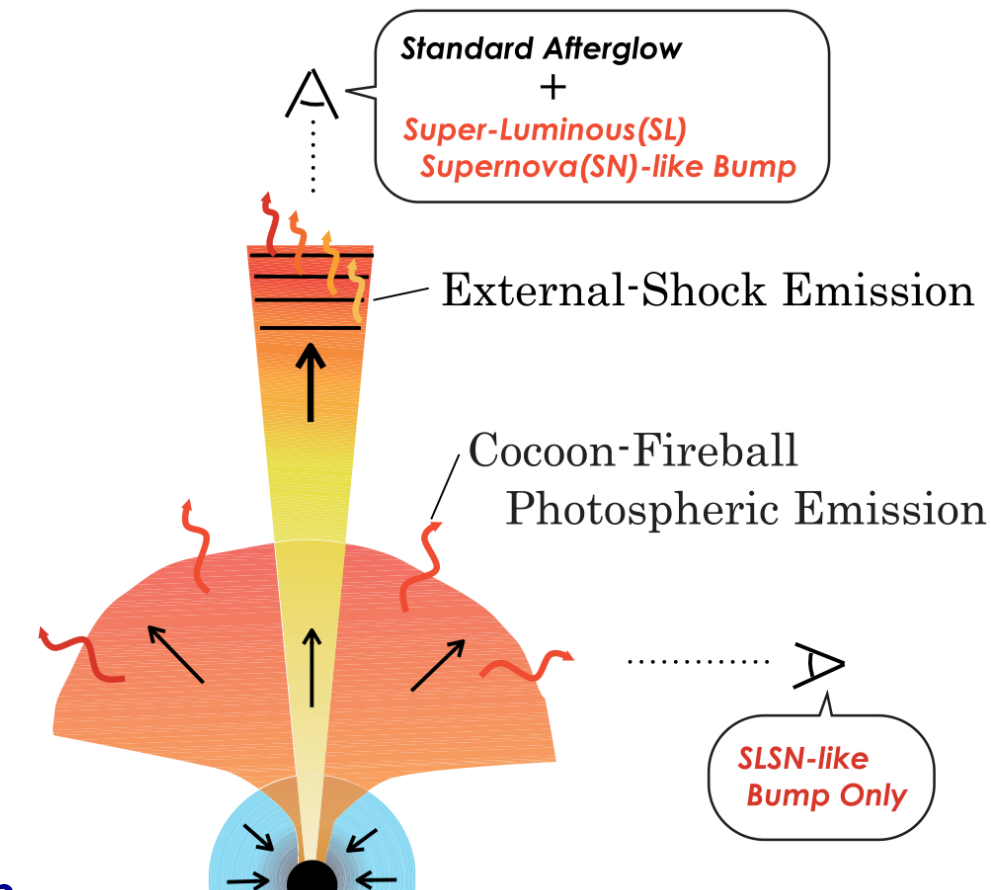


Cocoon Emission



Blue supergiant (BSG)
 $M=75M_{\odot}$, $Z=1e-4Z_{\odot}$, $R=8.6e12\text{cm}$
 $E_c=1e53 \text{ erg}$, $M_c=5.8M_{\odot}$

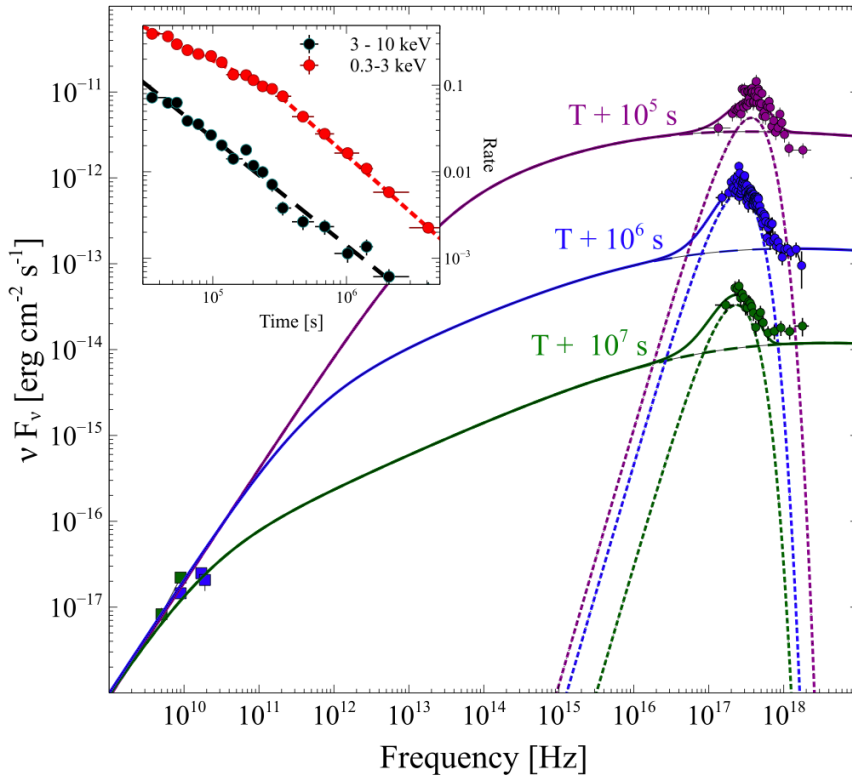
Nakauchi+ 13, 12; Kashiyama+ 13



**Cocoon thermal emission
 \approx Superluminous supernova**

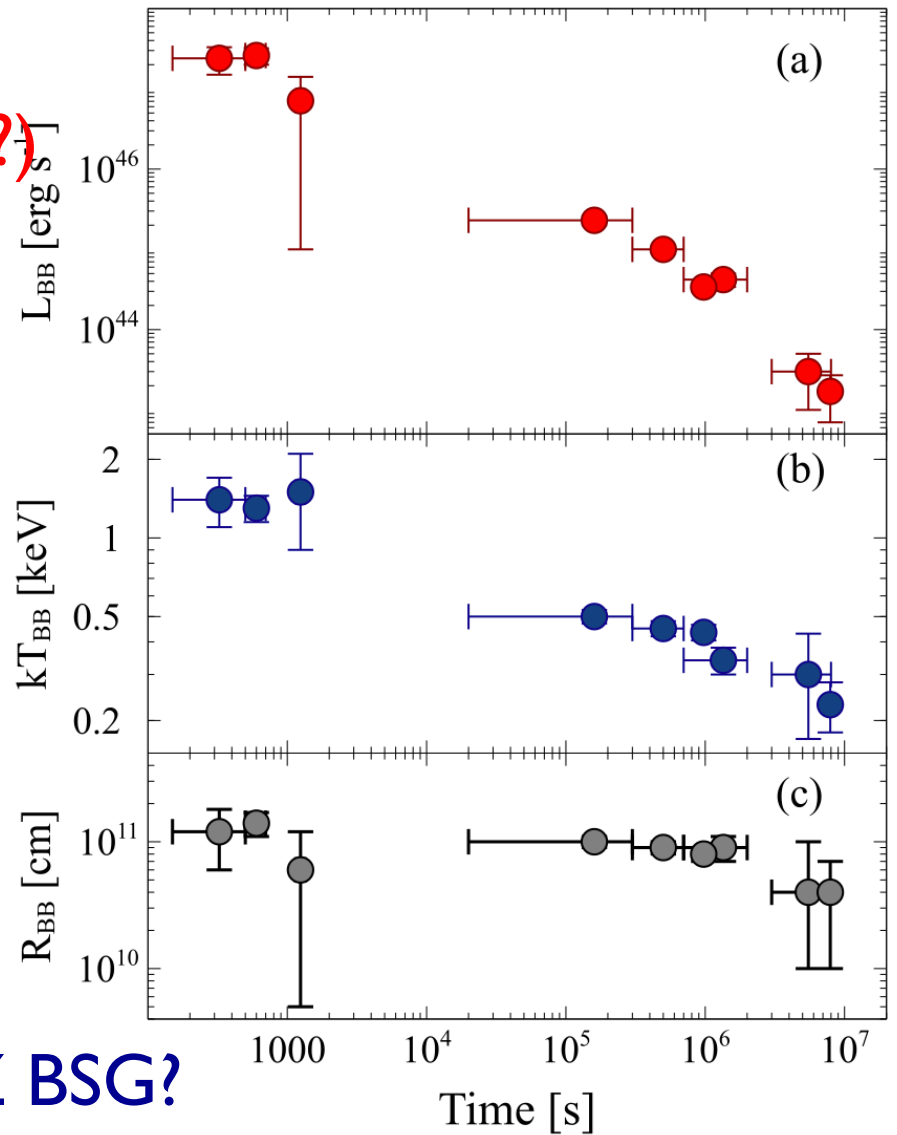
Ultralong GRB 130925A

**Afterglow in low density wind
+ Thermal component (Cocoon?)**

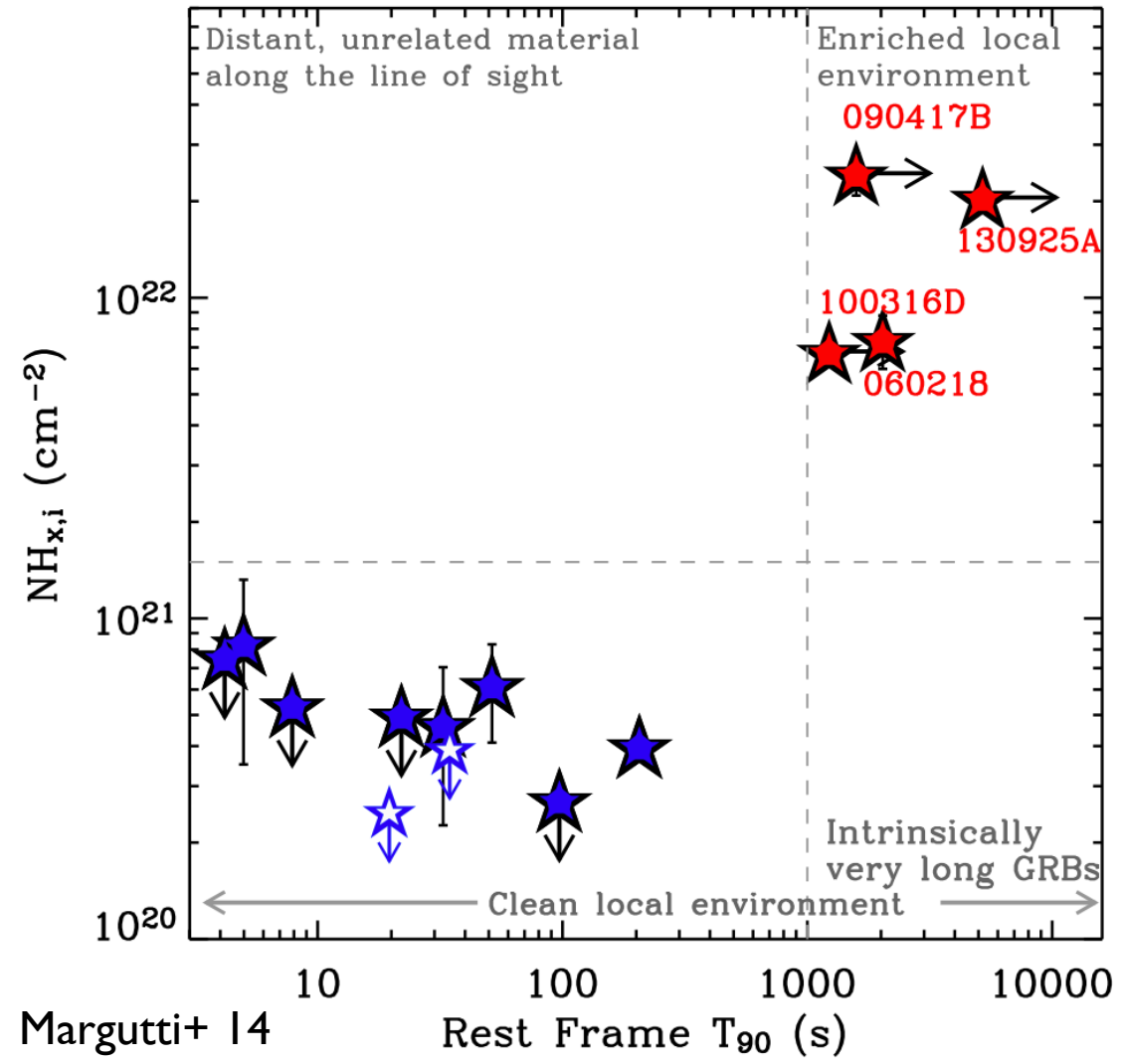


Piro+ 14; Zhao & Shao 14; Evans+ 14

$\sim 3 \times 10^{-8} M_\odot/\text{yr}$, $\sim 10^3 \text{ km/s} \Rightarrow \text{Low-Z BSG?}$



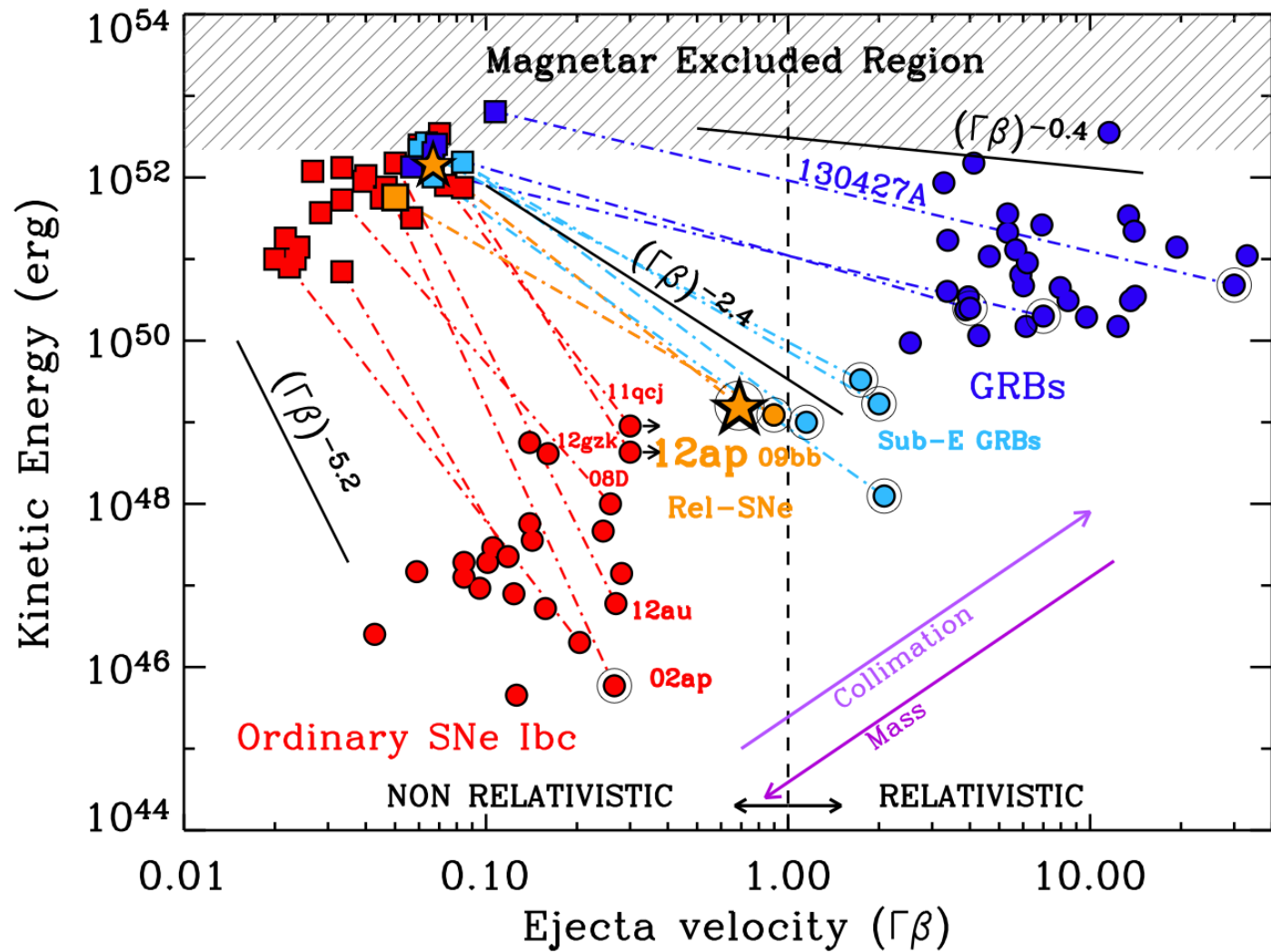
Mass Loss or Large Envelope?



\leftarrow with super-soft ($\Gamma > 3$)
late-time (>0.5 days)
X-ray emission
(not external shock)

- I. Recent mass loss**
 \Rightarrow Dust echo (late X) &
Wind-Jet shock (Long T)?
- 2. Large envelope**

Relativistic Supernova = Failed GRB?

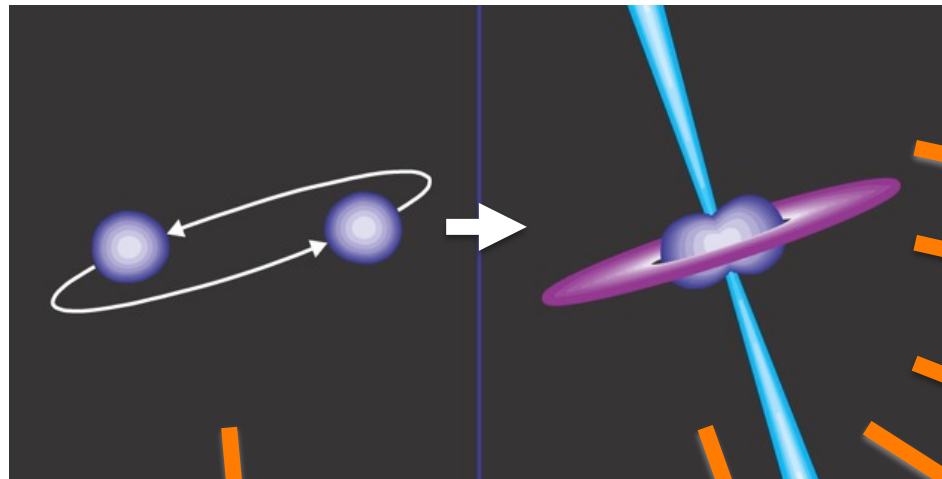


Contents for GRB

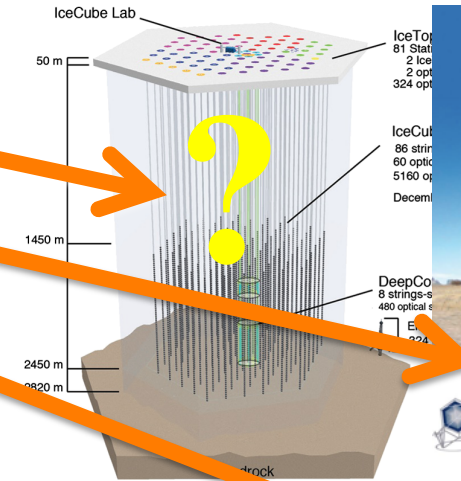
- GRB Cosmology
- Pop III GRB
- Ultralong GRB
- ***Short GRB***
- Other topics

Counterparts to GW

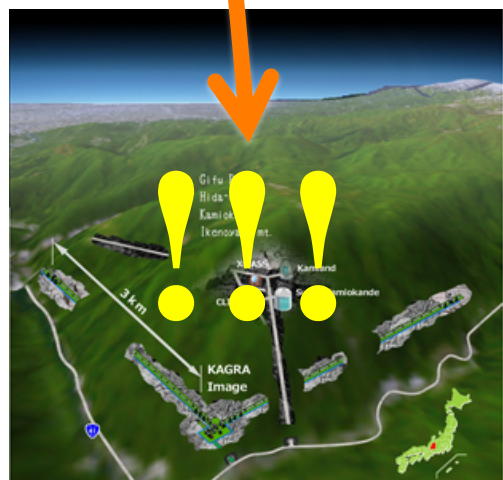
Gravitational Wave Sources



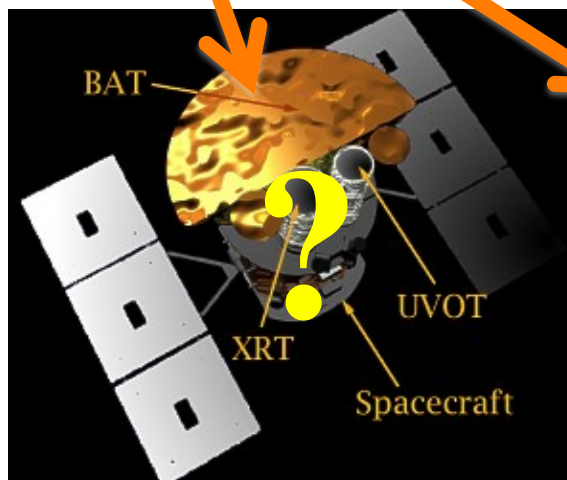
Neutrino



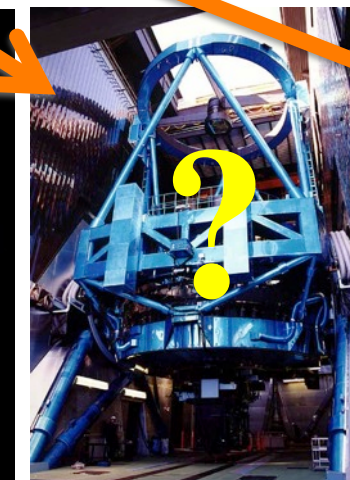
Gamma-ray



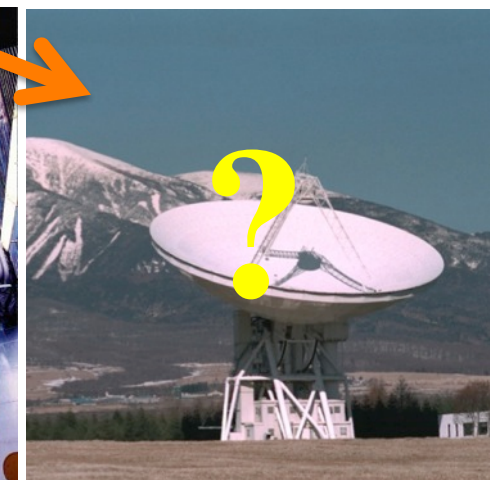
Gravitational wave



X-ray



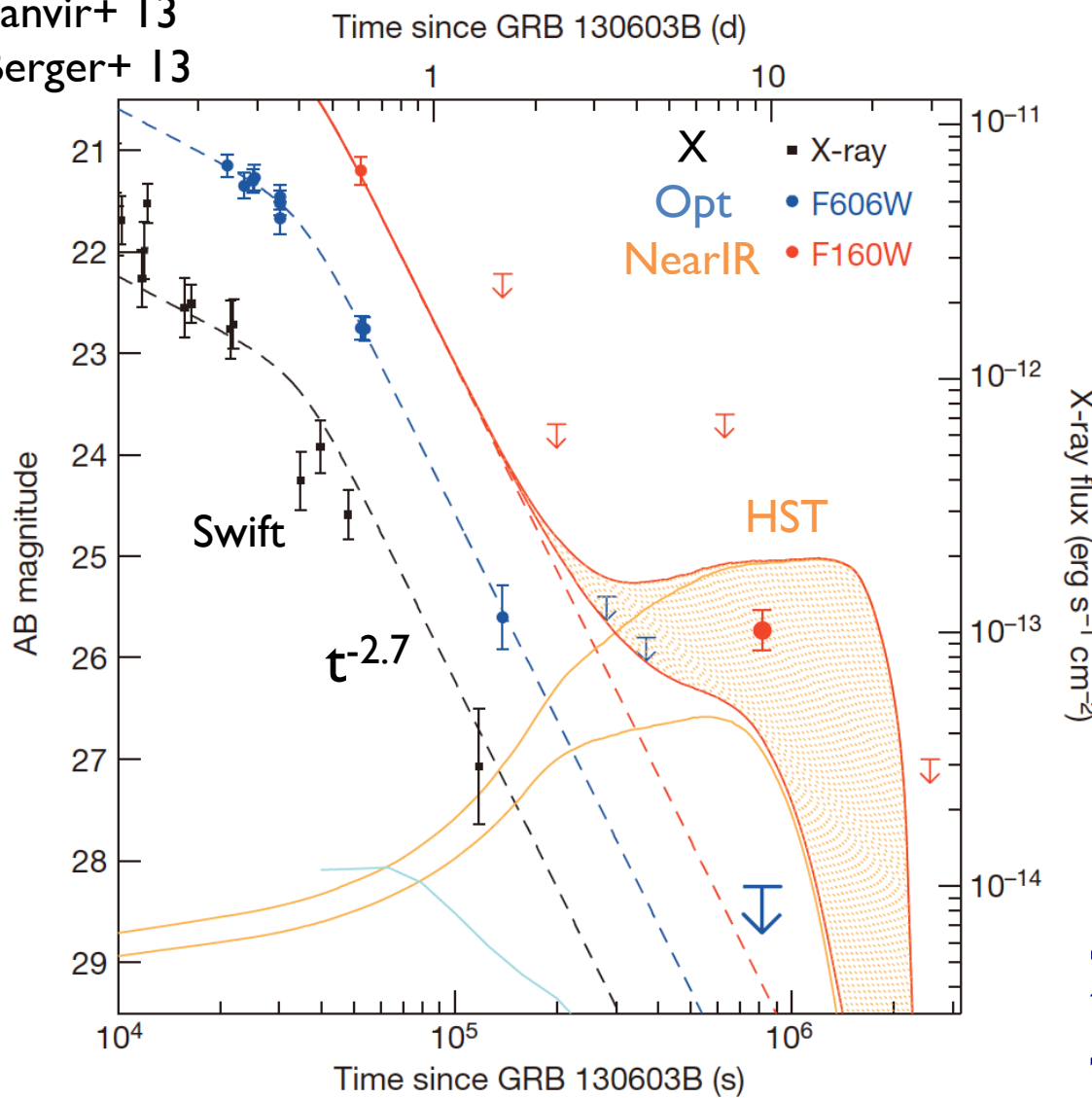
IR-Opt



Radio

Macro/Kilo/r-Process-Nova?

Tanvir+ 13
Berger+ 13

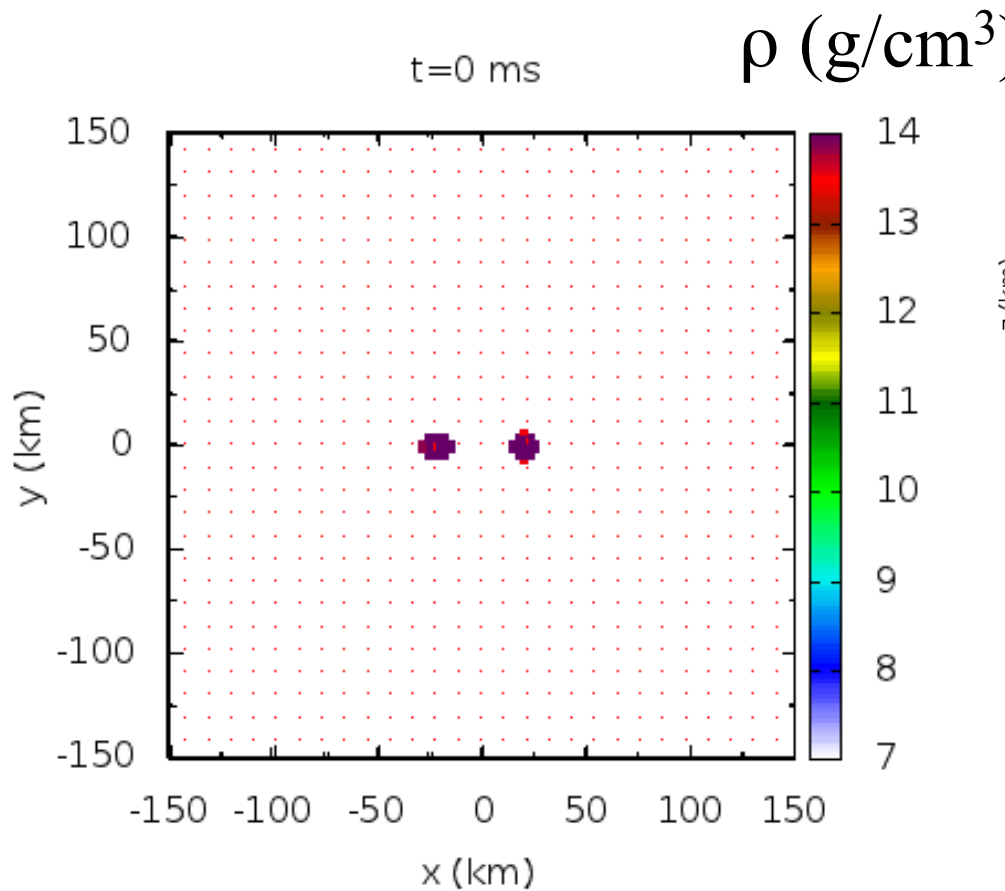


Ejecta with
 $\sim 0.01\text{-}0.1 M_{\odot}$
 $\sim 0.1\text{-}0.3 c$
 $\sim 10^{50}\text{-}10^{52} \text{erg}$
Radioactivity
 $f \sim \varepsilon_r / mc^2 \sim 3e-6$

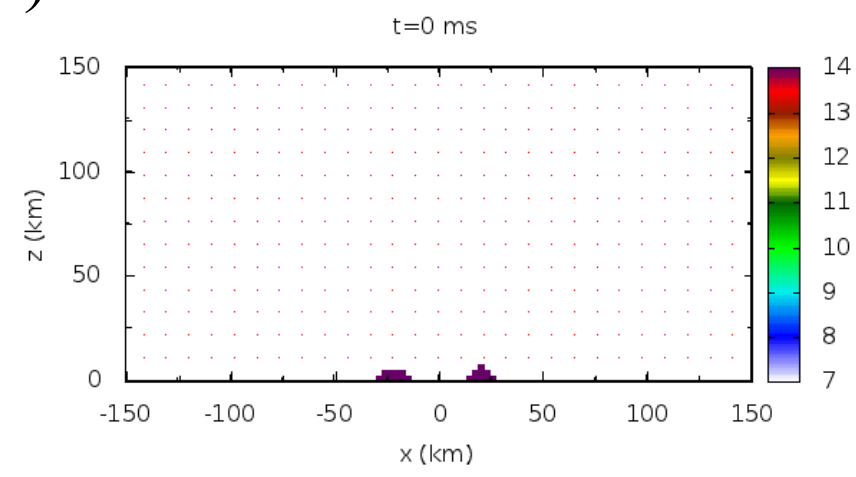
Li & Paczynski 98
Kulkarni 05

$L \sim 10^{41} \text{erg/s}$ @ $z \sim 0.356$
 22-23 mag if @ 200Mpc
 ~ 10 days

Merger of 1.3-1.4 M_{sun} NS: EOS=APR4: stiff but relatively soft



Orbital plane

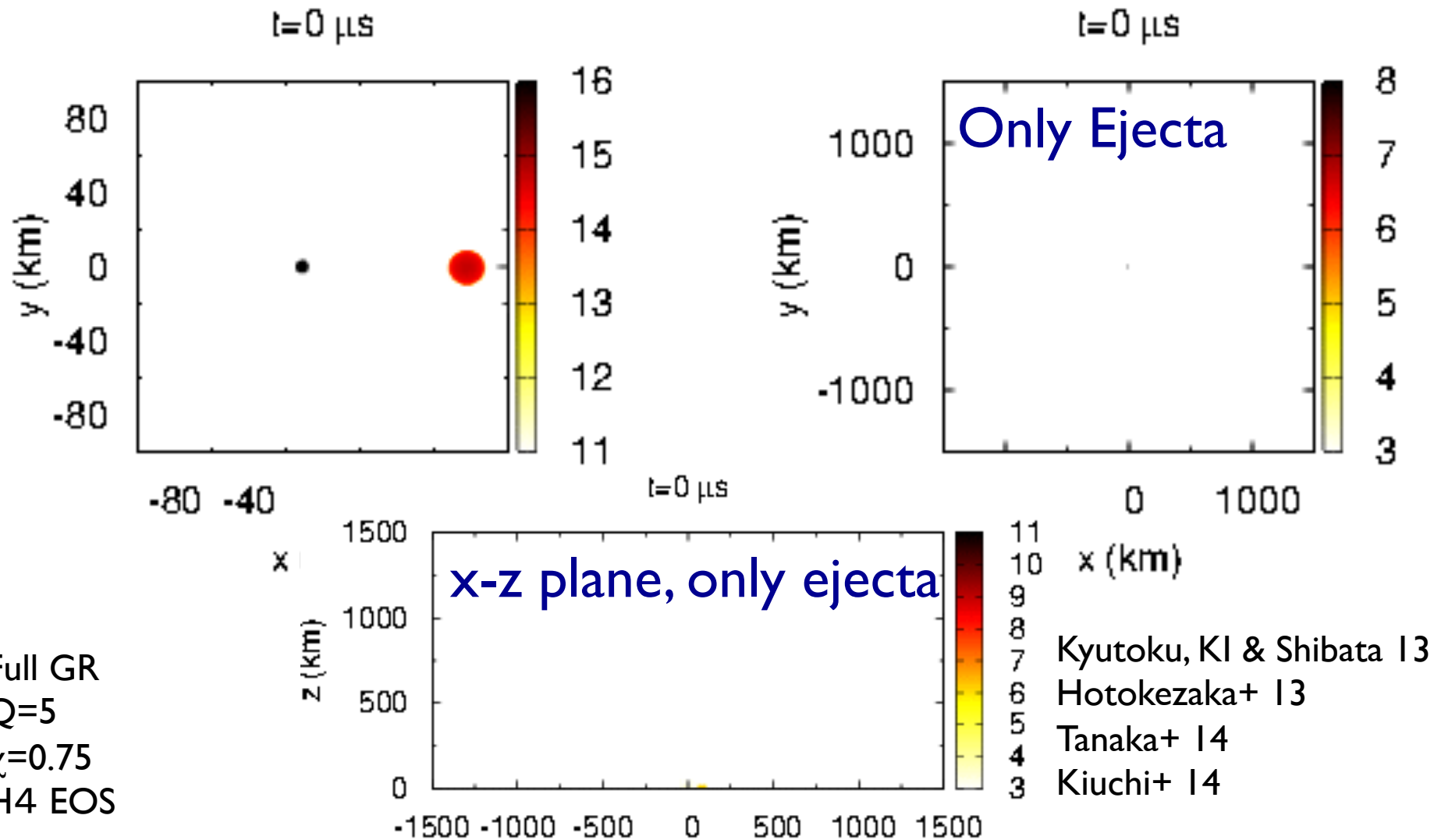


Relatively wider view

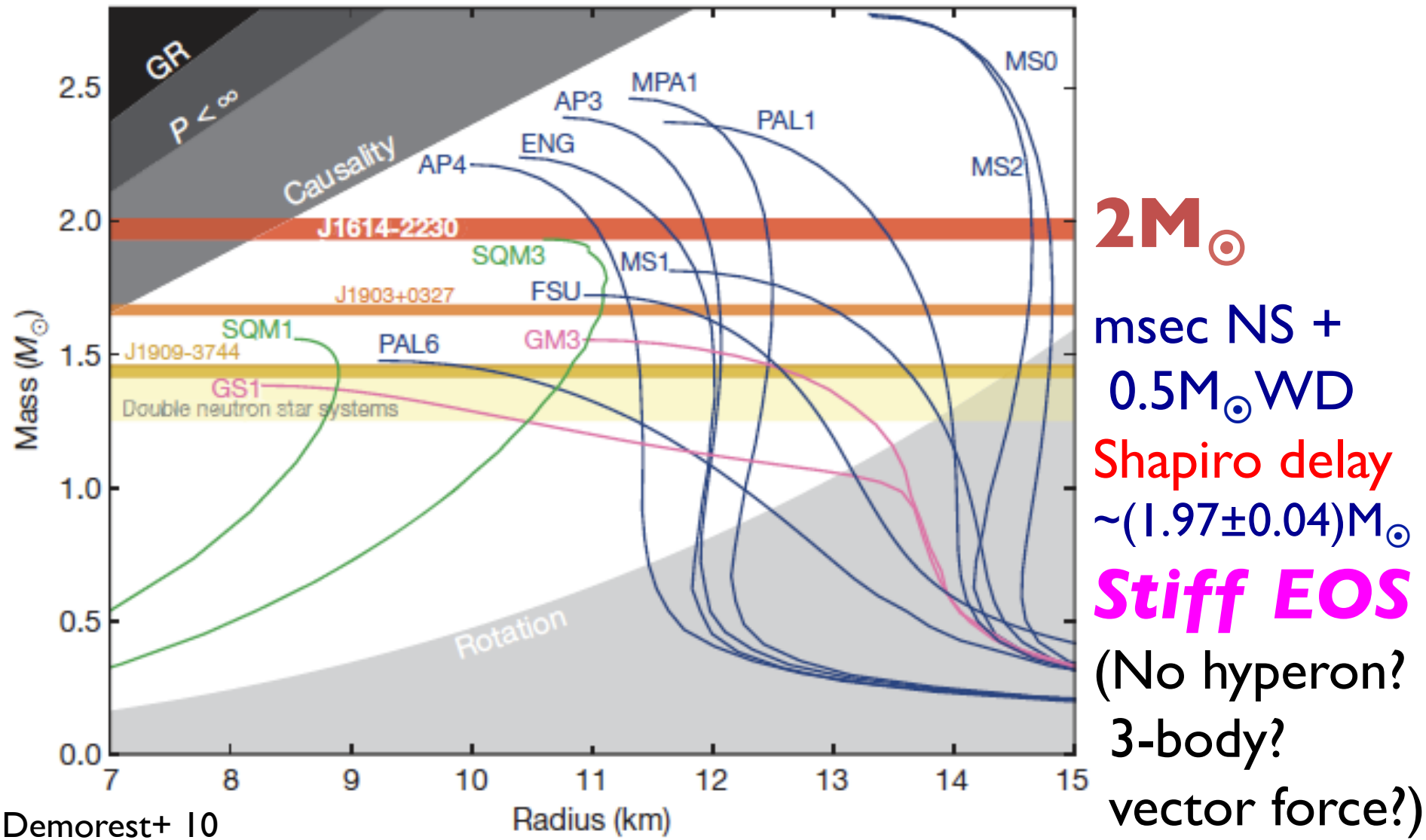
X-Z plane

BH-NS Merger

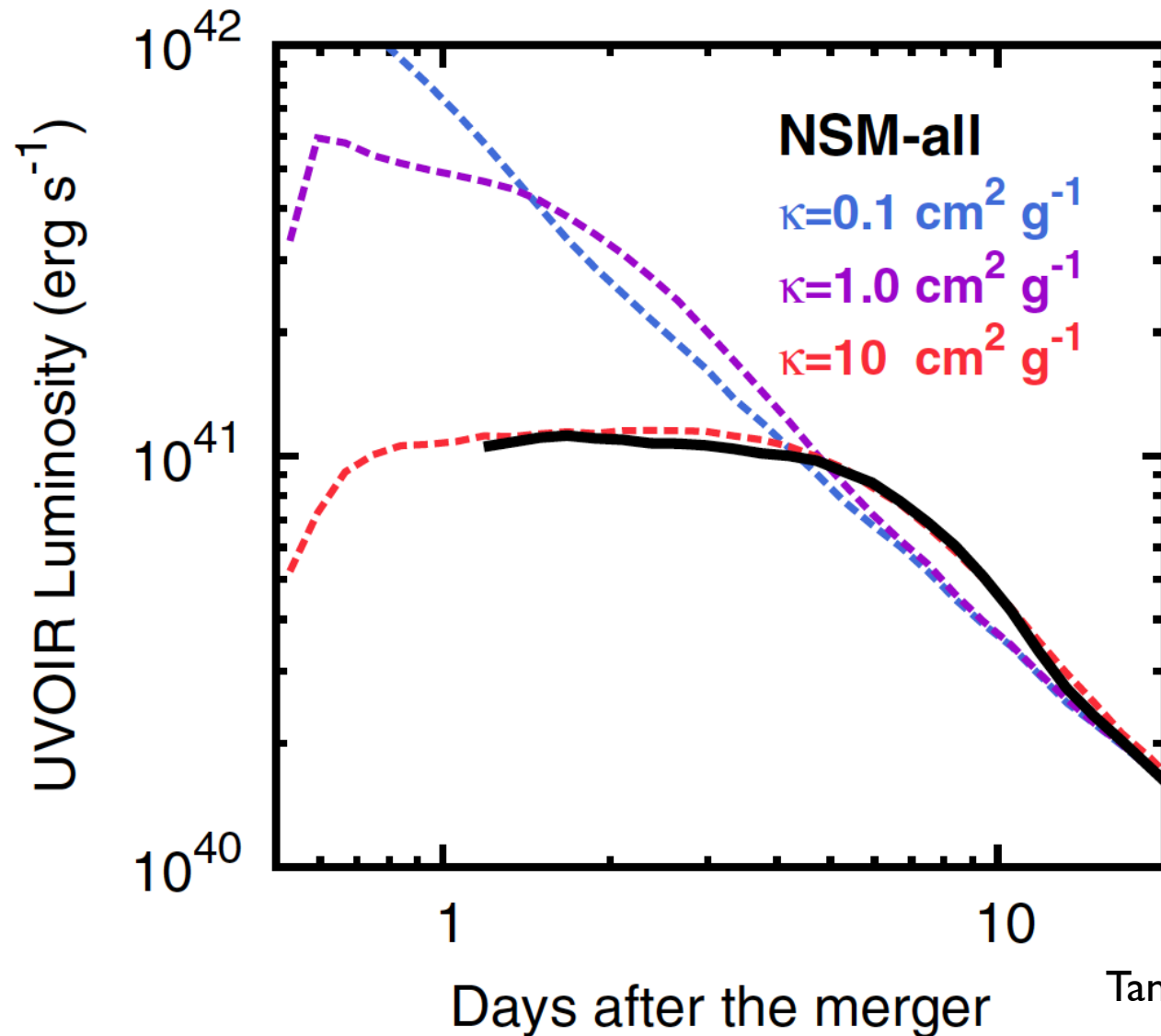
©Kyutoku



Maximum Mass



High Opacity

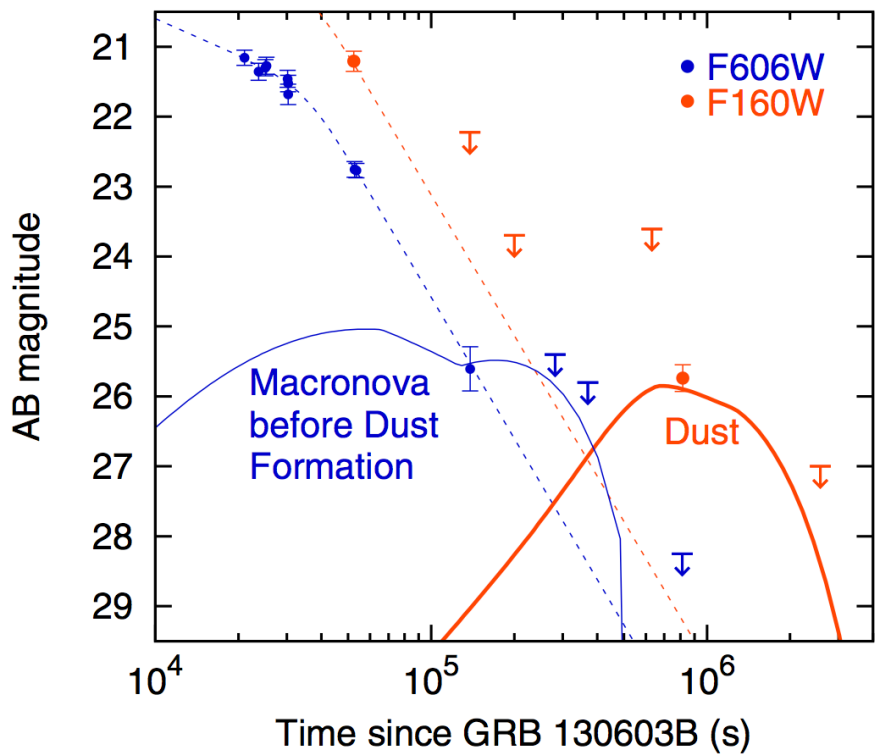


Supernova
Fe
 $\kappa \sim 0.1 \text{ cm}^2/\text{g}$

Macronova
r-process
 $\kappa \sim 10 \text{ cm}^2/\text{g}$

Alternative Models

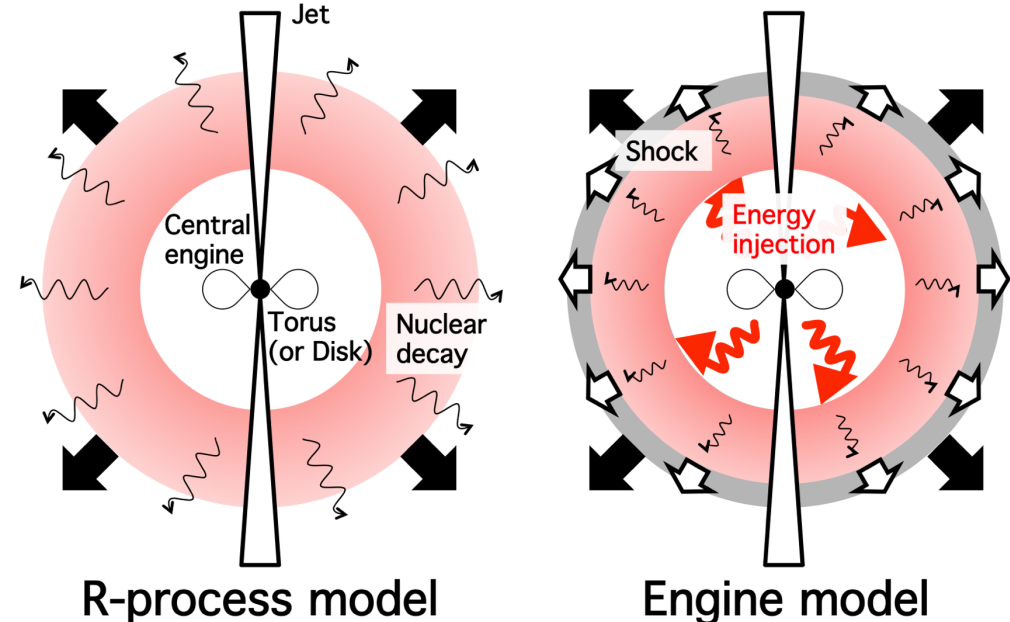
Dust for high opacity?



$$\kappa_{geometrical} = \frac{\pi r_{dust}^2}{m_{dust}} \sim \frac{\pi (N^{1/3} r_A)^2}{Nm_A} \sim 10^6 N^{-\frac{1}{3}} \text{ cm}^2 \text{ g}^{-1}$$

Takami, Nozawa & KI 14

Engine-Powered?



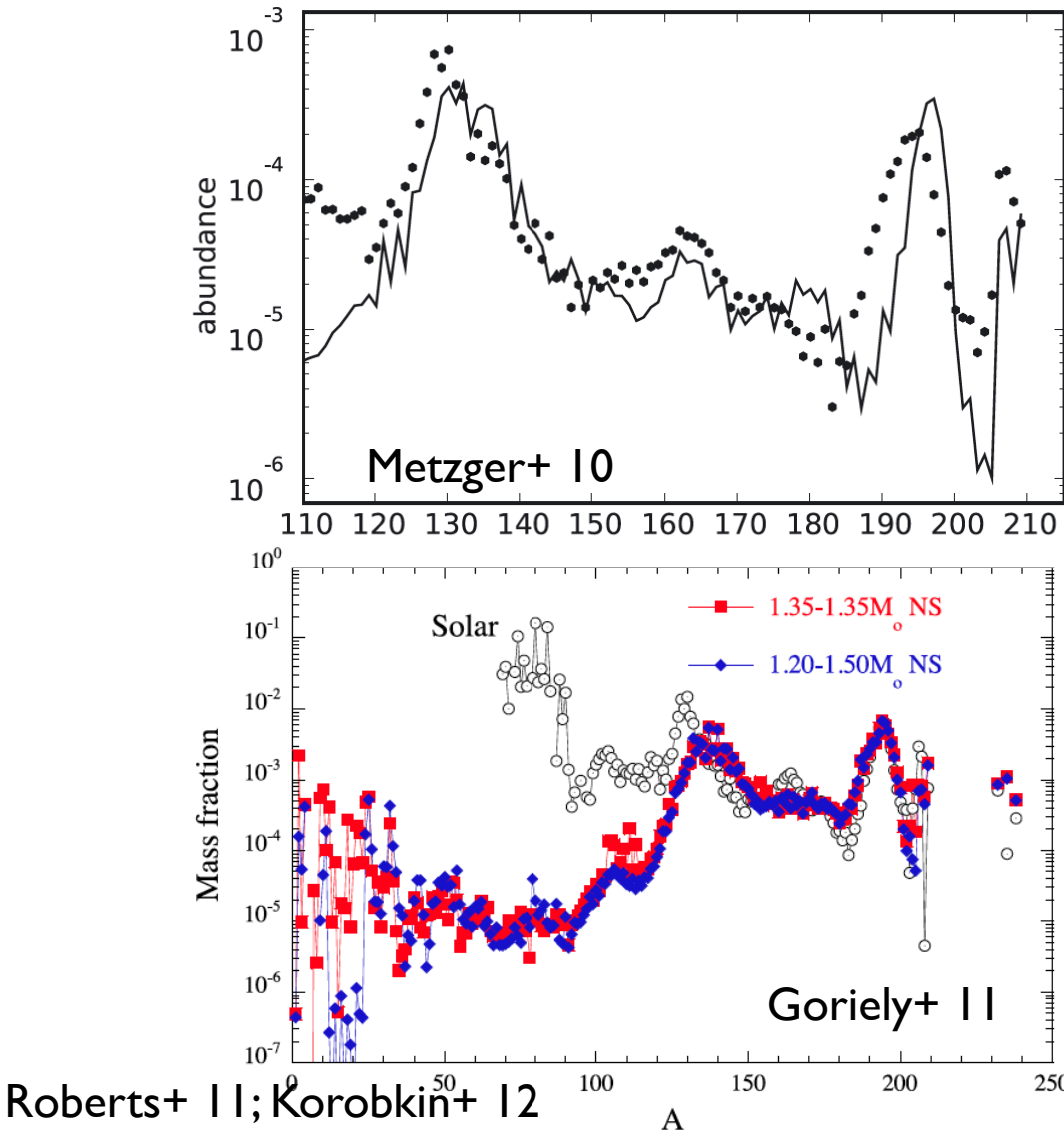
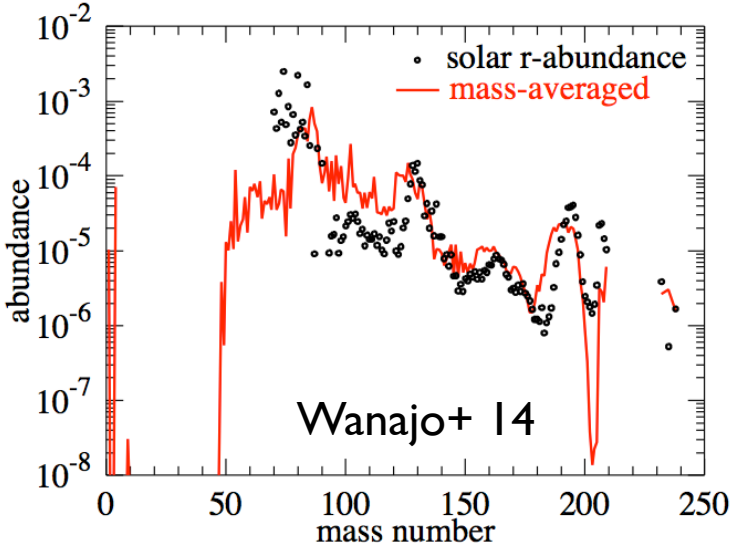
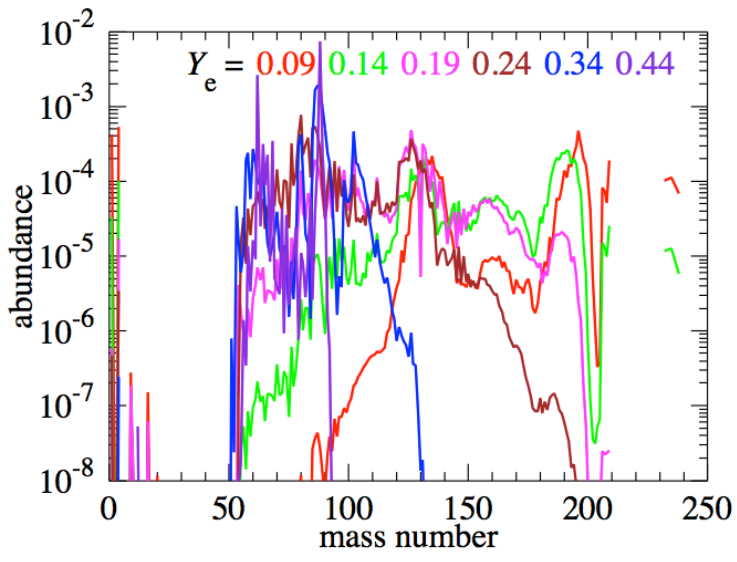
R-process model

$$L \sim \frac{E_{int0}}{t} \left(\frac{t}{t_{inj}} \right)^{-1} \sim 10^{41} \left(\frac{E_{int0}}{10^{51} \text{ erg}} \right) \left(\frac{t_{inj}}{10^2 \text{ s}} \right) \left(\frac{t}{10^6 \text{ s}} \right)^{-2} \text{ erg s}^{-1}$$

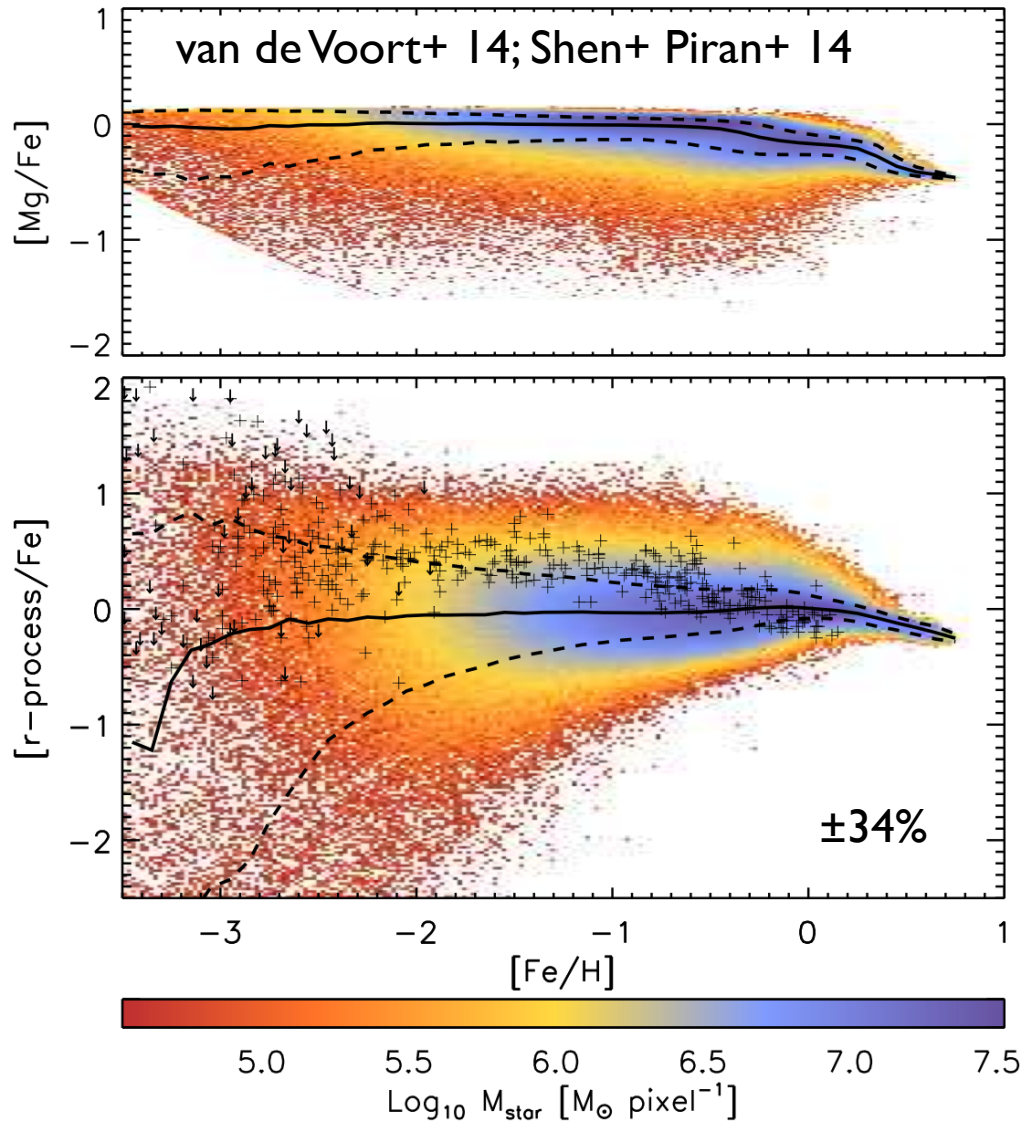
$$T \sim T_0 \left(\frac{t}{t_{inj}} \right)^{-1} \sim 2 \times 10^3 \left(\frac{E_{int0}}{10^{51} \text{ erg}} \right)^{1/4} \left(\frac{t_{inj}}{10^2 \text{ s}} \right)^{1/4} \times \left(\frac{v}{10^{10} \text{ cm s}^{-1}} \right)^{-3/4} \left(\frac{t}{10^6 \text{ s}} \right)^{-1} \text{ K.}$$

Kisaka, Takami & KI 14

r-Process Nucleosynthesis



r-Process Abundance



Cosmological zoom-in
simulation FIRE
Fe: Supernova
r-process: NS mergers

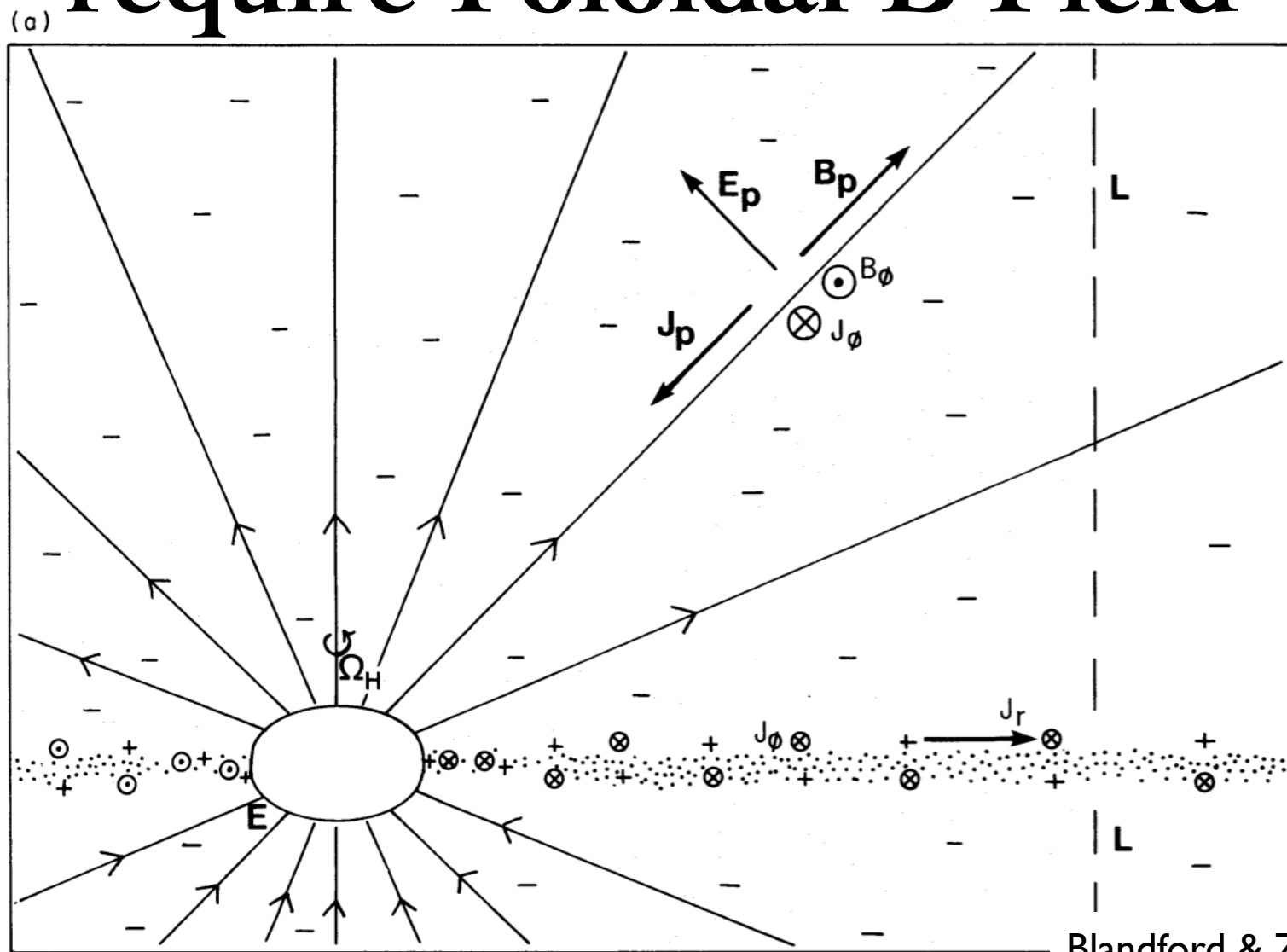
Mixing: wind, disk, ...
Less scatter in low metal
 $[r/\text{Fe}]$ decreases at large R_{gal}

Not converged yet at $\text{Fe} < -2$
< NS merger uncertainties
(Rate $\sim 1 \text{e-4}/\text{yr}$, $t_{\text{delay}} \sim 3 \times 10^7 \text{ yr}$)

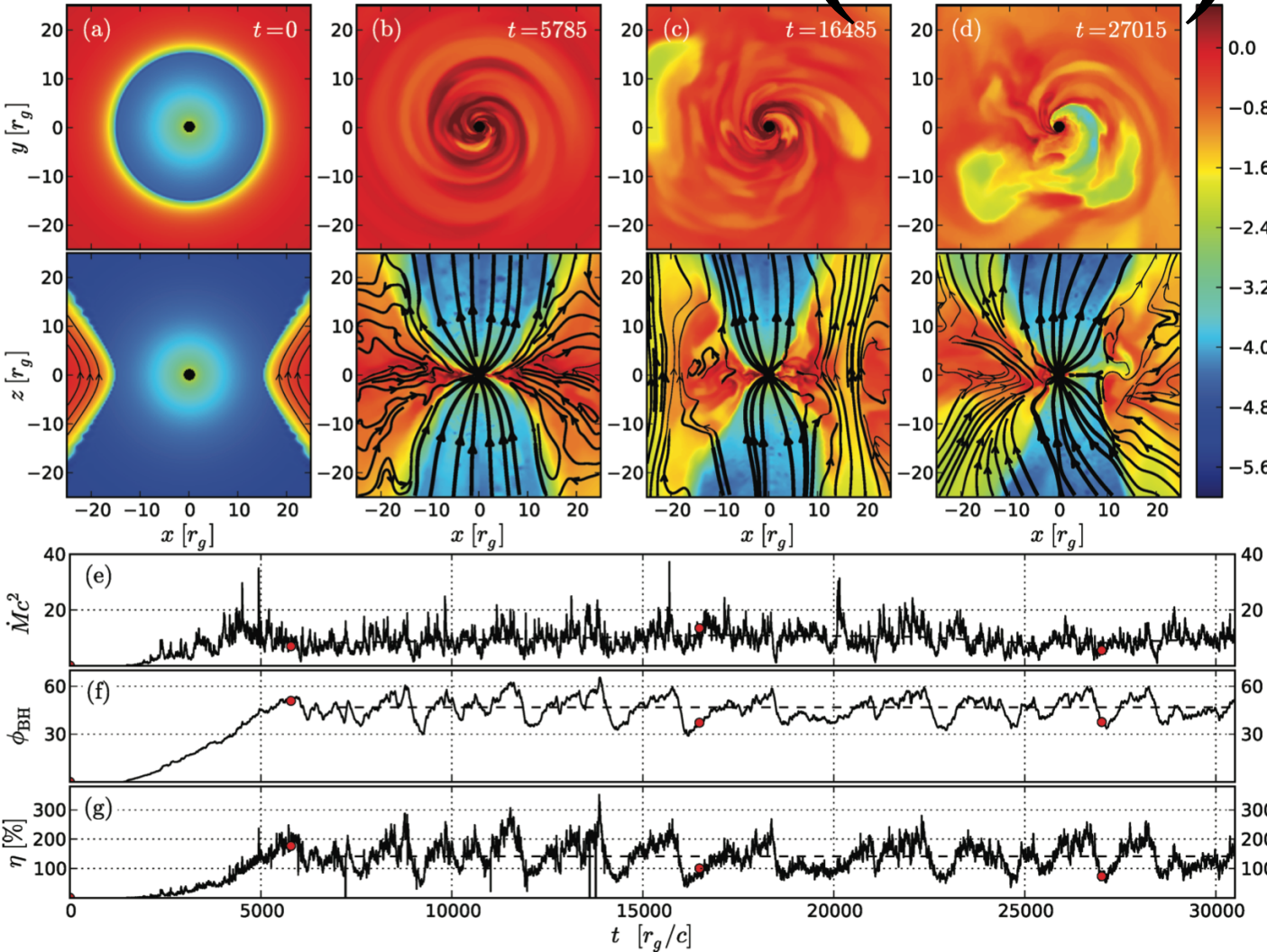
Contents for GRB

- GRB Cosmology
- Pop III GRB
- Ultralong GRB
- Short GRB
- *Other topics*

Blandford-Znajek Jets require Poloidal B Field



Magnetically Arrested Disk (MAD)



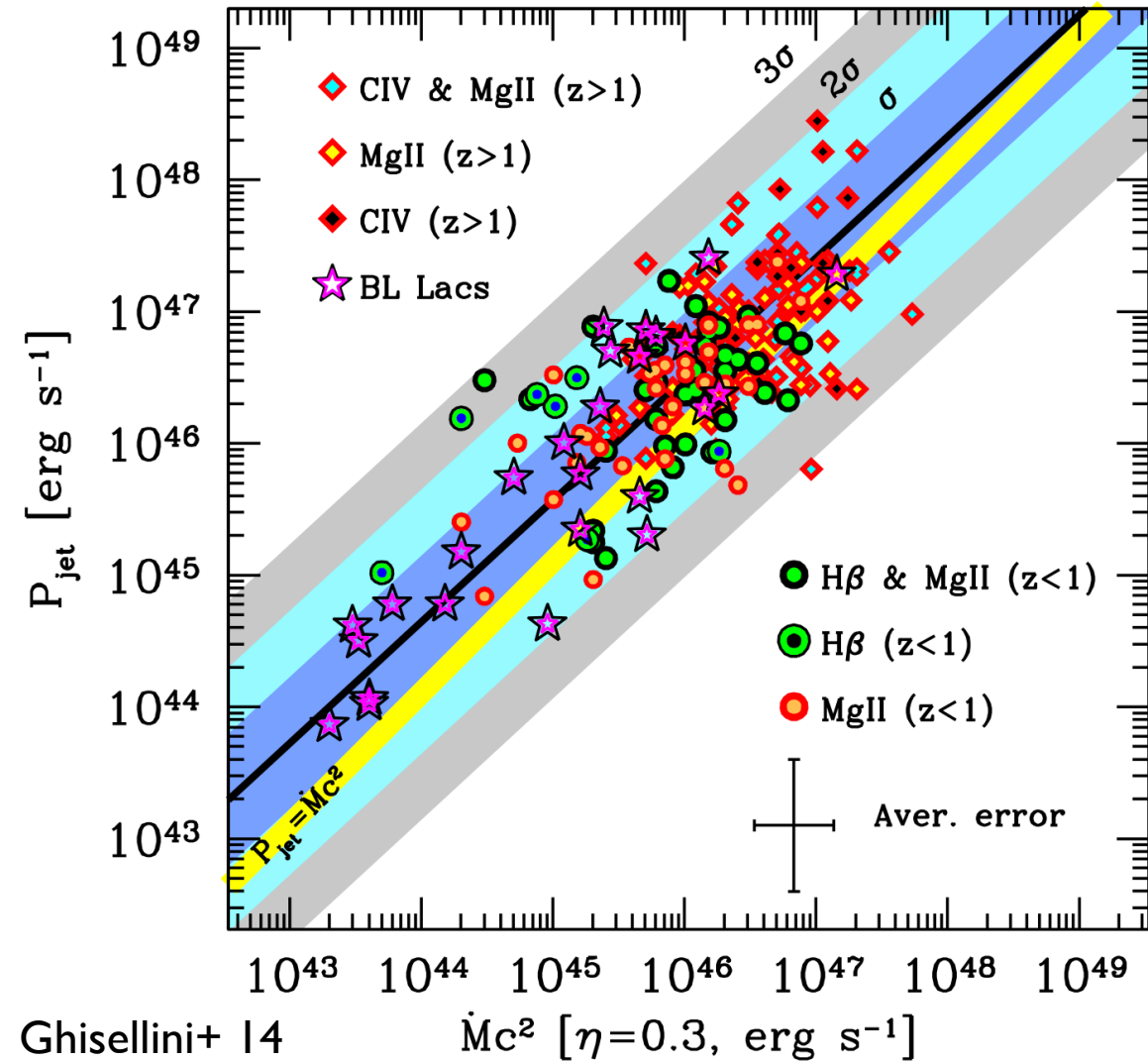
Poloidal
B-dominated
 $P_B > P_{\text{gas}}$

$P_{\text{jet}} > M_{\dot{\text{M}}} c^2$
 $\eta > 100\%!!!$

GR-MHD

Tchekhovskoy+ 11
McKinney+ 12
Narayan & Abramowicz 03

Observations of MAD



$$P_{\text{jet}} > M_{\text{dot}} c^2$$

$$\eta = L_{\text{disk}} / M_{\text{dot}} c^2 = 0.3$$

$$P_{\text{jet}} \approx 10 P_{\text{rad}}$$

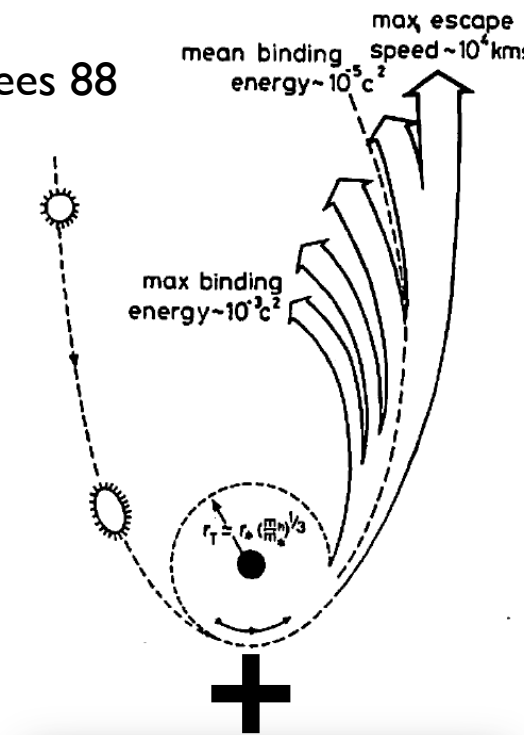
(one p per one e)

$$\log(P_{\text{jet}}) = 0.92 \log(M c^2) + 4.09$$

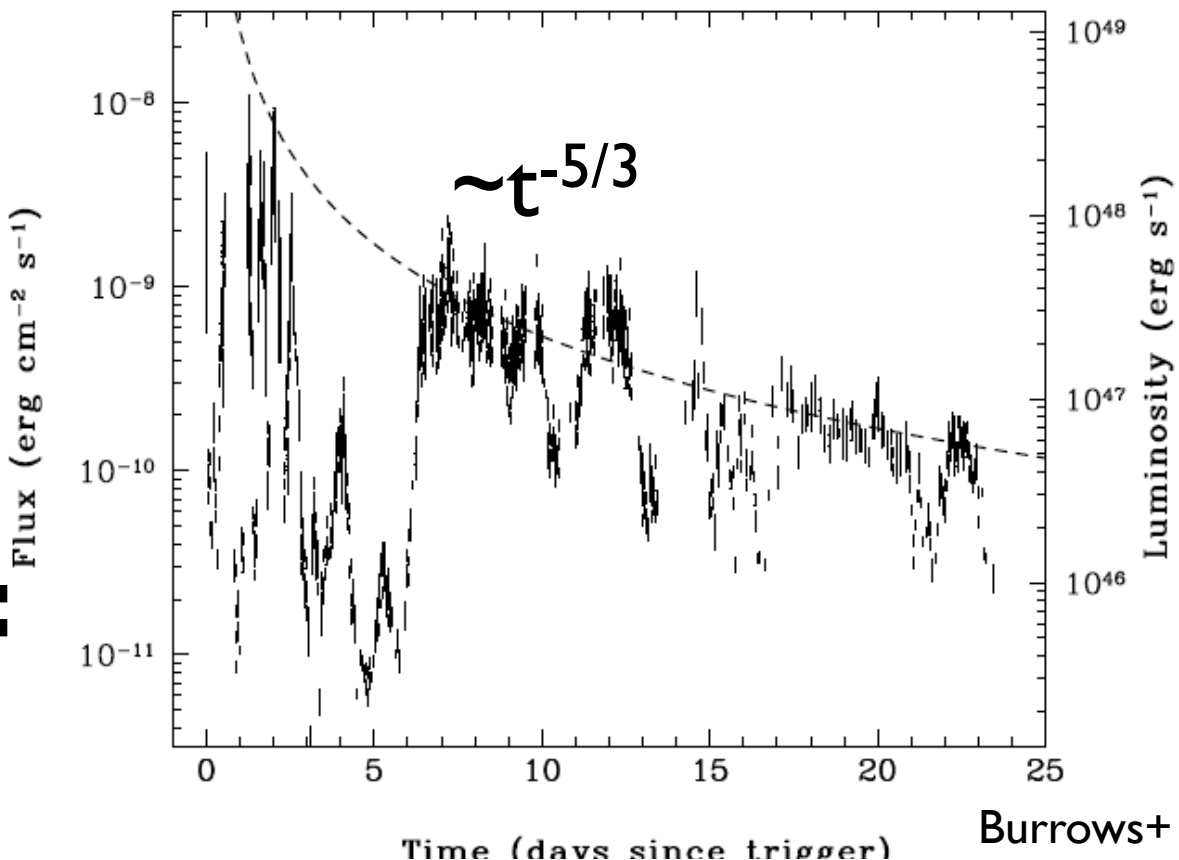
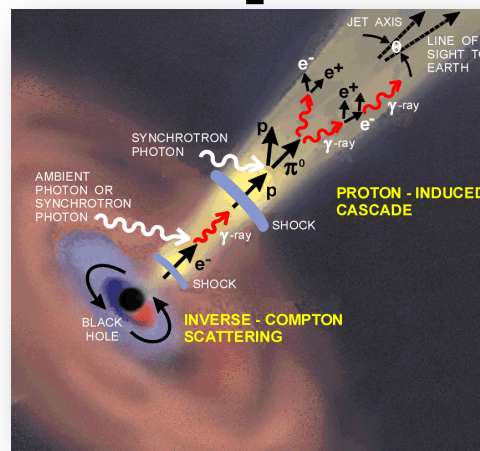
$$\sigma = 0.5 \text{ dex}$$

Tidal Disruption Jet

Rees 88



Massive BH tidally disrupt a star



Burrows+ 11

Jet formation (unexpected)

First 2 PeV vs

$\text{PeV} = 10^{15} \text{ eV}$

"Bert"

8 Aug 2011 3 Jan 2012

"Ernie"

Breakthrough of
the year 2013



$1.04 \pm 0.16 \text{ PeV}$

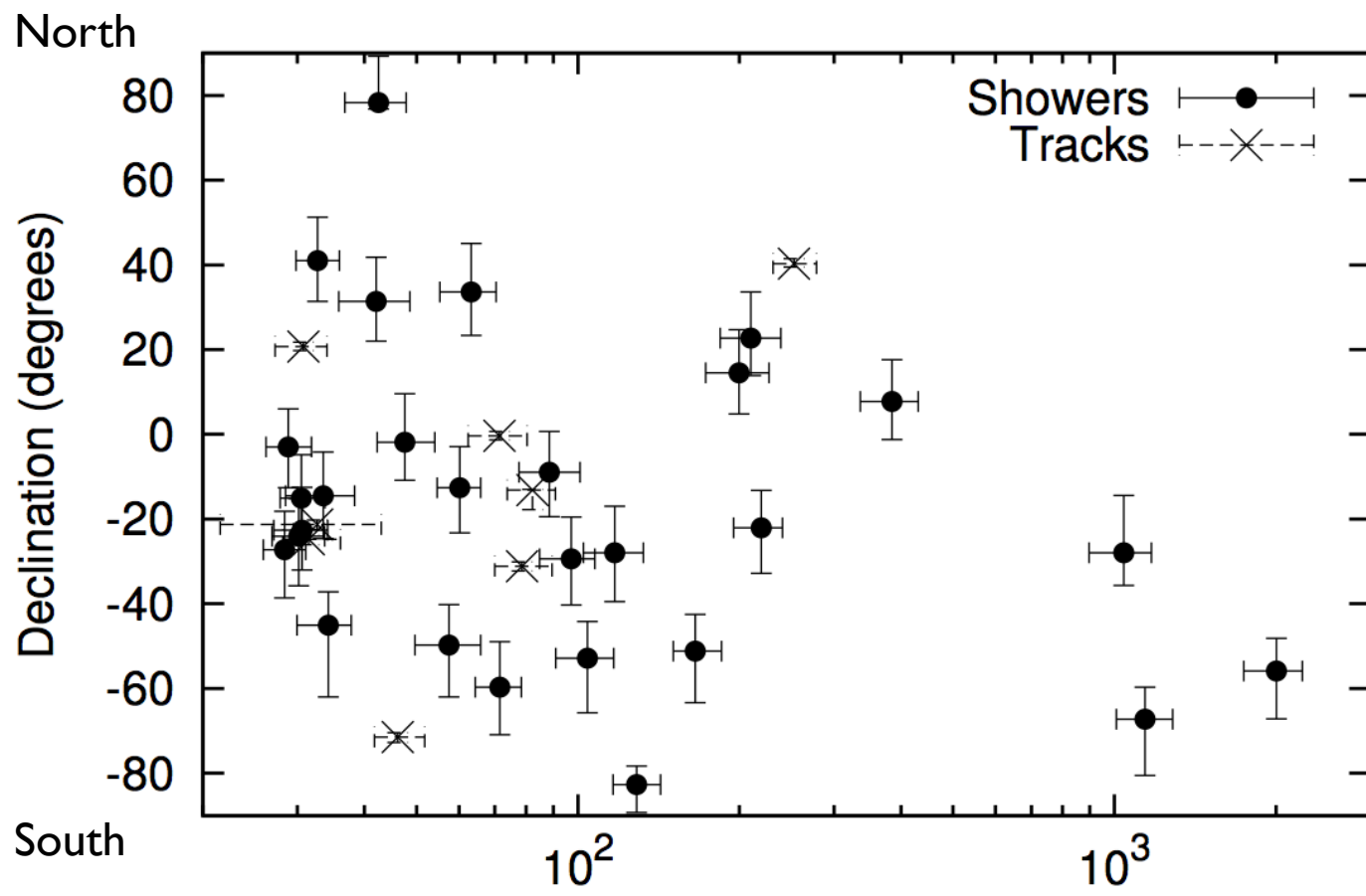
Reported in Kyoto v 2012

$1.14 \pm 0.17 \text{ PeV}$

Aartsen+(IceCube), arXiv:1304.5356

Dawn of High-Energy v Astronomy!!!

More Events



May 2010-May 2011 (79 strings)
 May 2011-May 2012 (86 strings)
 May 2012-May 2013 (86 strings)
 ~988 days

Big Bird



IceCube
1405.5303

Reject a purely atmospheric explanation at **5.7 σ**
 37 (9 μ + 28 showers), Background $8.4 \pm 4.2 \mu$ & $6.6^{+5.9}_{-1.6} \nu$

ν from GRBs

$$p\gamma \rightarrow n\pi^+, p\pi^0$$

At Δ -resonance

$$\pi^+ \rightarrow \mu^+ + \nu_\mu$$

$$\varepsilon_p \varepsilon_\gamma \approx 0.2 \Gamma^2 \text{ GeV}^2$$

$$\rightarrow e^+ + \nu_e + \nu_\mu + \bar{\nu}_\mu$$

$$\varepsilon_\nu \approx 0.05 \varepsilon_p$$

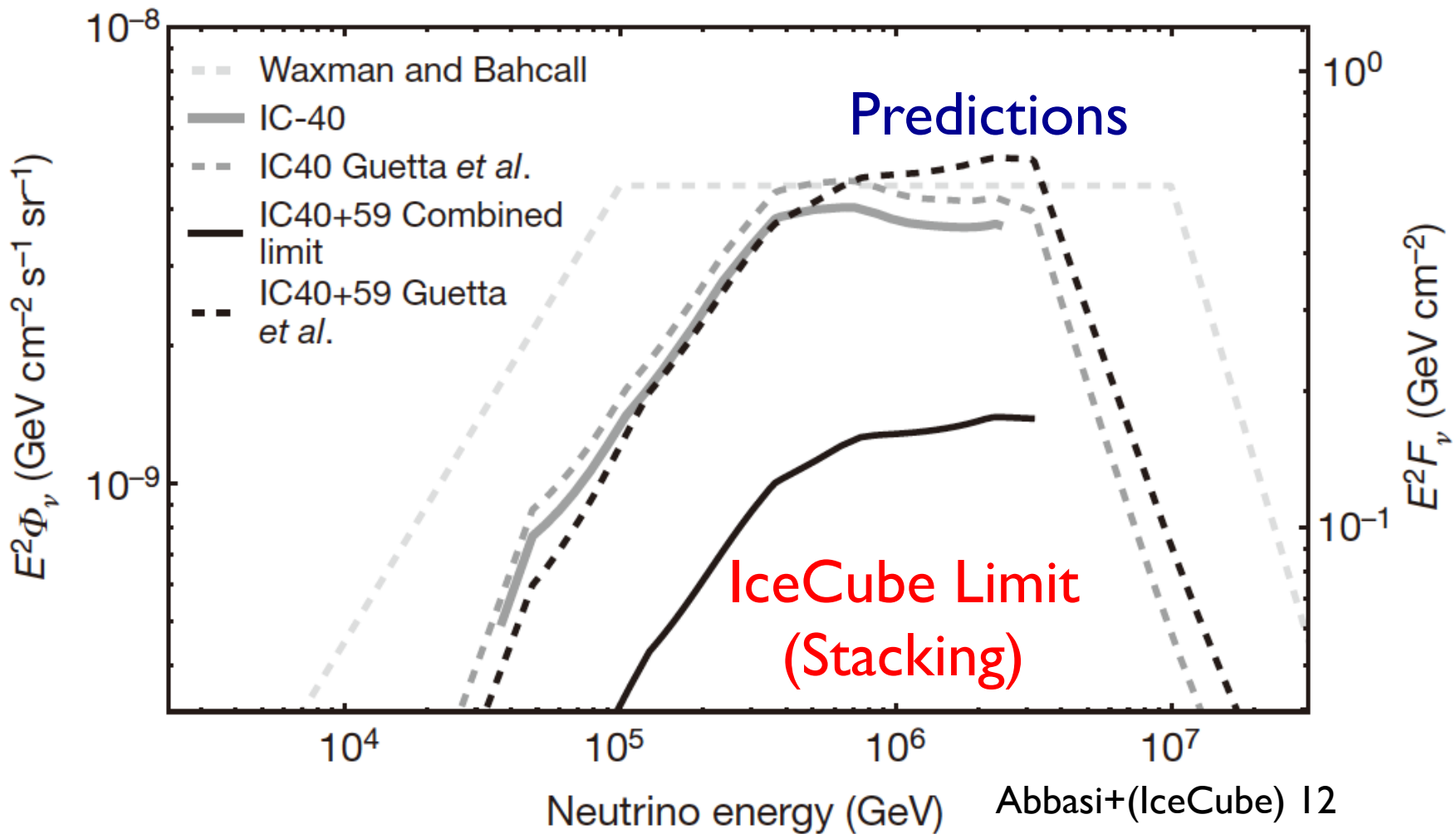
$$\pi^0 \rightarrow \gamma\gamma$$

$\varepsilon_\gamma \sim 1 \text{ MeV}, \Gamma \sim 1000$ (from obs.)

$$\Rightarrow \varepsilon_p \sim 10^{17} \text{ eV} \Rightarrow \varepsilon_\nu \sim \text{PeV}$$

$p\gamma$ efficiency can be $f_{p\gamma} \sim O(1)$ [for $\sigma_{p\gamma} \sim 3 \times 10^{-28} \text{ cm}^2$]

Limits on ν from GRBs

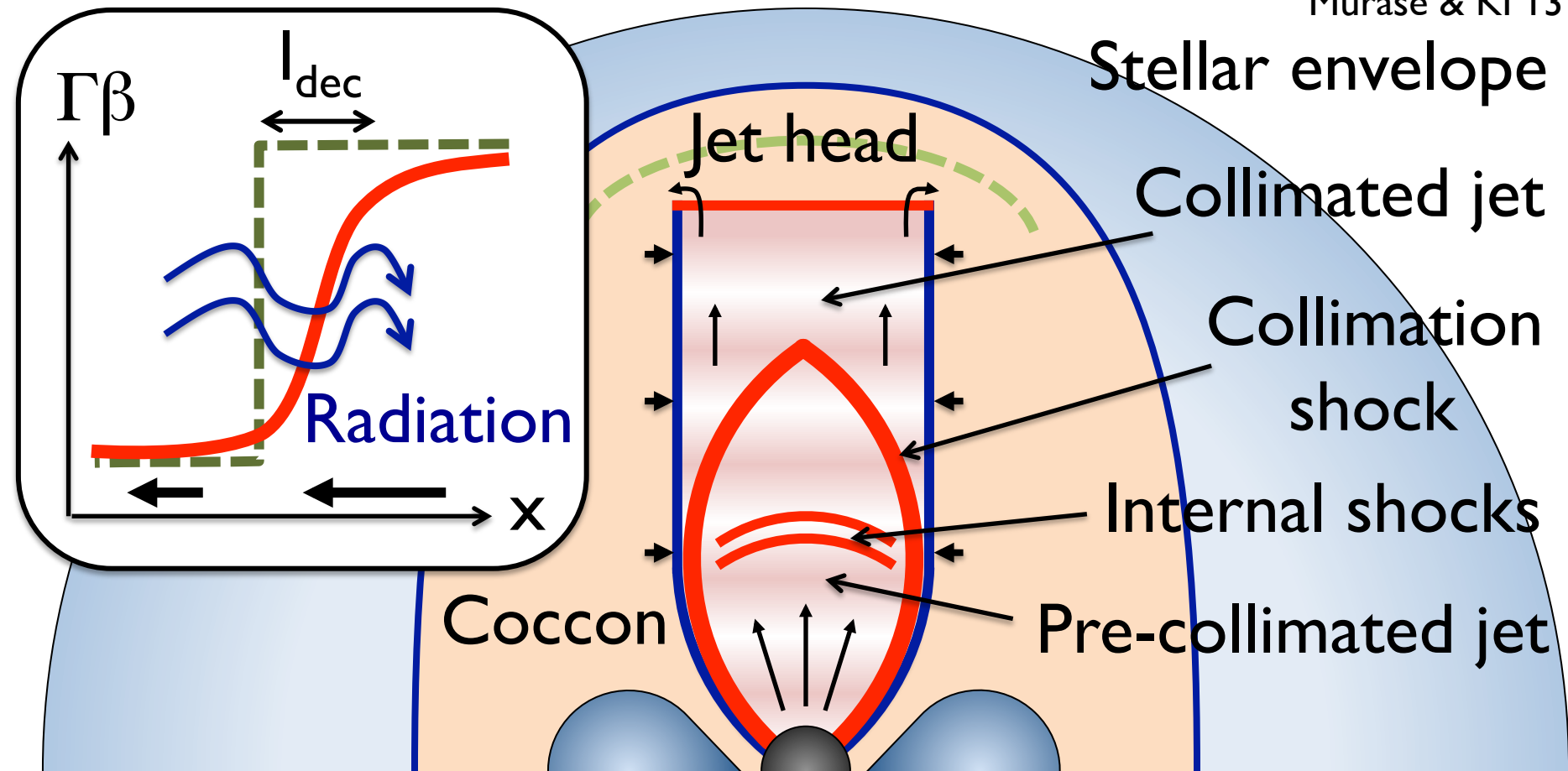


GRBs \neq PeV ν Sources? $\sim 10^{-8} \text{ GeV cm}^{-2} \text{s}^{-1} \text{sr}^{-1}$

GRB inside a Star?

Low-power GRB (Low-luminosity GRB, Ultra-long GRB)
Cutoff by E_{\max} , π/μ Cooling, or Absorption by envelope

Murase & KI 13



Contents

- **GRB**
 - GRB Cosmology
 - Pop III GRB
 - Ultralong GRB
 - Short GRB
 - Other topics
- **FRB**
 - Possible origins
 - Real cosmic signal?
 - Galactic?
 - FRB cosmology

Cosmic Transients for Probing High-z!

Thank You

Localization

- Single dish
 - $\sim(c/\text{GHz}) \times (64 \text{ m})^{-1} > 0.1 \text{ deg}$
- Long-baseline Interferometer
 - Not yet
 - will prove the extragalactic origin
 - will improve the counterpart searches

Table 1. Observed properties of FRB 140514

| | |
|---|-------------------------------|
| Event date UTC | 14 May, 2014 |
| Event time UTC, $\nu_{1.4}$ GHz | 17:14:11.06 |
| Event time, ν_∞ | 17:14:09.83 |
| Local date AEST | 15 May, 2014 |
| Local time AEST | 03:14:11.06 |
| RA | 22:34:06.2 |
| Dec | -12:18:46.5 |
| (ℓ, b) | ($50.8^\circ, -54.6^\circ$) |
| Beam diameter | $14.4'$ |
| DM _{FRB} (pc cm ⁻³) | 562.7(6) |
| DM _{MW} (pc cm ⁻³) | 34.9 |
| Detection S/N | 16(1) |
| Observed width, Δt (ms) | $2.8^{+3.5}_{-0.7}$ |
| Scattering timescale, $\tau_{1\text{GHz}}$ (ms) | 5.4(1) |
| Dispersion index, α | -2.000(4) |
| Peak flux density, $S_{\nu, 1400\text{MHz}}$ (Jy) | $0.47^{+0.11}_{-0.08}$ |
| Fluence, \mathcal{F} (Jy ms) | $1.3^{+2.3}_{-0.5}$ |

Table 2. Derived cosmological properties of FRB 140514

| | |
|---------------------------|--------------------------------------|
| z | $< 0.44(1)$ |
| Co-moving distance (Gpc) | $< 1.71(3)$ |
| Luminosity distance (Gpc) | $< 2.46^{+0.04}_{-0.06}$ |
| Energy (erg) | $< 3.7^{+4.7}_{-2.0} \times 10^{38}$ |
| Distance modulus (mag) | < 42.2 |

Luminosity-Rise time

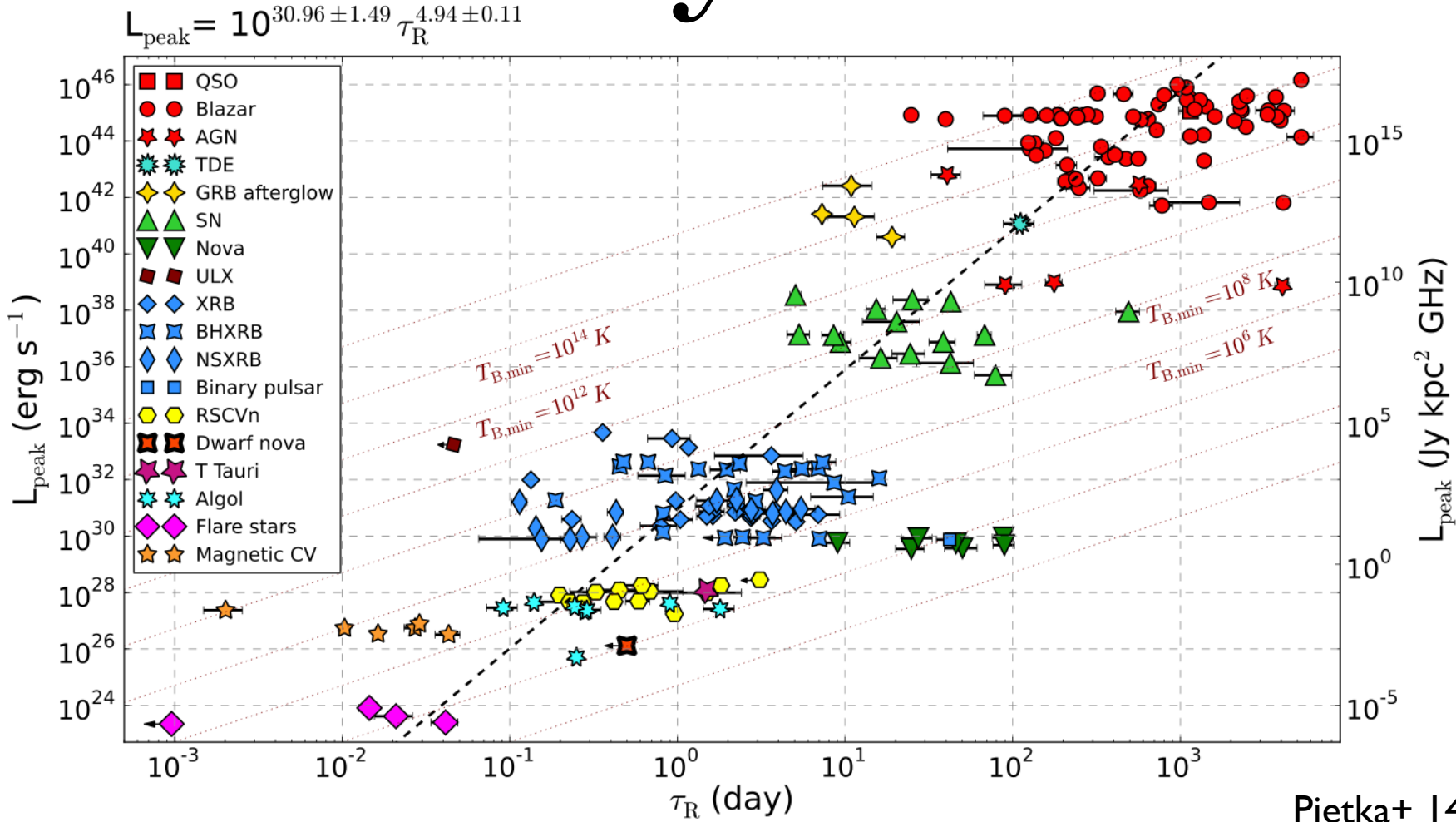


Figure 3. Exponential rise timescale as a function of peak radio luminosity for the entire set of radio flares studied. The overall relation is of the form $L \propto \tau^{4.94 \pm 0.11}$. Overplotted are lines corresponding to a fixed minimum brightness temperature ($T_{\text{B},\text{min}}$), under the assumption that the size of the emitting region $r = c\tau$, which have a form $L \propto \tau^2$, demonstrating clearly that $T_{\text{B},\text{min}}$ is an increasing function of luminosity, peaking just above the theoretical limit of 10^{12}K for the most luminous AGN (which are also likely to be beamed).

Brightness Temperature

$$F_\nu = \frac{\pi r_\perp^2}{d^2} \frac{2\nu^2}{c^2} kT$$

$$T \sim 3 \times 10^{41} \text{ K } L_{43} r_{emi,10}^{-2}$$

⇒ Coherent emission

$$\begin{aligned} P &\sim |E|^2 \sim |E_1 + E_2 + E_3 + \dots + E_N|^2 \\ &\sim N|E_1|^2 \quad (\text{incoherent}) \\ &\sim N^2|E_1|^2 \quad (\text{coherent}) \end{aligned}$$

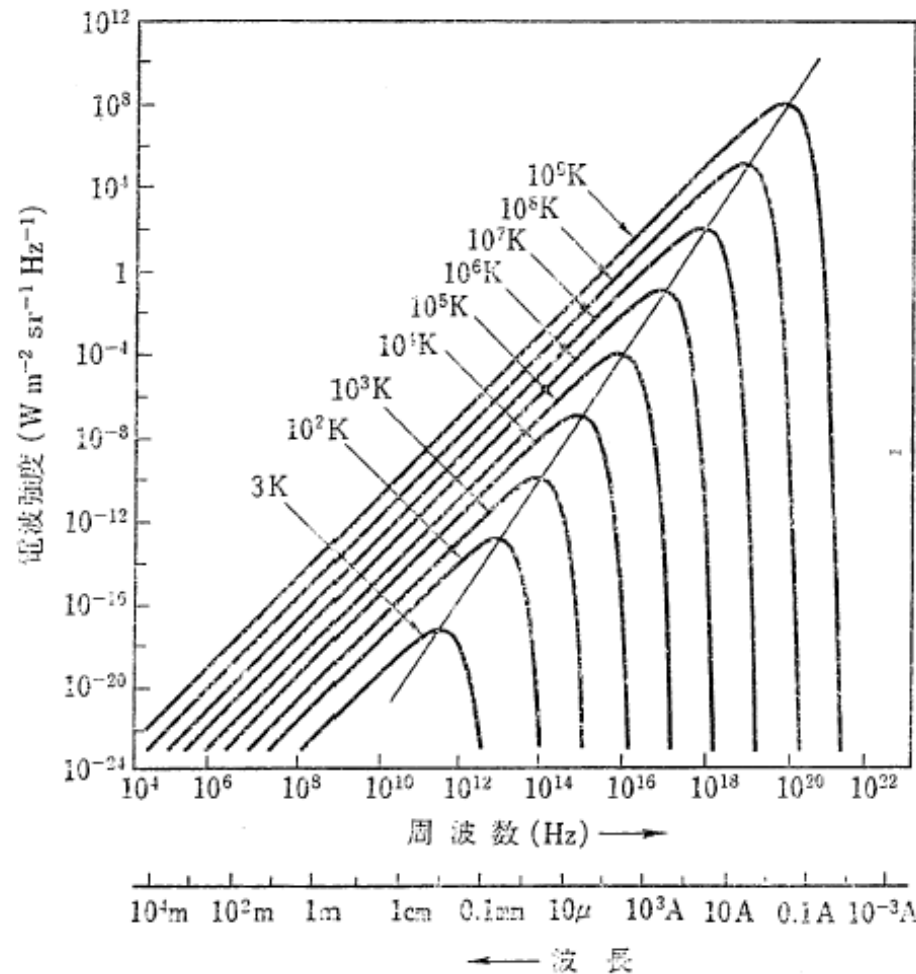


図 2・6 热放射（プランク放射）の强度スペクトル

FRB 010621 is Galactic?

Bannister & Madsen 14

- Keane FRB 010621
- Galactic?
- H_{α}, H_{β} towards FRB
 \Rightarrow Emission measure
 (with dust correction)
 \Rightarrow Contribution to DM
 \Rightarrow Galactic

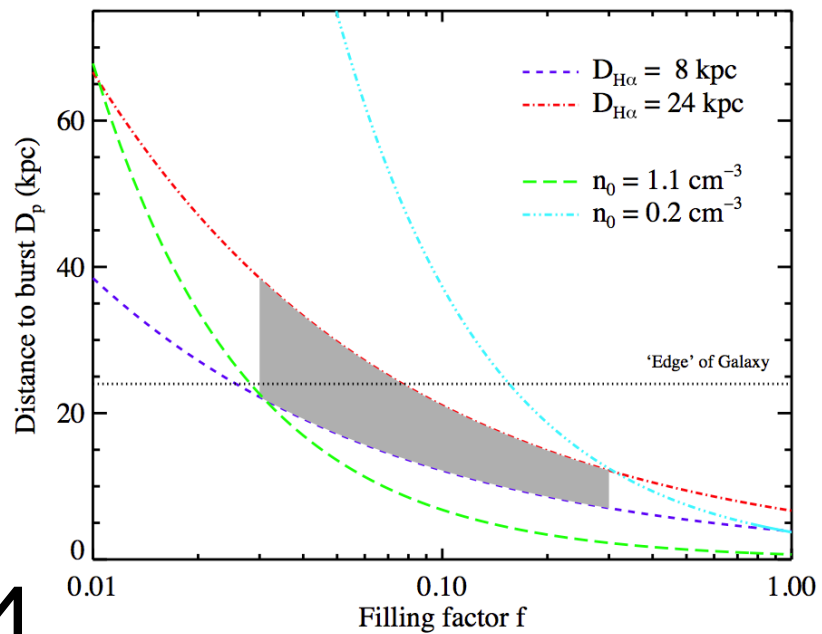


Figure 2. Distance to the burst as a function of filling factor of the ionised gas using an extinction corrected EM of $276 \text{ cm}^{-6}\text{pc}$. The grey shaded area shows the range of possible values of D_p bounded by $8 \text{ kpc} < D_{H\alpha} < 24 \text{ kpc}$ and $0.03 < f < 0.30$. The black horizontal dotted line is placed at the canonical ‘edge’ of the Galaxy along the line of sight to the burst (24 kpc). The lower and upper limits on the average electron density over the corresponding range of values of D_p are $0.2 < n < 1.1$; lines with these values of constant density are shown in aqua and green, respectively.

CONTOURS OF DISPERSION MEASURE

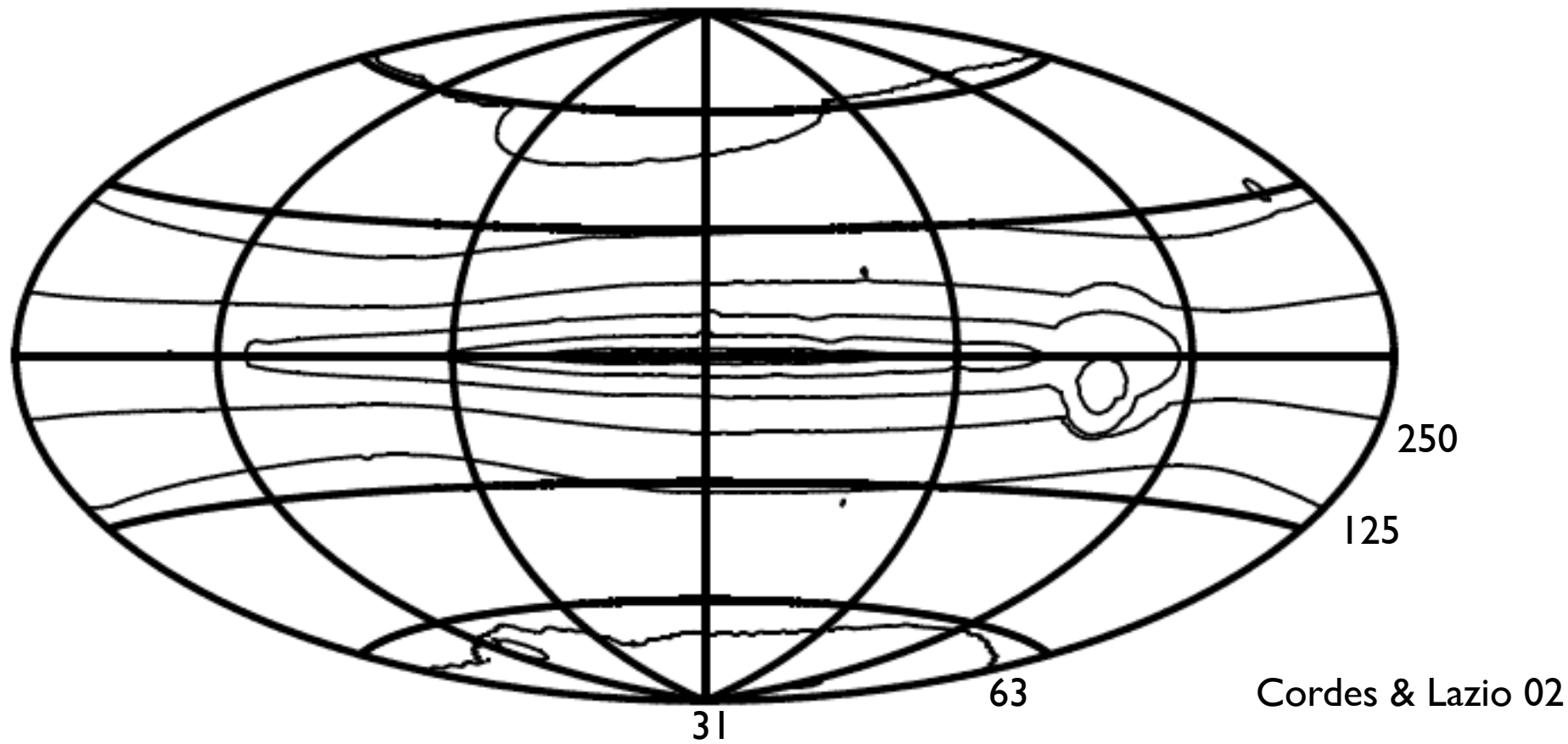


FIG. 15.— Contours of DM integrated to infinite distance and plotted against Galactic latitude and longitude on an Aitoff projection with the Galactic center in the middle and negative longitudes to the right. Contours are at $4000/2^n$ pc cm $^{-3}$ for $n = 0, 1, \dots, 7$, with the lowest contour at the Galactic poles.

Cordes & Lazio 02

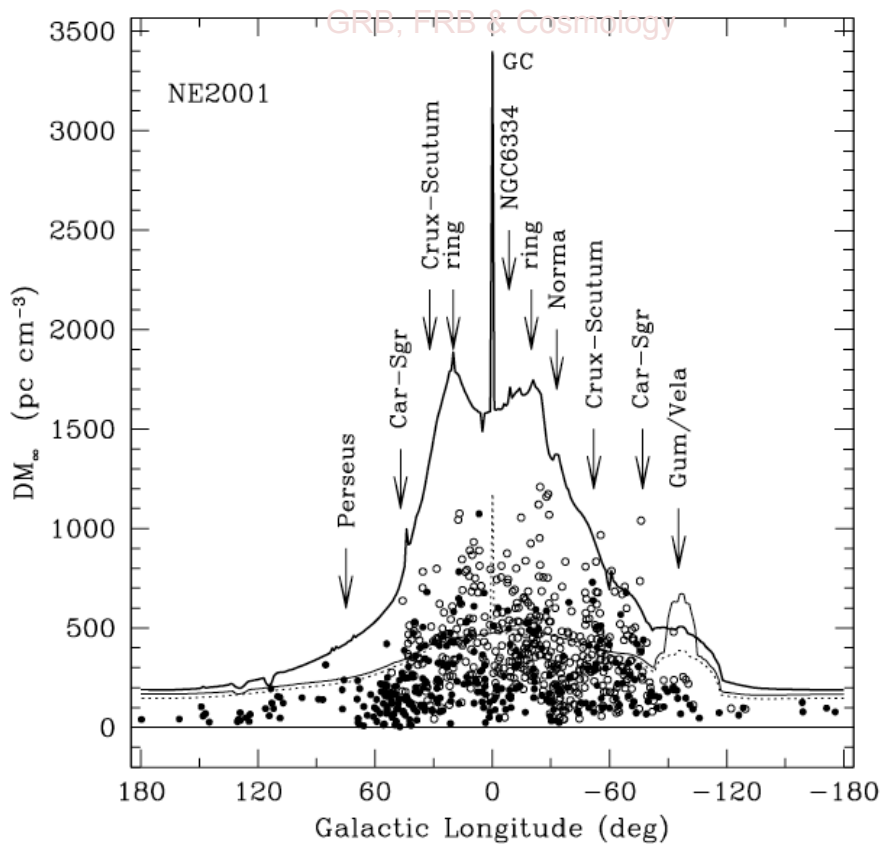


FIG. 11.— Plot of $\text{DM}_\infty(\ell, b)$, the maximum DM obtained by integrating the NE2001 model. Heavy solid line: $b = 0^\circ$. Light solid line: $b = -5^\circ$. Dotted line: $b = +5^\circ$ (offset by -20 pc cm^{-3} in the vertical direction for clarity). Plotted points are pulsars with $|b| < 5^\circ$. Filled circles: pulsars from the Princeton catalog. Open circles: pulsars from the public Parkes Multibeam catalog. Labelled features include tangents to the spiral arms and maxima associated with the ring component, the Gum Nebula and Vela supernova remnant, and the H II complex NGC 6334. The gaps near $\ell = +15^\circ$ and -20° and $\text{DM} \lesssim 200 \text{ pc cm}^{-3}$ are real, appearing in both samples, and signify either the real absence of pulsars in the corresponding volume or the presence of large electron densities in these directions fairly close to the solar system. The absence of pulsars above $\sim 1200 \text{ pc cm}^{-3}$ is due to selection against such objects by pulse broadening from dispersion smearing and scattering.

Cordes & Lazio 02

| Name | FRB 110220 | FRB 110627 | FRB 110703 | FRB 120127 |
|--|---------------------------------|---------------------------------|---------------------------------|---------------------------------|
| Beam Right Ascension (J2000) | 22 ^h 34 ^m | 21 ^h 03 ^m | 23 ^h 30 ^m | 23 ^h 15 ^m |
| Beam Declination (J2000) | -12° 24' | -44° 44' | -02° 52' | -18° 25' |
| Galactic Latitude, b (°) | -54.7 | -41.7 | -59.0 | -66.2 |
| Galactic Longitude, l (°) | +50.8 | +355.8 | +81.0 | +49.2 |
| UTC (dd/mm/yyyy hh:mm:ss.sss) | 20/02/2011 01:55:48.957 | 27/06/2011 21:33:17.474 | 03/07/2011 18:59:40.591 | 27/01/2012 08:11:21.723 |
| DM (cm ⁻³ pc) | 944.38 ± 0.05 | 723.0 ± 0.3 | 1103.6 ± 0.7 | 553.3 ± 0.3 |
| DM _E (cm ⁻³ pc) | 910 | 677 | 1072 | 521 |
| Redshift, z (DM _{Host} = 100 cm ⁻³ pc) | 0.81 | 0.61 | 0.96 | 0.45 |
| Co-moving Distance, D (Gpc) at z | 2.8 | 2.2 | 3.2 | 1.7 |
| Dispersion Index, α | -2.003 ± 0.006 | — | -2.000 ± 0.006 | — |
| Scattering Index, β | -4.0 ± 0.4 | — | — | — |
| Observed Width at 1.3 GHz, W (ms) | 5.6 ± 0.1 | < 1.4 | < 4.3 | < 1.1 |
| SNR | 49 | 11 | 16 | 11 |
| Minimum Peak Flux Density S_v (Jy) | 1.3 | 0.4 | 0.5 | 0.5 |
| Fluence at 1.3 GHz, F (Jy ms) | 8.0 | 0.7 | 1.8 | 0.6 |
| $S_v D^2$ ($\times 10^{12}$ Jy kpc ²) | 10.2 | 1.9 | 5.1 | 1.4 |
| Energy Released, E (J) | $\sim 10^{33}$ | $\sim 10^{31}$ | $\sim 10^{32}$ | $\sim 10^{31}$ |

Spectral index is difficult to infer due to position uncertainties

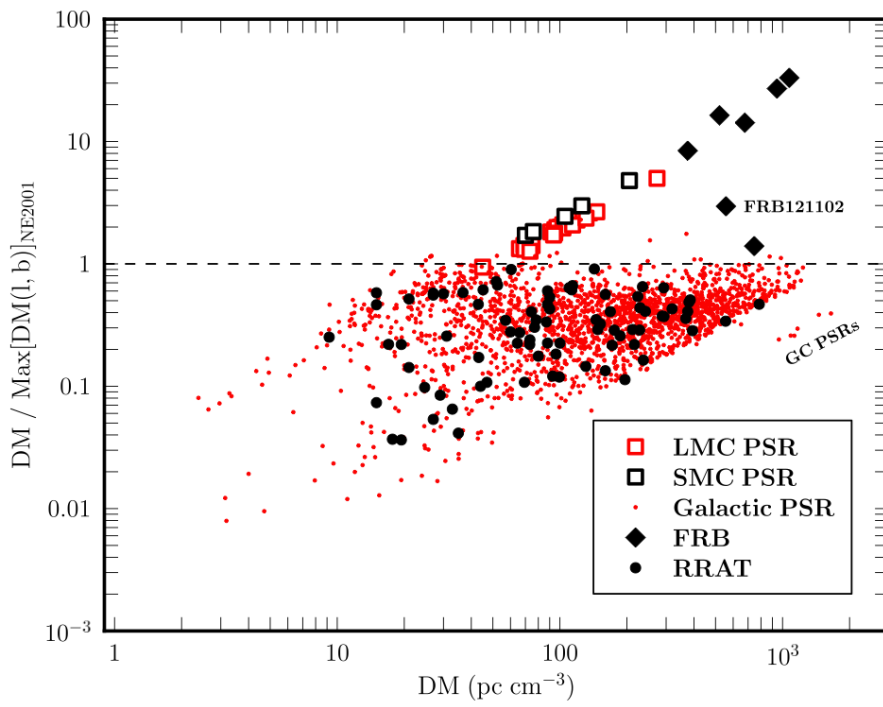


Figure 3. DM ratio (r_{DM}) of measured DM to maximum Galactic dispersion measure plotted against measured DM. The maximum Galactic DM is calculated by integrating the NE2001 model to the edge of the Galaxy for each pulsar line-of-sight. The dashed line shows the maximum unity ratio expected for Galactic objects if the electron density is accurate for all lines of sight. The six pulsars near the Galactic center are clustered on the far right of the plot. The RRATs have DM ratios consistent with the rest of the Galactic pulsar population. Known pulsars in the LMC and SMC have $r_{\text{DM}} \sim 1-5$, and the seven FRBs have ratios from 1.2 to 33. The Keane et al. (2012) burst has the lowest DM ratio of the FRBs and is located to the lower right of FRB 121102. The Lorimer et al. (2007) burst and Thornton et al. (2013) bursts fall along the line that extends from the LMC and SMC pulsars with the Lorimer et al. (2007) burst being the left-most point. (See Section 5 for data source references.)

Table 1
Observational Parameters of FRB 121102

| Parameter | Value |
|---|---|
| Date | 2012 Nov 02 |
| Time | 06:35:53 UT |
| MJD arrival time ^a | 56233.27492180 |
| Right Ascension ^b | 05 ^h 32 ^m 09.6 ^s |
| Declination ^b | 33°05' 13.4'' |
| Gal. long. ^b | 174.95° |
| Gal. lat. ^b | -0.223° |
| DM (pc cm ⁻³) | 557.4 ± 2.0 |
| DM _{NE2001,max} (pc cm ⁻³) | 188 |
| Dispersion index ^c | -2.01 ± 0.05 |
| Pulse width (ms) | 3.0 ± 0.5 |
| Pulse broadening (ms) ^d | < 1.5 |
| Flux density (Jy) ^e | 0.4 ^{+0.4} _{-0.1} |
| Spectral index range(α) ^f | 7 to 11 |

^a Barycentered arrival time referenced to infinite frequency.

^b The J2000 position of the center of beam 4.

^c $\text{DM} \propto \nu^\beta$

^d Flux density at 1 GHz

^e Flux estimation at 1.4 GHz assumes a side-lobe detection and a corresponding gain of $0.7 \pm 0.3 \text{ K Jy}^{-1}$.

^f $S(\nu) \propto \nu^\alpha$

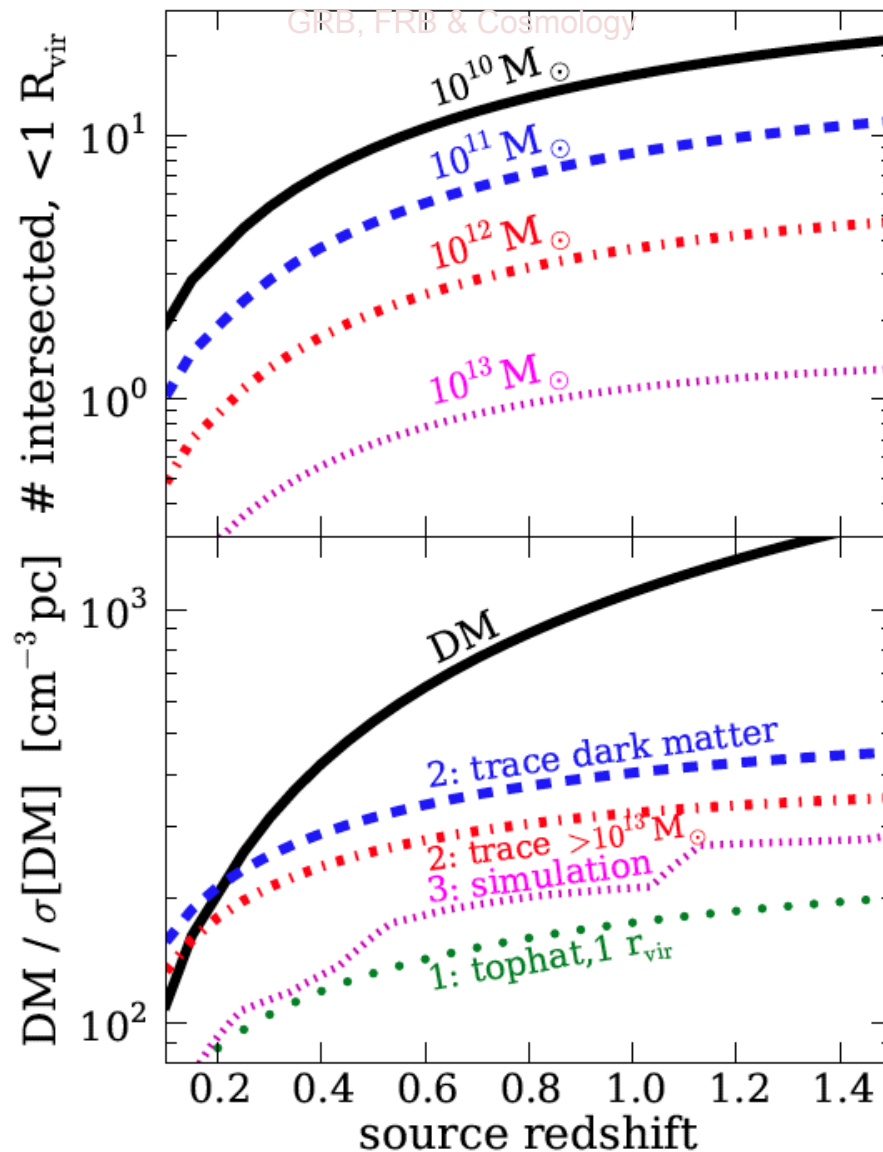


FIG. 1.— Top panel: The average number of halos above the specified mass thresholds that a sightline intersects within $1 r_{\text{vir}}$. Bottom panel: The mean dispersion measure (solid curve) as well as the standard deviation in its value for the considered models (other curves).

Volumetric Rates of Selected Cosmic Explosions

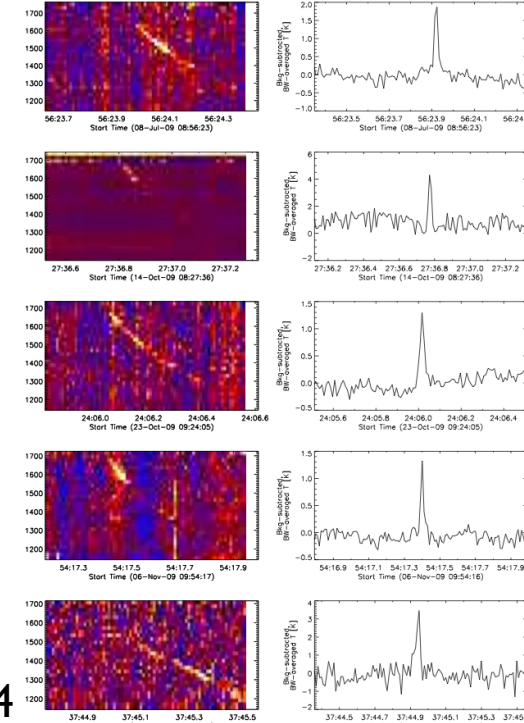
| Class | Type | Φ (Gpc $^{-3}$ yr $^{-1}$) | Ref |
|---------------|------|-------------------------------------|-------|
| LSB (low) | BC | 100–1800 | (1,2) |
| LSB(high) | Obs | 1 | (1) |
| | BC | 100–550 | (1) |
| SHB | Obs | >10 | (3a) |
| | BC | 500–2000 | (3b) |
| In-spiral | Th | 3×10^3 | (4) |
| SGR | Obs | $<2.5 \times 10^4$ | (5) |
| Type Ia | Obs | 10^5 | (6) |
| Core Collapse | Obs | 2×10^5 | (7) |
| FRB | Obs | $\approx 2 \times 10^4$ | (8,9) |

Notes. “Obs” is the annual rate inferred from observations. “BC” is the observed rate corrected for beaming. “Th” is the rate deduced from stellar models. LSB stands for GRBs of the long duration and soft spectrum variety. A gamma-ray luminosity of 10^{49} erg s $^{-1}$ divides the “low” and “high” subclasses (see Guetta & Della Valle 2007). SHB stands for GRBs of the short duration and hard spectrum class. SGR stands for soft gamma repeaters. Here we only include those giant flares with isotropic energy release $>4 \times 10^{46}$ erg.

References. (1) Guetta & Della Valle 2007; (2) Soderberg et al. 2006; (3a) Nakar et al. 2006; (3b) Coward et al. 2012; (4) Kalogera et al. 2004; (5) Ofek 2007; (6) Scannapieco & Bildsten 2005; (7) Li et al. 2011; (8) Lorimer et al. 2007; (9) Thornton et al. 2013.

Peryton

- Detected in multiple receiver beams with approximately the same S/N $\Rightarrow < 10\text{km}$
- $\sim 10^{-4}(d/10\text{km})^2 \text{ erg}$ (cf. cell phone $\sim 10^{-2}\text{erg}$)
- DM $\sim 300\text{pc/cc} \sim 1\text{mg/cc} \times \text{cm}$
- Possible origins
 - Lightning
 - Aircraft, GPS, etc.
 - Electronics



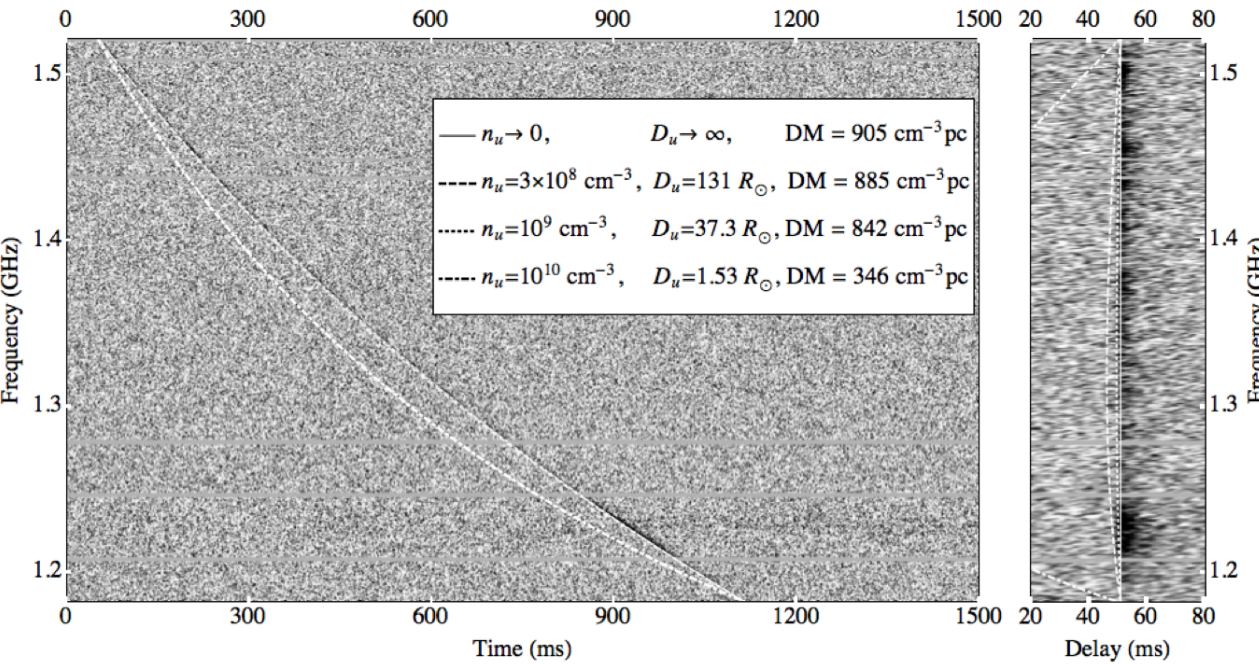
Danish Kahn 14

Saint-Hilaire+ 14

Dense Plasma Dispersion

$$t - t_0 \simeq \int \frac{dD}{c} \left[\frac{1}{2} \frac{f_p^2}{f^2} + \frac{3}{8} \left(\frac{f_p^2}{f^2} \right)^2 + \frac{5}{16} \left(\frac{f_p^2}{f^2} \right)^3 + \dots \right]$$

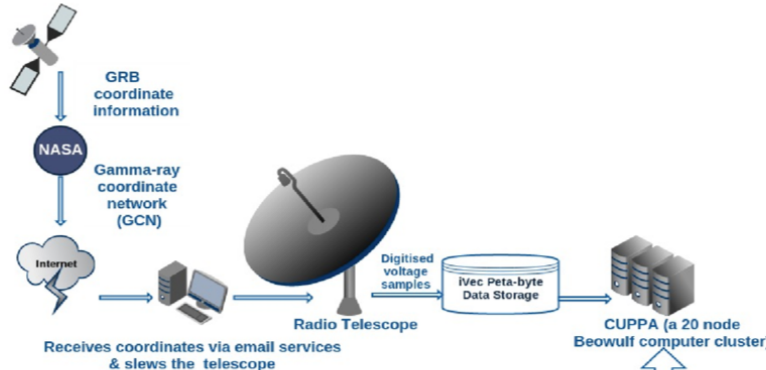
$$\approx \frac{cr_e}{2\pi f^2} \text{DM}, \quad \text{DM} \equiv \int n_e(D) dD.$$



$n_e < 10^{8-9}/\text{cc}$
Not nearby star

Tuntsov+ 14
Katz 14

No FRB-GRB Connection



2.3GHz
26 m radio telescope
Slew to GRB in \sim 140 s
No FRB detected

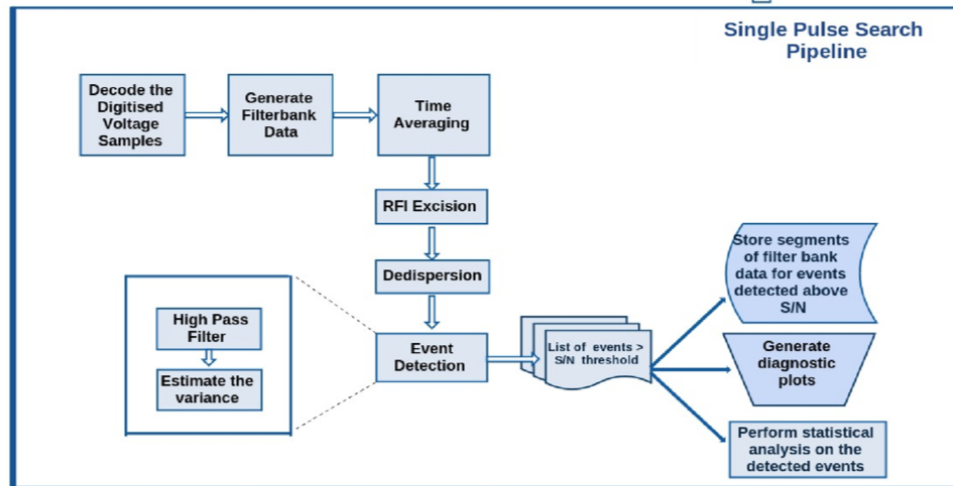


Fig. 1.— Top panel: A schematic representation of the system where the space-borne GRB telescope sends the position information for GRBs to our ground-based radio telescope through GCNs. The radio telescope is then slewed to the GRB positions and data are recorded. The recorded data are then transferred to the PetaByte data storage facility at iVEC, in Perth and processed on a 20 node Beowulf computer cluster, CUPPA. Bottom panel: Represents the single pulse search pipeline implemented in this paper, to search for FRBs from GRBs. The search pipeline has multiple stages: correlation; time averaging; radio frequency interference (RFI) excision; dedispersion; event detection and classification. In this experiment we generate time averages ranging from $640\ \mu\text{s}$ to $25.60\ \text{ms}$ (section 3.1.2). Each averaged time series go through the RFI excision, dedispersion, event detection and classification stages independently.

FRB-Macronova?

FRB-Macronova is detectable @ $z < \sim 0.3$ if exist

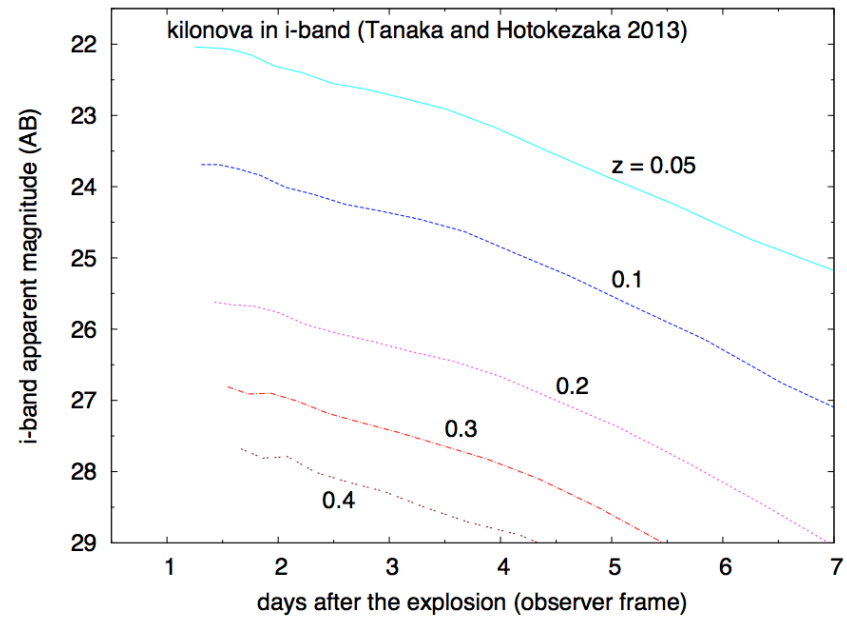
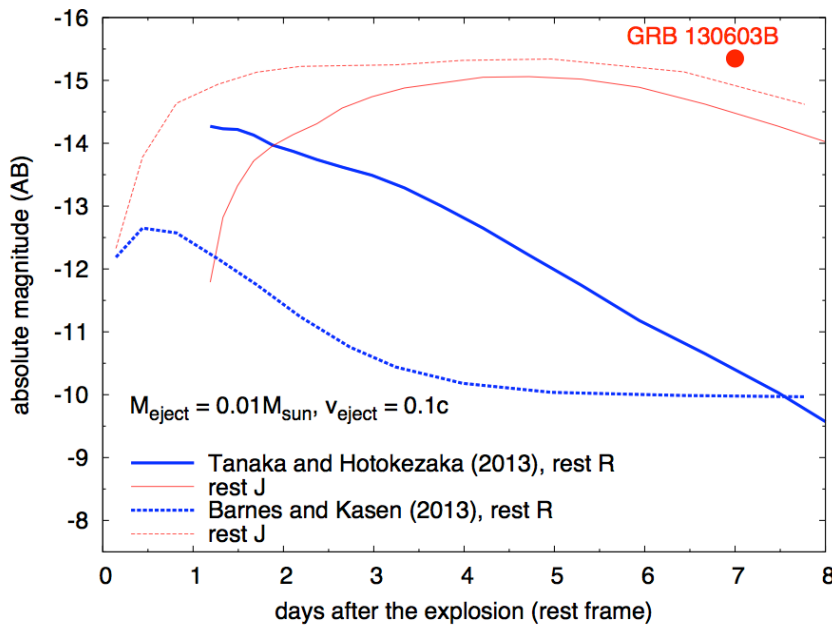
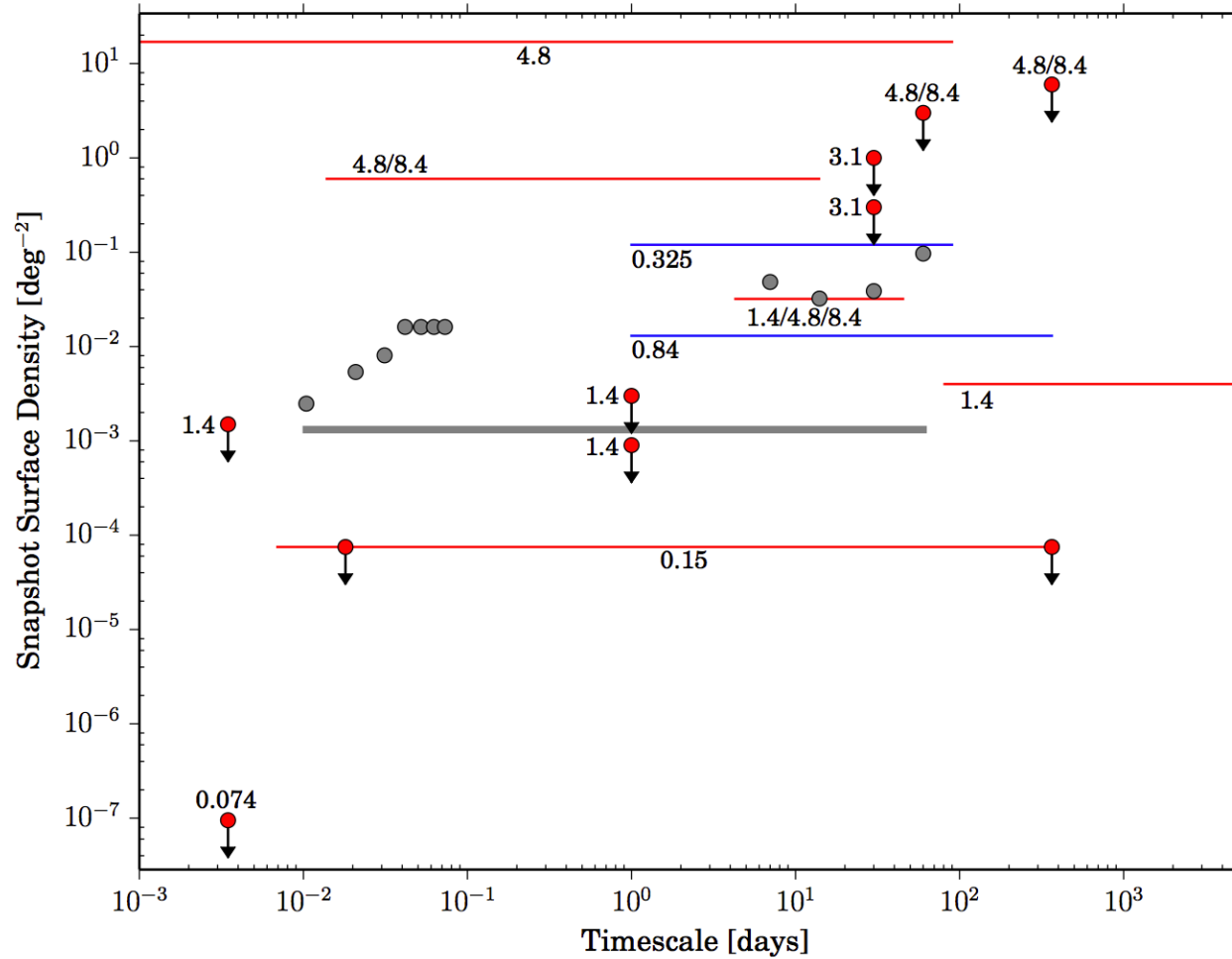


Fig. 1. Left panel: rest frame light curves of kilonovae in absolute magnitude predicted by the models of Tanaka & Hotokezaka (2013, TH13) and Barnes & Kasen (2013). The thick and thin lines represent the light curves in rest frame R -band and J -band, respectively. The circle at the top right indicates observing time and luminosity of the kilonova candidate associated with GRB 130603B ($z = 0.356$) in HST F160W filter which roughly corresponds to rest frame J -band. Right panel: apparent light curves in observer frame i -band predicted by the TH13 model at different redshifts.

LOFAR



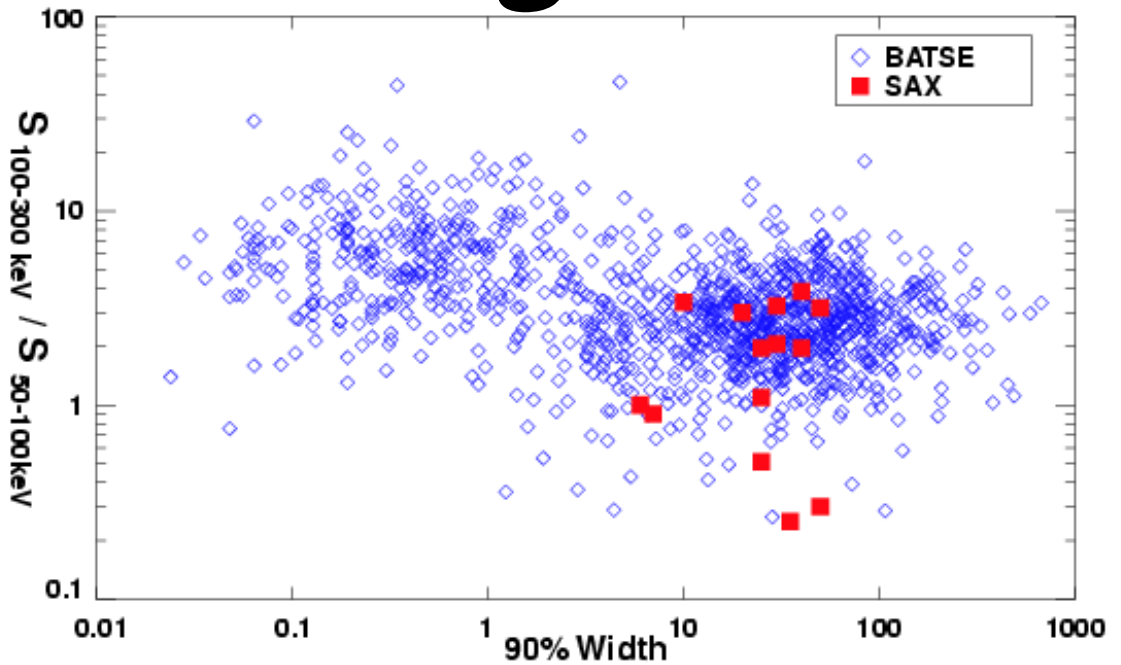
Carbone+ 14

Figure 4. Snapshot surface density (deg^{-2}) against time-scale of detections of transients (blue diamonds and lines) and upper limits based on non detections (red circles and lines). The numbers indicates the frequency in GHz at which each survey was conducted. The surveys displayed here are listed in Table 5. The grey circles indicate the upper limits derived from this work while the grey line represents the result from this work as displayed for the other surveys. It is clear how the grey line is a very rough approximation for the grey circles.

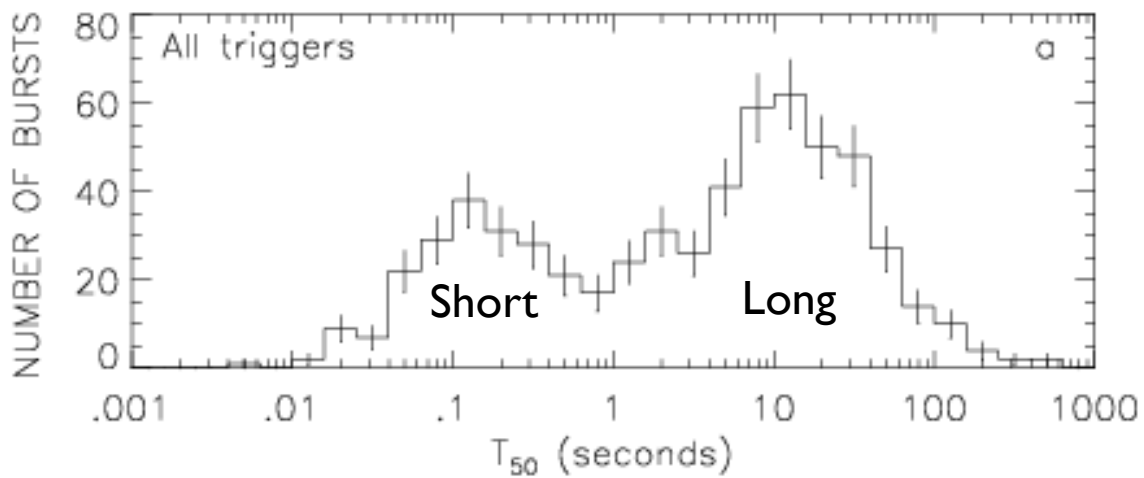
Thank

You

Long & Short GRB

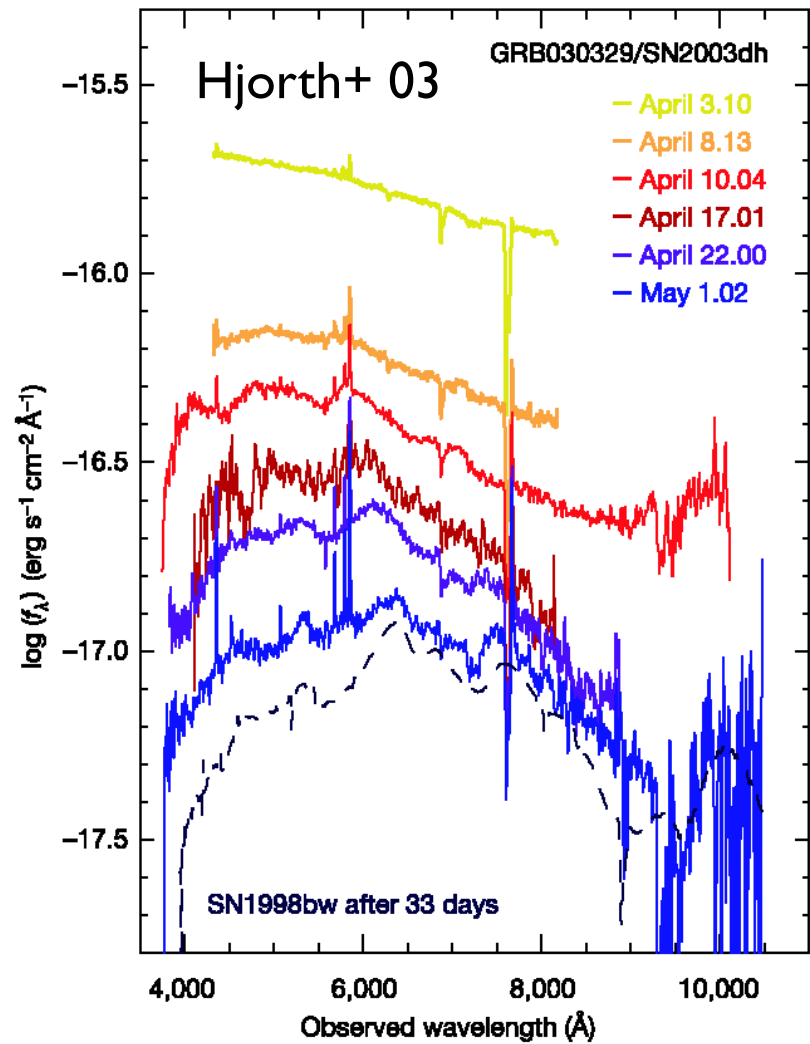
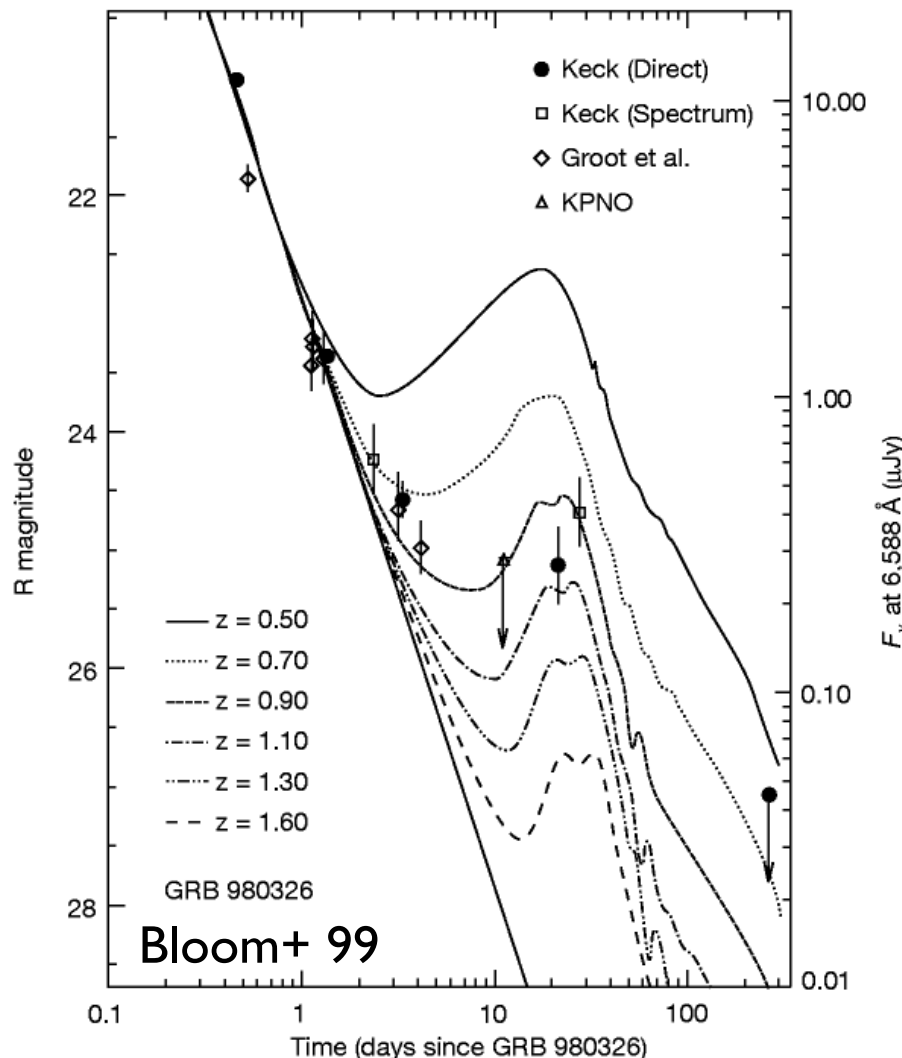


Long-soft
Short-hard



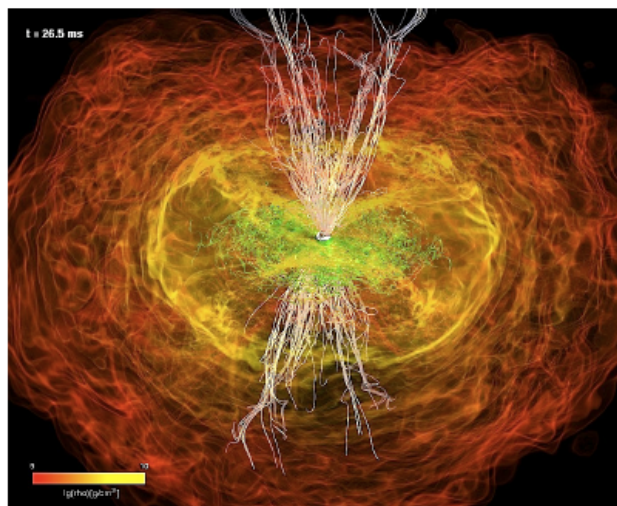
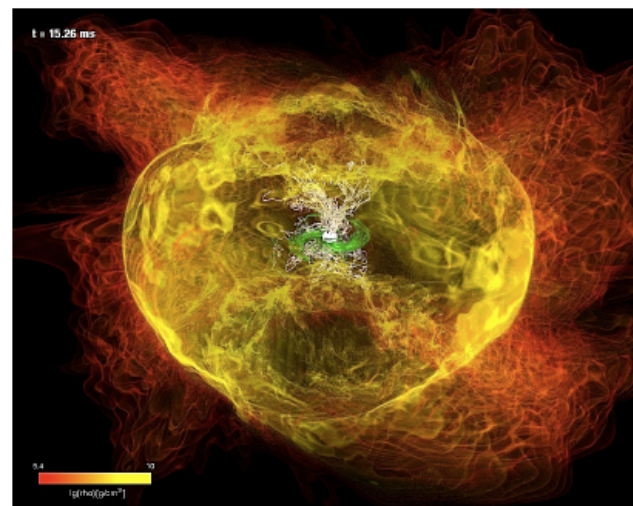
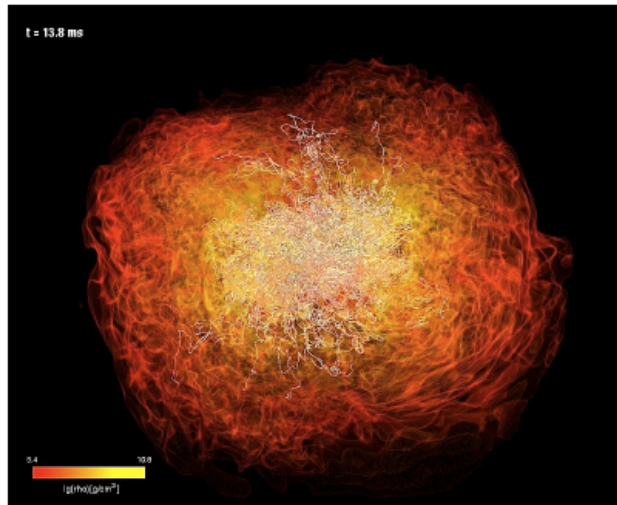
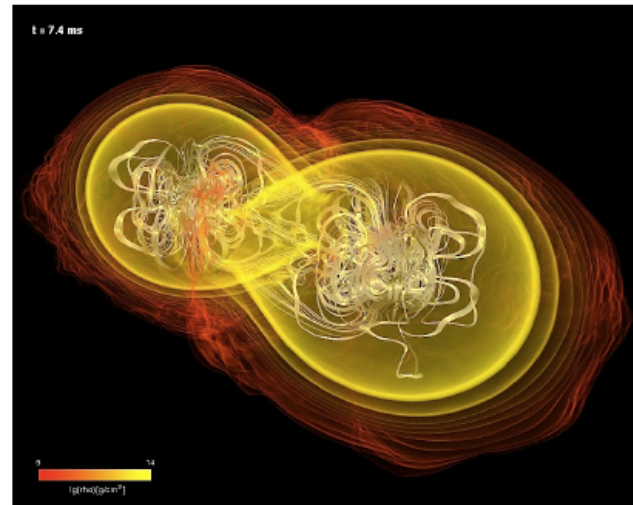
Long burst
Short burst

Supernova with Long GRB



Woosley 93 "Gamma-ray bursts from stellar mass accretion disks around black holes"

Short GRB

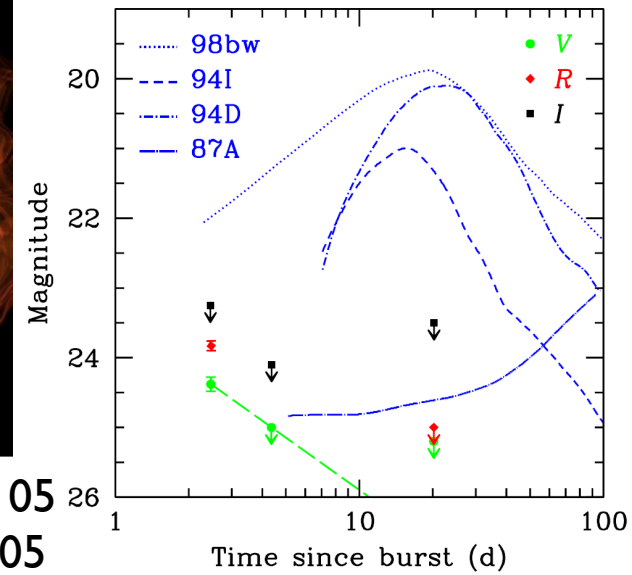


Rezzolla+ 11

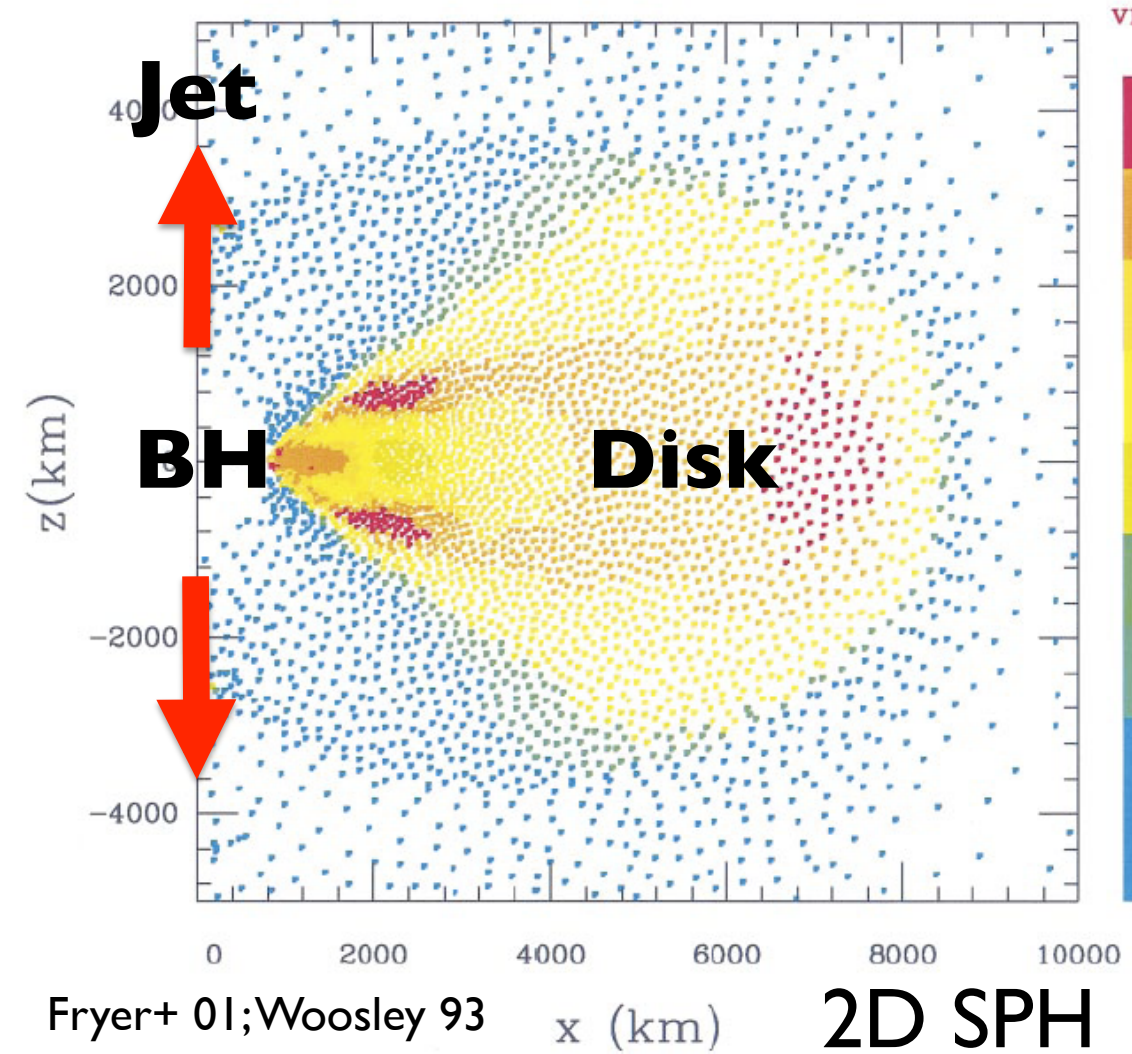
Covino+ 05
Hjorth+ 05

NS-NS / NS-BH
Magnetar (Svinkin+ 14)
WD/NS AIC
WD-WD

Not collapsar



Super Collapsar

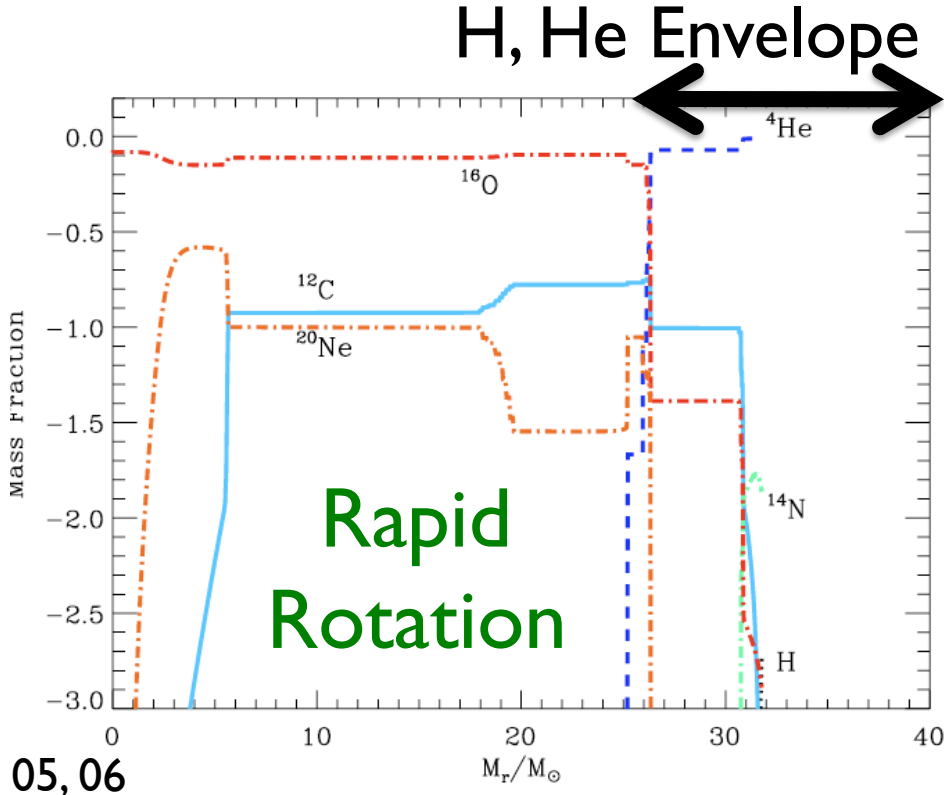
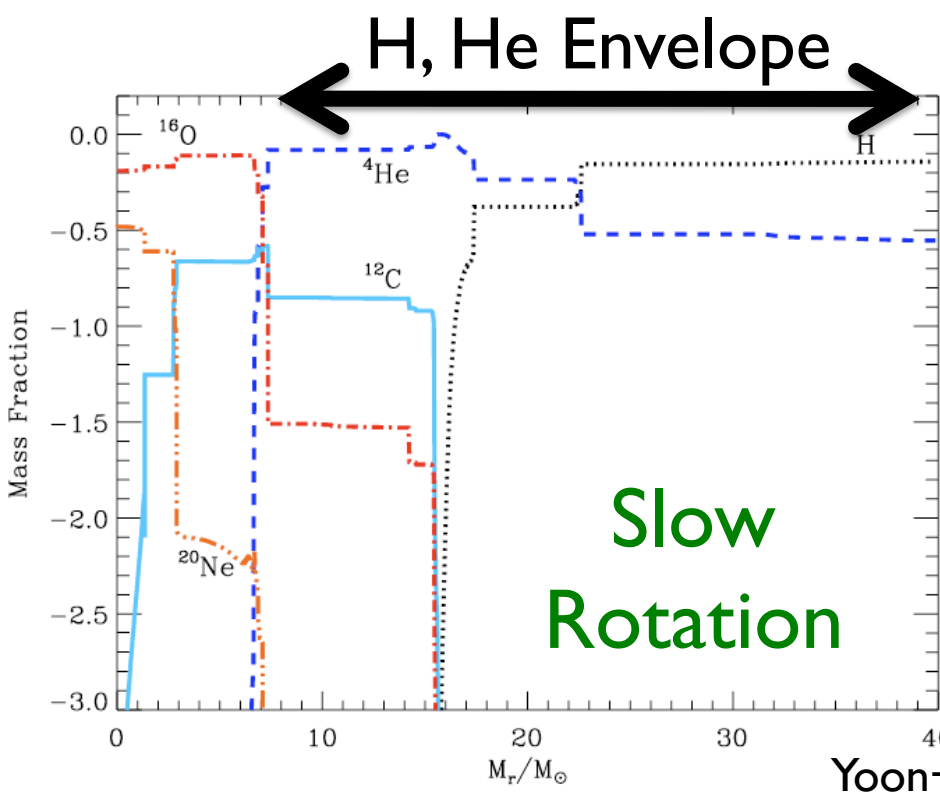
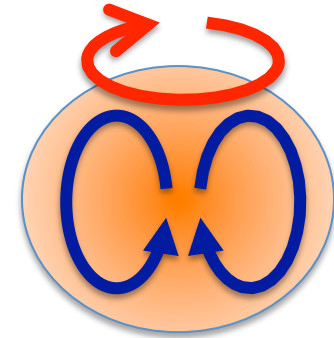


$50M_{\odot} < M < 160M_{\odot}$:
Black Hole
 $160M_{\odot} < M < 260M_{\odot}$:
Pair Instability SN
 $260M_{\odot} < M: BH$
 $\Rightarrow BH + Disk + Jet$
like Collapsar

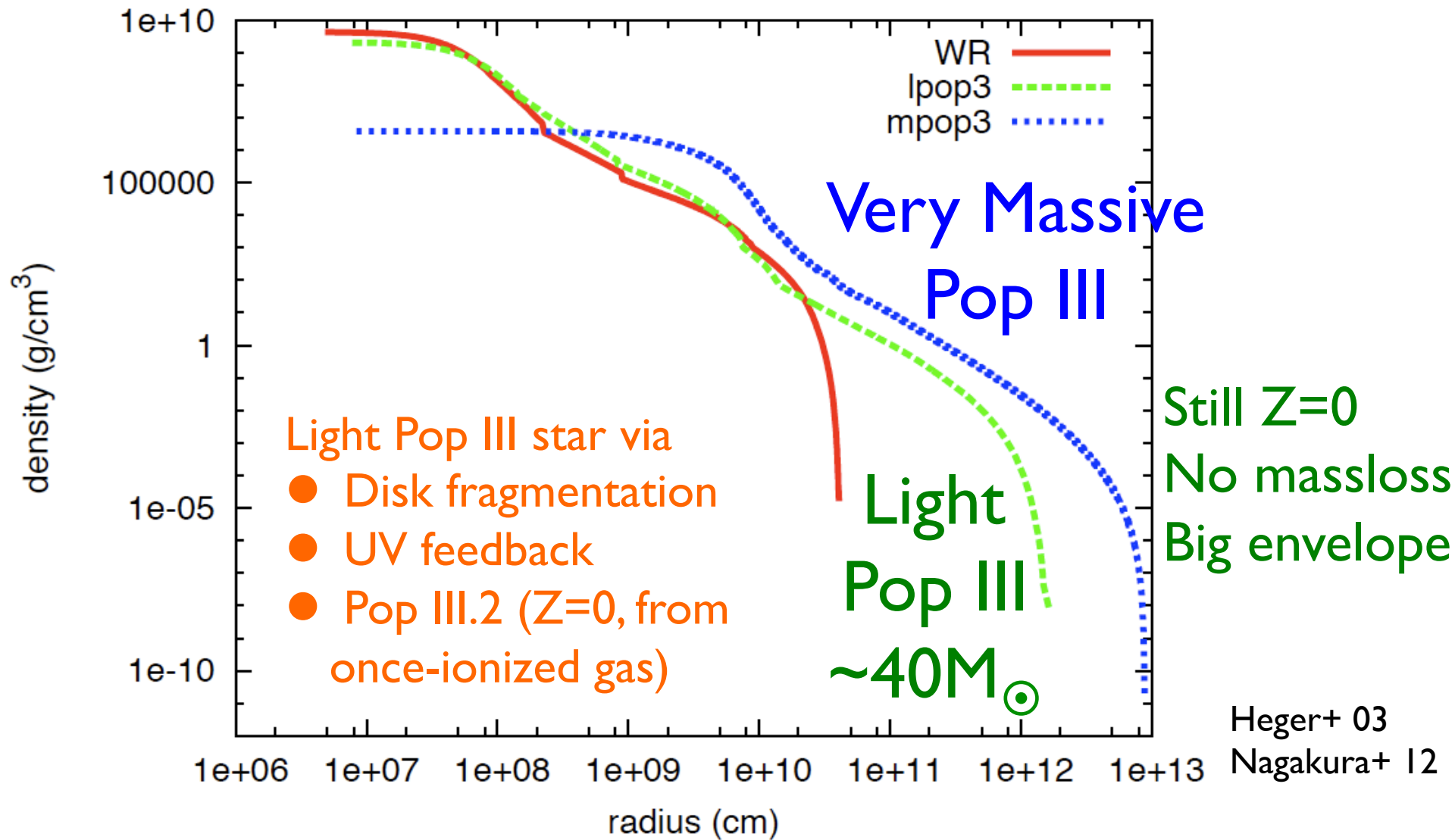
~ 100 times mass \Rightarrow
Super Collapsar
 v ann. is not effective
BZ could work

Chemically Homogeneous Evolution (CHE)?

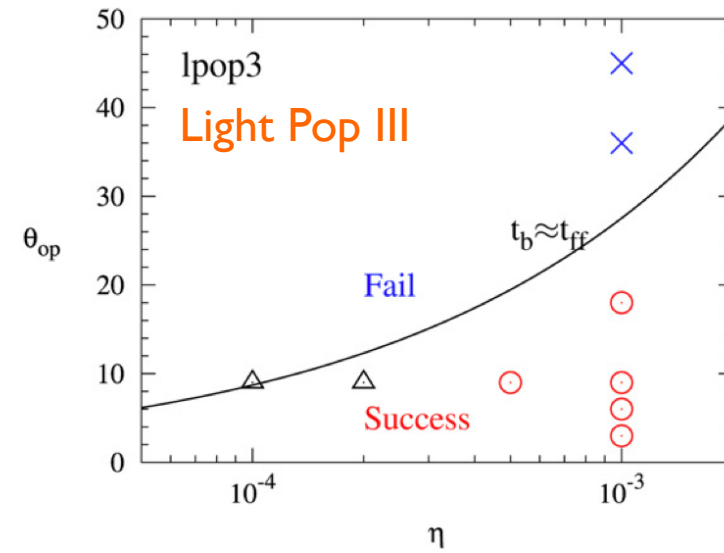
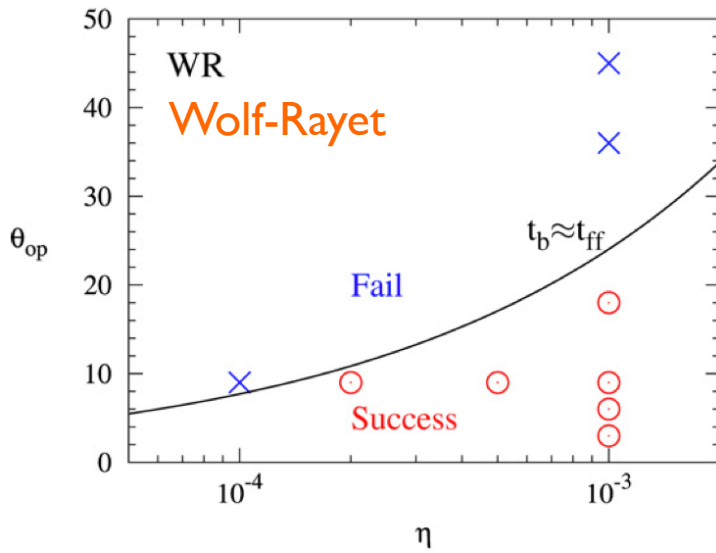
- Rotation \Rightarrow Mixing
 \Rightarrow Large CO Core & Small envelope



“Light” Pop III Star

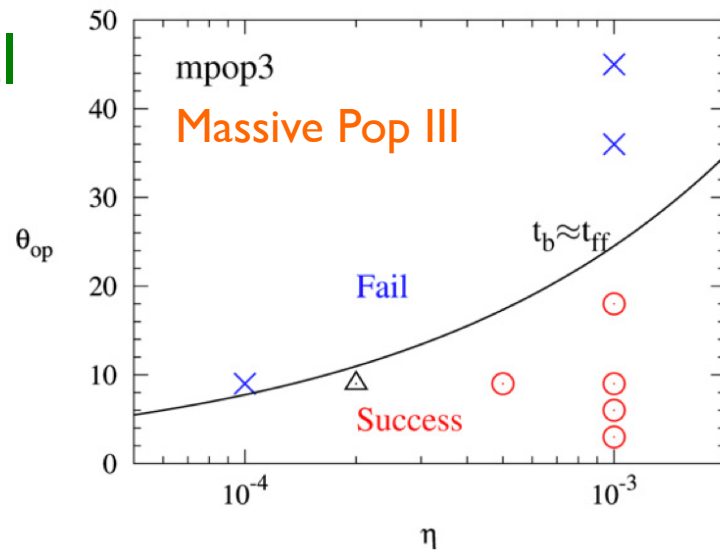


“Light” Pop III GRB



40 numerical
calculations
+ Analytical

Nagakura+ 12



**Breakout
is possible
also for
“Light” Pop III**

Polarized GRB 140206A

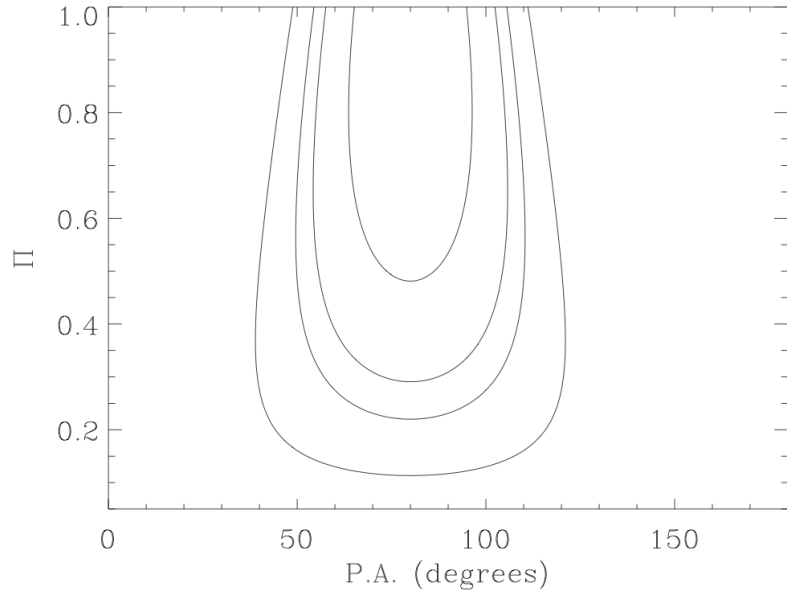
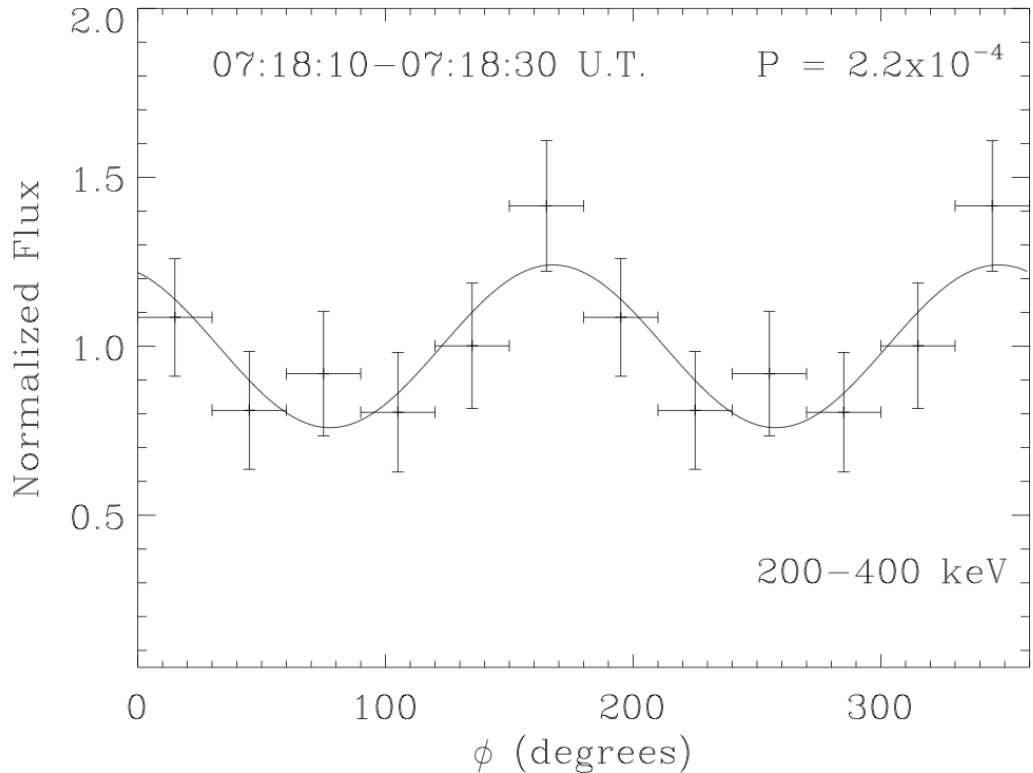
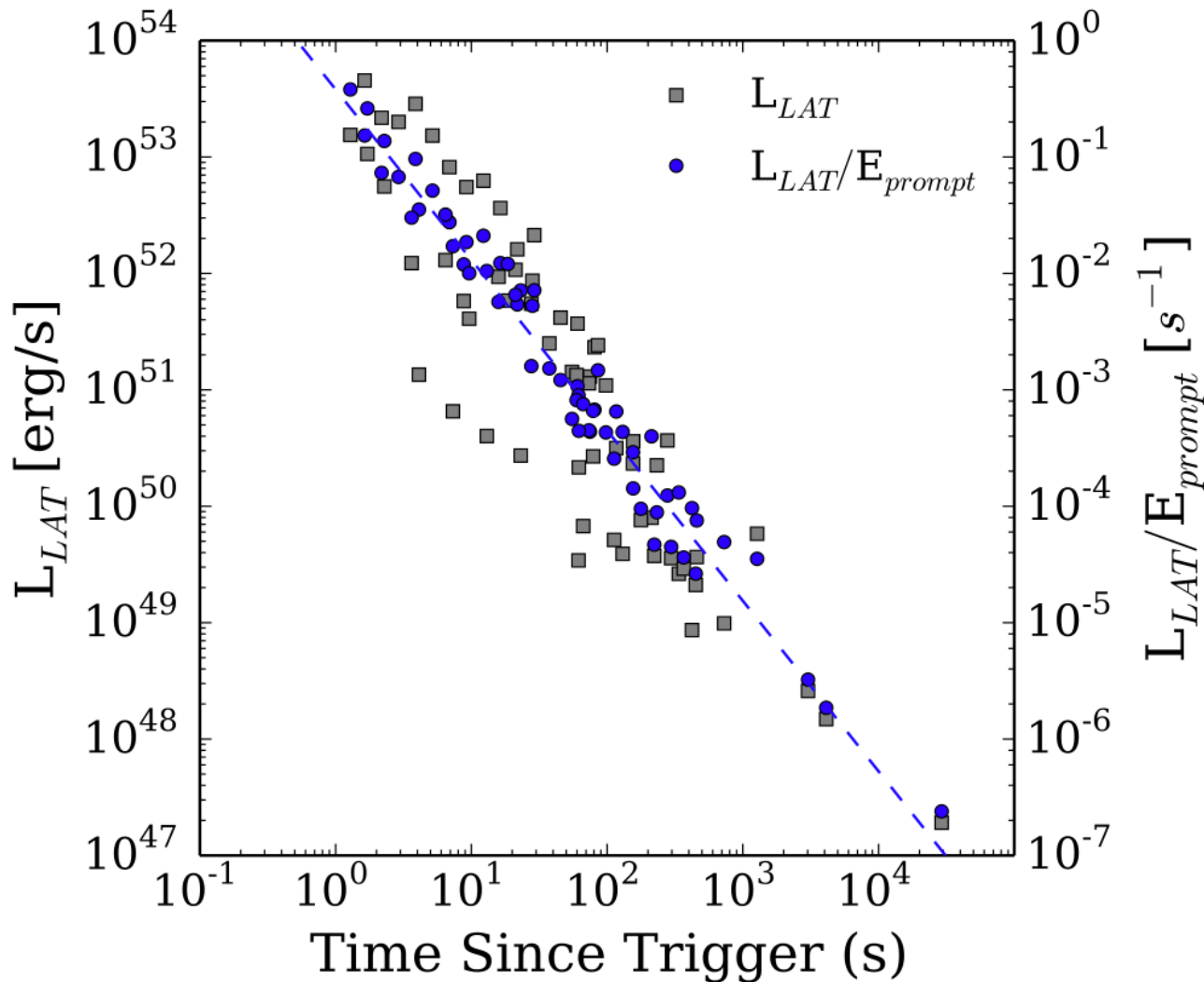


Table 2. Polarization measurements of GRB 140206A.

| Energy band (keV) | Π (%) (68% c.l.) | P.A. ($^{\circ}$) (68% c.l.) | Π (%) (90% c.l.) | P.A. ($^{\circ}$) (90% c.l.) |
|----------------------|-------------------------|-----------------------------------|-------------------------|-----------------------------------|
| 200–400 | >48 | 80 ± 15 | >28 | 80 ± 25 |

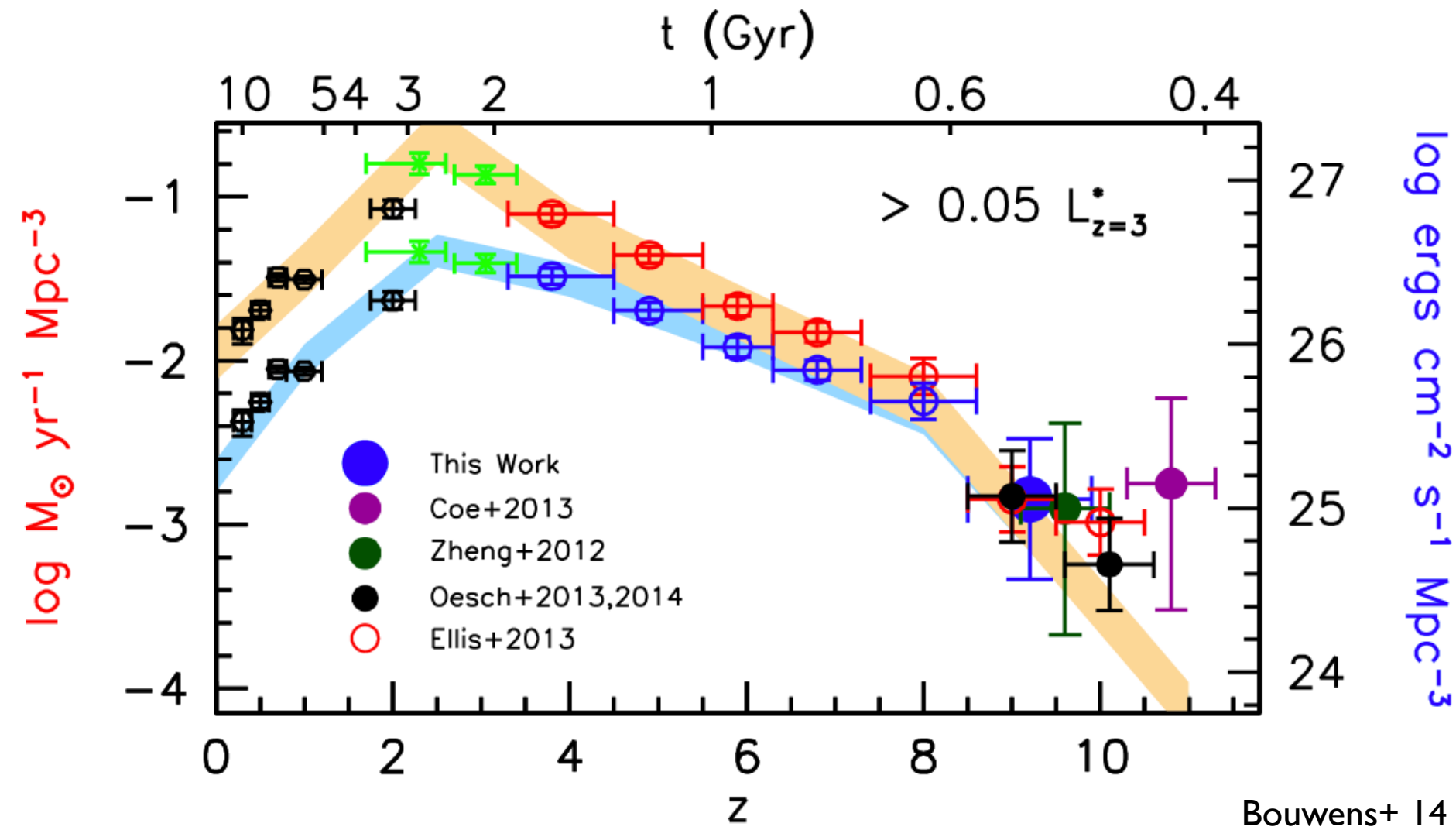
INTEGRAL/IBIS
 $z=2.739$
 $\xi < 1e-16$ on LIV

GeV Light Curve

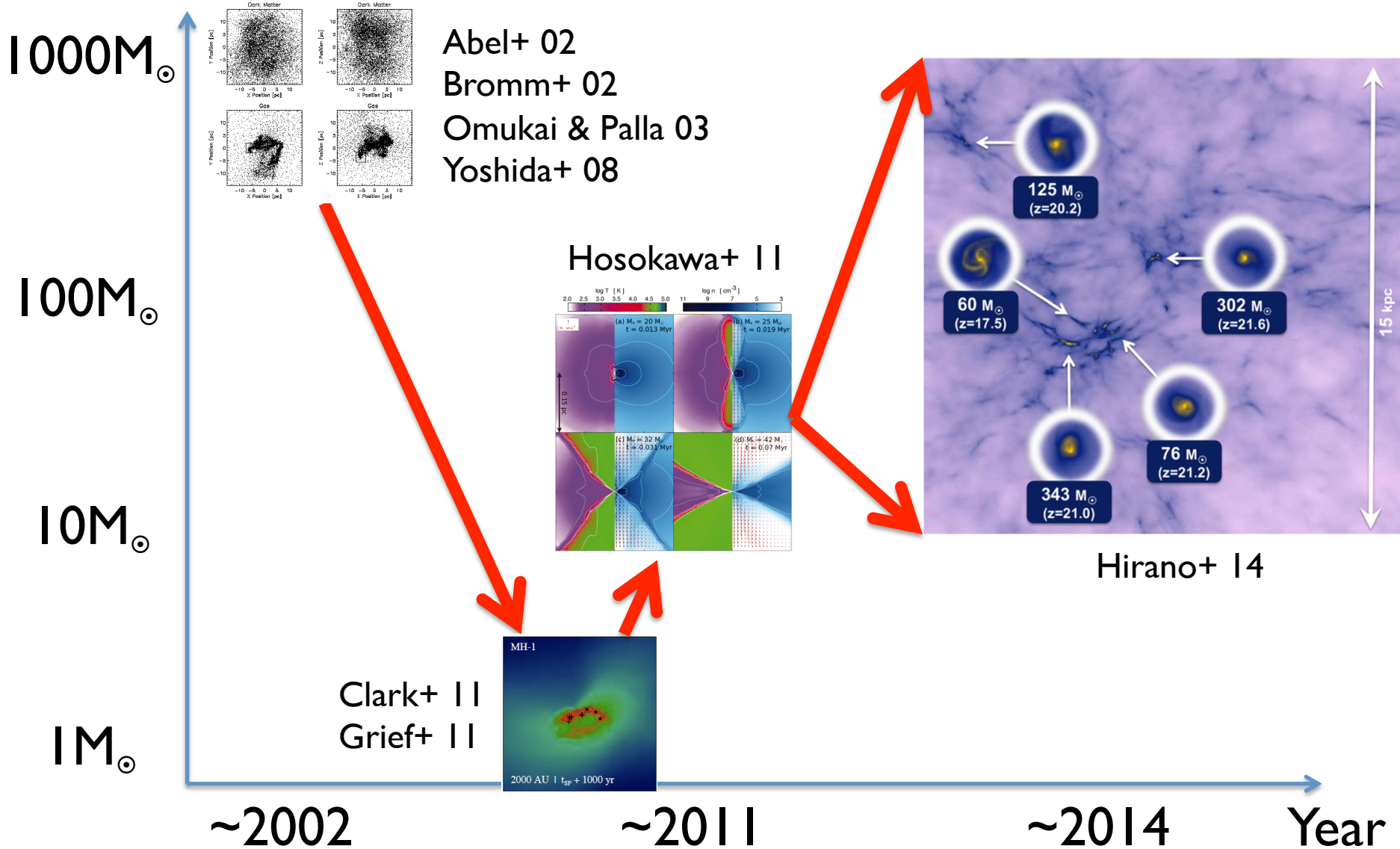


Clustering after
normalization
⇒ Extended GeV
emission from
external shocks

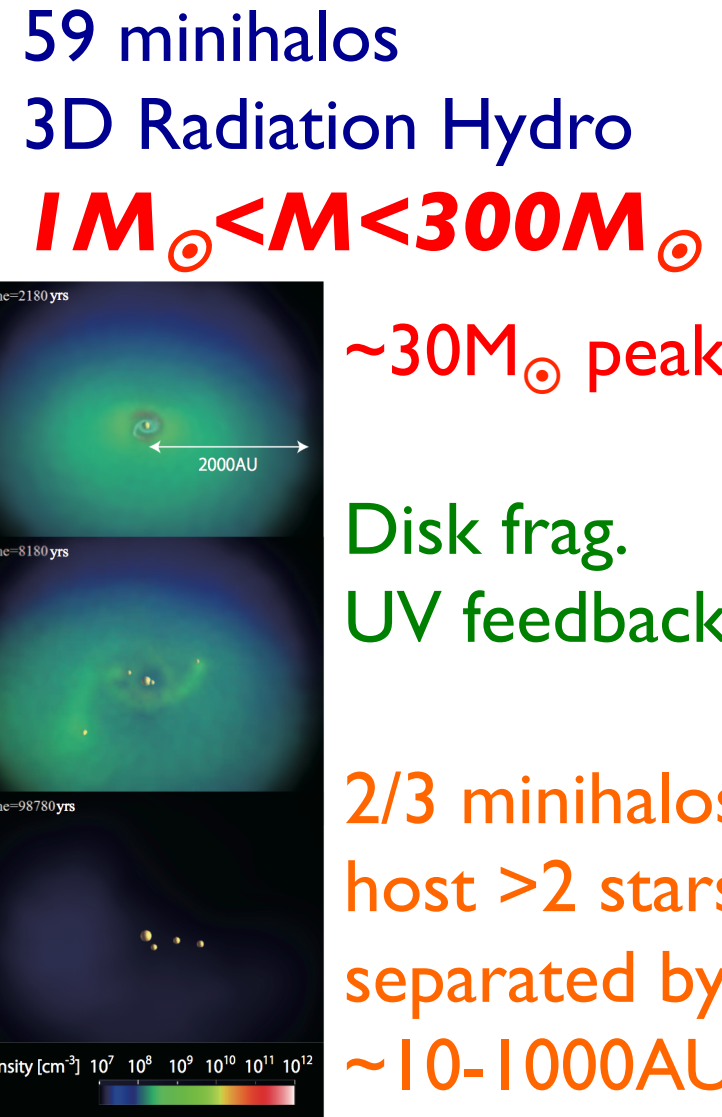
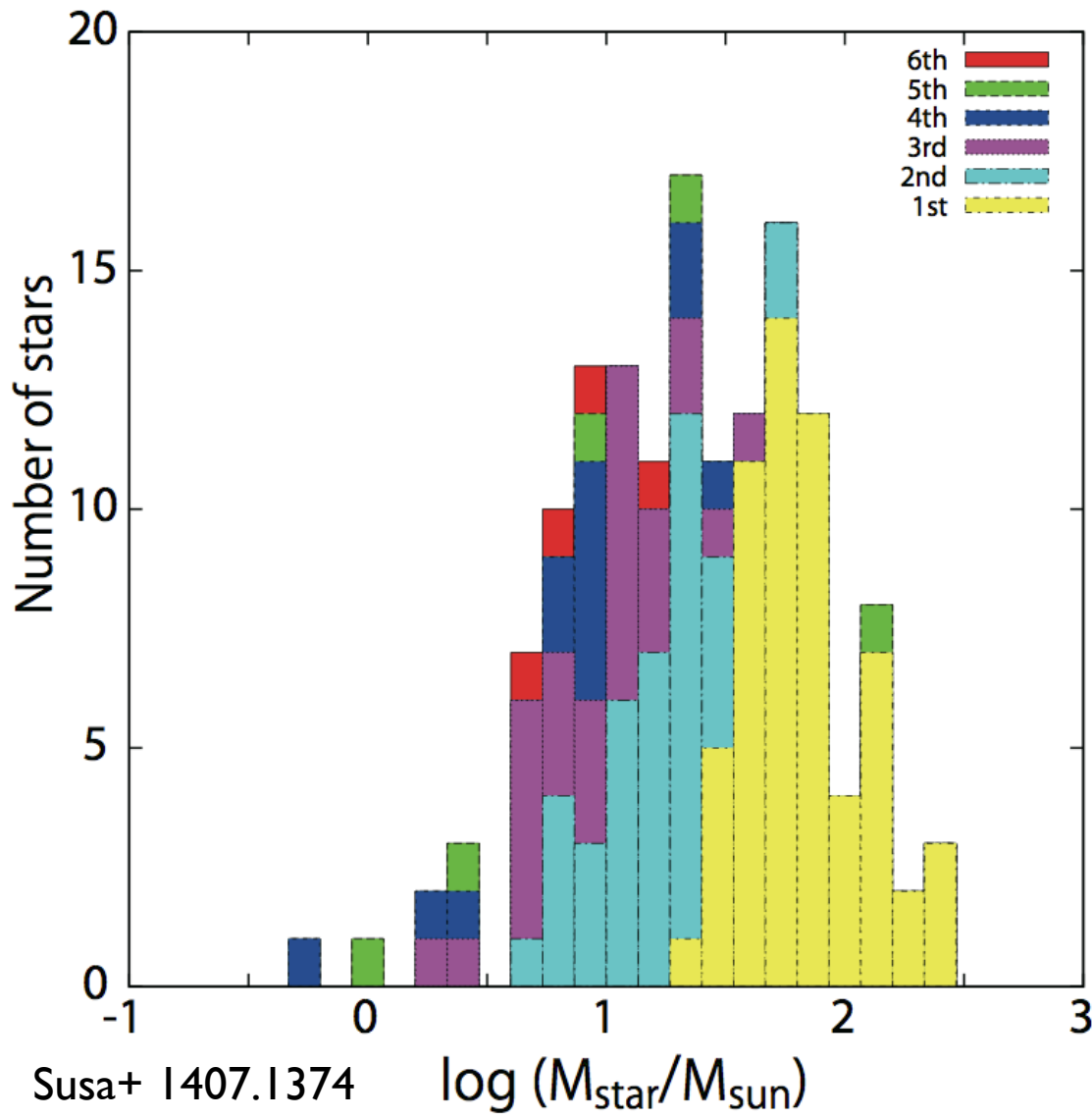
SFR up to $z \sim 10$

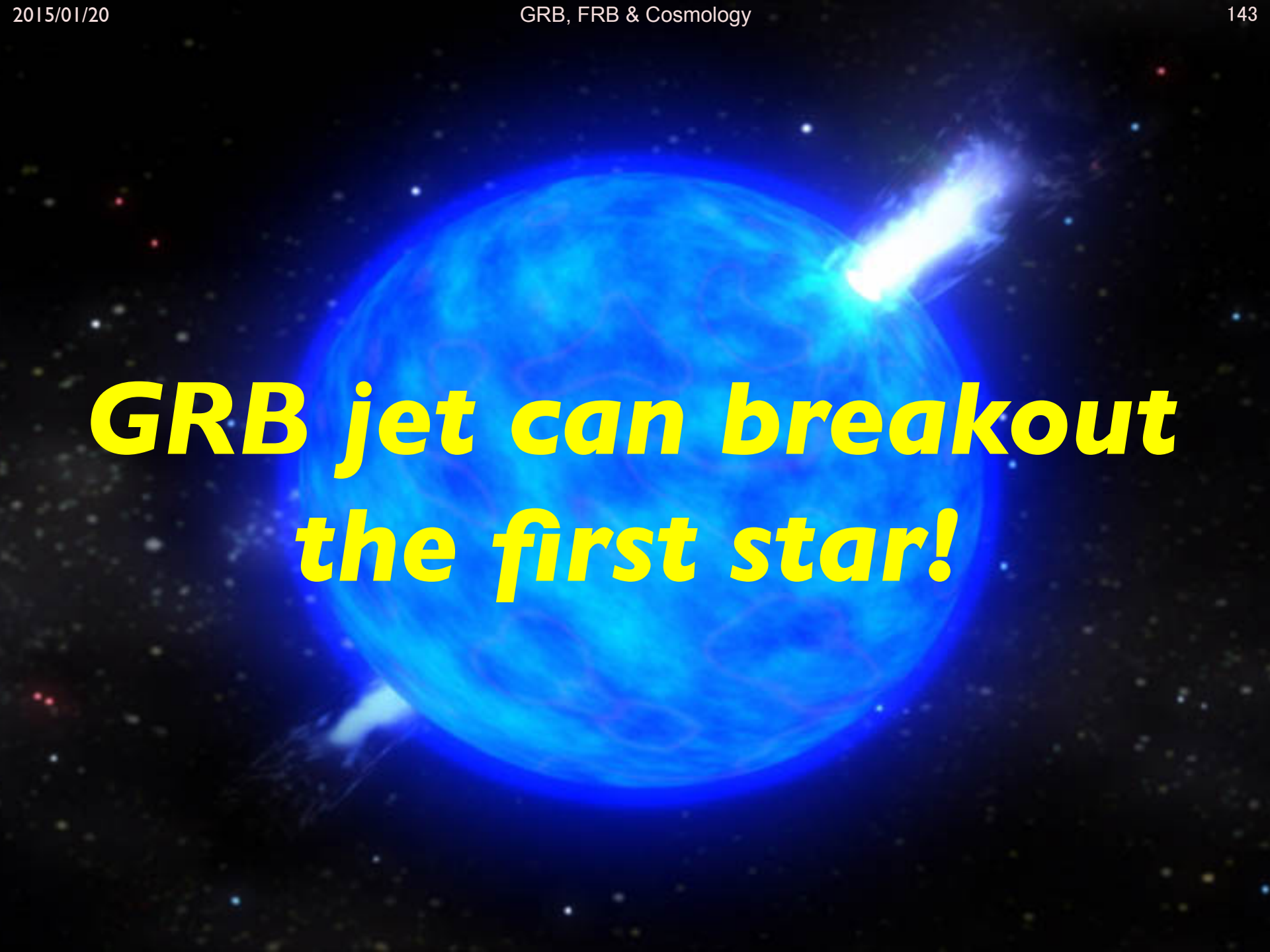


Mass Movement



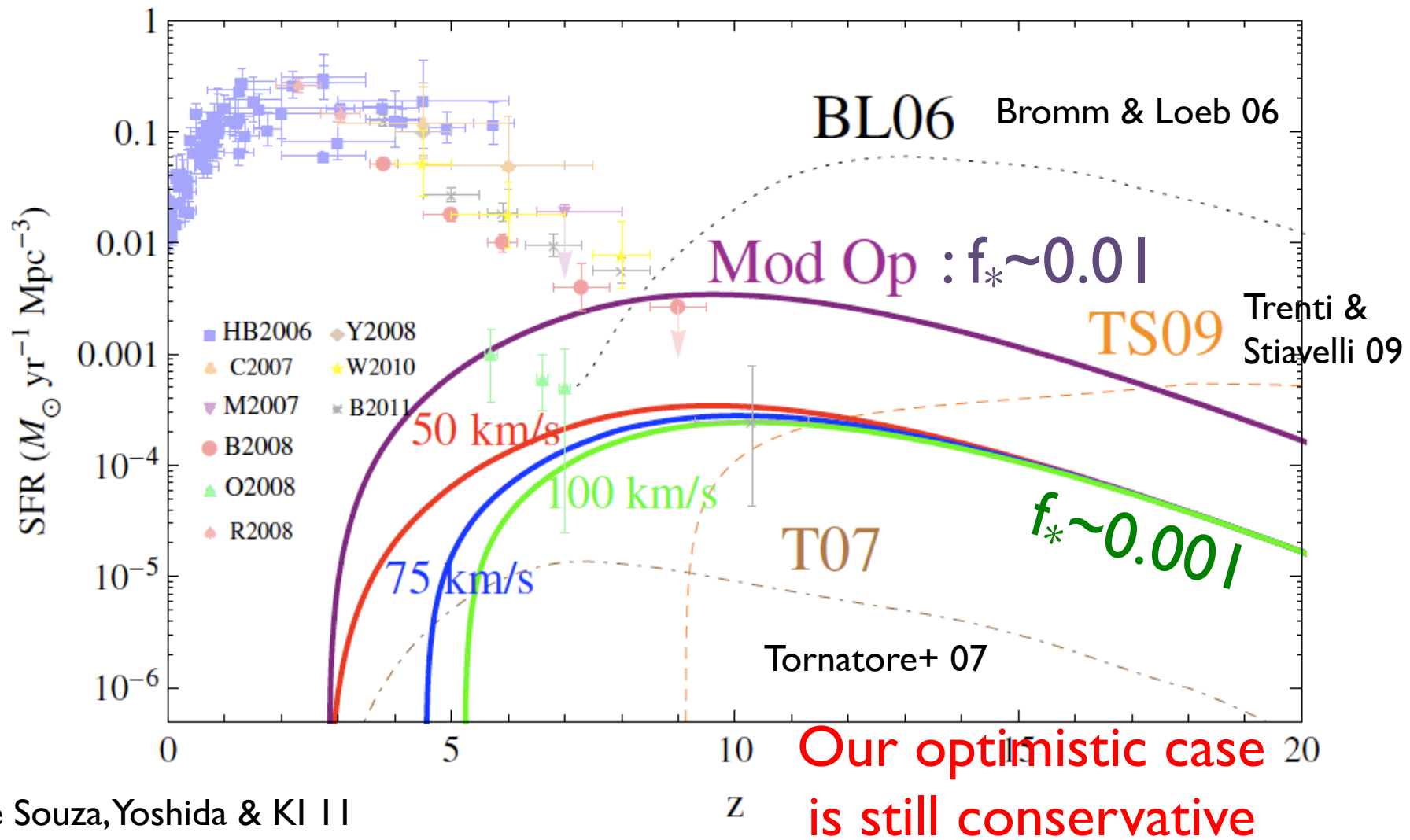
Pop III Mass Spectrum



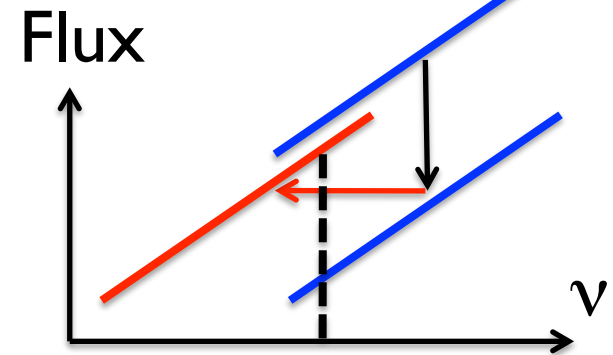
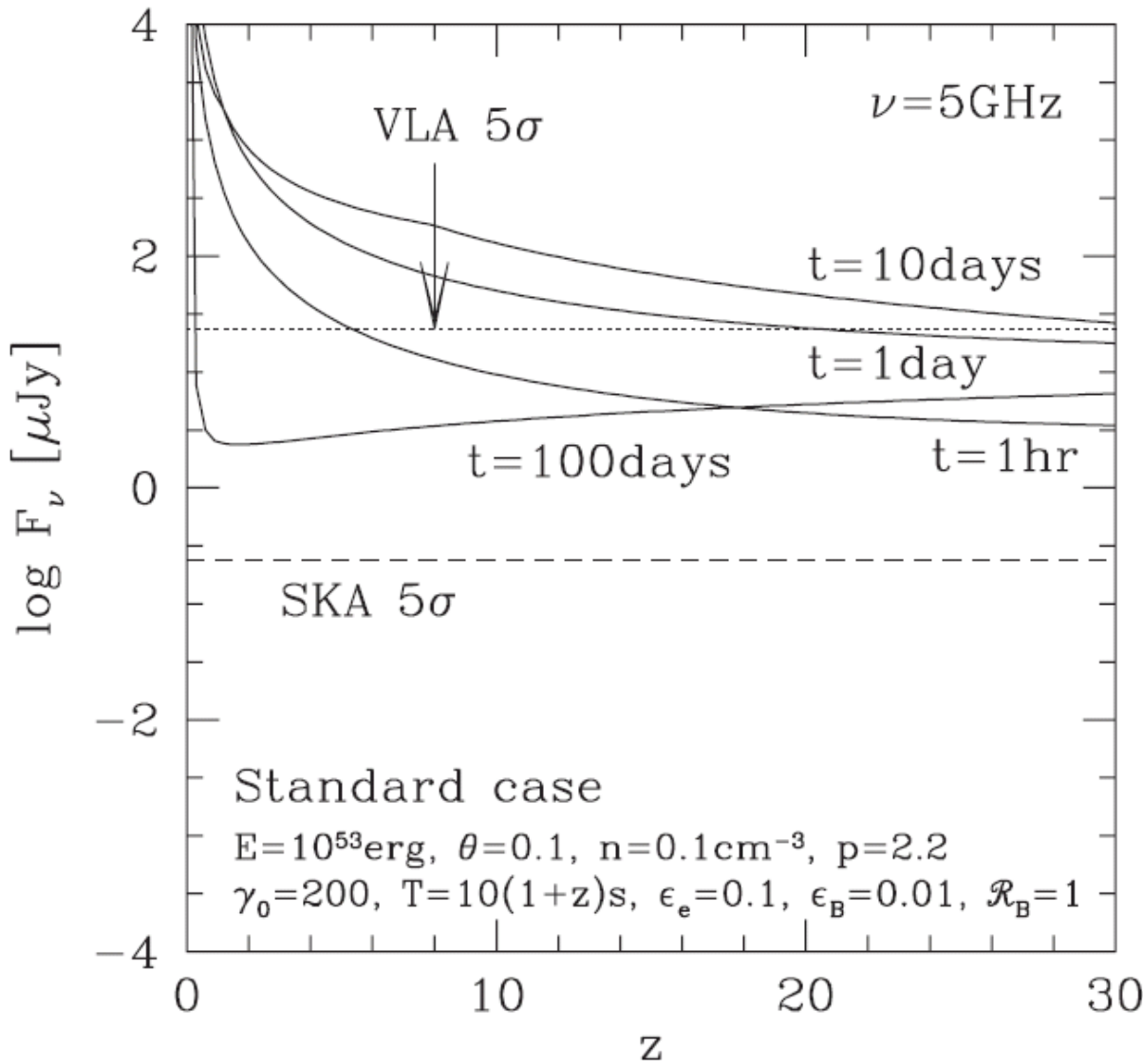
A blue and white illustration of a GRB jet breaking out from a star. The jet is a bright, luminous stream of light and energy, primarily blue and white, against a dark background. It appears to be emerging from a central point, possibly a star, which is partially visible at the bottom left. The surrounding space is filled with small, distant stars.

***GRB jet can breakout
the first star!***

Pop III.1 + III.2 Star Formation Rate



Radio Afterglow



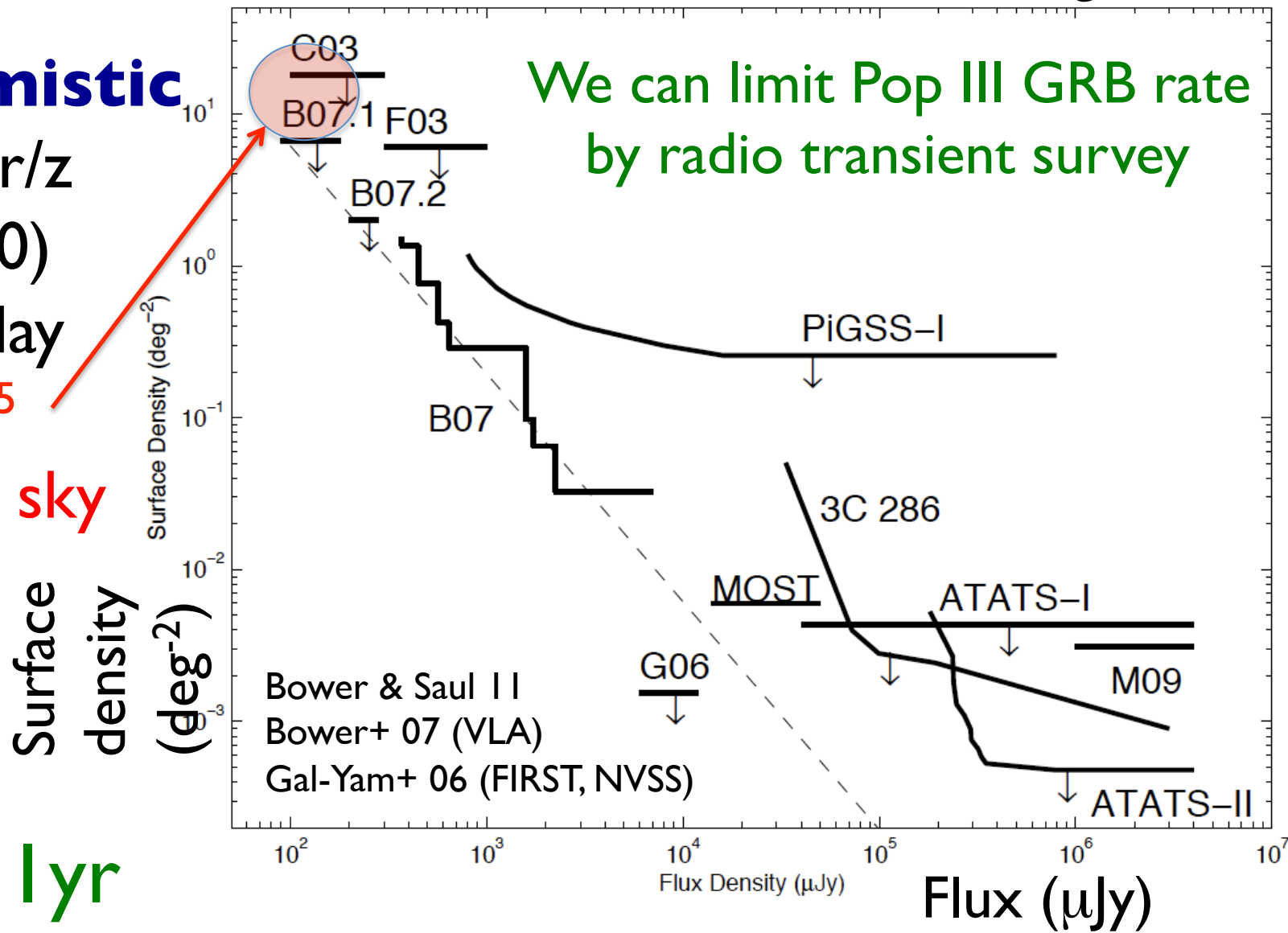
K-correction \Rightarrow
Not dim @high-z

Spherical after
jet break

KI & Meszaros 05
Inoue+ 07, Toma+ 10

Radio Transient Survey

Optimistic
 $\sim 10^5/\text{yr/z}$
 $\times (z \sim 10)$
 $\times 100\text{day}$
 $\sim 3 \times 10^5$
 on the sky



$\Delta t \sim 1\text{yr}$

Radio Transient Survey

Optimistic

$\sim 10^5/\text{yr/z}$

$\times (z \sim 10)$

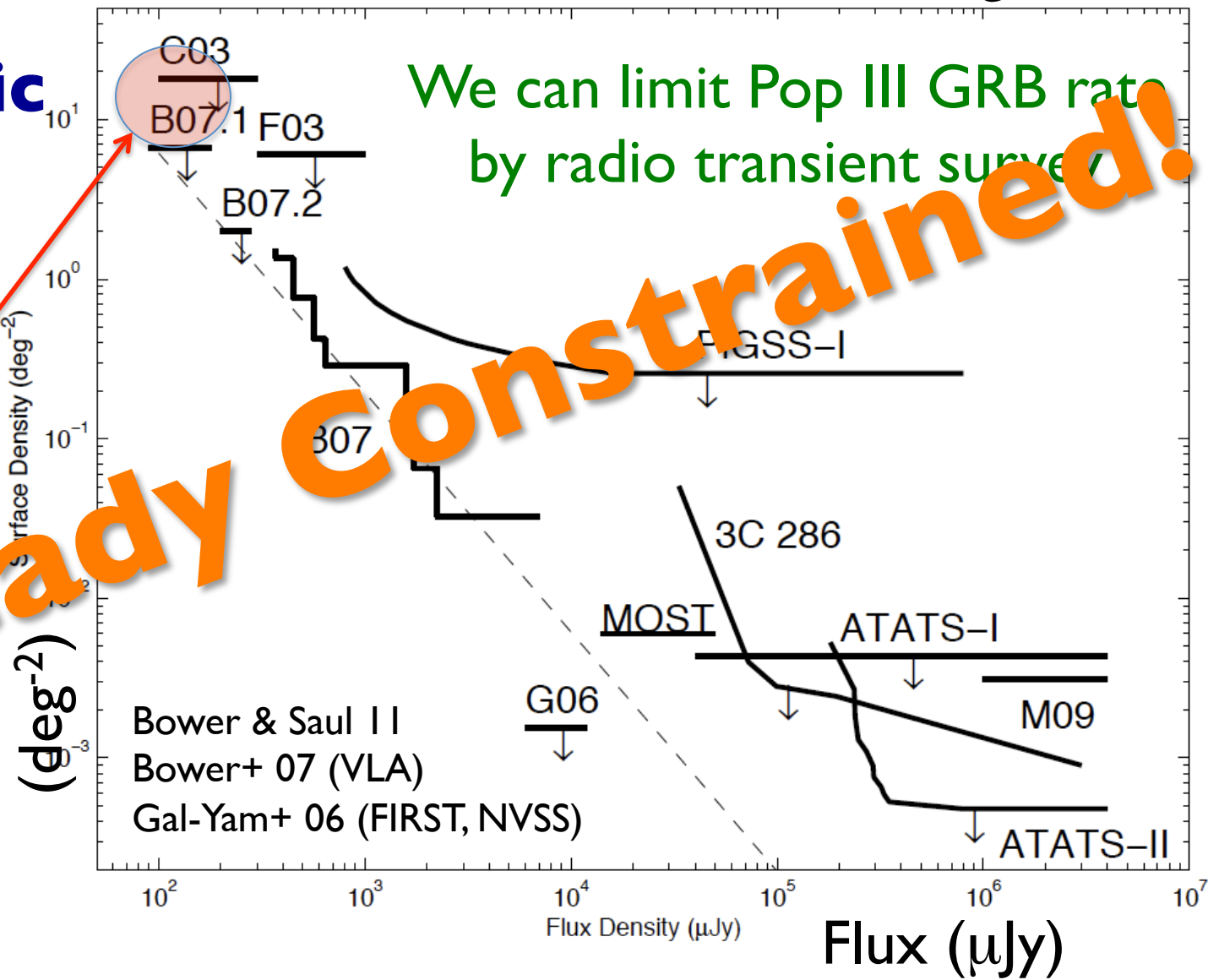
$\times 100\text{day}$

$\sim 3 \times 10^5$

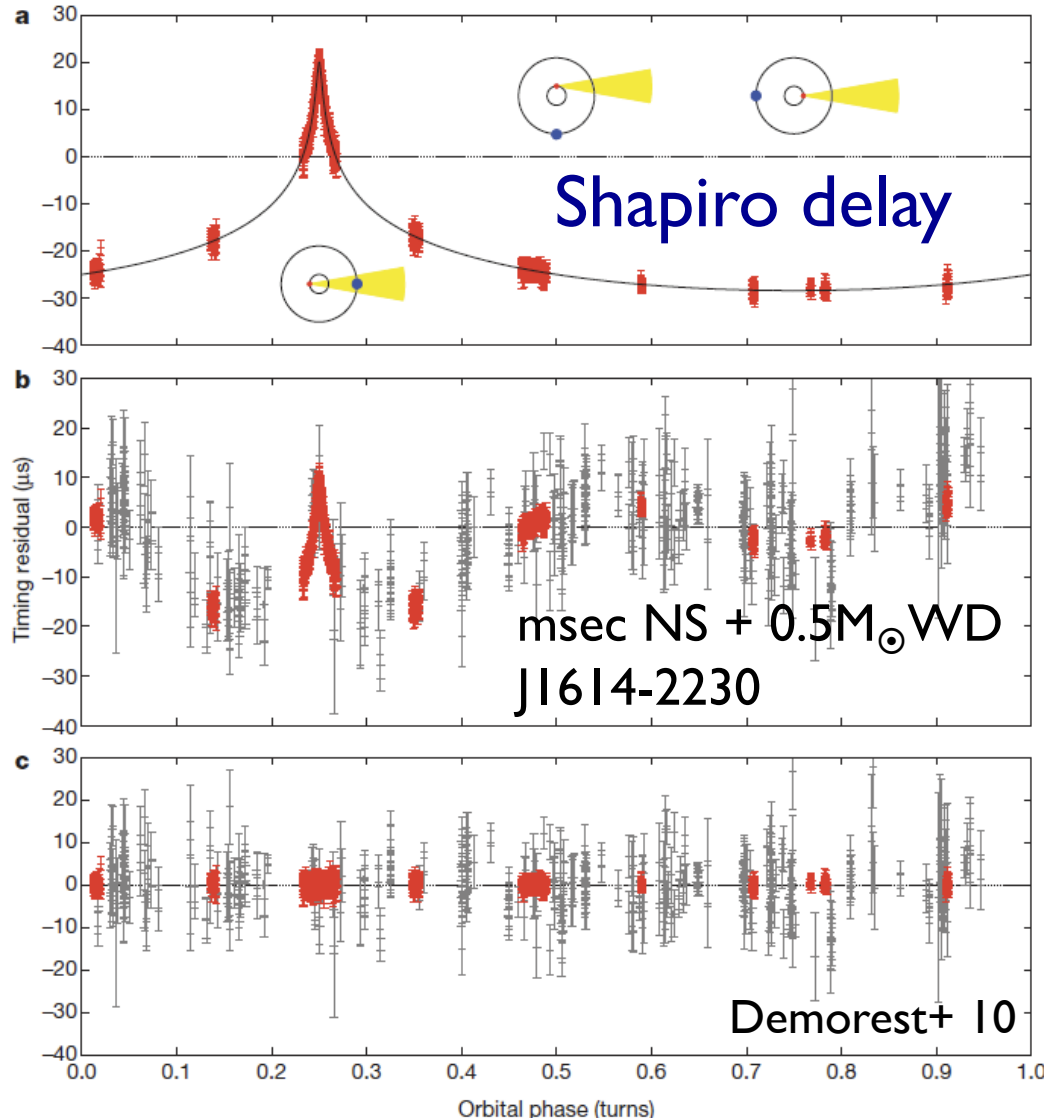
on the sky

Already constrained!

$\Delta t \sim 1\text{yr}$



$2M_{\odot}$ 中性子星



- $\sim(1.97 \pm 0.04)M_{\odot}$
- 硬い状態方程式
- 中性子星がブラックホールに崩壊しにくいため
- 連星中性子星合体
⇒ 超巨大中性子星
⇒ Short GRB
の可能性を高める

See also Antoniadis+ 13

ULX

CIBER

Fermi Bubble

EBL, CIBER